A STUDY ON THE SOLAR ENERGY HARVESTING POTENTIAL AT URBAN BLOCK LEVEL FOR BUSINESS DISTRICTS IN DHAKA

By

Sabbir Ahmed

A thesis submitted in partial fulfillment of the requirement for the degree of

MASTER OF ARCHITECTURE

June 2021

Department of Architecture

BANGLADESH UNIVERSITY OF ENGINEERING & TECHNOLOGY

Dhaka, Bangladesh.

Department of Architecture
Bangladesh University of Engineering and Technology
Dhaka-1000, Bangladesh.

The thesis titled "A STUDY ON THE SOLAR ENERGY HARVESTING POTENTIAL AT URBAN BLOCK LEVEL FOR BUSINESS DISTRICTS IN DHAKA" Submitted by Sabbir Ahmed, Roll No-1016012010 F, Session: October-2016, has been accepted as satisfactory in partial fulfillment of the requirements for the Degree of MASTER OF ARCHITECTURE on this day 1st June, 2021.

BOARD OF EXAMINERS

1.	Dr. Khandaker Shabbir Ahmed Professor Department of Architecture, BUET, Dhaka **(Supervisor)**	**Chairman**
2.	Dr. Shayer Ghafur Professor and Head Department of Architecture, BUET, Dhaka	**Member (Ex-Officio)**
3.	Dr. Zebun Nasreen Ahmed Professor Department of Architecture, BUET, Dhaka	**Member**
4.	Dr. Md. Ashikur Rahman Joarder Professor Department of Architecture, BUET, Dhaka	**Member**
5.	Dr. Abu Taib Mohammed Shahjahan Senior Assistant Professor Dept. of Architecture, American International University Bangladesh, Ka-66/1, Kuratoli Road, Kuril, Khilket, Dhaka-1229	**Member (External)**

CANDIDATE'S DECLARATION

It is declared that this thesis or any part of it has not been submitted elsewhere for the award of degree or diploma.

Signature:

Sabbir Ahmed

To my loving parents

Md. Ziaul Haque
Sabera Haque

Acknowledgments

Firstly, I would like to express my deep and sincere gratitude to my supervisor Dr. Khandaker Shabbir Ahmed, Professor, Department of Architecture, Bangladesh University of Engineering and Technology, for his valuable insight, prudent guidance, and profound inspiration throughout the period of my study.

It is also my genuine pleasure to be able to thank my teachers Prof. Dr. Zebun Nasreen Ahmed, Prof. Dr. Shayer Ghafur, Prof. Dr. Md. Ashikur Rahman Joarder, and Asst. Prof. Dr. Abu Taib Mohammed Shahjahan for their appreciation, comments, and careful guidance, without which this study could not have been completed. I am also thankful to Prof. Dr. S M Najmul Imam, Asst. Prof. Md. Mizanur Rahman, and Asst. Prof. Tasneem Tariq for their comments and support during my study.

I am greatly indebted to my colleagues Richie Renaissance Daru and Md. Raisul Mostafa Sajib for their logistic support; Ar. Sharfina Tasnim of DPDC and Debashish Chakraborty of BMD for helping me with the procurement of data; Chowdhury Ali Imam and Md. Shariful Alam for assisting in Grasshopper scripting; Md. Jakaria for helping me with python coding; and Nafisa Tasnim, Tasmim Fatima Wahhab, and S. M. Mashuk Hasan Nabil for their assistance while modeling in Rhinoceros. Without their invaluable support and assistance, my study would remain incomplete.

Last but not least, I am extremely grateful to my parents Md. Ziaul Haque and Sabera Haque, my elder brother Shahriar Tanvir and my elder sister Sajeda Sultana for their constant care and blessings throughout the entire research work.

Abstract

On-site production of electricity from solar energy using increasingly sophisticated technologies such as photovoltaics (PV) has been recognized as crucial for making cities energy-efficient. Urban configurations, which can be defined by urban design parameters that are governed by building regulations in Dhaka, highly influence the solar energy harvesting potential (or solar potential) of urban areas. This research aims to find out how the combined effect of urban parameters regulates the solar potential of urban blocks in the business districts of Dhaka, and explores the possibilities for the development of urban design strategies from such findings. Methods include an extensive theoretical framework, field investigation, parametric simulation study, and statistical analysis. For simulation, an integrated parametric interface combining Rhinoceros, Grasshopper, and Ladybug Tools was used. Field investigation generated insights about energy consumption in the buildings in an existing business district (Motijheel Commercial Area) in Dhaka, which is largely regulated by the combined effect of weather variables, and shows strong individual correlations with temperature variables. Moreover, airconditioning energy was found to dominate energy consumption in buildings. As such, solar energy can contribute to meeting energy demands in commercial office buildings more efficiently during the cooler and drier months of the year. Monthly Mean Temperature, Monthly Maximum Temperature (extreme variable), Monthly Average Sunshine Hours, Monthly Number of Workdays and Eid-ul-fitr Month (categorical variable) were all found statistically significant predictor variables for generating monthly energy consumption figures. Parametric study and analytics revealed that while the density and the compactness ratio of an urban block had negative and positive impacts respectively on its solar potential per unit floor area, the impact is governed by the combined effect of parameters such as the number of stories, ground coverage, street-to-surface distance, side-to-side distance, and orientation. Facades facing unobstructed south were found to increase solar potential more efficiently than facades facing other directions and with poorer setback conditions. Local building regulations should acknowledge compactness ratio and surface orientation as significant strategies for more efficient solar energy harvesting in the business districts in Dhaka. Urban designers, planners, architects, and engineers will be critically informed by this research about the impact of urban design decisions on the solar potential of urban blocks within the climatic and physical context of Dhaka.

Keywords:

Solar Potential, Energy and Environment, Commercial Buildings, Local Building Regulations, Urban Design.

Table of Contents

List of Figures

List of Tables

List of Abbreviations/Acronyms

Acronym	*Full Form*
3D	Three-dimensional
A/C	Airconditioning
ACSR	Annual Cumulative Solar Radiation
BERC	Bangladesh Energy Regulatory Commission
BIPV	Building-integrated Photovoltaics
BMD	Bangladesh Meteorological Department
BNBC	Bangladesh National Building Code
°C	Degrees Celcius
CAD	Computer-aided Design
CW	Clockwise
CCW	Counter-clockwise
Comp	Compactness Ratio
DAP	Detail Area Plan
DPDC	Dhaka Power Distribution Company Ltd.
EPW	EnergyPlus Weather file format
Env	Total Building Envelope Area
FAR	Floor Area Ratio
FSI	Floor Space Index
GC	Ground Coverage
GOB	Government of the People's Republic of Bangladesh
HVAC	Heating, ventilation, and airconditioning
IEA	International Energy Agency
IEA-PVPS	International Energy Agency's Photovoltaic Power Systems program
INB2008	Dhaka Mahanagar "Imarat Nirman Bidhimala" – 2008 (translated as Dhaka Metropolitan Building Construction Rules 2008)
KB	Kawran Bazar Commercial Area
kWh	Kilowatt-hour
kWh/m²	Kilowatt-hour per square meter
MCA	Motijheel Commercial Area
MWh	Megawatt-hour
MGC	Maximum Ground Coverage
NOAA	National Oceanic and Atmospheric Administration, United States
OSM	Open Street Map
P.I.	Annual Solar Performance Indicator
PV	Photovoltaics, i. e. electric power generation with solar cells
ST	Solar Thermal, i. e. solar thermal energy system
TFA	Total Floor Area
WMO	World Meteorological Organization
UN	United Nations

CHAPTER 1: PREAMBLE

1.1 Background

More than 50% of the global population reside in cities today and by 2050, the proportion is expected to increase to 68.4% (UN, 2018). Cities account for nearly two-thirds of global energy demand and 70% of energy-related CO_2 emissions (IEA, 2019). This has made urban areas a particularly important concern for reducing energy consumption and carbon emission. Applications of cost-effective on-site renewable energy generation such as photovoltaic (PV) systems on building surfaces could technically meet one-third of cities' electricity demand by 2050 (IEA, 2019). PV, one of the most efficient ways to harness solar energy (Peng, et al., 2011), has gradually started dominating the global market with the promise of aesthetical, economic, and technical solutions (Jelle & Breivik, 2012); for example, BIPV (Building-integrated photovoltaics) for facade PV generation (Brito, et al., 2017; Jelle & Breivik, 2012).

However, solar harvesting capacity is not only decided by PV cell, module, and system technologies which have progressed substantially in previous decades (Zhang, et al., 2019), but also significantly by the intensity of insolation in a given geographic and climatic context and the availability of spaces suitable for system deployment, the latter being massively influenced by urban design strategies and building design solutions adopted. High-density cities, such as Dhaka, face many challenges in terms of harvesting solar energy compared to cities with relatively low density. Solar energy harvesting in the urban context is massively dependent upon available areas for PV installation and degrees of obstruction resulting from compact urban form. When buildings in high-density cities get substantial shading from their surroundings, they have less suitable rooftop and facade surfaces to deploy PV panels (Zhang, et al., 2019).

In order to create a sustainable urban environment, it is essential to improve old and new buildings' energy efficiency by reducing their energy demands by means of passive design which utilizes natural ventilation and daylighting, as well as to use a significant portion of renewable energy sources integrated into the urban context (IEA, 2019). While integrating solar energy systems in buildings is generally conceived as an important local solution for providing renewable energy, the formal characteristics of these buildings, their orientations, configuration, and the nature of spaces between them heavily influence their respective solar energy harvesting potentials (Arboit, et al., 2008; Zhang, et al., 2019). For example, a study shows that by introducing changes in aggregated descriptors of the urban form, insolation in roofs could be increased by around 9%, and in facades by up to 45% (Sarralde, et al., 2015).

Current legislation in many cities of the world is already directing towards energy-producing buildings (Kanters & Wall, 2015). More importantly, Bangladesh adopted the Renewable Energy Policy in 2008, which acknowledges the use of PV systems for harnessing solar energy in urban areas and offers subsidies for installation, exemption of taxes, and tariffs for generated electricity (GOB, 2008). The important players from the building sector, such as urban planners, architects, and engineers, should be able to make well-informed decisions in the very beginning, in order not to put constraints on the solar potential of the buildings further in the design phase (Todorov, 2015). These professionals, also important actors in urban development (Kanters & Wall, 2014), will be critically informed by this research about the impact of urban design decisions on the solar potential of the urban blocks in the context of Dhaka, Bangladesh's densely populated capital.

1.2 Problem Statement

The research questions were:

- In what manner does the combined effect of urban parameters regulate the solar potential of urban blocks in the business districts of Dhaka?
- In reference to existing building regulations, what are the possible urban design strategies that can be adopted to maximize the solar potential of urban blocks in the business districts of Dhaka?

1.3 Aim and Objectives

To explore the potential of an urban block in a business district in Dhaka for harvesting solar energy and to study the Urban design implications in terms of existing building regulations. The objectives of the study were to:

1. To identify and study the components of the existing regulations responsible for the spatial arrangement of urban blocks in a business district in Dhaka in terms of insolation and overshadowing.
2. To investigate the solar potential of urban surfaces of the said district at the urban block level.
3. To explore possibilities for the development of urban design strategies that will potentially maximize solar energy harvesting in the business districts of Dhaka.

1.4 Overview of Research Methodology

To respond to the objectives, the design of the research process needed to combine various methodologies within a multidisciplinary approach. The overall design could be classified as Experimental Research, which includes a combination of case studies, simulation, and analysis.

A theoretical framework encompassing the concepts of solar energy and urban parameters affecting solar potential was executed in detail, along with how these parameters relate to insolation and overshadowing. Dhaka Metropolitan Building Construction Rules (Imarat Nirman Bidhimala) and existing regulations were also studied to investigate how urban parameters are defined in the study area. Moreover, theoretical knowledge on previous research on solar potential in the urban context, electricity consumption, and production in buildings, the microclimate of Dhaka with particular focus on sun paths, seasonal variations, standards for software data input, and validation of the methods and tools to be used was also assembled.

Field Investigation was carried out for supporting the theoretical framework with knowledge regarding local energy consumption patterns and the local urban context. During physical surveys, thermal images of urban surfaces were also taken and were utilized for a comparison study between the actual scenario and the simulated scenario to better understand the effect of parameters.

Solar potential was determined at the building level and the district level, before conducting experiments at the urban block level, which is the generic unit of business districts. At the district level, two case study areas in Dhaka with differing building morphologies: Kawran Bazar and Motijheel were studied. At the building level, seven buildings from Motijheel Commercial Area were studied. At the urban block level, the experimentation was carried out on projected district models from a generic commercial plot layout in Purbachal New Town – a newly planned urban area in Dhaka. A combination of data obtained from satellite images and Field Investigation were utilized for modeling the case study districts and buildings, which was carried out in a commercial 3D computer graphics and computer-aided design (CAD) tool and its parametric modeling plugin that uses a visual programming language and environment. Using this parametric interface, the calculation of urban parameters was also performed and recorded. The solar radiation incident on urban blocks and the amount that can be converted into electricity using PV systems were calculated and mapped with the help of simulation techniques using an environmental component group integrated within the mentioned parametric interface.

Simulations were conducted primarily on an annual basis to explore the solar potentials of the district and building models on which parametric studies were performed. However, to address seasonal variations, the outcome of simulations on a monthly basis was also compared with the monthly energy consumption figures to investigate how much energy demand can be met for each month. Finally, the data from the aforementioned simulations were analyzed to find out which parameters influence the solar potential to what degree, and how these parameters relate to existing building regulations for business districts in Dhaka. Data analysis was performed using validated statistical models.

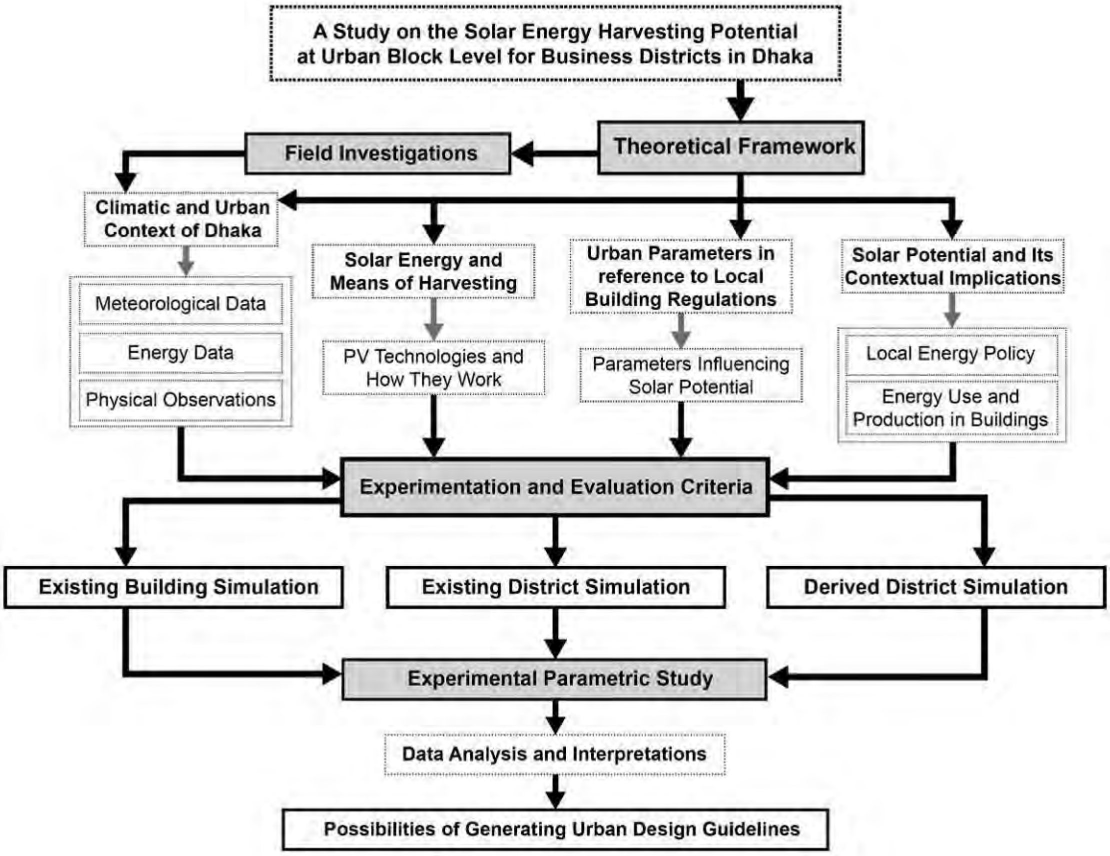

Figure 1.1: Flow diagram of the research process.

1.5 Scope and Limitations

While harvesting solar energy largely depends on exposed surfaces for insolation, urban areas pose a particular challenge in acquiring such exposed surfaces within them. Besides the formal characteristics of individual urban blocks (Kanters & Horvat, 2012), the solar potential of an urban area is influenced by parameters such as Urban Density (Kanters & Wall, 2014), Compactness Ratio (Zhang, et al., 2019), and Mean Height of Buildings (Lobaccaro, et al., 2012). In the context of Dhaka, these parameters are governed by the existing parameters of building regulations, such as FAR (Floor Area Ratio), MGC (Maximum Ground Coverage), Street Width, and Setback (GOB, 2008). Business districts in Dhaka, e.g. Kawran Bazar and Motijheel, boasts highrise buildings with large facade and roof areas that can potentially be utilized for generating electricity through solar power subject to urban configurations and volumetric design in reference to solar geometry and urban weather variables. This research focuses on parametric studies to generate urban design strategies for business districts in Dhaka so that the design of the urban blocks, as well as individual buildings, can be explored to maximize their solar potential in terms of using PV systems.

The methodology of this solar potential study can be applied all over the world. However, this study strictly uses the weather data for Dhaka, and therefore the results are valid for Dhaka only. Moreover, planning regulations are not the same everywhere. In Dhaka, urban areas predominantly follow local building regulations and are therefore shaped by these regulations. This study is limited to the application of building regulations in Dhaka. Therefore, urban parameters are also defined and interpreted in terms of local building regulations.

Additionally, the research limits its scope to investigating the solar potential for solar photovoltaic (PV) systems and does not take into consideration other types of solar systems, such as Solar Thermal (ST). However, since solar radiation values remain the same for all solar systems, the results of simulations could also be utilized for other solar systems with some modifications. This study does not also take into account all the financial implications of PV systems such as Payback Time and does not include calculations regarding the feasibility of the system, which creates a gap for future research in this field of study. Another limitation of the research is its focus exclusively on commercial buildings of a certain category that largely comprise business districts in Dhaka. An analysis of buildings of other categories should require major adjustments and will deliver different results. For ease of calculations, the experiments featured buildings as simplified geometric elements within various urban settings and ignored minor building features and details. Details of PV systems such as tilt angles and spacing are not also taken into account. Besides, the calculation of energy consumption would be more accurate with further study on building dynamics and configurations. This inaccuracy can also be attributed to a lack of detailed previous research on the energy consumption patterns of business districts in Dhaka.

The average efficiency of PV panels is expected to reach about 20% by 2025 (Brito, et al., 2017), meaning a 30% increase in the overall solar potential, i.e. electricity produced from PV systems. In order to keep the option for natural ventilation by means of providing operable windows, photovoltaic glass has not been considered for facade glazing in this study, but if considered, it would mean about a 16.67% increase in the facade solar potential, assuming that photovoltaic glass systems are half as efficient. This study does not consider PV glass due to a few other aspects: shading devices should affect their effectiveness, and exposing them to insolation could increase building heat gain. Moreover, although not considered in this study, applying tilt angles could increase roof solar potential by up to 12% (Obaidullah & Sarkar, 2004) and facade solar potential by up to 20% (Brito, et al., 2017). The research will need a few modifications to accommodate these cases, but it should provide the means and tools to find out which urban settings perform better in terms of efficient harvesting of solar energy.

1.6 Summary

The amount of energy that can be produced annually using building surfaces for solar harvesting is termed as that building's solar potential. Optimizing some features of a group of buildings in the district morphology, the "urban block" being one such distinguishable group, should lead to increased energy production from integrated solar systems such as PV (Lobaccaro, et al., 2012). However, some challenges arise when it comes to implementing solar systems in the urban context; for instance, due to overshadowing by surrounding buildings or other objects, unfavorable surface orientation, and limited surface area (roof and facade) per floor area, the harvesting of direct solar energy can be massively reduced. In this research, a parametric study is carried out, based on commercial urban blocks of varying densities in Dhaka in order to investigate the effect of the urban design parameters on the solar potential in terms of local building regulations. The results of this analysis will help develop strategies for urban planners and policymakers when designing new urban districts.

1.7 Structure of the Thesis

The thesis is developed using a linear-analytic model. Figure 1.2 shows the organization of the chapters and the structure of the thesis.

1.8 Key Findings

With the gradual development of the research, the incorporation of research findings at each stage made the objectives, methods, and limitations of the research more defined, refined, and detailed. Findings have been listed in Section 6.2. Appendix A presents a summary of the key findings of the research in relation to the objectives, methodologies, and concerned chapters.

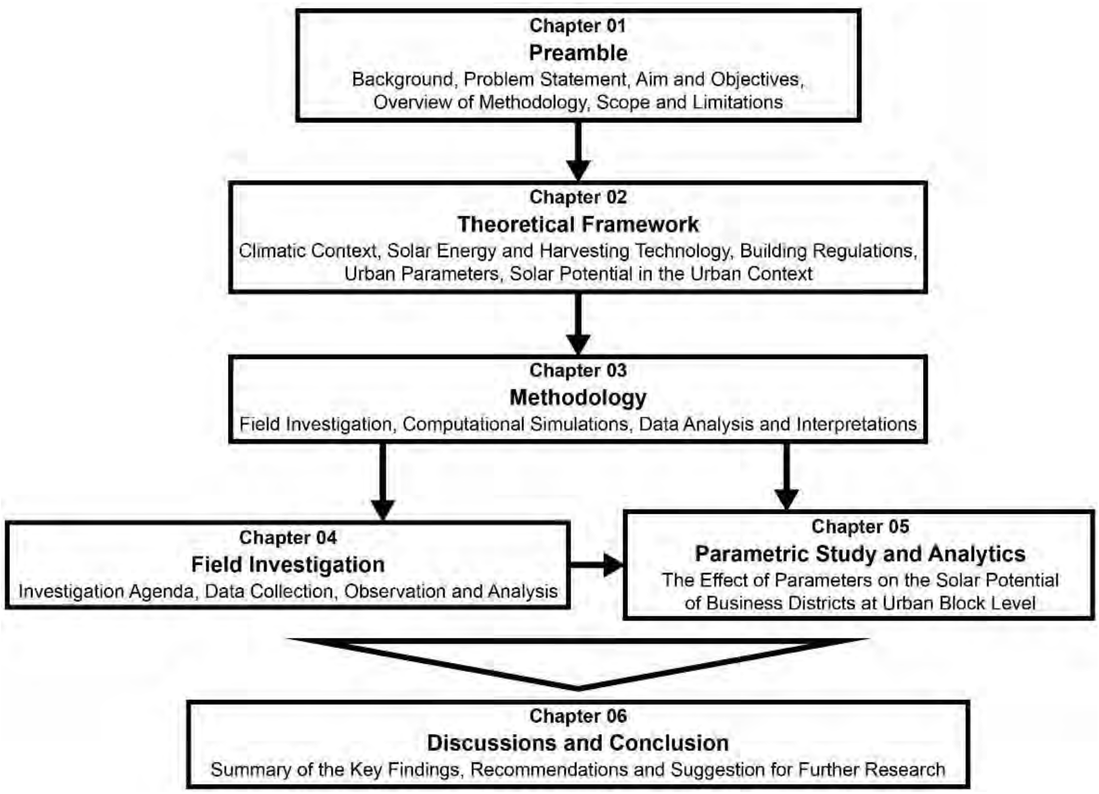

Figure 1.2: Organisation of the chapters and structure of the thesis.

References

Arboit, M., Diblasi, A., Fernandez Llano, J. & de Rosa, C., 2008. Assessing the solar potential of low-density urban environments in Andean cities with desert climates: The case of the city of Mendoza, in Argentina. *Renewable Energy,* 33(2008), p. 1733–1748.

Brito, M. et al., 2017. The importance of facades for the solar PV potential of a Mediterranean city using LiDAR data. *Renewable Energy,* 111(2017), pp. 85-94.

GOB, 2008. *Bangladesh Gazette,* Dhaka: Government of Bangladesh.

GOB, 2008. *Renewable Energy Policy of Bangladesh,* Dhaka: Power Division, Ministry of Power, Energy and Mineral Resources, Government of the People's Republic of Bangladesh.

IEA, 2019. *World Energy Outlook 2019.* [Online] Available at: https://www.iea.org/reports/world-energy-outlook-2019 [Accessed 22 April 2020].

Jelle, B. P. & Breivik, C., 2012. State-of-the-art building integrated photovoltaics. *Energy Procedia,* 20(2012), pp. 68-77.

Kanters, J. & Horvat, M., 2012. Solar Energy as a Design Parameter in Urban Planning. *Energy Procedia,* pp. 1143-1152.

Kanters, J. & Wall, M., 2014. The impact of urban design decisions on net zero energy solar buildings in Sweden. *Urban, Planning and Transport Research: An Open Access Journal,* 2(1), pp. 312-332.

Kanters, J. & Wall, M., 2015. A planning process map for solar buildings in urban environments. *Renewable and Sustainable Energy Reviews,* p. 173–185.

Lobaccaro, G., Fiorito, F., Masera, G. & Poli, T., 2012. District geometry simulation: a study for the optimization of solar façades in urban canopy layers. *Energy Procedia,* 30(2012), p. 1163 – 1172.

Lobaccaro, G., Frontini, F., Masera, G. & Poli, T., 2012. SolarPW: A new solar design tool to exploit solar potential in existing urban areas. *Energy Procedia,* 30(2012), p. 1173 – 1183.

Obaidullah, M. & Sarkar, M., 2004. Performance and Life Cycle Cost Analysis of a Stand Alone PV Lighting System. *Journal of Energy & Environment,* 3(1), pp. 25-32.

Peng, C., Huang, Y. & Wu, Z., 2011. Building-integrated photovoltaics (BIPV) in architectural design in China. *Energy and Buildings,* pp. 3592-3598.

Sarralde, J. J., Quinn, D. J., Wiesmann, D. & Koen, S., 2015. Solar energy and urban morphology: Scenarios for increasing the renewable energy potential of neighbourhoods in London. *Renewable Energy,* 73(2015), pp. 10-17.

Todorov, M., 2015. *Implementation of Solar Energy in Urban Planning,* Malmo: Lund University.

UN, 2018. *World Urbanization Prospects 2018.* [Online] Available at: https://population.un.org/wup/ [Accessed 22 April 2020].

Zhang, J. et al., 2019. Impact of urban block typology on building solar potential and energy use efficiency in tropical high-density city. *Applied Energy,* pp. 513-533.

CHAPTER 2: THEORETICAL FRAMEWORK

2.1 Introduction

Since the contemporary world widely recognizes energy implications of the built environment as a key issue for sustainable urban development (Arboit, et al., 2008), the urban context, in the future, will not only consume energy but will also partially meet its huge energy demands (Kanters & Wall, 2015). With solar energy proven as a valid strategy for producing on-site renewable energy (Kanters & Wall, 2015), buildings can successfully reduce their impact on the environment and reduce dependence on imported energy by adopting solar energy (Kanters & Wall, 2015). As highlighted earlier, the majority of the world's current population live and work in cities, where up to 80% of all available energy is consumed and over half of the greenhouse gas emissions are produced. Therefore, making cities energy-efficient has been recognized to be crucial to the de-carbonization of the economy (Lobaccaro, et al., 2012). A new set of urban design strategies are required to guide the design of new buildings in cities with particular attention to volume, shape, layout, and orientation of each building and its relationship with the urban context and thus, more efficient utilization of solar energy can be integrated into their envelopes (Lobaccaro, et al., 2012).

Intending to understand this particular dynamic and its regional implication, this chapter builds up the theoretical knowledge that is important for the development of this research. The concepts of solar energy and urban parameters affecting solar potential are introduced and discussed in detail. Concerned parameters are also understood in reference to building regulations. Moreover, previous research on the solar potential in the urban context, as well as electricity use and production in buildings are analyzed and discussed.

2.2 Related Terminology

Solar potential, shortened from solar energy harvesting potential, is an expression of the annual cumulative solar radiation receivable (Zhang, et al., 2019). It is defined as the amount of electricity that can be generated per year using building surfaces, such as facades and roofs, covered with photovoltaic (PV) systems. It is also termed PV potential or solar PV potential.

Photovoltaics is the branch of technology concerned with the production of electric current at the junction of two substances. Throughout this study, photovoltaics or PV has been used to refer to its popular meaning i.e. devices having a photovoltaic junction. Building Integrated Photovoltaics (BIPV) are defined as photovoltaic cells integrated into the building envelope as part of the building structure.

Urban Design looks into the creation of three-dimensional city features including buildings and interfaces, public space, infrastructure, transport, landscapes, and community facilities. On the other hand, the planning of city structures such as policies, zones, neighborhoods, infrastructure, standards, and building codes is generally termed as Urban Planning. Planning facilitates the presence, absence, and state of open spaces and building infrastructure, which are significant elements of urban design. In this research, the term 'urban design' is used considering this relationship acknowledging that planning provisions, such as building codes are important generators of its strategies.

A business district is understood in comparison with the "Central Business District (CBD)" or "Financial District" of a city. Dhaka has a number of financial cores, with the more robust ones located at MCA (Motijheel Commercial Area) and Kawran Bazar. Others include zones at Gulshan and Uttara, which are smaller but growing. The main component of these city areas is corporate office buildings, which are often highrises. Such areas, with comparatively higher density than other parts of the city, have been considered as business districts in this study.

Urban Block level refers to the selection of "urban block" as the basic unit of analysis in the final phase of this study. An urban block is the basic component of the urban fabric and is defined as the smallest area in urban planning that is surrounded by external streets. The urban block is usually subdivided into smaller land plots and is primarily composed of buildings of similar typology in terms of their form, function, and spatial relationship between each other. In this study, buildings are interpreted as simplified geometric entities that mainly comprise orthogonal surface planes potentially suitable for PV deployment. All other details of the study area including building elements such as fenestration details and shading devices, and street elements such as street furniture, trees, signage, poles, and posts are not taken into account. Building materials, service infrastructure, and other physical entities are also excluded from consideration for the sake of avoiding complications in simulation and analysis.

Insolation refers to the level of exposure a building has to the sun's rays. It can be measured by the amount of solar radiation reaching the building's surfaces. **Overshadowing** is the phenomenon by which the insolation of a building is reduced because of obstructions or casting of shadows by its surroundings.

2.3 Climatic Context of Bangladesh

This section investigates the climatic scenario for the study, which helps the understanding of how weather variables vary during different months of the year, and how these variations affect the insolation of urban surfaces and energy consumption in buildings.

2.3.1 General Overview of the Climate of Bangladesh

Bangladesh, lying between 20°34′ N to 26°33′ N and 88°01′E to 92°41′E and straddling the Tropic of Cancer, has a tropical monsoon climate with wide seasonal variations in rainfall, high temperatures, and high humidity. Flood plains, with minor climatic differences by region, dominate Bangladesh's landforms. The monsoon, characterized by overcast skies, varies in dates from year to year. Three seasons are generally recognized: a hot, muggy summer from March to June; a hot, humid, and rainy monsoon season from June to November; and a relatively cooler, drier winter from December to February. In general, the summer temperatures can rise up to 40.6°C or more, while it is characterized by a very high rate of evaporation, and erratic but occasional heavy rainfall (Agrawala, et al., 2003). The majority of maximum temperatures are recorded in April: the hottest month in most parts of the country, and January is the coolest month, although frost is extremely rare. The sun reaches its maximum inclination towards the south in January. The average temperature in winter is 7.2 to 12.8˚C to a maximum of 23.9 to 31.1˚C in most parts of Bangladesh (Agrawala, et al., 2003).

2.3.2 The Microclimate of Dhaka City

The climate of Dhaka is subtropical. It has a distinct rainy season, which occurs from May to September, and monsoons peak from June to August when flooding can be severe (NOAA, 2020). Approximately 80% of the annual average rainfall of 1,854 millimetres (73.0 in) occurs during the rainy season (Weatherbase, 2008). The Tropic of Cancer (23° 26′ N) runs through the districts to the immediate south of Dhaka (23° 46' N at the city-centre). At about 12.30 pm on the summer solstice (June 21), the sun shines almost directly overhead and casts no shadow of any erect object. Increasing air and water pollution caused by traffic congestion and indiscriminate disposal of municipal wastes are seriously affecting public health and the quality of life in the city. Moreover, water bodies and wetlands around Dhaka are facing destruction as these are being filled up to construct multi-storied buildings and the development of physical infrastructure. Pollution and the consequent erosion of natural habitats constantly result in increased temperatures and dust-laden cityscapes. Figures 2.1-3 show charts of temperatures, rainfall, and daylight availability – the key climatic features of Dhaka related to solar irradiation – implying that prolonged rainfall, characterized by overcast skies, may variably affect solar irradiation in the months of solar abundance.

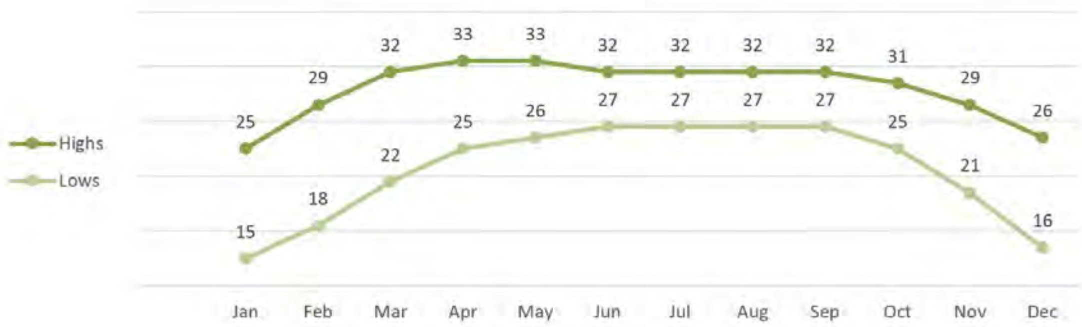

Figure 2.1: Temperatures (°C) in Dhaka by month (NOAA, 2020).

Figure 2.2: Rainfall in Dhaka by month (NOAA, 2020).

Figure 2.3: Daylight availability in Dhaka by month (NOAA, 2020).

2.4 Solar Energy

The highest level of solar radiation that reaches the earth is 1000 W/m^2, down from an average of 1367 W/m^2, due to the absorption or scattering of molecules in the atmosphere (Beckman & Duffie, 1991). The solar radiation towards a horizontal plane can be classified into direct, diffuse, and ground-reflected radiations (Ahmed, 1994). Direct radiation is the radiation that is not intercepted by any obstructions such as clouds; diffuse radiation is the one that is blocked by clouds and objects and is then reflected; and ground reflected radiation is the radiation reflected from the ground plane (Beckman & Duffie, 1991). The latter two vary depending on the reflectance properties of the insolation surface. The fourth type, called circumsolar diffuse radiation, occurs when a surface is tilted, coming from the same direction as the direct beam (Beckman & Duffie, 1991), while being scattered by water vapor and aerosols in the atmosphere (see Figure 2.4). With this general dynamic considered, this section discusses the local solar context and technologies. The monthly average daily solar radiation, sun path diagram, and solar elevation diagram for Dhaka City are given in Figures 2.5-7.

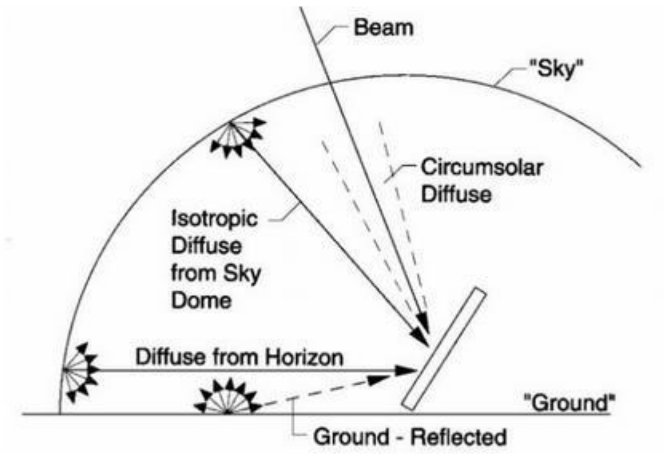

Figure 2.4: Solar radiation toward a tilted surface (Beckman & Duffie, 1991).

2.4.1 Solar Irradiation in Dhaka

Irradiation (or irradiance) is defined as the amount of solar radiation obtained per unit area by a given surface (W/m^2). The solar irradiation towards a horizontal or inclined surface varies by latitude. Situated between latitudes 23°42' and 23°54' N, Dhaka has an average of 5 kWh / m^2 solar radiation falling on its ground for over 300 days per annum. The maximum amount of radiation is available during March and April and the minimum in December and January. A 2012 study found the daily sunlight hours in Dhaka to be within 7 to 10 hours; which was further reduced by 54% (to 4.6 hours) to account for rainfall, cloud, and fog (Ghosh, et al., 2002). This abundance of solar energy has a large potential for producing energy that can be used by buildings in urban areas, ensuring sustainable development (Deb, et al., 2013). It can be utilized in the buildings passively for natural lighting, as well as actively for solar harvesting using PV panels and ST collectors.

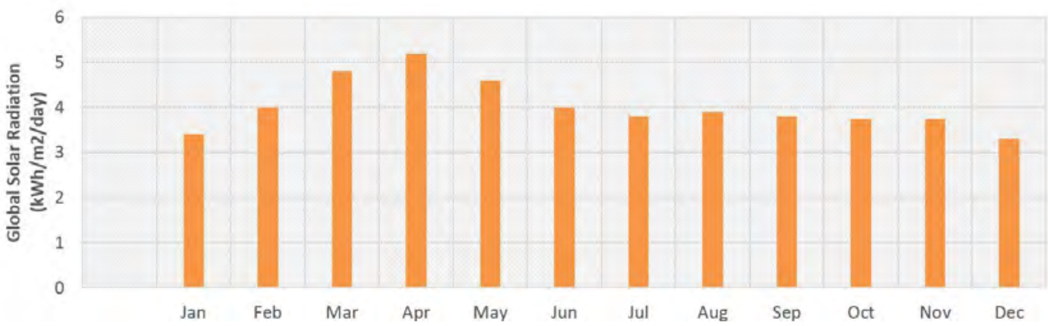

Figure 2.5: Monthly average daily solar radiation for Dhaka City (Obaidullah & Sarkar, 2004).

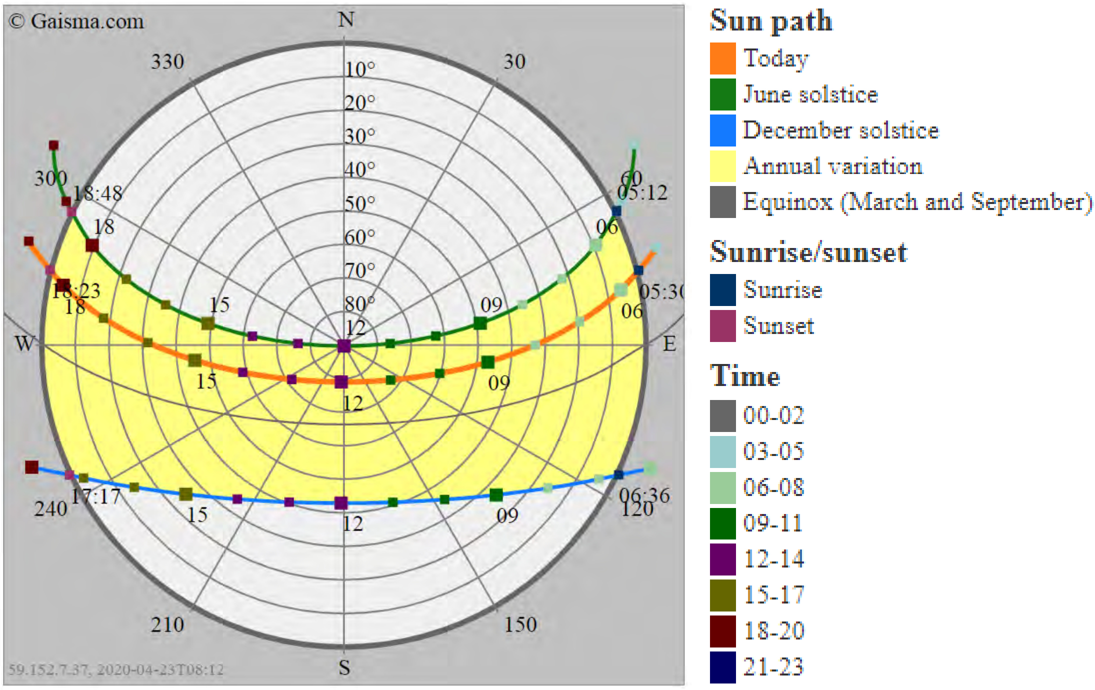

Figure 2.6: Sunpath diagram: Dhaka, accessed 23 Apr 2020 (GAISMA, 2020).

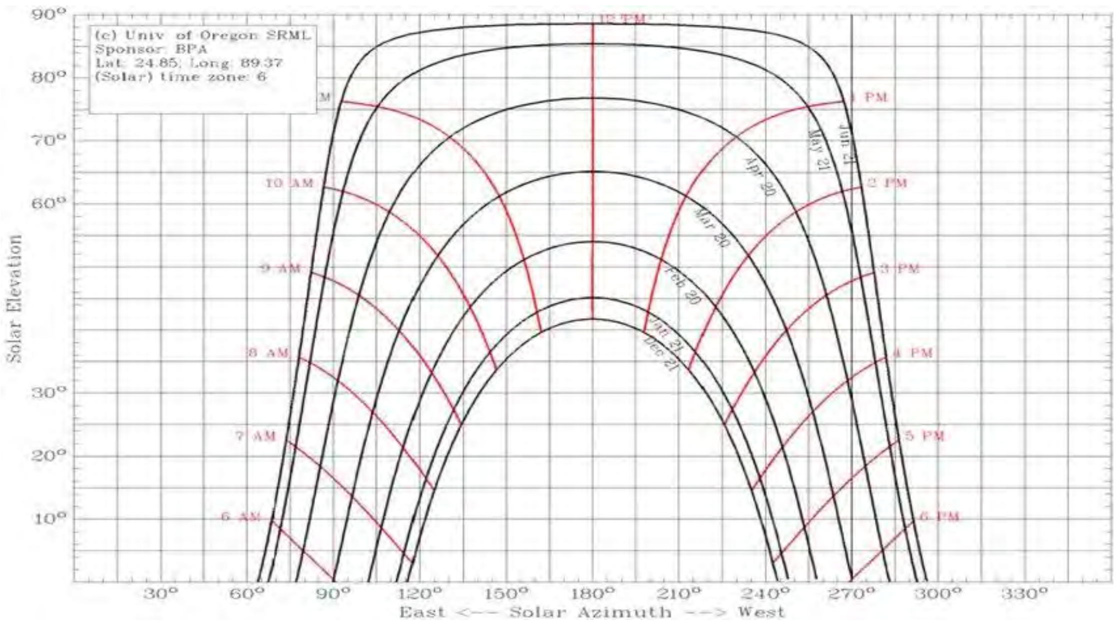

Figure 2.7: Solar elevation diagram for Dhaka showing a maximum approximate difference of 47 degrees between solar inclinations on summer solstice and winter solstice (Khan, et al., 2015).

2.4.2 Photovoltaic Technology

Light is directly converted into electricity by photovoltaic (PV) devices as opposed to other related technologies such as concentrated solar power (CSP) or solar thermal (ST), which are used for heating and cooling (IEA-PVPS, 2019). In an urban environment, PV systems are generally connected to the electricity grid. Interconnected and encapsulated PV cells, which form a photovoltaic module, are the key components of a grid-connected PV system, along with the mounting structure for the module, the inverter, the storage battery (often not required), and charge controller (IEA-PVPS, 2019). Crystalline silicon cells with an efficiency of 15-20% are the most widely used PV cells, and crystalline silicon technologies account for above 97% of global cell production and more than 94% in the countries under the International Energy Agency's Photovoltaic Power Systems Programme (IEA-PVPS, 2019). Various mounting structures have been developed for PV and BIPV (Building-integrated Photovoltaics) systems such as PV facades, sloped and flat roof mountings, integrated glass-glass modules (opaque or semi-transparent), and PV tiles. (IEA-PVPS, 2019). BIPV is elaborated in Section 2.4.3.

In the urban context, the efficiency of PV panels deployed on building envelopes can drop significantly due to overshadowing by surrounding buildings, building elements, vegetation, or other objects, and as a result, the electricity output may suffer (Todorov, 2015). Since the cells inside the module are connected in series, it may lead to current failure in the whole string if a single cell is shaded (Gomes, et al., 2014). Bypass diodes can redirect current flow in the alternate path to allow for the other cells to operate, and thus the effect of shading can be reduced (Gomes, et al., 2014).

Another issue that affects the output is that when deployed on a typical flat roof, the panels are shaded mutually. Heat gain in the panels due to high ambient temperatures and solar radiation, inverter losses, DC and AC cable losses, soiling, etc. can also have negative effects on the efficiency and output (Todorov, 2015). Research is being conducted to find the optimum spacing and tilt angles for PV panels in Bangladesh to account for all these losses. An estimation of tilt angles for maximizing the output is presented in Table 2.1. The application of optimum tilt on flat roofs could result in a 12% increase in the solar potential of an urban area (Obaidullah & Sarkar, 2004). PV technologies can be integrated into the building envelope in several ways as shown in Figures 2.8 and 2.9.

Table 2.1: Optimum tilt angles for PV panels in Dhaka (Adopted from Obaidullah & Sarkar, 2004).

One Tilt Angle for the Whole Year System	**Two Tilt Angles for Two Halves of a Year System**		**Four Tilt Angles for Four Quarters of a Year System**			
Optimum Tilt Angle in Degrees (January-December)	**Optimum Tilt Angle in Degrees (April-September)**	**Optimum Tilt Angle in Degrees (October-March)**	**Optimum Tilt Angle in Degrees (January to March)**	**Optimum Tilt Angle in Degrees (April to June)**	**Optimum Tilt Angle in Degrees (July to September)**	**Optimum Tilt Angle in Degrees (October to December)**
21.40°	8.70°	37.90°	35.30°	6.40°	11.00°	40.60°

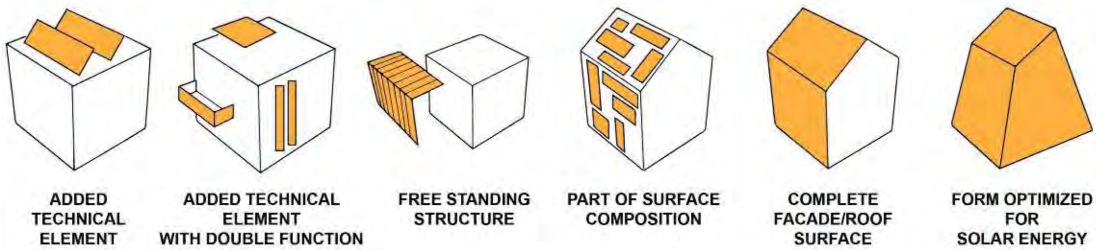

Figure 2.8: Conceptual Integration Typologies (Farkas, K., et al., 2013).

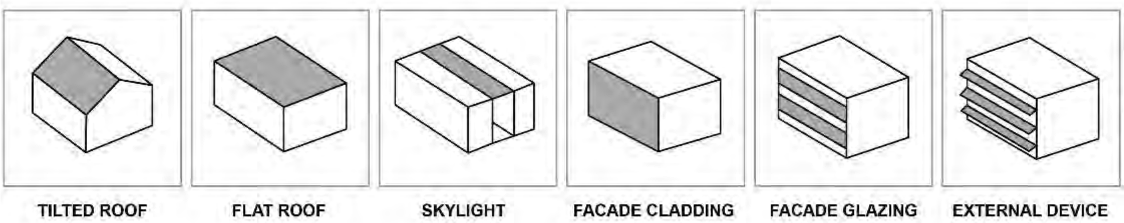

Figure 2.9: Conceptual Integration Typologies into the Building Envelope (Farkas, K., et al., 2013).

2.4.3 Building-integrated Photovoltaics (BIPV)

Solar power being the most abundant, inexhaustible and clean of all the available energy resources in cities such as Dhaka, minimization of energy waste and maximization of the potential use of solar energy requires physical, economical, and legally feasible alternatives and eventually, ‘‘on-site’’ PV generation needs to be considered for all potential urban surfaces including facades (Arboit, et al., 2008). The solar radiation received on vertical urban surfaces such as facades can be harnessed efficiently by means of Building Integrated Photovoltaics (BIPV) to produce energy, which, in turn, can be used to fulfill the energy needs of buildings (Peng, et al., 2011). BIPV offers an aesthetical, economical, and technical solution to engage solar cells in solar harvesting, producing electricity within the climatic envelopes of buildings (Jelle & Breivik, 2012). BIPV systems can provide shading for buildings which reduces solar heat gains through the building envelope and, consequently, reduces building cooling loads and cooling energy consumption (Jelle & Breivik, 2012). Moreover, it can replace conventional building materials whilst creating a harmonious architecture by blending into the design of the building (Peng, et al., 2011). Besides opaque BIPV modules, semitransparent modules are also available, which can be used for fenestration, allowing daylight to enter the interior spaces. Also, system efficiency and longevity can be improved by the air flow behind modules, which reduces their temperature (Brito, et al., 2017). On the other hand, the electricity generated from BIPV systems along with roof PV systems can help offset local electricity demands more efficiently, thus reducing the electricity to be purchased from the power grid and relieving peak electricity demand (Zhang, et al., 2019). The recent trend of rapidly decreasing costs of PV opens a massive window of opportunity for this kind of application.

In a building with 4 or more floors, the facade area is more than at least twice the roof area, and if PV could be deployed in the entire facade area of such a building, the amount of annual electricity produced would at least equal that of the roof assuming there is no shading from the surroundings. This ratio should increase further for taller buildings. However, it is important to note that the cost of producing this electricity would also be a few times higher. Therefore, the deployment of PV on less than optimum inclination or orientation has to be weighted by economic constraints (Brito, et al., 2017). Vertical PV facades should produce relatively more power in winter and less in summer, and more in the early and late hours of the day when the sun is lower in the sky (Brito, et al., 2017). Since a building typically has four, or at least two, exposed facades with opposite orientations, the different solar facades of a building should produce maximum power at different times of the day (Brito, et al., 2017).

For facades, however, the vertical assumption (instead of tilted sunscreens) represents an underestimation of the solar potential of about 20% (Brito, et al., 2017). Although fenestrations may be used as solar active areas, e.g. by using semi-transparent PV modules, the average conversion efficiency is about 50% of standard opaque PV modules (Brito, et al., 2017). Onyx Solar provides PV glass solutions commercially in Bangladesh, the corporate headquarters of Eastern Bank Ltd. in Gulshan, Dhaka being one of their customers of note, with the building featuring a slatted amorphous silicon photovoltaic glass.

The scarcity of lands in Bangladesh has been blamed as a huge obstacle towards materializing projects such as large-scale solar PV power plants that require vast stretches of land (Chowdhury, 2018). Besides, these ideas are also hindered by cyclones and monsoon flooding, resulting in higher operation and maintenance costs (Chowdhury, 2018). This emphasizes that building surfaces in urban areas such as Dhaka need to be utilized for PV generation, as the largest consumption of electricity is generally attributed to urban areas.

2.5 Building and Planning Regulations in Dhaka

Current legislation in many cities of the world is already directing towards such energy-efficient and energy-producing buildings, with the European directive for the energy performance of buildings a prominent example (Kanters & Wall, 2015). Urban design plays a significant role in maximizing the on-site production of electricity from solar energy (Zhang, et al., 2019). Distribution of volumes, street layout pattern, building/street orientation, street width, and relative building height are all potential Urban design parameters that affect insolation on building surfaces (Lobaccaro, et al., 2012).

Institutions such as the Rajdhani Unnayan Kartripakkha (RAJUK, The Dhaka Capital Development Authority) and Dhaka City Corporation (DCC) are key to urban planning and implementation in Dhaka (World Bank, 2008). To provide zoning for various urban activities, Dhaka Metropolitan Development Plan (DMDP) was prepared for the years 1995-2015 (World Bank, 2008). Since then, Dhaka's urban planning issues have been addressed at three geographic levels: subregional (Dhaka Structure Plan), urban (Urban Area Plan), and sub-urban (Detailed Area Plans - DAPs) (World Bank, 2008). The Dhaka Capital Development Authority (RAJUK) is the key agency responsible for the further development of the DMDP and the Detailed Area Plans (DAPs), which supersede the Urban Area Plans and are conceived as the third and lowest tier of the DMDP urban plans (World Bank, 2008).

The Dhaka Metropolitan Building Construction Rules (Imarat Nirman Bidhimala) proposed in 2008 (here referred to as INB2008) is solely responsible for the construction, development, conservation, and removal of buildings in any area of Dhaka Metropolitan City under RAJUK jurisdiction (GOB, 2008). It focuses on the policies on Floor Area Ratio (FAR) and mandatory open space such as Setback and MGC (Maximum Ground Coverage). By proposing guidelines for each building plot, it regulates urban density, porosity, and spacing of urban districts. Because it delineates policies as per building typology, the urban features of districts also differ by typology. For example, it proposes separate sets of rules for commercial and residential buildings, and so the features of a business district are expected to be different from that of a residential district in terms of urban parameters such as urban density.

2.6 Urban Design Parameters

2.6.1 Urban Density, FAR and Street Width

For urban sustainability, the urban design parameter that must be considered with vast importance is Urban Density. A higher density reduces transportation energy and optimizes the use of land; but on the contrary, it affects solar access and natural lighting, leading to an increase in the use of artificial lighting and reduced insolation for PV systems to utilize (O'Brien, et al., 2010). Therefore, it is important to consider density at the early design phase for creating a balance among solar access, daylight, and energy consumption (Todorov, 2015). A recognized way to represent urban density is the Floor Space Index (FSI), which is the total gross floor area (TFA; m^2) divided by the plot area (A_{plot}; m^2) exploited by the building (Todorov, 2015). Based on a study of urban planning in Malmö, Sweden, A_{plot} is calculated by adding together the land area assigned to the building, and the area that represents half of surrounding streets or a park, and if the adjacent street or park is larger than 30m, then a fixed distance of 15m is taken (Todorov, 2015). Thus, in an urban area without parks or assigned open space, A_{plot} is the total of all the building plot areas plus half the area of the streets, provided the streets have buildings on both sides. This is applicable for street widths below 30m. TFA for an urban area is considered as the summation of all total floor areas of all the buildings within the area of study.

$$FSI = TFA / A_{plot} \text{ (Building)} \tag{2.1}$$

$$FSI = \sum TFA \ / \ \sum A_{plot} \text{ (Urban Area)} \tag{2.2}$$

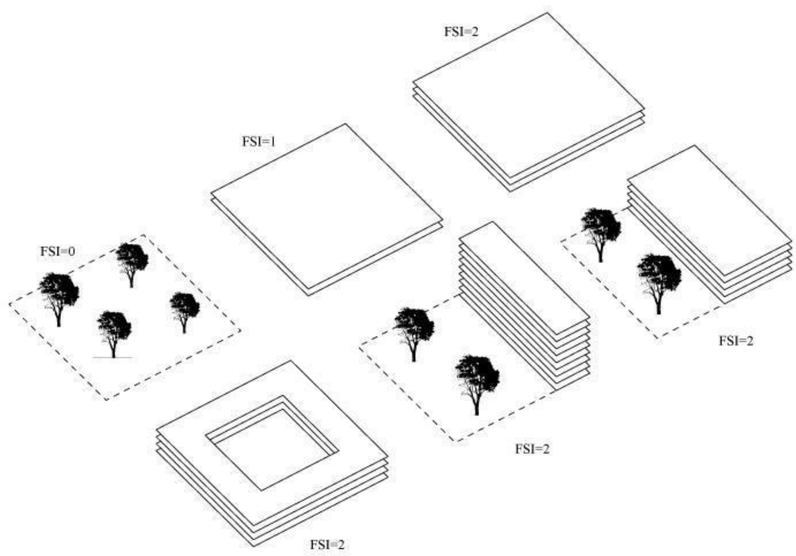

Figure 2.10: Principles of Floor Space Index (FSI), when FSI=FAR. (Kanters, et al., 2014).

Figure 2.5 shows that the expression of FSI can be different depending on the geometry of the building. For example, when FSI=0 the plot is empty. When the FSI=1, this means that the whole plot is built with a one-story building. If the FSI=2, this means that the whole plot is occupied by a two-story building or half of the plot by a four-story building and so on (Kanters, et al., 2014).

This research is limited to urban contexts with streets below the 30m street width limit. INB2008 recommends street widths and Floor Area Ratios (FAR) according to plot size (GOB, 2008). For an individual building, FAR is defined as the building's total gross floor area (TFA; m^2) divided by the building plot area (A_{bplot}; m^2) (GOB, 2008). It should be noted that when adjacent open spaces such as streets are not considered, FAR equals FSI. In this study, FAR is considered as a measure for the individual building, and FSI is considered as a measure for the study area representing the urban context. Street width is an important parameter since it impacts insolation and overshadowing in the urban context, considering streets as the open spaces between buildings. FSI accounts for both FAR and street width and represents urban density for various plot sizes as categorized in INB2008.

The limited space between buildings in the urban context is responsible for restricting one another's daylight and solar access. In Dhaka, the space between buildings is largely regulated by the Setback rules recommended in INB2008. Setback is defined as the measure of mandatory open space a building must consider between the building's plot boundary and its built surface. The mandatory open spaces are also regulated by GC or Ground Coverage, which is defined as the percentage ratio of the building's footprint to its plot area. INB2008 proposes Maximum Ground Coverage (MGC) for all buildings in Dhaka according to their respective plot sizes. Some studies have referred to Ground Coverage as "covering ratio" and outlined its importance in terms of solar access (Lobaccaro, et al., 2012). Thus, FAR, street width, setback, and GC are all responsible for the density of an urban context.

$$FAR = TFA / A_{bplot} \quad (2.3)$$

$$GC = (Building\ Footprint / A_{bplot}) \times 100\% \quad (2.4)$$

However, in case of an urban block, GC will take into account the footprints of all buildings in the block and the Effective Plot Area ($\sum A_{plot}$), which includes half the area of the surrounding streets:

$$GC = (All\ Buildings'\ Total\ Footprint / \sum A_{plot})\ x\ 100\% \quad (2.5)$$

2.6.2 Compactness Ratio

Compactness Ratio (Comp) of a building is a measure of the ratio of the total external envelope area (Env; m^2) to the total floor area (TFA; m^2) of the building (Todorov, 2015).

$$Comp = Env / TFA \quad \text{(Building)} \quad (2.6)$$

$$Comp = \sum Env / \sum TFA \quad \text{(Urban Area)} \quad (2.7)$$

Since the distribution of a volume has been found to be able to maximize insolation on building envelope (Lobaccaro, et al., 2012), the understanding of compactness ratio is important for evaluating energy performance as it expresses the total external envelope area in proportion to the total floor area of the building (Zhang, et al., 2019). Lower values of this ratio correspond to a more compact building, and this could mean lower heat gain by the envelope; in terms of solar potential, however, it is more likely to have a reversed effect considering energy performance, as the more compact a building is, the less envelope (Zhang, et al., 2019). The evaluation of energy performance could be more accurate with Compacity, which takes into account the volume of the building rather than its total floor area. However, since this research assumes that the floor height is the same for all floors of the building, Compacity is a function of Compactness Ratio and can be measured by dividing Compactness Ratio by the constant floor height – in which case their relationships with other factors should also be similar. This research, therefore, takes into account only one of the two – Compactness Ratio.

2.6.3 *Building Layout*

Building layout is a significant parameter that influences the solar potential of individual buildings as well as urban districts. The layout is the horizontal configuration of a building, which can vary according to design decisions. In this research, layouts were investigated in physical surveys of business districts. Layouts can heavily influence insolation, self-shading, and overshadowing.

Compagnon (2004) uses case studies to investigate the impact of urban form on PV electricity production. Using the validated Perez all-weather sky model for a fairly accurate simulation, he shows that solar potentials vary significantly across five different building layouts within the same urban context and under the same density (Compagnon, 2004). Moreover, he finds that solar availability in dense urban areas is significant, and can be increased significantly in even denser areas by planning provisions such as layouts (Compagnon, 2004).

2.7 Solar Potential in the Urban Context

Recent studies indicate that there is limited knowledge regarding how much energy demand can be met through on-site utilization of solar energy by the buildings in an urban context, and about the effect of urban design and planning decisions on the solar potential of buildings (Kanters & Wall, 2014; Zhang, et al., 2019). Self-shading and overshadowing by adjacent buildings in a high-density urban environment can dominate solar potential and daylight availability (Lobaccaro & Frontini, 2014), because buildings within an urban area that are surrounded by other buildings could see the contribution of solar energy decreased by 10-75% (Kanters & Horvat, 2012).

Nevertheless, solar energy is gradually becoming one of the key components urban planners have to take into account among other factors in the complex process of planning (Kanters & Horvat, 2012). They should be informed about the consequences of urban blocks' features on solar potential because taking solar energy into account when designing a new urban district can provide significant benefits in terms of the production of renewable energy (Kanters & Horvat, 2012). The urban context offers a complex environment, which presents many obstacles and opportunities for the utilization of solar energy. Certain methods and tools are necessary for the quantitative and visual evaluation of solar potential, which could assist the decision-making of authorities, planners, and other involved actors (Kanters & Wall, 2015).

Sarralde, Quinn, Wiesmann, and Steemers (2015) expanded the study of the impact of urban morphology on solar potential to city-scale for Greater London. They found that the combined effect of several urban form parameters led to 9% and 45% increase in receivable solar irradiance for roof and façade surfaces, respectively, such as average spacing between buildings, variation in building heights, average building perimeter, etc., although the potential conflict between the parameters might need prioritization for more concrete results (Sarralde, et al., 2015).

Lobaccaro, Frontini, Masera, and Poli (2012) have assessed a design tool in terms of its efficacy to optimize the shape of buildings in a designed urban scenario by maximizing solar access, finding significant effects of overshadowing and solar reflection from surrounding buildings. They have sketched out some new basic design principles suggesting the use of the tool to support the use of solar energy as one of the measures that can improve the energy efficiency of districts (Lobaccaro, et al., 2012). In another study published in the same year, Lobaccaro, Fiorito, Masera, and Poli (2012) highlight the importance of facades in terms of solar potential as well as energy production by conducting experiments on a reference building within a simple district composed of nine blocks. Under different Ground Coverage (GC) or "covering ratio" conditions, they found that the distribution of the volume, or in other words, a higher Compactness Ratio (Comp) successfully increases solar access on building envelopes (Lobaccaro, et al., 2012). A later study by Lobaccaro and Frontini (2014) attempts to analyze the efficacy of another design tool for optimizing building shape in a dense urban environment and comes up with an interesting finding. Although optimized buildings were found to have maximized their solar access, insolation and daylight availability for other buildings and public spaces in the surroundings were significantly compromised.

Kanters and Wall (2014) tested the solar potential metric for four building blocks typical for southern Sweden using the DIVA4RHINO platform, where they partly examined the effect of design decisions regarding building density, orientation, and roof type. The results showed that building density was the most influential parameter on solar potential (Kanters & Wall, 2014). In another study conducted on both existing and planned city blocks in Malmo and Lund using the same platform, Kanters, Wall, and Dubois (2014) found that density has a negative impact on both annual electricity coverage using PV systems and annual heating coverage using ST systems. Moreover, at higher densities, the differences among the solar potentials of differently oriented city blocks become less significant (Kanters, et al., 2014).

Brito, Freitas, Guimaraes, Catita, and Redweik (2017) highlights the importance of facades for the solar potential of two representative areas in the city of Lisbon measuring 500m x 500m each using LiDAR data, showing that the non-baseload electricity demand could be satisfied by cost-effective PV investments on roofs and facades considering contemporary market conditions for up to 10 months of the year (Brito, et al., 2017).

In a more recent study, Zhang, Xu, Shabunko, Tay, Sun, Lau, and Reindl (2019) investigates the solar potential and building energy-use efficiency of thirty generic urban blocks in six typology categories using an integrated workflow comprising a modeling platform (Rhinoceros + Grasshopper with Ladybug and Honeybee) and a simulation engine (Radiance + EnergyPlus) for calculating and visualizing several urban design parameters, performance indicators, and analysis – all requiring intensive scripting in Grasshopper. (Zhang, et al., 2019) Conducted in the context of Singapore, the study provides significant evidence that solar potential and energy-use efficiency significantly vary across various urban block typologies that feature different layouts (Zhang, et al., 2019).

Although the impact of urban design parameters on the solar performance of buildings has been addressed in previous studies from different perspectives, how these parameters influence solar potential in the context of high-density tropical cities has not been evaluated in detail. Moreover, it also remains to be seen how local urban design policies can accommodate solar potential as an important feature for energy-efficient districts.

2.8 Further Significance of Solar Potential

This section deals with two important issues. Firstly, considering that the produced energy is used to meet energy demand, it recognizes the role of energy consumption and its relationship with energy production. Secondly, local policies that make solar harvesting a feasible initiative are discussed.

2.8.1 Electricity Consumption and Production in Buildings

Policymakers and real-estate developers are interested in the ratio of how much electricity can be contributed annually by solar energy systems in reference to the consumed electricity, represented by the solar fraction (Kanters & Wall, 2014). Electricity is the dominant energy used in Bangladesh. In recent years, buildings have been a major target in Bangladesh for energy optimization that could be achieved by reducing the energy consumption in buildings, as well as by providing energy using the application of on-site renewable energy. Many buildings in Dhaka have adopted the strategy of harvesting solar energy by using PV systems in their roofs .

Business districts in Dhaka city, such as MCA (Motijheel Commercial Area), are gradually becoming high energy demand areas for accommodating elevated business and commerce activities. Buildings of these areas consume a significant amount of electricity to accommodate lighting facilities, mechanical means for ensuring thermal comfort, and operating electrical appliances for a large number of occupants. These buildings go nearly vacant except during the peak time of this demand, from 9 a.m. to 5 p.m., which is the peak working hours. A 2015 study found the average electricity demand in the buildings in MCA to be 2.3 kWh/sft/month, which is equivalent to 297 kWh/m^2/year (Debnath, et al., 2015).

A study on the electricity consumption characteristics of 10 air-conditioned office buildings in subtropical Hong Kong found the ranges of percentage consumption for the four major electricity end-users – namely heating, ventilation, and airconditioning (HVAC), lighting, electrical equipment, and lifts and escalators – to be 40.1–50.7%, 22.1–29%, 16.6–32.9% and 2.2–5.3%, respectively (Lam, et al., 2008). These figures are expected to be similar for Dhaka. However, both the degrees of energy consumption and production of energy through solar harvesting in buildings fluctuate during different months of the year due to the variation of weather variables, such as Temperature. Although energy consumption from lighting, electrical equipment, lifts, and escalators is expected to remain the same throughout the year, energy consumption from HVAC systems can be expected to vary considerably on a monthly basis. On the other hand, solar harvesting is highly subject to seasonal variation. South-facing facades are expected to enjoy a significantly greater degree of insolation during winter and lower during summer. The degree of insolation should drop entirely during monsoon due to overcast skies.

2.8.2 Government Energy Policy

Bangladesh adopted the Renewable Energy Policy in 2008, which acknowledges the use of photovoltaics for harnessing solar energy in urban areas and offers subsidies for installation, exemption of taxes, and tariffs for generated electricity (GOB, 2008). The Government of Bangladesh plays an active role in the promotion of solar energy through the Bangladesh Energy Regulatory Commission (BERC). Towards facilitating about 27% of the population that are still without access to electricity, the Government of Bangladesh has around 5 million solar-home systems (SHS) already developed at the beginning of 2018, each with a system size of around 50-60 W that can be utilized for lighting, TV connections and mobile phone charging. (IEA, 2020). Led by the Infrastructure Development Company Limited (IDCOL), the government is promoting incentive schemes to encourage entrepreneurs who wish to start PV actions under the Bangladesh zero-interest loan from the World Bank Group as well as support from a range of other donors (IEA-PVPS, 2019).

The country targets 3.2 GW of renewables by 2021, including 1.7 GW of PV with more than 325 MW operational at the beginning of 2019 (IEA-PVPS, 2019). Considering these steps taken by the Government, PV generation for buildings in high-density urban areas that feature large roofs and facades remains a lucrative opportunity for entrepreneurs in Bangladesh, with business districts such as Kawran Bazar and MCA as interesting options.

2.9 Summary

A comprehensive understanding of the climatic context of the study area was developed along with the local implications of insolation and solar energy. Later on, solar energy and the means of harnessing it were discussed in detail. Next, urban regulations were studied in terms of relevant urban parameters responsible for insolation and overshadowing in buildings. It was also important to reflect on previous studies on the solar potential of urban areas and previously used tools and methods along with relevant findings of these studies. Lastly, the dynamics of energy consumption and production in buildings were studied, while local and global initiatives to promote renewable energy production were found to be encouraging, which highlighted the significance of solar potential in the context of Dhaka. Key findings were:

- Weather variables vary significantly by month in Dhaka and are likely to impact monthly energy consumption and solar irradiation in buildings.
- FSI, compactness ratio, street width, setback, layout, and orientation (due to sun's inclination) are important parameters that impact insolation in urban blocks.
- Solar potential should be evaluated in terms of energy consumption.

Theoretical knowledge was later combined with the findings of Field Investigation, simulation, and analysis towards arriving at the conclusive findings of the research and their interpretations. However, this chapter is an important catalog of relevant information which can be used for any study involving the solar potential of urban areas in Dhaka.

References

Agrawala, S. et al., 2003. *Development and Climate Change in Bangladesh: Focus on Coastal Flooding and the Sundarbans,* Dhaka: Organisation for Economic Co-operation and Development.

Ahmed, Z. N., 1994. *Assessment of residential sites in Dhaka with respect to solar radiation gains (Unpublished Ph. D. Thesis),* Leicester: De Montfort University, UK.

Arboit, M., Diblasi, A., Fernandez Llano, J. & de Rosa, C., 2008. Assessing the solar potential of low-density urban environments in Andean cities with desert climates: The case of the city of Mendoza, in Argentina. *Renewable Energy,* 33(2008), p. 1733–1748.

Beckman, J. & Duffie, W., 1991. *Solar engineering of thermal processes.* 1st ed. New York: John Wiley & Sons, Inc.

Brito, M. et al., 2017. The importance of facades for the solar PV potential of a Mediterranean city using LiDAR data. *Renewable Energy,* 111(2017), pp. 85-94.

Chowdhury, S. A., 2018. *Indicative Tariff for Utility-Scale Solar IPP in Bangladesh,* Dhaka: Centre for Energy Research, United International University.

Compagnon, R., 2004. Solar and daylight availability in the urban fabric. *Energy and Buildings,* 36(2004), p. 321–328.

Deb, A., Bhuiyan, M. A. & Nasir, A., 2013. Prospects of Solar Energy in Bangladesh. *IOSR Journal of Electrical and Electronics Engineering (IOSR-JEEE),* 4(5), pp. 46-57.

Debnath, K. B., Hossain, M. T., Rezwan, S. M. & Iqbal, M. N., 2015. *Exploring the solar energy potential for multistoried commercial office buildings in a dense CBD area of a mega city.* Dhaka, ResearchGate.

Farkas, K., et al., 2013. *IEA SHC Task 41: Solar Energy Systems in Architecture - Integration Criteria and Guidelines,* Paris, France: M. C. M. Probst, C. Roecker (editors).

GAISMA, 2020. *GAISMA.* [Online] Available at: https://www.gaisma.com/en/location/dhaka.html [Accessed 23 April 2020].

Ghosh, H. et al., 2002. *Measurement and Estimation of Sunshine Duration for Bangladesh,* Dhaka: Renewable Energy Research Center, University of Dhaka, Bangladesh.

GOB, 2008. *Bangladesh Gazette,* Dhaka: Government of Bangladesh.

GOB, 2008. *Renewable Energy Policy of Bangladesh,* Dhaka: Power Division, Ministry of Power, Energy and Mineral Resources, Government of the People's Republic of Bangladesh.

Gomes, J., Diwan, L., Bernardo, R. & Karlsson, B., 2014. Minimizing the Impact of Shading at Oblique Solar Angles in a Fully Enclosed Asymmetric Concentrating PVT Collector. *Energy Procedia,* 57(2014), pp. 2176-2185.

IEA, 2020. *IEA - International Energy Agency.* [Online]

Available at: https://www.iea.org/data-and-statistics/charts/share-of-population-without-access-to-electricity-or-water-in-rural-areas-2017
[Accessed 27 April 2020].

IEA-PVPS, 2019. *Trends in Photovoltaic Applications 2019,* Stockholm, Sweden: IEA Photovoltaic Power Systems Programme.

Jelle, B. P. & Breivik, C., 2012. State-of-the-art building integrated photovoltaics. *Energy Procedia,* 20(2012), pp. 68-77.

Kanters, J. & Horvat, M., 2012. Solar Energy as a Design Parameter in Urban Planning. *Energy Procedia,* pp. 1143-1152.

Kanters, J. & Wall, M., 2014. The impact of urban design decisions on net zero energy solar buildings in Sweden. *Urban, Planning and Transport Research: An Open Access Journal,* 2(1), pp. 312-332.

Kanters, J. & Wall, M., 2015. A planning process map for solar buildings in urban environments. *Renewable and Sustainable Energy Reviews,* p. 173–185.

Kanters, J., Wall, M. & Dubois, M.-C., 2014. Typical values for active solar energy in urban planning. *Energy Procedia,* 48(2014), pp. 1607-1616.

Khan, A. H., Islam, A., Islam, M. & Rahman, M. S., 2015. *A systematic approach to find the optimum tilt angle for meeting the maximum energy demand of an isolated area.* Dhaka, Jahangirnagar University.

Lam, J. C., Wan, K. K. & Yang, L., 2008. Sensitivity analysis and energy conservation measures implications. *Energy Conversion and Management,* 49(2008), pp. 3170-3177.

Lobaccaro, G., Fiorito, F., Masera, G. & Poli, T., 2012. District geometry simulation: a study for the optimization of solar façades in urban canopy layers. *Energy Procedia,* 30(2012), p. 1163 – 1172.

Lobaccaro, G. & Frontini, F., 2014. Solar energy in urban environment: how urban densification affects existing buildings. *Energy Procedia,* 48(2014), pp. 1559-1569.

Lobaccaro, G., Frontini, F., Masera, G. & Poli, T., 2012. SolarPW: A new solar design tool to exploit solar potential in existing urban areas. *Energy Procedia,* 30(2012), p. 1173 – 1183.

NOAA, 2020. *National Centers for Environmental Information.* [Online] Available at: https://www.ncdc.noaa.gov/
[Accessed 24 April 2020].

Obaidullah, M. & Sarkar, M., 2004. Performance and Life Cycle Cost Analysis of a Stand Alone PV Lighting System. *Journal of Energy & Environment,* 3(1), pp. 25-32.

O'Brien, W. T., Kennedy, C. A., Athienitis, A. K. & Kesik, T. J., 2010. The relationship between net energy use and the urban density of solar buildings. *Environment and Planning B Planning and Design,* 37(6), pp. 1002-1021.

Peng, C., Huang, Y. & Wu, Z., 2011. Building-integrated photovoltaics (BIPV) in architectural design in China. *Energy and Buildings,* pp. 3592-3598.

Sarralde, J. J., Quinn, D. J., Wiesmann, D. & Koen, S., 2015. Solar energy and urban morphology: Scenarios for increasing the renewable energy potential of neighbourhoods in London. *Renewable Energy,* 73(2015), pp. 10-17.

Todorov, M., 2015. *Implementation of Solar Energy in Urban Planning,* Malmo: Lund University.

Weatherbase, 2008. *Weatherbase: Historical Weather for Dhaka, Bangladesh.* [Online] Available at: http://www.weatherbase.com/weather/weather.php3?s=032914&refer=/ [Accessed 24 April 2020].

World Bank, 2008. *Policies for Mainstreaming Strategic Environmental Assessment in the Urban Development of Greater Dhaka,* Dhaka: World Bank.

Zhang, J. et al., 2019. Impact of urban block typology on building solar potential and energy use efficiency in tropical high-density city. *Applied Energy,* pp. 513-533.

CHAPTER 3: METHODOLOGY

3.1 Introduction

This chapter firstly outlines an overview of the overall work process and identifies key steps. Next, it delineates the purpose and modes of Field Investigation that solidifies the grounds for further study. Afterward, it explains the tools and software used for performative evaluation by simulation along with the parameters and values that were used for the investigation of solar potential. The methods and tools for analyzing and interpreting output data are also discussed. All key procedures in this research, along with the methods and tools used in each step, are delineated in this chapter so that it is possible to relate and estimate how and why these methods and tools were used to ultimately fulfill the objectives of the research.

3.2 Overview

To fulfill the objectives of the study, conducting an elaborate theoretical framework was considered vital. It was followed by a combination of a rigorous Field Investigation, case studies, simulation, and analysis – all adopted within the framework of Experimental Research.

Theoretical Framework enabled the research process to be informed about how the spaces between buildings are regulated by existing building regulations in the urban context and how urban parameters behave in reference to those spaces and configurations. It is obvious that these parameters are responsible for the degree of insolation in urban surfaces, and tweaking these parameters could result in massive changes in insolation and overshadowing. The theoretical study also informed about how PV systems work and to what extent it is applicable for energy production by using on urban surfaces.

The patterns of energy usage in buildings, more specifically, in the commercial buildings in Dhaka, were investigated by means of an elaborate analysis and detailed understanding of field data. Moreover, Field Investigation enabled the research to understand the urban context affecting insolation as well as the degree of energy consumption of individual buildings. Obtained data helped to record and relate how the weather variables impact energy consumption and solar energy harvesting in buildings.

The simulation study is divided into three parts. The first part deals with individual buildings and assesses the urban context influencing the degree of possible electricity generation and how much energy demand can be met during each month of the year. The second part deals with selected areas of existing business districts in Kawran Bazar and MCA and assesses their solar potential in terms of urban parameters. These experimentations helped the understanding of solar potential at the individual building level as well as within the urban scenario in the business districts in Dhaka. The findings from Field Investigation and theoretical framework helped to gather the input settings and parameters for these experimentations, while the overall understanding at this point was utilized for the third and final part of the simulation study. In this part, projected district settings modeled according to existing building regulations were used to assess the solar potential at the urban block level. These settings were varied based on urban parameters in terms of building regulations in the business districts in Dhaka so that the effect of various parameters can be evaluated in reference to the comparative solar potential and energy demand of urban blocks.

Modeling, simulation, and analysis were performed using an integrated parametric interface consisting of Rhinoceros, Grasshopper, and Ladybug Tools, which are all validated and extensively used in previous studies. Numerical data were analyzed using statistical models such as regression analysis models. Analyses were needed vigorously to sort and interpret the findings and generate conclusions in terms of urban parameters' effect on solar potential and possibilities of providing urban design guidelines with a view to maximizing energy production.

The process adopted is mostly linear and was completed in a number of important steps as shown in Figure 3.1.

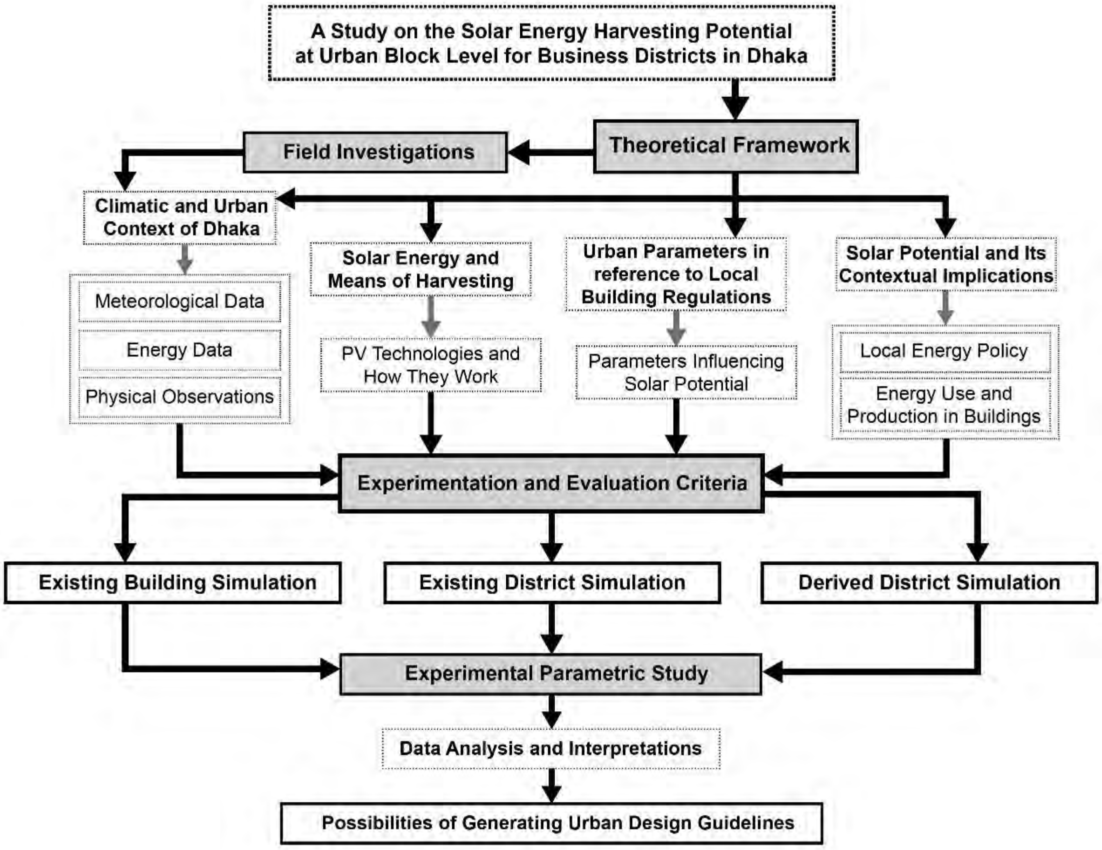

Figure 3.1: Overview of Methodology by a flow diagram of key steps.

3.3 Field Investigation

It was important to combine theoretical knowledge with in-situ findings to generate and verify the information needed for the final experimentations. An elaborate Field Investigation was carried out for the following purposes:

1. To procure physical, climatic, and energy data as required for intended study and analysis.
2. To understand how urban and weather variables impact energy consumption and the degree of insolation in the commercial buildings in Dhaka by looking for specific patterns in the obtained data.
3. To obtain necessary data for three-dimensional modeling used in the simulation study of existing buildings and districts.
4. To study the urban scenario and to investigate or verify the input parameters used in the simulation study.
5. To investigate the nature of insolation on building surfaces in reality.

To serve the above-mentioned purposes the investigation was carried out in several steps. The steps of Field Investigation are described as follows:

Collection of Climatic and Energy Data: Required climatic data was procured from the Bangladesh Meteorological Department (BMD). To obtain energy consumption data, monthly electricity consumption figures were extracted from Dhaka Power Distribution Company Ltd's (DPDC) monthly reports. Later, these sets of data were processed and analyzed using statistical methods.

Physical Survey: Physical Survey was carried out in Kawran Bazar and Motijheel Commercial Area (MCA), which are the two most prominent business districts in Dhaka. Seven buildings in MCA were studied separately for energy analysis, and for this purpose, their surrounding urban areas were also mapped three-dimensionally. Three-dimensional mapping was performed using a combination of site sketches, notes, site photographs, Google Maps, Google Earth, Google Streetview, and Open Street Map (OSM). Internet data were scrutinized and verified during physical surveys. Site mapping culminated in 3D models within the commercial 3D modeling software Rhinoceros. The same mapping technique was also applied for creating 3D models of two selected 500m x 500m areas, one each in Kawran Bazar and MCA. Finally, physical observations facilitated the evaluation of existing urban conditions in terms of the existing building code as per INB2008. Figure 3.2 lists the building-level physical observations that were conducted in situ.

Activity and Scenario Study: Street-level physical circumstances and public activities were investigated to find out to what degree they affect insolation and potential solar energy harvesting. Moreover, building elevations were also documented to study how they can efficiently harvest solar energy, the scope of available technologies to be used, and the measures that need to be taken to harvest solar energy as per existing circumstances. This study also explored what architectural features of the existing commercial buildings are the most convenient for solar energy harvesting.

Thermal Image Study: Thermal images were taken to understand insolation patterns in various parts of buildings. Figure 3.2 shows four building-level observations performed with the help of thermal images: insolation pattern at different times of the day, the height from ground up to which deploying PV is ineffective, percentage of glazed areas on the facade, and overshadowing due to setback conditions. Thermal imaging is being extensively used worldwide for examining solar installations and documenting key external features of buildings such as emissivity (Drone Media Imaging, 2021; Insectapedia, 2021).

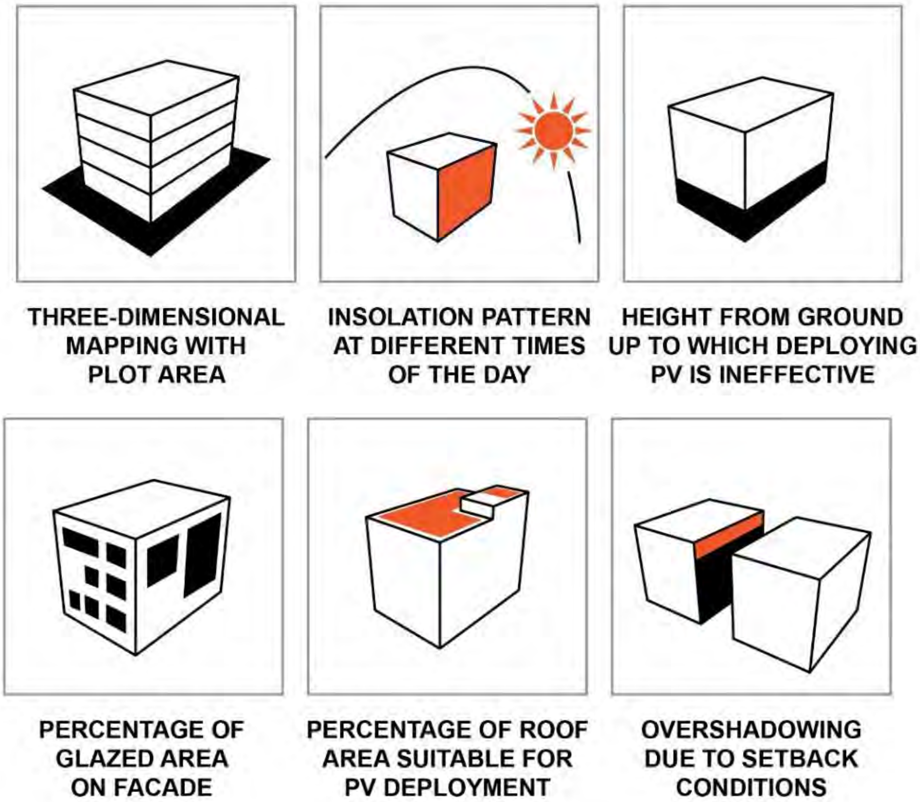

Figure 3.2: Criteria for Building-level Physical Observations.

Other Issues: To understand the collected data, the data providers were consulted. For example, to understand DPDC's monthly reports, a department of DPDC called Network Operations and Customer Services (NOCS) was contacted and was asked to provide information. The number of workdays in a month was obtained by studying the Government Holiday Calendars. Physical surveys also enabled the investigation of the usage of HVAC systems in buildings: the kinds of HVAC that are being used, the tentative percentage of the usage of air conditioning systems as opposed to the usage of natural ventilation, the rate of energy consumption for air conditioning compared to other electric appliances in buildings and the resultant effect on facades. Another important task was to examine the suitability and availability of roofs and facades for the installation of PV panels by looking into the current conditions, uses, and features of these urban surfaces.

An overview of the Field Investigation process is presented in Figure 3.2.

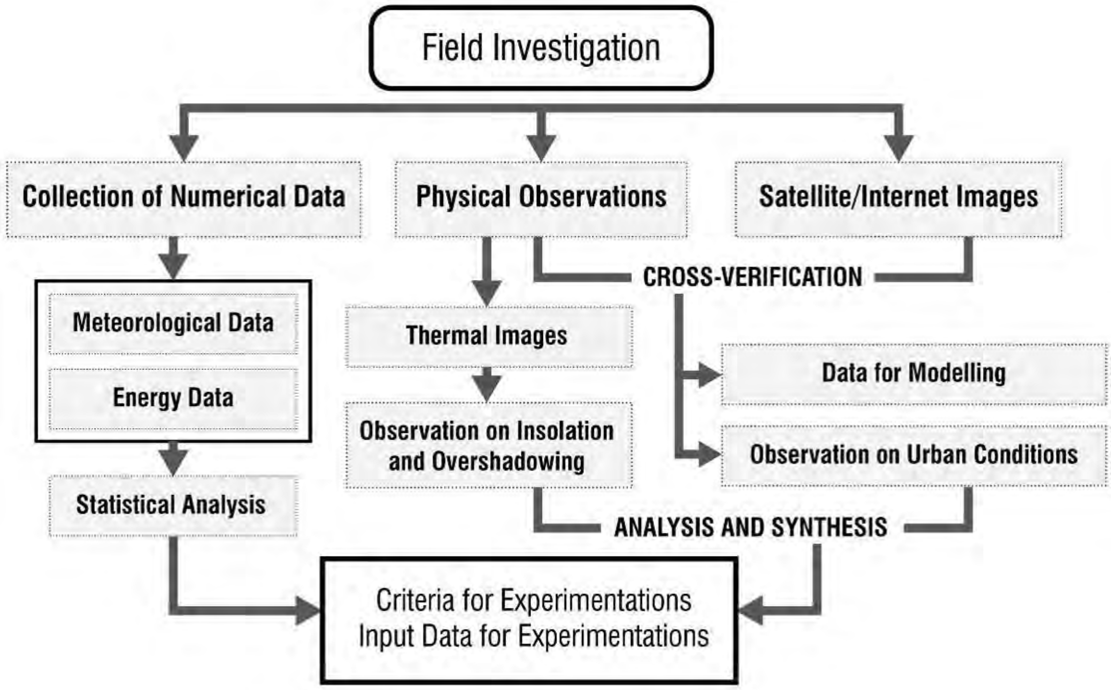

Figure 3.3: Flow Diagram representing an overview of Field Investigation.

3.4 Computational Simulations

Computational Simulations were mainly used for the parametric study and analysis of the solar potential of existing buildings, existing districts, and projected districts – the experimentations that helped to develop an understanding of solar potential at urban block level in reference to urban and weather variables. The continuous task from modeling and solar radiation analysis to the estimation of the amount of electricity that can be generated using PV systems was performed using an integrated parametric interface combining Rhinoceros, Grasshopper, and Ladybug Tools. Figure 3.3 illustrates how the integrated interface provided the means for analysis and interpretations – which was later utilized to generate conclusions and guidelines.

3.4.1 Modeling process in Rhinoceros and Grasshopper

Rhinoceros is a validated commercial 3D computer graphics and computer-aided design (CAD) application software that can be used for various parametric simulation and analysis purposes using an array of different plugins and their extensions, many of which are validated as well. Grasshopper is a parametric modeling plugin within the Rhinoceros 3D application. It uses a validated visual programming language plus environment and supports other validated plugin packages itself, which can be used for a wide range of modeling, simulation, and analysis purposes.

For modeling existing scenarios (existing individual buildings with their surrounding urban context and existing district areas), the buildings from the site were represented as simplified polysurfaces in Rhinoceros utilizing the data obtained from Field Investigation. The model comprised only representative building surfaces and the ground surface, while other elements such as street furniture, wirings, trees, and animated objects were excluded.

Projected scenarios were modeled according to a generic format of commercial block in the Detailed Land Use Map of Purbachal proposed by RAJUK (Rajdhani Unnoyon Korttripokkho – Dhaka's Development Authority) as of 2020. This generic urban block comprises 6 building plots of the same configuration arranged in a rectangular format, separated from each other by property boundaries, and separated from the surroundings by streets on all sides. For modeling, the districts' 2D layouts were drawn using Rhinoceros and Grasshopper. From this 2D drawing, representative building polysurfaces were modeled using the same Grasshopper script, which would later be used for assigning and varying parameters, providing input data, and conducting simulation and further calculation. Built-in components of Grasshopper were used to assign size, height, and relative position to the buildings, which were subject to necessary changes for simulation. Moreover, to identify and separate surfaces that are required for solar radiation analysis, the script also relied on internal algorithms. The Ladybug algorithm used for solar radiation analysis requires the reference geometry and the surrounding geometry as separate input data, which is why a host of built-in components were used to separately group these two kinds of geometry. Projected district models have a single urban block as the reference geometry, surrounded by streets on four sides with similar buildings on the other side of the street, which were assigned as the context geometry along with the ground plane. Buildings on the side of the street opposite the urban block have profiles as same as the ones inside the block. The square layout was maintained for all buildings for all simulation instances so that comparisons are valid based on the considered parameters.

3.4.2 Algorithms used in Grasshopper

Grasshopper offers a visual programming language that is very convenient for conducting a large array of parametric modeling, simulation, and evaluation, visualized within the interface of Rhinoceros. Besides built-in algorithms, an extension called Ladybug was used for solar radiation analysis. Ladybug, an open-source plugin for environmental analysis started by Mustapha Sadeghipour Roudsari, is built on top of several validated simulation engines: Radiance, EnergyPlus/ OpenStudio, Therm/ Window, and OpenFOAM (Roudsari, 2013). Ladybug offers components for solar radiation analysis that takes in time period, weather data, reference geometry, surrounding geometry, and an orientation cue as inputs to provide a visual color graph along with radiation amounts based on a fixed assigned grid size for the surfaces that make up the reference geometry. Built-in algorithms in Grasshopper also help data processing for the analysis of simulation results.

An algorithm is a series of calculations or steps by which computation is performed. It offers a solution to a mathematical or statistical conundrum through a finite sequence of instructions that can be implemented by computer software. A grasshopper component holds an algorithm and is able to take in certain input information in order to provide the intended output information that is processed by that algorithm. A script is generally a sequence of components, in which the output data of one component is considered as the input data of another component towards generating the final output. Grasshopper scripts used for the simulation study are presented in Figures D1, D2, and D3 in Appendix D.

3.4.3 Input Data

A list of input parameters that were used for computational simulations with the respective values considered in this research is presented in Table 3.1.

Table 3.1: Input parameters for simulations and their values.

Input Parameter	Considered Value
Building Type[1]	F1 (Office)
Floor Height for all instances	3.6 m
Weather Data	Dhaka, Bangladesh (EPW file)
Grid Size	1.0 m^2
Distance From Base	1.0 m
Test Duration	Annual (January 1 – December 31) or Monthly (According to the duration of each Calendar Month)
Facade offset from Ground Level	3.6 m
Annual Cumulative Irradiance Threshold	650 kWh/m^2
Qualified Surfaces Irradiance	>650 kWh/m^2/year (for both Monthly and Yearly simulations)
Solar Panels	PV cells
Facade Glazing Area	25 %
Roof Offset (non-usable area)	25%
PV Efficiency	15%
Additional System Losses (for PV)	10%
Further Losses (Due to grid inaccuracy)	10%
Semitransparent BIPV for Glazing	Not considered (If considered, it'd be half as efficient)

[1] Building Type refers to the building types given in INB2008 according to which building features, such as FAR and MGC, were recommended. F1 is for commercial buildings and 'Office' is a subcategory.

The electricity generated from PV panels as deployed across building surfaces depends on the minimum Annual Cumulative Irradiance Threshold level to be adopted below which the deployment of PV panels may not be economical (Zhang, et al., 2019). Therefore, surfaces with annual solar radiation above 650 kWh/m^2/year were identified and selected. This value was chosen because they can produce around 100 kWh/m^2/year with a 15% efficient PV cell. Furthermore, the area for deploying PV was considered to be 75% of the facade area, leaving 25% for fenestration. The tentative value of 25% for fenestration was adopted from the findings of the Field Investigation. This figure is realistic since too much fenestration can lead to glare and overheating. The same ratio was chosen for the roof since a certain portion of the roof surface is needed for the maintenance of the building and building service installations.

Dhaka city's weather data in the EPW file format was used as input for the solar radiation analyses which includes the statistically representative data of some of the key meteorological parameters for a particular location, such as hourly global horizontal radiation, dry bulb temperature, relative humidity, wind speed, etc. EPW file format is validated and has been used in a significant number of previous research works for similar analyses.

3.4.4 Output Data

Two kinds of output data were used in analyses. The first one is the visual output, and the second one is the numerical output. Solar Radiation Analysis in Ladybug generates a color graph that shows a particular color on each surface grid, from red through yellow and light blue to blue, graduated according to the intensity of insolation during the assigned period of time. The same Grasshopper script also generates the overall radiation amount for all input surfaces as output, along with the radiation amount for each grid as a list. These output data were collected and processed for further analysis and interpretations. The overall Grasshopper script ultimately generates the annual or monthly PV potential of the concerned reference building or reference district as the amount of generated electricity in MWh, kWh, or GWh – whichever is necessary. For this purpose, the numerical output from Solar Radiation

Analysis was utilized within the script. The output data was taken as input data for several built-in Grasshopper components for filtering and processing the data as per the concerned equations and criteria.

3.4.5 Simulation Process

The customized workflow adopted for the simulation study, as shown in Figure 3.3, integrates the functions of parametric 3D modeling of buildings or the urban block, performance simulation, calculation of variables and performance indicators, data processing, and visualization of results in a seamless way.

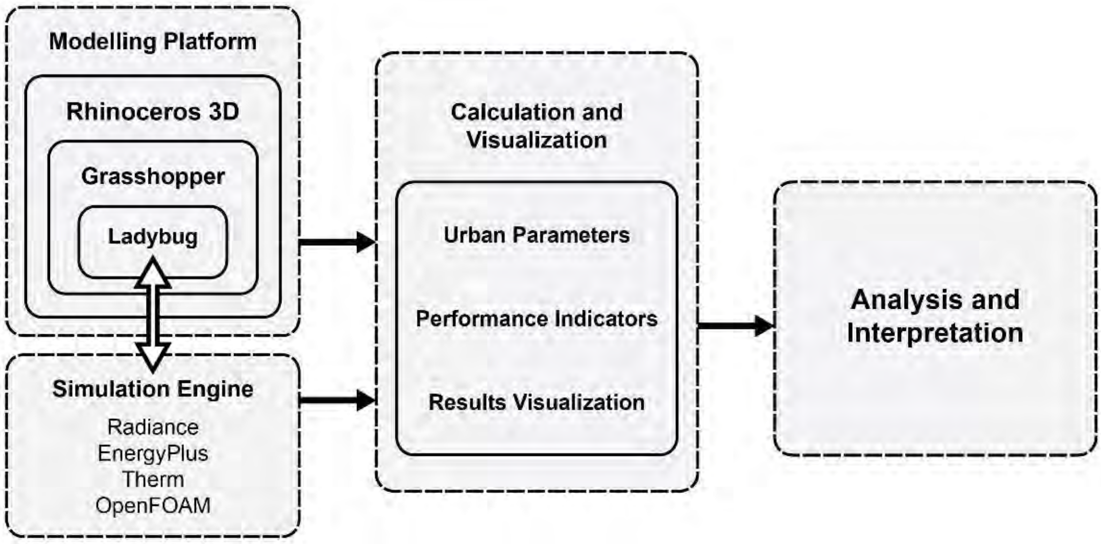

Figure 3.4: Flow Diagram showing the workflow of the simulation study.

For each existing district simulation or existing building simulation, a separate Rhinoceros model was considered, but the Grasshopper script for simulation featured minor changes according to the unique characteristics of the model, or to address specific simulation requirements. For projected district models, however, some adjustments were needed in the script to address the particular requirements of the experiment. According to the specific requirements of a particular experiment, the simulation was performed one by one with customized models by tweaking certain parameters of the initial setup, such as orientation, building height, ground coverage, and relative position within the integrated parametric interface. For each unique instance, a result was recorded.

3.5 Data Analysis

Data analysis was used for developing an understanding of field data as well as simulation data. In this section, data analysis methods will be discussed in two categories:

1. Analysis of field data
2. Analysis of simulation data

3.5.1 Analysis of Field data

For analyzing field data, data cleaning, filtering and sorting were necessary to avoid data anomalies and to examine the nature of relationships. Analysis of field data primarily assumes that the Annual Energy Consumption Rate (E_r) is the same for all commercial buildings in MCA[2], and considers the total energy consumption from March 2019 to February 2020 as the Annual Total Energy Consumption (E_y) for each building entity. For convenient handling of data, a metric called Monthly Energy Consumption Indicator (E_{mo}) was used. For each building entity of which energy consumption data were available, the Monthly Energy Consumption Indicator (E_{mo}) for a calendar month (e.g. September 2018, July 2019, etc.) was calculated by using equation 3.1.

$$E_{mo} = \frac{E_m}{E_y} = \frac{Units\ Sold\ by\ DPDC\ in\ a\ Particular\ Calendar\ Month}{Units\ Sold\ by\ DPDC\ throughout\ One\ Year} \tag{3.1}$$

E_{mo} was used for canceling out the floor area factor (see equation 3.2), due to which the energy consumption figures are different for different buildings – provided that the Annual Energy Consumption Rate (E_r) is the same for all commercial buildings in MCA. Thus it was used as a universal coefficient that can be considered for any commercial building in MCA.

$$\begin{gathered} E_m = E_{mr} \times TFA \\ E_y = E_r \times TFA \\ E_{mo} = \frac{E_m}{E_y} = \frac{E_{mr} \times TFA}{E_r \times TFA} = \frac{E_{mr}}{E_r} \\ E_{mr} = E_{mo} \times E_r \end{gathered} \tag{3.2}$$

[2] This is possible when energy consumption is strictly a function of TFA or Total Floor Area.

Hence, $$E_m = E_{mo} \times E_r \times TFA \quad (3.3)$$

Here,

TFA = Total Floor Area of a building/ group of buildings, m^2

E_{mr} = Energy Consumption Rate for a Particular Calendar Month, kWh/m^2

E_m = Energy Consumption in a Particular Calendar Month = Units Sold by DPDC in that Month, kWh

E_r = Annual energy consumption rate, kWh/m^2

E_y = Annual Total Energy Consumption = Units sold by DPDC throughout 12 consecutive months (in this case from Mar 2019 to Feb 2020), kWh

E_{mo} = Monthly Energy Consumption Indicator = Ratio of energy consumption in a particular calendar month to that of the entire year

E_{mo} was taken as the dependent variable (y), whereas several weather variables and other related factors were considered as independent variables (x_1, x_2, x_3, etc.) for the regression analyses that followed. Regression analysis was applied to determine to what extent a particular independent variable is related to the dependent variable. By determining these relationships, it is possible to develop a firm understanding of the causes of the monthly variation of energy consumption in commercial buildings as well as the factors responsible for the pattern of energy consumption throughout the course of the year. However, the median E_{mo} value was considered for regression analyses out of the E_{mo} values of a number of building entities. The analysis of field data is elaborated in Sections 4.3.4 and 4.3.5.

3.5.2 Analysis of Simulation Data

Three categories of simulation studies were necessary for the research to develop an understanding of solar potential at the urban block level and to reach conclusions that eventually generated final research findings. These categories are:

1. Simulation study of existing buildings,
2. Simulation study of existing districts, and
3. Simulation study of projected districts.

A different approach is needed for data analysis in each category. However, these approaches are mainly of two types:

1. Analysis of qualitative data, and
2. Analysis of quantitative data.

Qualitative data were analyzed using the inductive reasoning method supported by findings from Field Investigation. Quantitative data were analyzed using statistical methods such as linear regression analysis. Scikit-learn, an extensive and widely used machine learning library for the Python programming language (Pedregosa, et al., 2011), was used as a software tool for statistical analysis. Scikit-learn is free and offers fast and reliable options for statistical modeling. However, for convenient analysis, a number of metrics and equations were used. The most important metric used for the analysis of quantitative data generated from simulation are Annual Solar Performance Indicator (P.I.), Monthly Solar Performance Indicator (M.P.I.), and Monthly Solar Fraction (S_{mo}).

Solar Radiation Analysis in Ladybug generates Annual Cumulative Solar Radiation (ACSR) values in kWh, which were converted into the possible amount of electricity that can be generated annually from PV systems (E_{pv}) by utilizing Equation 3.4. However, for monthly simulations, a similar equation was used to obtain the amount of electricity that can be generated in a particular month (E_{mpv}) from Monthly Cumulative Solar Radiation (MCSR) values (see Equation 3.5). Similar equations and values have been used in other research works on solar potential including Brito et. al. (2017) and Kanters et. al. (2014).

$$E_{pv} = R_{surf} \times \eta_{pv} \times R_{syst} \times L_{surf} \times ACSR \\ = 0.091125 \times ACSR \tag{3.4}$$

$$E_{mpv} = R_{surf} \times \eta_{pv} \times R_{syst} \times L_{surf} \times MCSR \\ = 0.091125 \times MCSR \tag{3.5}$$

Here,

E_{pv} = Electricity Generated Annually from PV

E_{mpv} = Electricity Generated during a particular Month from PV

R_{surf} = Percentage of Surface Area Suitable for PV deployment (75%)

η_{pv} = Efficiency of PV systems (15%)

R_{syst} = A Multiplication Factor to account for System Losses of 10% (0.9)

L_{syst} = A Multiplication Factor to account for Losses due to Overestimation of Qualified Surfaces[3] (90%)

ACSR = Annual Cumulative Solar Radiation

MCSR = Monthly Cumulative Solar Radiation

To set the values for coefficients, Equation 3.5 uses the values assumed in Table 3.1, which lists all input data for simulation. To account for the relative energy demand that can be met throughout the year and during a particular month, two performance indicators were used considering that energy consumption is a function of the Total Floor Area (TFA) of any concerned building entity. These two indicators, namely Annual Solar Performance Indicator (P.I.) and Monthly Solar Performance Indicator (M.P.I.) were calculated using Equations 3.6 and 3.7. A similar metric was used by Zhang et. al. (2019) for their solar potential studies.

$$P.I. = \frac{E_{pv}}{TFA} \tag{3.6}$$

$$M.P.I. = \frac{E_{mpv}}{TFA} \tag{3.7}$$

The Monthly Solar Fraction (S_{mo}) of a building for a particular month (e.g. January, February, etc.) was calculated using Equation 3.8. This metric was used to analyze how monthly figures of energy demand that can be met varied across the year.

$$S_{mo} = \frac{S_m}{\sum S_m} = \frac{E_{mpv}/E_m}{\sum(E_{mpv}/E_m)} \tag{3.8}$$

In this equation,

S_{mo} = Monthly Solar Fraction

---

[3] The grid size of 1.0 m^2 is the avaerage grid size for analysis of all reference surfaces in simulation, but not necessarily the average grid size of qualified surfaces which were separated out. Experiments showed that the count of grids is generally 8-10 percent more for qualified surfaces than the count of grids that would originally account for the qualified surface area. Hence, a 10 percent loss "due to overestimation" has been taken into account.

S_m = Percentage of Energy Demand that can be met in a Particular Calendar Month, E_{mpv} = Electricity Generated during a Particular Calendar Month from PV, E_m = Energy Consumption in a Particular Calendar Month, and Summation (∑) refers to the addition of all monthly values throughout the entire year for a particular building.

Additionally, azimuth angles were categorized into 12 distinct 15° angle directions as shown in Figure 3.5 for identifying building orientations and facade orientations in the study of existing buildings and districts. Facades were categorized according to the directions of their outward surface normals falling within specific azimuth angle categories.

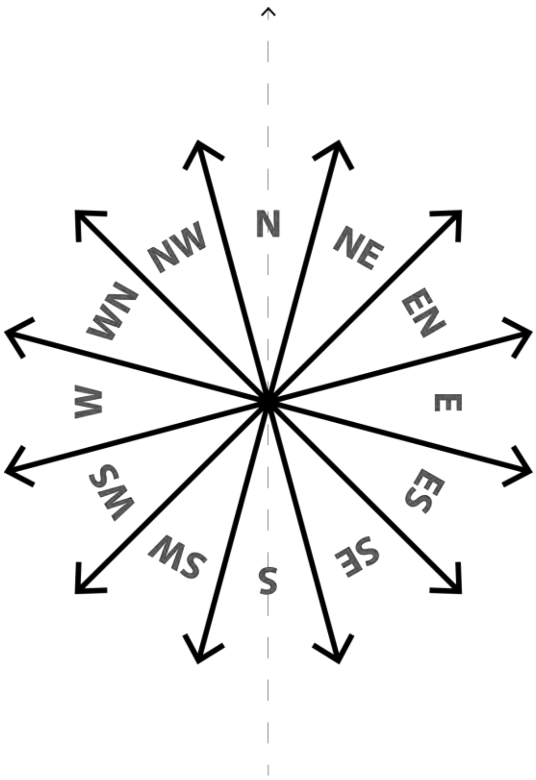

Figure 3.5: Distribution of azimuth angles into 15°-angle discrete categories.

3.5.3 Urban Block Parameters

The experimentation on projected districts considers an urban block with identical buildings resulting from identical layouts (square), identical individual ground coverages leading to identical individual heights. To assess the impact of building regulations on solar potential, variations in P.I. were observed in terms of various urban block parameters that:

1. Have direct relationships with local building regulations
2. Are assumed to be directly influencing surface insolation.

The locations of the building surfaces within the urban block are governed by three urban block parameters: Side-to-side Distance, Back-to-back Distance, and Street-to-surface Distance. These parameters are directly related to the Side Setback, Back Setback, and Front Setback guidelines in INB2008 respectively. However, these distances are impacted by the urban block's ground coverage (GC), which is directly related to GC guidelines for the individual building in INB2008 since the effective plot area of the urban block is kept fixed throughout the experimentation[4]. Additionally, the building height should heavily govern insolation and overshadowing and so Number of Stories has been included in analysis as an urban block parameter. The orientation of the urban block has also been taken into account because the relative position of the sun in reference to the direction of building surfaces could cause solar potential to vary significantly.

Besides, density and envelope area are key issues to consider in Urban Design and therefore two urban block parameters, the impact of which could be of interest to important players in the urban design process, were also taken into account: Urban Density (FSI) and Compactness Ratio[5]. It is primarily assumed that the combined effect of these parameters is responsible for the variation in solar potential per unit floor area (P.I.). Urban Density (FSI) is directly related to FAR regulations in INB2008 since the effective plot area is fixed, and is regulated by building height and GC. Compactness Ratio of the considered urban block is the same as that of any component building and is also regulated by building height and GC. Figure 3.6 shows which urban block parameters were considered and their connections to local building regulations.[6]

---

[4] See Section 2.6.1 for how GC for the urban block is calculated.

[5] Section 2.6 elaborates on why these two parameters are important to consider.

[6] Urban block parameters were used in analysis instead of individual building parameters for several reasons. The first issue is street width. For varying street widths, the implication of urban parameters FSI, GC and Street-to-surface Distance are different from related building parameters such as FAR, GC and Front Setback. Another reason is that there could be same values of urban block parameters for different values of building parameters for the constituent buildings.

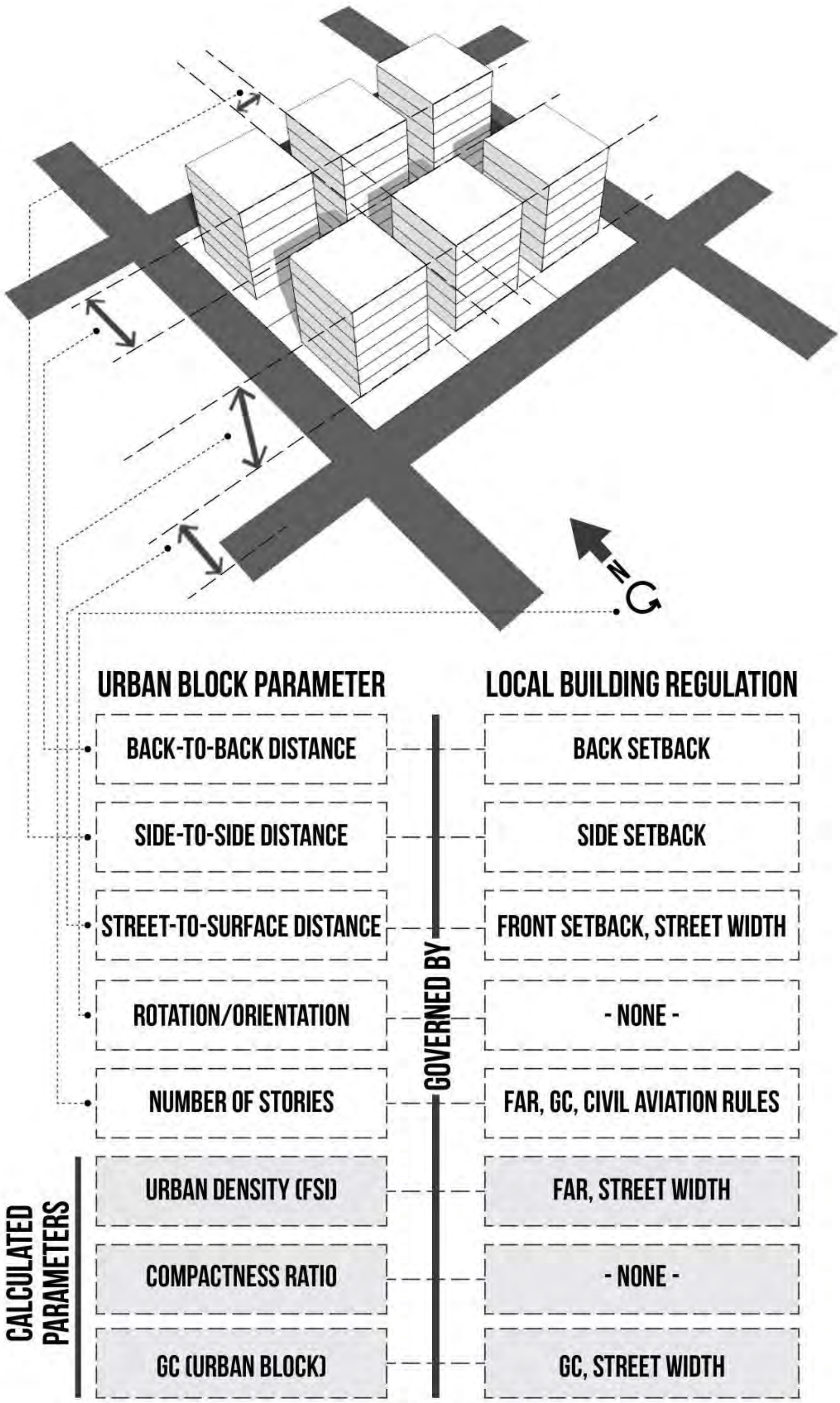

Figure 3.6: Urban block parameters used in this study with references to related building regulation strategies.

3.6 Validity of used values and tools

Rhinoceros, Grasshopper, and Ladybug were also used to build an integrated parametric interface for simulation, calculation, and visualization by Zhang, et al. in their 2019 study of the solar potential of various urban block typologies (Zhang, et al., 2019). However, software package Rhinoceros+Grasshopper is validated and has been used extensively in numerous research works (Giani, et al., 2013; Amado & Poggi, 2014; Kanters, et al., 2014; Zhang, et al., 2019). Ladybug was built on top of several simulation engines as shown in Figure 3.3, which are also validated (Roudsari, 2013). The Annual Cumulative Irradiance Threshold of 650 kWh/m^2, 15% efficiency of PV cells, 10% system losses, and a grid size of 1.0 m^2 have also been used as justified values in a number of research works (Zhang, et al., 2019; Kanters, et al., 2014). EPW weather file has also been extensively used for similar research works, and the research outcomes are also widely accepted (Zhang, et al., 2019; Todorov, 2015). Statistical models used in this study are also well-established as data analysis methods. Comparisons are based on performance metrics and imagined variables which are all mathematical functions of the output from the validated set of tools used in the simulation study. Parameters carry their usual meaning and units have their usual values.

3.7 Summary

Theoretical Framework, supported by an extensive Field Investigation, strengthens the foundation of the overall research work. The Simulation Study, which was used for experimentation and evaluation, was conducted in three individual categories, each developing useful insights toward conclusions. Assumption of several metrics and customized equations were considered necessary for data analysis, while statistical methods helped generate inferences regarding correlations among variables. Finally, discussions have enabled researchers to explore possibilities of developing urban design guidelines for the business district in Dhaka. The validity of tools, methods, and interpretations was also confirmed by referring them to previous works.

References

Amado, M. & Poggi, F., 2014. Solar urban planning: a parametric approach. *Energy Procedia,* 48(2014), pp. 1539-1548.

Drone Media Imaging, 2021. *Solar Panels and Drone Thermal Imaging.* [Online] Available at: https://www.dronemediaimaging.co.uk/solar-panels-and-drone-thermal-imaging/
[Accessed 3 July 2021].

Giani, M. et al., 2013. *A Design Approach for the Solar Optimization of Built Volumes.* Lausanne, s.n.

Insectapedia, 2021. *Thermography 101: Thermal Imaging in Buildings.* [Online] Available at: https://inspectapedia.com/home_inspection/Thermography_Info.php
[Accessed 3 July 2021].

Kanters, J., Wall, M. & Dubois, M.-C., 2014. Development of a Façade Assessment and Design Tool for Solar Energy (FASSADES). *Buildings,* 4(2014), pp. 43-59.

Kanters, J., Wall, M. & Dubois, M.-C., 2014. Typical values for active solar energy in urban planning. *Energy Procedia,* 48(2014), pp. 1607-1616.

Pedregosa, F. et al., 2011. Scikit-learn: Machine Learning in Python. *Journal of Machine Learning Research,* 12(2011), pp. 2825-2830.

Roudsari, M. S., 2013. *Ladybug: A Parametric Environmental Plugin for Grasshopper to Help Designers Create an Environmentally Conscious Design.* Chambery, France, ResearchGate.

Todorov, M., 2015. *Implementation of Solar Energy in Urban Planning,* Malmo: Lund University.

Zhang, J. et al., 2019. Impact of urban block typology on building solar potential and energy use efficiency in tropical high-density city. *Applied Energy,* pp. 513-533.

CHAPTER 4: FIELD INVESTIGATION

4.1 Introduction

Field Investigation was the primary mode of data collection for case studies, simulation, and analysis - the basic framework for the overall research work. Field Investigation involved physical and online surveys of Kawran Bazar and MCA (Motijheel Commercial Area), while the majority of the work was conducted in MCA, the most recognizable and prominent business district in Dhaka. Besides an elaborate site mapping which was completed with the help of observations from physical surveys and satellite data available on various internet sources, Climatic data and Energy data were also collected from concerned organizations such as Dhaka Power Distribution Company Ltd. (DPDC) and Bangladesh Meteorological Department (BMD). This chapter mainly deals with data collected from Field Investigation, their interpretations, and analysis, along with derivations from the data that helped the research process and generated understandings, resources, criteria, and parameters for final experimentations. Although there are explanations of all the forms of field works conducted, this chapter will mainly focus on the processing, analysis, and interpretation of numerical data.

4.2 Field Investigation Agenda

Field Investigation was carried out according to the agenda described in Section 3.3.

4.3 Physical Survey

4.3.1 Key Observations

This section discusses the building-level physical observations in MCA. Seven buildings, namely SBB, JBB, BCIC, SKB, KRB, AGB, and NCC, and their surrounding urban conditions were mainly observed. These buildings are listed in Table 4.2, and elaborations of acronyms used have been given in Table E1 in Appendix E. Their location map is provided in Figure 4.8.

Street-level observation:

Figure 4.1 shows street-level images and thermal images showing shaded areas at ground-floor level. The top pair show street activities including retails and casual parking in the street adjacent to AGB, the middle pair show the entrance to BCIC and the bottom pair show the street-level physical condition of JBB – all demonstrating reasons due to which PV deployment at ground-floor facade should be problematic or ineffective.

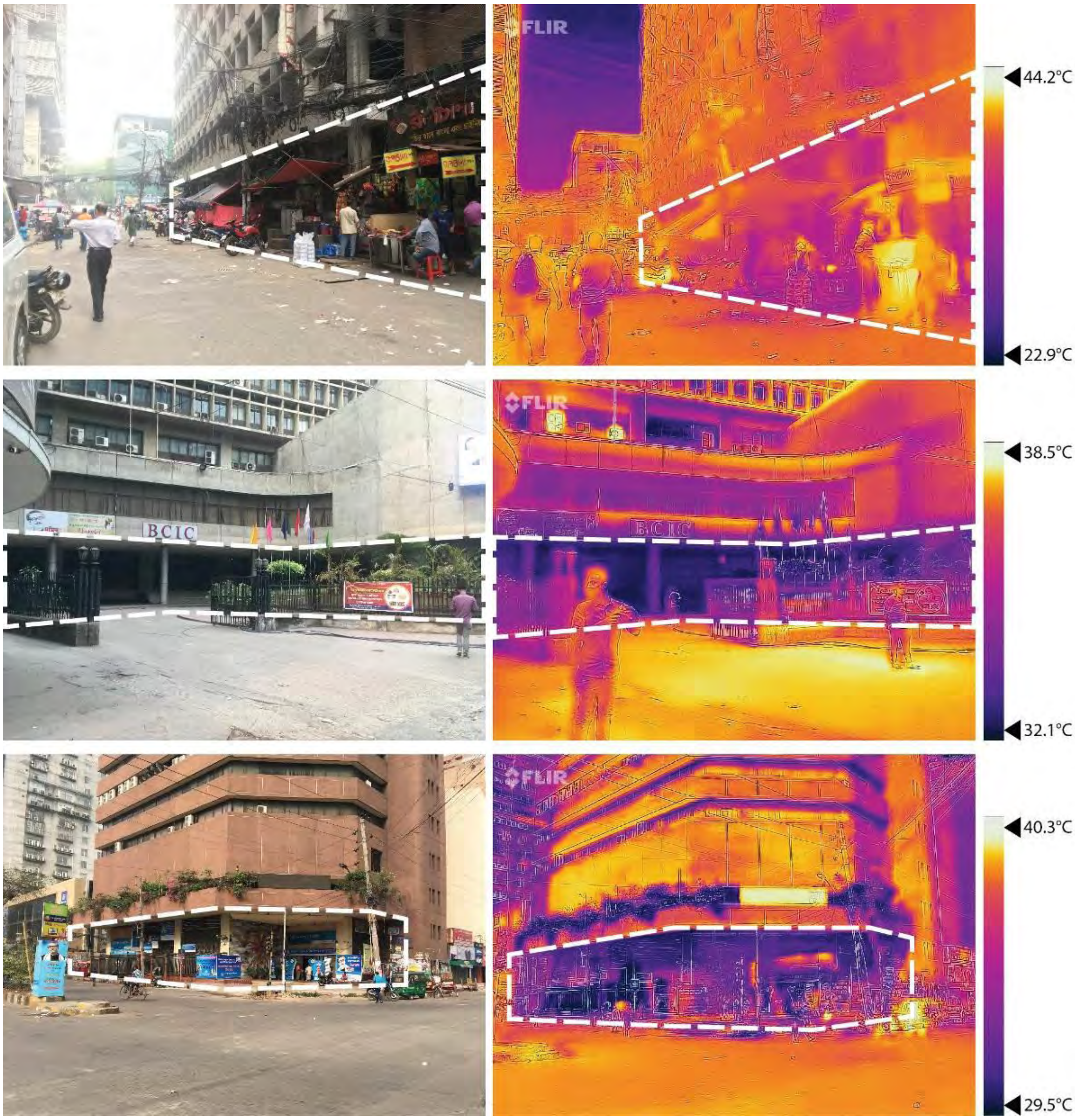

Figure 4.1: Street-view images and thermal images of MCA showing shaded areas at ground-floor level.

Facade feature observation: The south facade of BCIC with many split A/C discharge units is shown in Figure 4.2. The thermal image shows that the glazing is cooler than other parts of the facade. BCIC's facade condition suggests that buildings with central A/C systems should be more suitable for PV deployment in their facades. The thermal image of the south facade of the centrally airconditioned NCC (see Figure 4.3) shows that horizontal shading devices are hotter than vertical surfaces (alucobond) because of greater insolation, suggesting that shading devices could be an interesting option for PV modeling. Photos were taken at 6:13 PM on 3 April 2021.

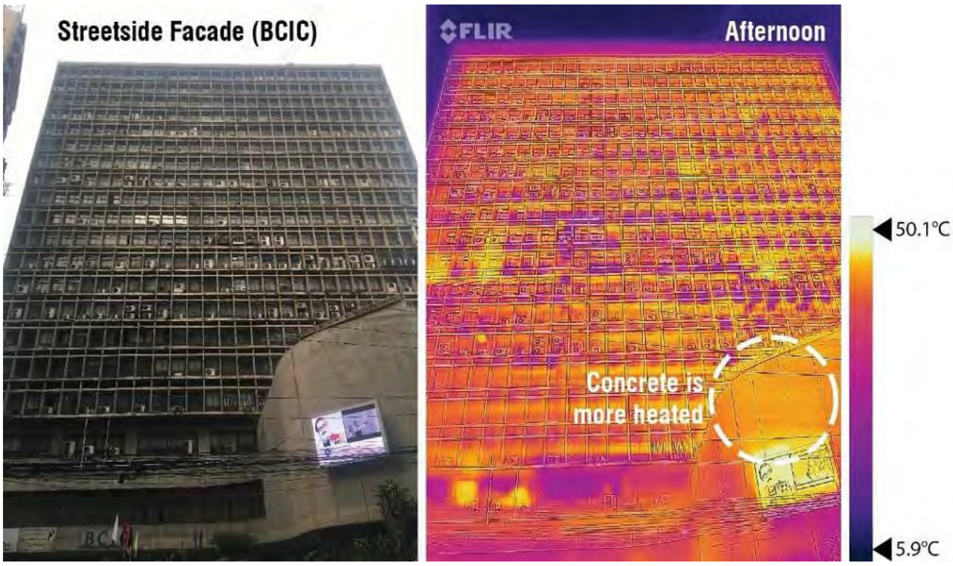

Figure 4.2: Investigation of the streetside facade of BCIC.

Figure 4.3: Investigation of the streetside facade of NCC.

North facade of SKB showing a large continuous facade suitable for installing BIPV but with an unfavorable orientation. Thermal image separates glazing as fenestration from glazing covering concrete surfaces. Buildings intent on solar harvesting should direct their largest facades toward the south.

Figure 4.4: Investigation of the streetside facade of SKB.

Setback effect observation: The west facade of KRB (building at the middle of either photo in Figure 4.5) is shaded by a much higher adjacent building with a shifting facade. Notice that the lower part of the facade (beside writing 'BADC') is cooler than the top part.

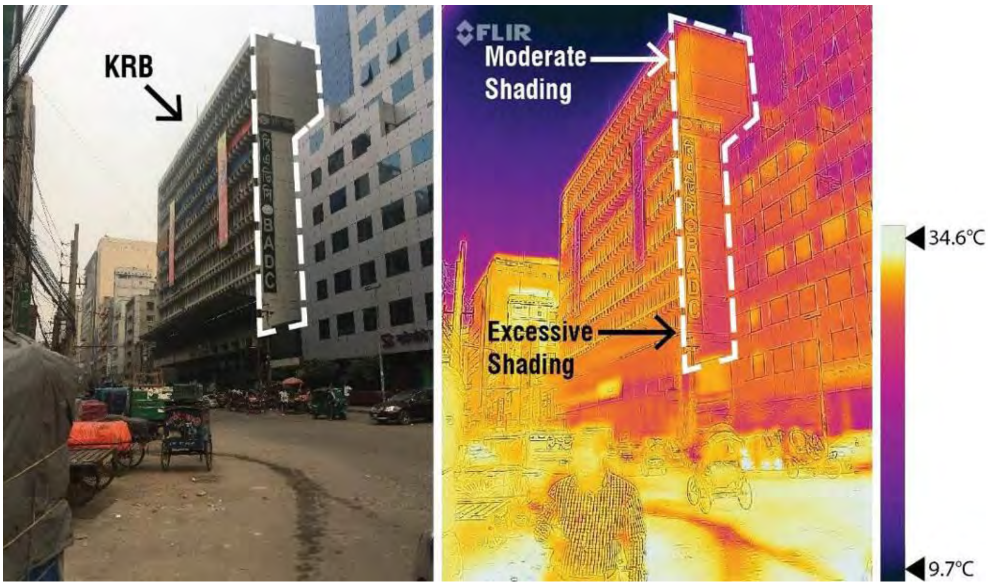

Figure 4.5: Observation of setback between KRB and adjacent building.

Orientation effect observation: Although a streetside facade, the north-east facade of SBB does not capture much insolation (see Figure 4.6, photos were taken at 9:37 AM on 3 April 2021). A difference between the temperatures of facades of JBB is also observed (see the difference between top (morning) and bottom pair (afternoon) of photos in Figure 4.7). The top pair were taken at 8:43 AM and the bottom at 4:10 PM on 4 April 2021 from the south. The variation is due to the shift of the sun from east to west.

Figure 4.6: Streetside facade observation of SBB.

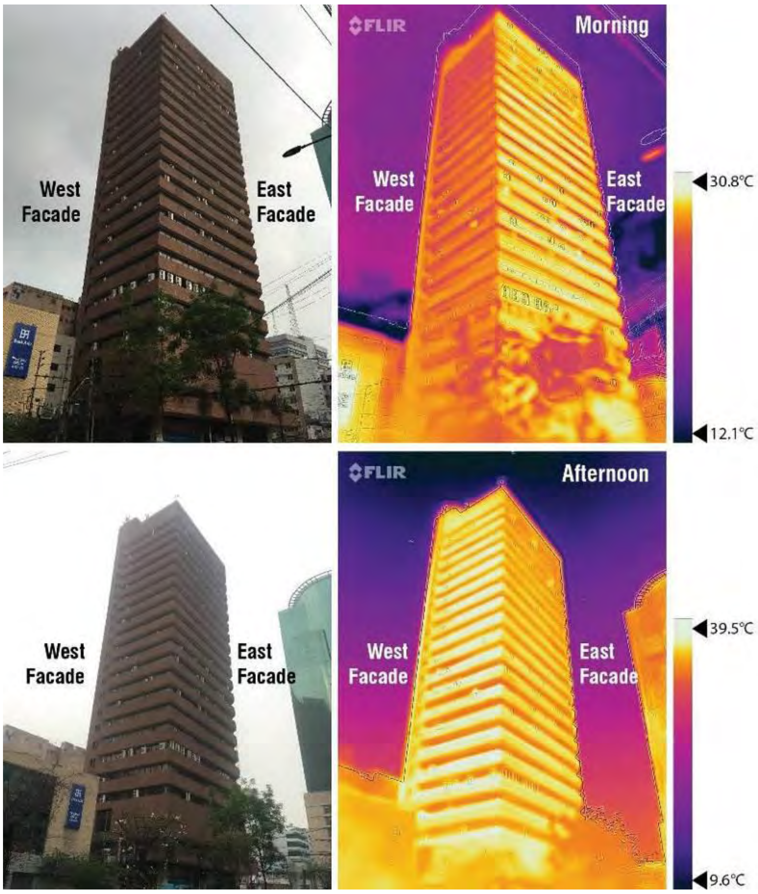

Figure 4.7: Facade insolation at different times of the day for JBB.

4.3.2 Discussion

The lowest facade areas, especially the ground-floor facades were found to be unsuitable for installing BIPV because of retails, entrances, and parking provisions, and are generally the most shaded area due to street trees, street furniture, utility installations, signages, and nearby buildings. For all simulations, facades of the reference building up to the ground floor ceiling, in other words, up to an estimated height of 3.6m from the Ground level, were excluded from calculations (see input parameters in Section 3.4.3).

For generating PV potential, a facade glazing of 25% was considered. This tentative figure was supported by detailed mapping of the facades of the seven buildings that were studied. Lower floors were excluded from this calculation because in all the cases, almost the entirety of qualified surface areas for BIPV was found towards the top of the buildings. Building facades were mapped with the help of photogrammetry, and a tentative value for the percentage of glazing area was calculated for each facade and also for the overall facade area. For example, in the particular case of BCIC, the south-west, south-east, north-east, and north-west facades have approximately 37.5%, 100%, 33.5%, and 100% glazing areas respectively, whereas the overall glazing area was about 22% of the overall facade area. An example of facade mapping and breakdown is shown in Figure C1 in Appendix C. Similarly, a suitable roof area for the installation of PV cells was estimated to be 75% (tentative) of the roof's total area. This tentative value was estimated by mapping the building roofs from Google satellite images (see Figure 4.10 for an MCA image). A certain portion of the roof surface is needed for the maintenance of the building and building service installations. However, other than the mentioned purposes, almost all the roofs in both the business districts (Kawran Bazar and MCA) were left unused, and therefore, potentially suitable for the installation of solar PV panels.

Other important findings from physical observations are listed as under:

1. All commercial office buildings in MCA are either fully or partially airconditioned. However, buildings with central A/C systems seem to be more suitable for facade PV deployment due to their facade features.
2. Setback should be considered as an important parameter that regulates insolation.
3. There are many buildings in MCA with huge facade areas that provide important opportunities for solar energy harvesting.
4. Streetside facades have lower chances of overshadowing.

4.4 Numerical Data Collection and Observation

Numerical data collected from various sources were observed and interpreted in this section. Policymakers are interested in the percentage ratio of how much electricity can be contributed by solar energy systems in reference to the consumed electricity (Kanters & Wall, 2014). This percentage can be increased in twofold ways:

1. By increasing electricity production from solar energy, and
2. By decreasing energy consumption in buildings.

However, due to the effect of multiple weather variables, both energy production and energy consumption can vary on a monthly basis. Since minimizing energy consumption is essential for better solar performance, it is important to understand which factors are responsible for the monthly variation in energy consumption. Therefore, monthly weather data and monthly energy consumption data were collected and observed to identify the said factors. A closer look will enable us to understand which months of the year are more suitable for solar energy harvesting and due to which factors, considering that the percentage ratio of energy production to energy consumption can be diminished due to higher rates of energy consumption in some months. Moreover, if the identified factors can be altered, it is possible to decrease energy consumption rates in buildings.

4.4.1 Weather Data

The categories of weather data procured from Bangladesh Meteorological Department (BMD) is outlined in Table 4.1. This set of data was later processed for further analysis.

Table 4.1: Types of Data Collected from BMD.

Serial	Category	Basis	Unit	Time Period
1	Maximum Temperature	Monthly	Degrees Celcius	Jan 2015 - Oct 2020
2	Minimum Temperature	Monthly	Degrees Celcius	Jan 2015 - Oct 2020
3	Mean Temperature	Monthly	Degrees Celcius	Jan 2015 - Oct 2020
4	Average Cloud Amount	Monthly	Octa	Jan 2015 - Oct 2020
5	Average Sunshine Hours	Monthly	Number of Hours	Jan 2015 - Oct 2020

The primary assumption is that the monthly energy consumption in buildings should vary due to the effect of the variables (category of data) listed in Table 4.1. As described in Section 2.8.1, the entirety of energy consumption in commercial office buildings can be attributed to four categories:

1. Heating, ventilation, and airconditioning (HVAC)
2. Lighting
3. Electrical Equipment, and
4. Lifts and Escalators

Among these categories, category 3 and 4 is not influenced by weather variables and therefore, do not vary on a monthly basis. The first two categories of energy consumption vary on a monthly basis and are highly dependent on weather variables.

Temperature in Dhaka varies on a monthly basis (as mentioned in Section 2.3.2) and so does the cooling load in buildings. Therefore, an increase in temperature can cause an increase in the energy required for HVAC systems. It is important to look at how energy consumption varies with each of Monthly Maximum Temperature, Monthly Minimum Temperature, and Monthly Mean Temperature. **Cloud amount** and the length of **sunshine hours** can affect indoor lighting in buildings. Therefore, the relationship of these variables with energy consumption should help us investigate whether, and to what extent the studied buildings are using natural lighting for their interiors. In terms of lighting energy, these two variables should have an increasing and a decreasing effect on energy consumption. Cloud amount also corresponds to humidity, which can affect indoor comfort and as a result, HVAC requirements can go up. However, in terms of HVAC energy, sunshine hours should generate a reverse effect. More sunshine hours mean prolonged exposure to the sun and a greater heat gain in buildings, resulting in the use of more air-conditioning. The combined effect of these variables, the nomenclature of which follows World Meteorological Organisation (WMO) guidelines (WMO, 2017), is responsible for the monthly variation of energy consumption in buildings.

4.4.2 Energy Consumption Data

Energy consumption data were procured from Dhaka Power Distribution Company Ltd. (DPDC). DPDC, the principal power provider in the MCA zone, generates monthly reports of power consumption for different zones in Dhaka under their jurisdiction. The monthly report from DPDC includes a Table, which provides Customer Numbers and Units Sold in kWh in various tariff categories (for example, LT-A, LT-B, LT-C, LT-D, LT-E, MT-1, MT-2, MT-3, etc.) for 27 “Feeders” across MCA. A Feeder is a hub from which power is distributed to one or more customers, serving either an entire building or a collection of buildings in the MCA. A single building can have multiple customers. Amongst the tariff categories, the MT-2 category was declared as strictly commercial, and therefore, data from the MT-2 column was utilized for further processing. A sample table from DPDC’s monthly report is provided in Figure F1 in Appendix F. It should be noted that in some cases, the customer number varied across monthly reports due to their switching of zones from MCA to an adjacent zone, or from an adjacent zone to MCA according to DPDC’s disposal. For processing and analysis, “Units Sold” figures that showed variable customer numbers were avoided by excluding the Feeder entirely from data processing.

Seven buildings were identified from the list of Feeders and their tentative floor areas were calculated. The buildings were located in the Google satellite image of MCA in Figure 4.8. The representative monthly energy consumption data over a year from March 2019 to February 2020, which correspond to the "Units Sold" figures of DPDC's monthly reports, along with their total floor areas are listed in Table 4.2. All these buildings have the "Units Sold" figures only in the "MT-2" category, and their respective customer numbers didn't vary during the year from March 2019 to February 2020, and figures derived only from these months were utilized for calculating the yearly energy consumption rate (E_r). Table 4.2 calculates the average E_r to be 255 kWh/m^2 with a standard deviation of 40. The E_r of NCC, SBB, SKB and AGB are below average, and that of JBB, BCIC and KRB are above average. The variation of energy consumption is down to building features and surrounding conditions analyzed in Section 5.2.

Figure 4.8: Google Satellite image showing the locations of 7 buildings listed as column headings in Table 4.2.

Table 4.2: Building energy consumption figures at MCA.

Name of Building with Acronym Used	Month	Sonali Bank Bhaban (SBB)	Janata Bank Bhaban (JBB)	BCIC Building (BCIC)	Senakallyan Bhaban (SKB)	Krishi Bhaban (KRB)	Agrani Bank Building (AGB)	NCC Bank Building (NCC)
Energy Consumption Figures in kWh (Units Sold by DPDC)	Jan	448460	225858	742670	655238	655238	170560	190000
	Feb	470288	312294	897275	654860	654860	255432	228000
	Mar	476674	306716	752743	689440	689440	235916	222000
	Apr	501782	317244	740742	507458	507458	166800	242000
	May	458068	314089	774928	763735	763735	273000	270000

Name of Building with Acronym Used	Month	Sonali Bank Bhaban (SBB)	Janata Bank Bhaban (JBB)	BCIC Building (BCIC)	Senakallyan Bhaban (SKB)	Krishi Bhaban (KRB)	Agrani Bank Building (AGB)	NCC Bank Building (NCC)
	Jun	524072	355528	837930	679548	679548	270000	230000
	Jul	458740	355520	837155	772931	772931	211200	248000
	Aug	490886	318694	751321	652006	652006	217800	244000
	Sep	373666	253369	635200	522583	522583	175800	206000
	Oct	338082	200307	470638	440410	440410	144000	168000
	Nov	302606	183232	466952	397464	397464	136800	178000
	Dec	300352	183400	434420	393749	393749	116400	180000
	Annual	5143676	3326251	8341974	7129422	7129422	2373708	2606000
Total Floor Area (m^2)		23369	12996	29327	30554	21739	9555	12237
Annual Cons. Rate (E_r)		220	256	284	233	328	248	213
Average E_r (kWh/m^2)					255			

4.4.3 Data Analysis and Interpretation

Analysis and observation on 2019 data: Building electricity consumption figures by month, and the corresponding Monthly Energy Consumption Indicator (E_{mo}) is listed in tabular form in Appendix E for 14 building entities in Motijheel. E_{mo} was calculated using Equation 3.1. Acronyms used for building entities in Tables E2-E6 are elaborated in Table E1. Each entity is either a single building as in the case of the seven buildings listed in Table 4.1 or a small group of buildings – all commercial buildings with office functions. The fixed customer number that was considered for any electricity consumption data to be accounted for is also mentioned in Tables E2-E6 in Appendix E. However, this chart only includes data from July 2017 to February 2020 that were made available by DPDC. Some fields are kept blank due to irregular customer numbers or the unavailability of data. Initial data analysis generates insight into the relationship of the degree of energy consumption to the values of weather variables for each month in 2019 which is plotted in multiple-axes graphs in Figures 4.9, 4.11, 4.13, 4.15, and 4.17. The energy consumption figures of 2019 used in the mentioned figures follow table 4.2, whereas the weather data, which remained identical for all the mentioned figures, were collected from BMD.

Dashed lines represent the average figures for each group of data. Observations on five buildings for the year 2019 helped consider and examine variables for further analysis. Figure 4.9 shows that for BCIC, the increase in energy consumption in mid-year corresponds with increases in temperature and cloud amount and a drop in sunshine hours. For NCC and SBB, a similar pattern is observed (see Figure 4.11 and Figure 4.13). For SBB, however, the mid-year energy curve is relatively flatter. For SKB (see Figure 4.15), the temperature curve is relatively flat during mid-year months, but the energy curve fluctuates. Moreover, an uncharacteristic drop in energy consumption is observed in June. Note that June 2019 was the month of Eid-ul-fitr. The bumpiness of the energy curve and the uncharacteristic drop in June is also observed in case of AGB (see Figure 4.17).

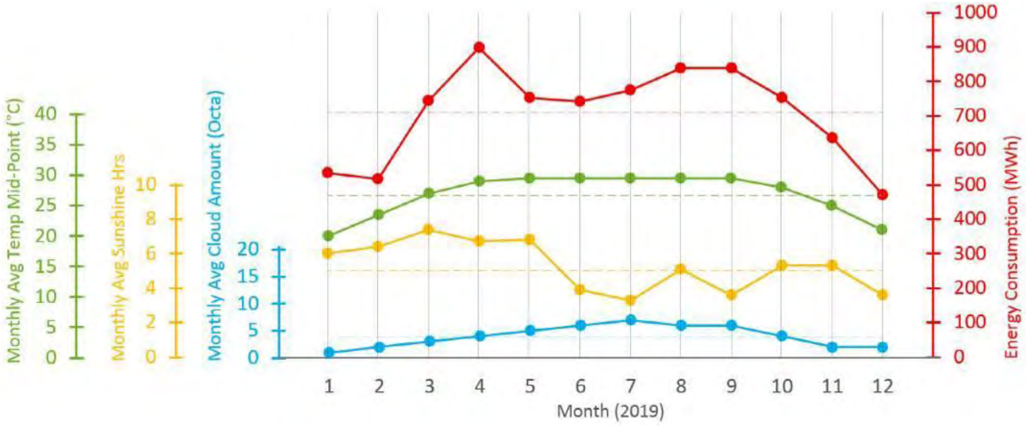

Figure 4.9: Primary observation on energy data for BCIC.

Figure 4.10: Street views of BCIC Building.

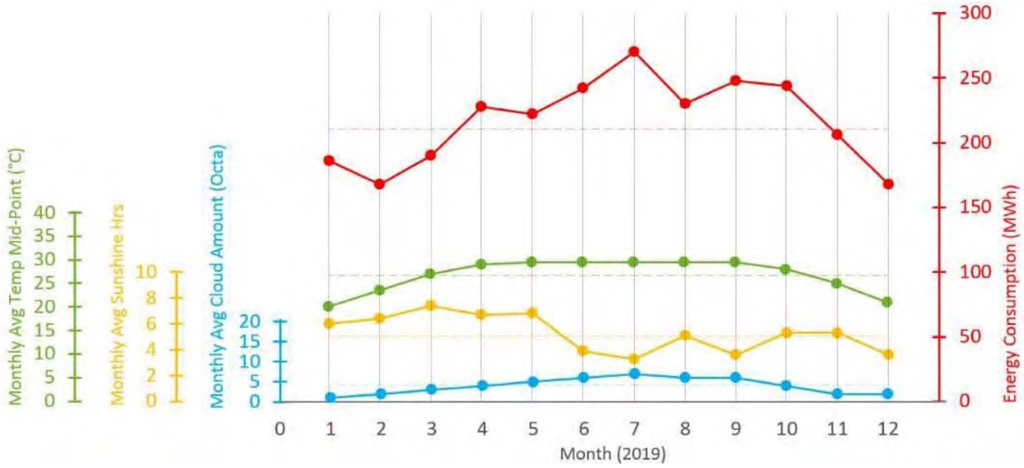

Figure 4.11: Primary observation on energy data for NCC.

Figure 4.12: Street views of NCC.

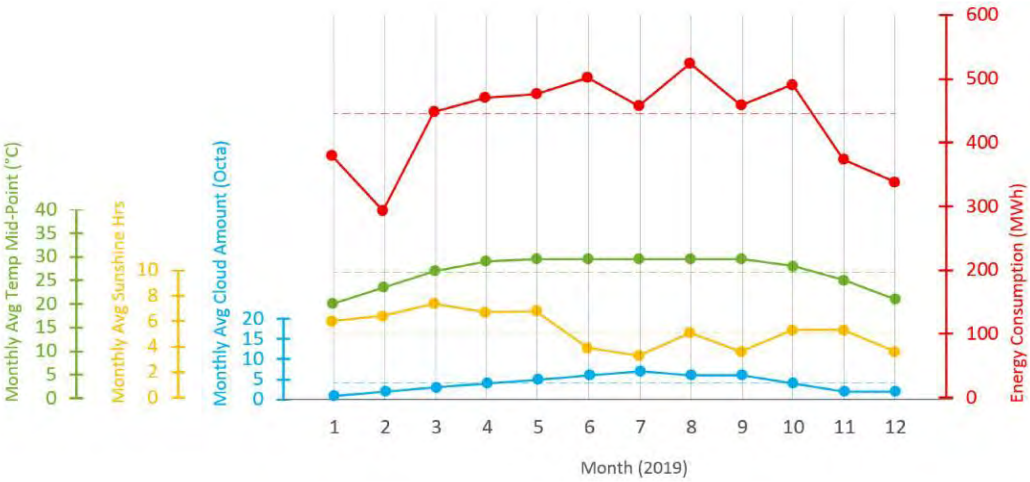

Figure 4.13: Primary observation on energy data for SBB.

Figure 4.14: Panoramic image depicting SBB (left, yellow), the top portion of NCC (middle, blue), and SKB (right, highrise with black vertical stripes).

An important overall observation is that the energy consumption curve is bumpy and irregular, unlike other weather variables' curves, probably because of the variation of active office hours each month. Therefore, the Monthly Number of Workdays (W) could be an important variable to consider. Observations on the monthly energy data of individual buildings for the year 2019 and the corresponding weather data indicated that positive relationships exist between Monthly Energy Consumption (E_m) and each of Monthly Mean Temperature (T_{avg}) and Monthly Average Cloud Amount (C_{avg}). The figures for 2019 also tend to show a negative relationship between Monthly Average Sunshine Hours (S_{avg}) and Monthly Energy Consumption (E_m), albeit unclear and fluctuating. However, the average temperature (T_{avg}) curve is relatively flat during the mid-year months unlike the energy consumption (E_m) curve, which goes up and down. For further scrutiny, the relationship of energy consumption could be investigated in terms of another temperature variable with a slightly loftier curve: Monthly Maximum Temperature (T_{max}). For in-depth statistical analysis, data from a longer period was utilized, and all variables that could potentially impact monthly variation in energy consumption were taken into consideration. Note that other variables impacting energy consumption, for example, indoor activities, building volume, etc. were excluded because they do not vary on a monthly basis. The metric used to estimate monthly variation is E_{mo}.[7]

[7] See Section 3.5.1 for the definition of Monthly Energy Consumption Indicator (E_{mo}).

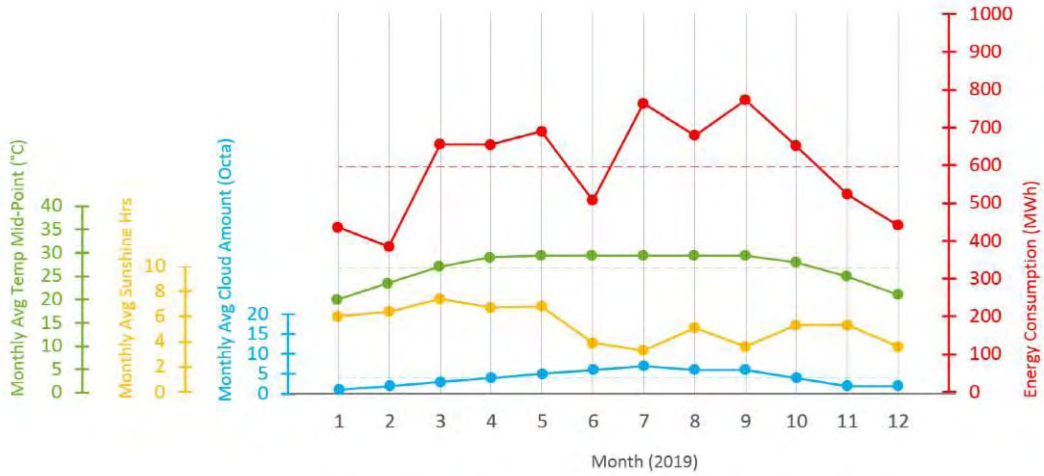

Figure 4.15: Primary observation on energy data for SKB.

Figure 4.16: Street views of SKB.

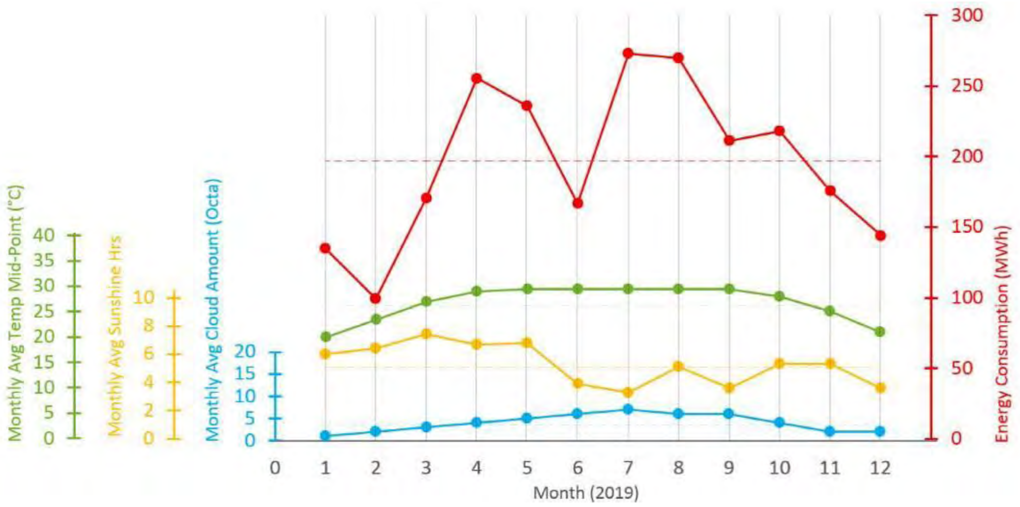

Figure 4.17: Primary observation on energy data for AGB.

Figure 4.18: Street views of AGB.

Analysis of data from 2017-2020: Table 4.3 lists the median values calculated from the corresponding E_{mo} values of all the building entities mentioned in Tables E2-E6 (see Appendix E), along with the weather data for the respective months. Weather variables include Monthly Maximum Temperature (T_{max}), Monthly Minimum Temperature (T_{min}), Monthly Mean Temperature (T_{avg}), Monthly Average Cloud Amount (C_{avg}), and Monthly Average Sunshine Hours (S_{avg}). Besides, Table 4.3 also includes the Number of Workdays (W) by month, which was calculated from the Government's Holiday Calendar, and an Annual factor (A), which denotes the number of years passed from the start of July 2017 to the start of each month. To account for the drop in energy consumption in the month of Eid-ul-fitr, a categorical variable R is included. The value of R is 1 for an Eid-ul-fitr month, and 0 for a non-Eid-ul-fitr month.

Table 4.3: Monthly values for Regression Analysis. A, W, R, T_{max}, T_{min}, T_{avg}, C_{avg}, and S_{avg} are independent variables while E_{mo} is a dependent variable.

YYYY	MMM	A	W	R	T_{max}	T_{min}	T_{avg}	C_{avg}	S_{avg}	E_{mo} (Median)
2017	**Jul**	0.000	22	0	35.8	24.8	30.3	7	3	0.0895
2017	**Aug**	0.085	21	0	34.2	25.2	29.7	7	3.4	0.1078

YYYY	MMM	A	W	R	T_{max}	T_{min}	T_{avg}	C_{avg}	S_{avg}	E_{mo} (Median)
2017	**Sep**	0.170	19	0	36	24.0	30	6	3.8	0.0940
2017	**Oct**	0.252	22	0	36.5	19.1	27.8	5	4.9	0.1021
2017	**Nov**	0.337	22	0	33.2	17.1	25.15	2	5.6	0.0876
2017	**Dec**	0.419	20	0	29.4	14.2	21.8	1	4.4	0.0747
2018	**Jan**	0.504	23	0	26.8	9.5	18.15	0	5.3	0.0602
2018	**Feb**	0.589	19	0	33.6	14.4	24	1	5.5	0.0565
2018	**Mar**	0.666	20	0	34.6	17.5	26.05	2	7.4	0.0877
2018	**Apr**	0.751	21	0	36.5	19.4	27.95	4	6.8	0.0930
2018	**May**	0.833	21	0	36.3	20.8	28.55	6	4.7	0.0888
2018	**Jun**	0.918	18	1	35.6	23.6	29.6	6	4.2	0.0725
2018	**Jul**	1.000	23	0	37.6	24.8	31.2	7	3.5	0.1076
2018	**Aug**	1.085	18	0	36.5	25.4	30.95	7	4.4	0.1003
2018	**Sep**	1.170	20	0	36.5	25.0	30.75	5	5.4	0.1009
2018	**Dec**	1.252	20	0	28.9	11.8	20.35	2	4.3	0.0629
2019	**Jan**	1.504	23	0	31.3	12.0	21.65	1	6	0.0607
2019	**Feb**	1.589	19	0	32	13.2	22.6	2	6.4	0.0577
2019	**Mar**	1.666	19	0	35.1	13.2	24.15	3	7.4	0.0769
2019	**Apr**	1.751	20	0	37.1	17.9	27.5	4	6.7	0.0931
2019	**May**	1.833	21	0	36.6	17.9	27.25	5	6.8	0.0947
2019	**Jun**	1.918	17	1	36.6	22.3	29.45	6	3.9	0.0889
2019	**Jul**	2.000	23	0	35.7	24.4	30.05	7	3.3	0.1033
2019	**Aug**	2.085	17	0	36.4	25.0	30.7	6	5.1	0.0993
2019	**Sep**	2.170	21	0	36.3	23.7	30	6	3.6	0.0998
2019	**Oct**	2.252	22	0	35.2	21.5	28.35	4	5.3	0.0937
2019	**Nov**	2.337	19	0	32.7	18.2	25.45	2	5.3	0.0743
2019	**Dec**	2.419	21	0	31.5	12.2	21.85	2	3.6	0.0612
2020	**Jan**	2.504	22	0	29.6	11.6	20.6	3	4	0.0568
2020	**Feb**	2.589	20	0	32	11.3	21.65	2	6.7	0.0548

A multiple linear regression assuming A, W, R, T_{max}, T_{min}, T_{avg}, C_{avg}, and S_{avg} as independent variables and E_{mo} as the dependent variable was conducted, which generated the P-value and the t-Statistic value of each independent variable (see Table 4.4). An adjusted R-square value of 0.8598 was returned.

Table 4.4: t-Statistic values and P-values of Intercept / Independent variables returned by multiple linear regression conducted with A, W, R, T_{max}, T_{min}, T_{avg}, C_{avg}, and S_{avg} as independent variables and E_{mo} as the dependent variable.

Intercept/Variable	***t-Stat***	***P-value***
Intercept	-1.207669339	0.24060042
T_{max}	-1.07443261	0.294819671
T_{min}	0.135350015	0.89362413
T_{avg}	2.960205236	0.007470148
C_{avg}	-0.286797681	0.777077847
S_{avg}	-0.643060441	0.527144905
A	-0.160085935	0.874343232
W	2.482637709	0.021571462
R	-2.486816462	0.021378013

Selection of variables: Table 4.4 shows that the P-values of T_{max}, T_{min}, C_{avg}, S_{avg}, and A are greater than the significance threshold of $\alpha = 0.05$, and therefore are not statistically significant in the prediction of E_{mo}. However, the t-Statistic values of T_{min}, C_{avg}, and A are also close to the zero point, and so removing them from the regression model altogether was at first considered for a better outcome. Additionally, T_{max}^2 was added as another independent variable to the model, since the observation from individual linear regression with each of T_{max}, T_{avg}, S_{avg}, and W is that, T_{max} shows a significantly better R^2 score for a polynomial regression of order 2, unlike the other variables. Table 4.5 lists the R^2 values for the individual regression of each of the independent variables T_{max}, T_{avg}, S_{avg}, and W with E_{mo} as the dependent variable. Figure 4.19 also shows that a polynomial order 2 regression line has a much better visual fit to the data than a linear regression line for T_{max} against E_{mo}.

Table 4.5: Observations on regression analysis with each independent variable for finding possible relationships with dependent variable E_{mo}.

Independent Variable	***Label***	***Regression Type***	***Order***	***Equation***	***R^2 Value***
Monthly Maximum Temperature	T_{max}	Linear	-	y = 0.0049x - 0.0831	0.6236
Monthly Maximum Temperature	T_{max}	Polynomial	2	$y = 0.0005x^2 - 0.0293x + 0.4718$	0.6784
Monthly Maximum Temperature	T_{max}	Polynomial	3	$y = -5E-05x^3 + 0.0053x^2 - 0.1833x + 2.1116$	0.6827
Monthly Mean Temperature	T_{avg}	Linear	-	y = 0.004x - 0.0215	0.7658
Monthly Mean Temperature	T_{avg}	Polynomial	2	$y = 4E-05x^2 + 0.0018x + 0.005$	0.7667
Monthly Average Sunshine Hours	S_{avg}	Linear	-	y = -0.0032x + 0.0996	0.0573
Monthly Average Sunshine Hours	S_{avg}	Polynomial	2	$y = 0.0023x^2 - 0.0275x + 0.159$	0.0995
Workdays	W	Linear	-	y = 0.0005x + 0.0724	0.0028
Workdays	W	Polynomial	2	$y = 0.0007x^2 - 0.0288x + 0.3666$	0.0207

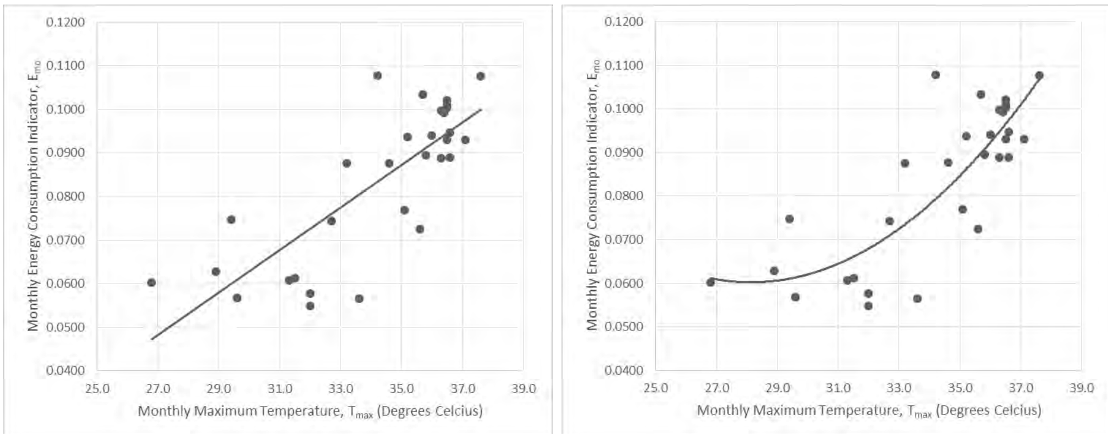

Figure 4.19: T_{max} vs E_{mo} graphs with a linear regression line (left) and a polynomial order 2 regression line (right). The latter shows a much better fit.

Selection of regression model: With T_{max}^2, T_{max}, T_{avg}, S_{avg}, W, and R selected as the independent variables, a multiple linear regression was again carried out maintaining E_{mo} as the dependent variable. This regression model returns a much increased Adjusted R-square value of 0.8886. The Coefficient, P-value, Lower 95% value, and Upper 95% value of each independent variable returned by this model are listed in Table 4.6.

Table 4.6: Output of multiple linear regression with T_{max}^2, T_{max}, T_{avg}, S_{avg}, W, and R as independent variables and E_{mo} as the dependent variable.

Intercept/Variable	***Coefficients***	***P-value***	***Lower 95%***	***Upper 95%***
Intercept	0.262453583	0.110395773	-0.064520124	0.58942729
T_{max}^2	0.000275783	0.069572924	-2.39395E-05	0.000575506
T_{max}	-0.019421743	0.049994585	-0.038842988	-4.9916E-07
T_{avg}	0.005041003	4.43803E-06	0.00329207	0.006789935
S_{avg}	-0.001189239	0.219714086	-0.003139139	0.000760662
W	0.001793107	0.030859641	0.000180358	0.003405857
R	-0.016118018	0.004448544	-0.026692269	-0.005543767

For detailed results of regression analysis for this model, see Tables E8-E12 in Appendix E. Although S_{avg} (t-Stat = -1.26) and T_{max}^2 (t-Stat = 1.9) have P-values greater than α = 0.05, removing them from the model does not increase the Adjusted R-square value of the model, which is evident from Table 4.7. This is because of their t-Statistic value, which is significantly away from the zero-point.

Table 4.7: Regression models considered in the analysis: each row represents a separate model and lists the adjusted R-square value for each.

Considered Variables in Multiple Linear Regression Model		**Adjusted R-square Value of Model**
Dependent Variable	**Independent Variables**	
E_{mo}	T_{avg}, R, W, T_{max}, S_{avg}, C_{avg}, A, T_{min}	0.859823668
E_{mo}	T_{avg}, R, W, T_{max}, T_{max}^2, S_{avg}	0.888600256
E_{mo}	T_{avg}, R, W, T_{max}, T_{max}^2	0.885853293
E_{mo}	T_{avg}, R, W, T_{max}	0.873835762
E_{mo}	T_{avg}, R, W	0.861881147

The key finding at this point is that T_{avg}, R, W, T_{max}, T_{max}^2, S_{avg} are all significant predictor variables[8], and their combined effect is responsible for the monthly variation in energy consumption. See Section 6.3.3 for the regression equation. It is important to note that the median values of E_{mo} were used for this analysis to avoid data anomalies and unexpected occurrences in the energy data of the studied building entities. However, an analysis considering the average E_{mo} values returns similar results with similar relationships among the variables. Table E7 in Appendix E lists the average values alongside the median values, along with their mathematical differences, which were found to be minor. Moreover, a t-test of the "paired" type and two-tailed distribution run between the median dataset and the average dataset returns a p-value of 0.402, which is greater than the significance threshold of $\alpha = 0.05$, meaning that the null hypothesis between these two datasets cannot be rejected, and so there is no significant statistical difference between the two groups of data.

4.4.4 Key Observations

The combined effect of variables: A multiple linear regression model with T_{max}^2, T_{max}, T_{avg}, S_{avg}, W, and R as independent variables and E_{mo} as the dependent variable was found to be able to predict E_{mo} very accurately (Adj. $R^2 = 0.89$), suggesting that monthly energy consumption in MCA varies due to the combined effect of these variables. Observations include:

1. It is evident from the strong positive coefficient (0.005) of T_{avg} that temperature governs energy consumption, while at extreme temperatures it is likely to rise at a higher rate (minor effect of T_{max}^2 and T_{max}). The coefficient of T_{max}^2 and T_{max} was returned positive and negative respectively, which is understood from the polynomial regression equation of order 2 listed in Table 4.5. This suggests that airconditioning energy dominates energy consumption. Physical surveys in MCA also inform that commercial office buildings in MCA are either partially or fully airconditioned (e.g. SBB: partial, split; NCC: full, central).

[8] Predictor variable refers to an independent variable that provides useful information in the prediction of the dependent variable using a multiple regression equation.

2. Monthly energy consumption varies significantly due to the monthly number of workdays (W) and is likely to drop during the month of Eid-ul-fitr due to changes in active occupancy hours in commercial buildings. This phenomenon is clarified by the strong coefficients of W (0.002) and R (0.016). However, it is also understood that the drop during the calendar month of Eid-ul-fitr (June) is not due to a perceived lack of activity during the Arabic month of Ramadan (more than half of it is in the previous calendar month), but due to the lack of occupants during the Eid-ul-fitr vacation period when more than half of Dhaka's population leave the city for festivities (The Daily Star, 2019).
3. Monthly average sunshine hours (S_{avg}) was found to have a minor effect, and its lower 95% and upper 95% values indicate a range of -0.0031 to 0.0007 for its coefficient, which is inclined to be negative. The effect of sunshine hours is unclear because it could reduce the energy required for lighting, but could increase airconditioning energy requirements nonetheless, given the fact that exposed glass facades are fairly common in MCA. Since monthly average cloud amount (C_{avg}) was found to have no effect at all on overall energy consumption, we can conclude that there is little use of natural lighting in MCA buildings, and lighting energy requirements are relatively minor. Having said that, the energy-consumption-reducing effect of S_{avg} seemed to dominate its energy-consumption-increasing effect in the final regression model.

Individual relationships with weather variables:

Weather variable – Monthly Maximum Temperature: Monthly Energy Consumption is closely related to the square of Monthly Maximum Temperature (T_{max}), meaning that at high temperatures, energy consumption increases at a higher rate due to an increase in temperature (see graph in Figure 4.20). An R-square value of 0.6784 for the polynomial order 2 regression line confirms a strong positive relationship between E_{mo} and T_{max} in Figure 4.20.

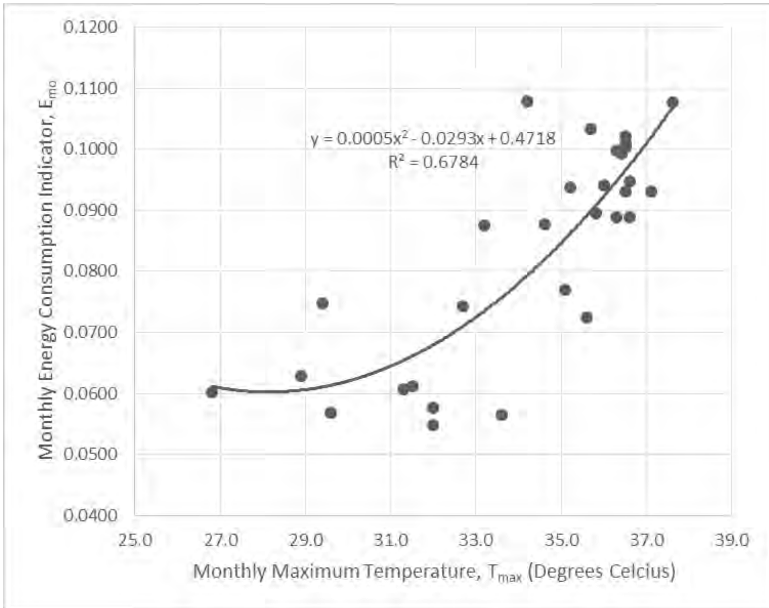

Figure 4.20: T_{max} vs E_{mo} graph showing the relationship between maximum temperature and energy consumption.

Weather variable – Monthly Mean Temperature: Monthly Mean Temperature (T_{avg}) shows a positive linear relationship (see graph in Figure 4.21) with energy consumption, which is the strongest among the considered variables, implying that the cooling load in the commercial office buildings in MCA contributes highly to their energy consumption. An R-square value of 0.7615 for the linear regression line in Figure 4.21 confirms a positive relationship between T_{avg} and E_{mo} – the strongest relationship found among the considered variables.

Weather variable – Monthly Minimum Temperature: Monthly Minimum Temperature (T_{min}) shows a strong positive linear relationship (see graph in Figure 4.22) with Monthly Energy Consumption Indicator (E_{mo}), suggesting that the lower the minimum extreme in a month, the lower is the energy consumption, and vice versa. An R-square value of 0.7369 for the linear regression line confirms a strong positive relationship between T_{min} and E_{mo} (see Figure 4.22). However, among temperature variables, T_{avg} turned out to be the most significant predictor variable, and so the importance of T_{min} in the prediction of E_{mo} is diminished in any multiple regression analysis that considers all three temperature variables.

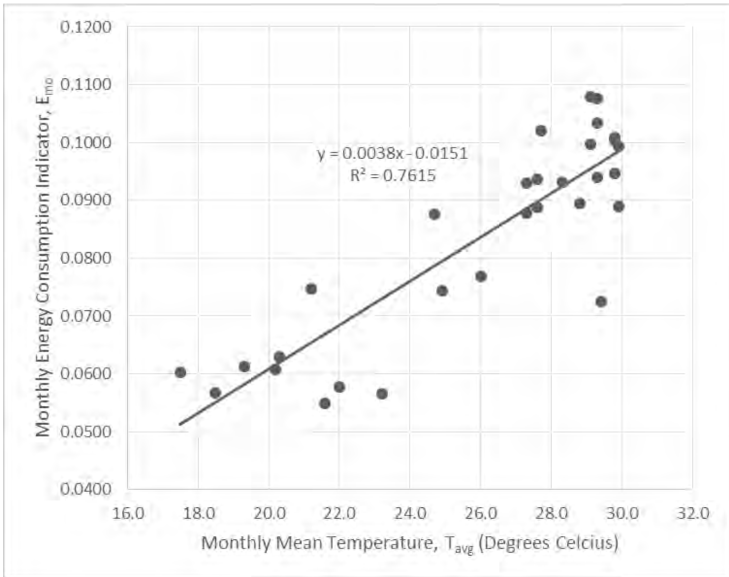

Figure 4.21: T_{avg} vs E_{mo} graph showing the relationship between mean temperature and energy consumption.

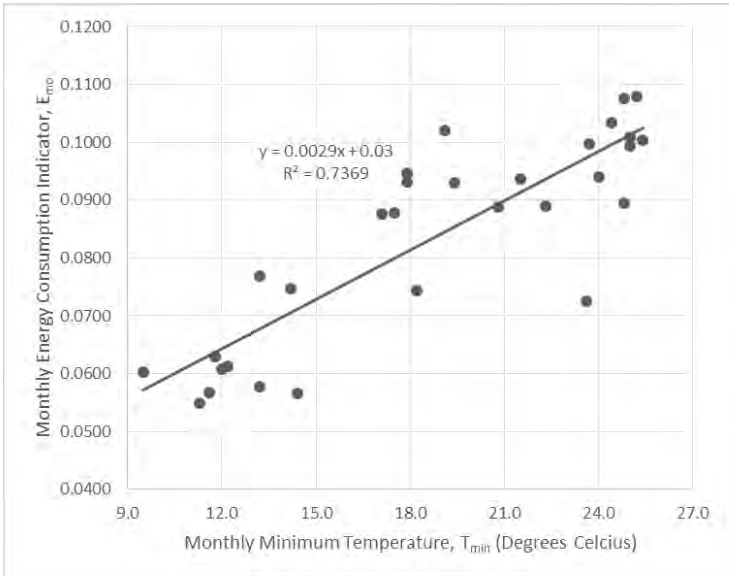

Figure 4.22: T_{min} vs E_{mo} graph showing the relationship between minimum temperature and energy consumption.

Weather variable – Monthly Average Cloud Amount: C_{avg} also shows a strong linear relationship with E_{mo} (see Figure 4.23) despite being an insignificant variable in the multiple regression model due to its P-value (see Table 4.4). This can be explained from the graph shown in Figure 4.24, which shows that the C_{avg} curve has a similar profile to T_{avg} during the given time period. As a result of having similar profiles, their regression lines with E_{mo} are also similar.

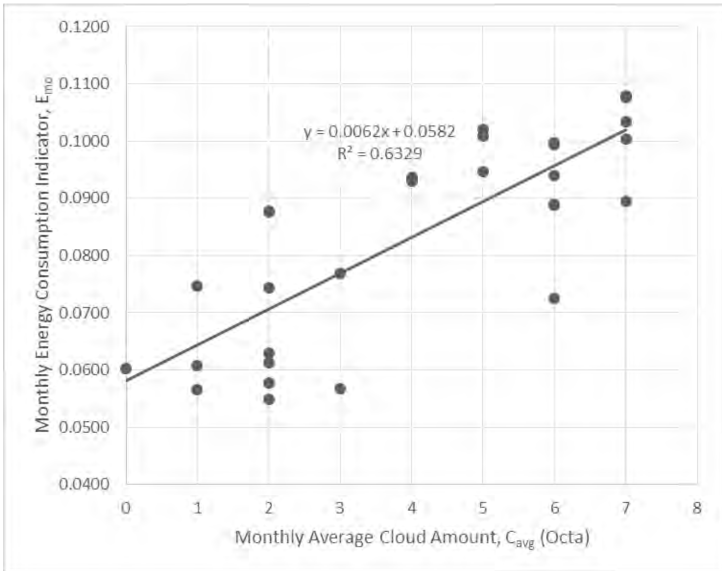

Figure 4.23: C_{avg} vs E_{mo} graph showing the relationship between cloud amount and energy consumption.

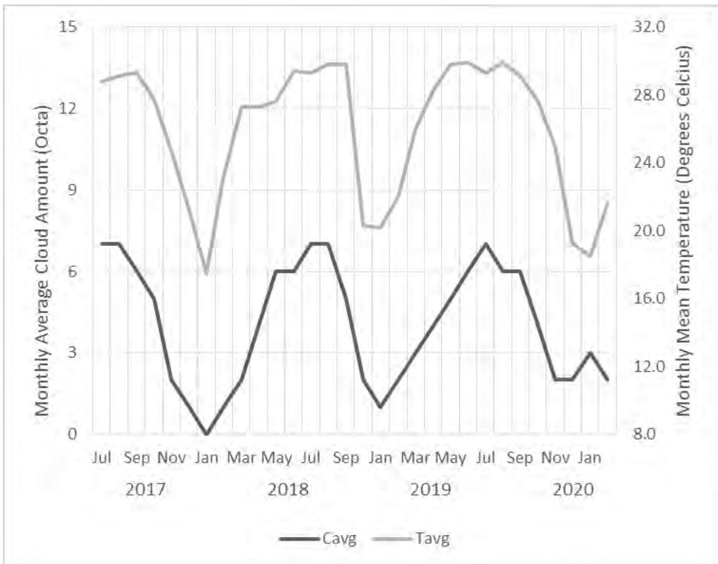

Figure 4.24: Demonstration that in the observed dataset, the T_{avg} curve exhibits a journey similar to the C_{avg} curve.

Weather variable – Monthly Average Sunshine Hours: Monthly Average Sunshine Hours (S_{avg}) shows no clear relationship with Monthly Energy Consumption in the commercial buildings of MCA. However, the overall trend is negative (see Figure 4.25) suggesting that prolonged sunshine hours could make a minor contribution toward saving lighting energy. The data points in Figure 4.25 are too scattered to hint at any obvious correlation.

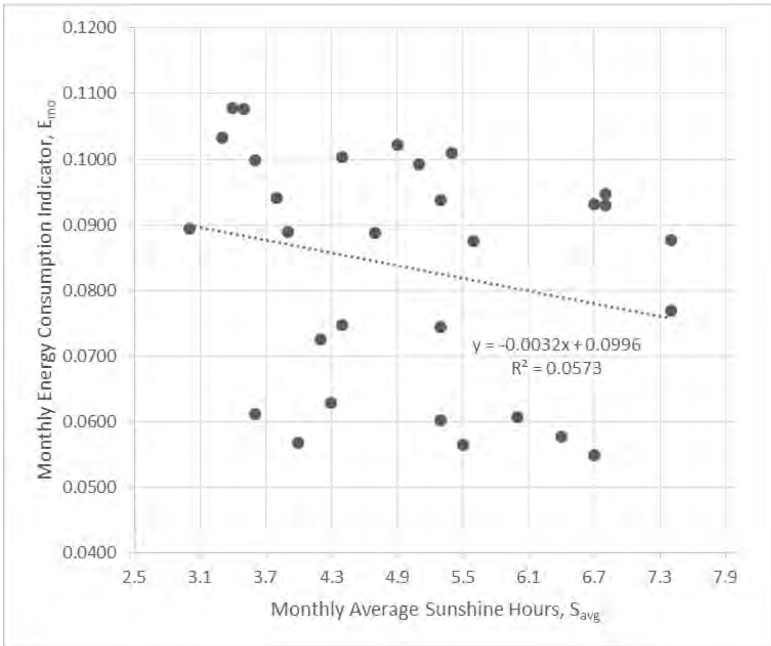

Figure 4.25: S_{avg} vs E_{mo} graph showing a very weak negative relationship between sunshine hours and energy consumption.

Individual relationships with workdays and annual factor:

The arbitrary and insignificant relationship of the annual factor (A) with energy consumption assured that the energy consumption pattern in the buildings of MCA did not alter during the three years of study. There was not a clear hint of a general increase or decrease in energy consumption per year, which is evident from Figure 4.26.

Figure 4.27 shows that between W and E_{mo}, no obvious relationship was found as indicated by the scattered data points around the linear regression line. Despite showing no clear individual relationship with Monthly Energy Consumption, the Monthly Number of Workdays (W) was found to be an influential variable in combination with other factors in the multiple regression model. The underlying reason, most possibly, is that the removal of a few points from the given dataset could yet hint of a rather strong individual relationship (R^2 = 0.367), which is also illustrated in Figure 4.27. Omitting red data points generates the red-dotted linear regression line, which implies that a reasonably strong positive relationship potentially exists between the variables.

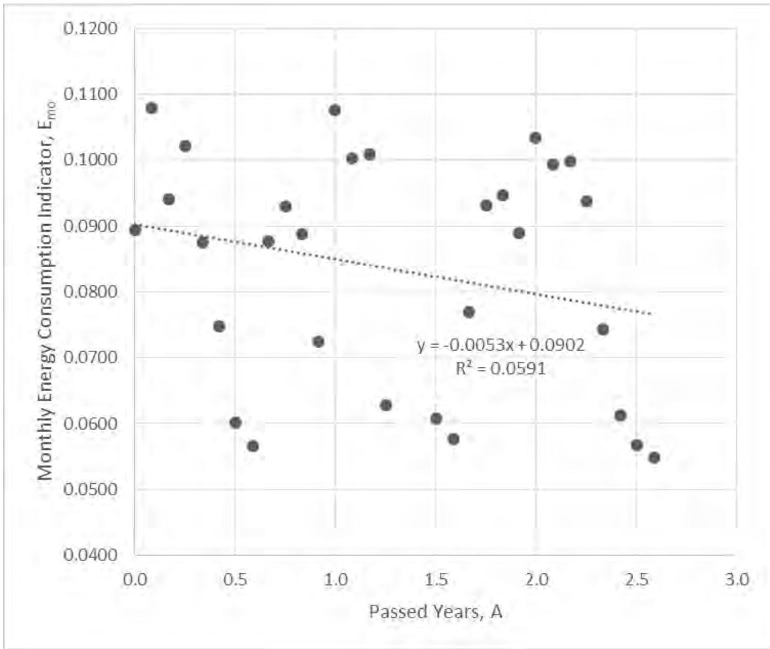

Figure 4.26: A vs E_{mo} plot showing no obvious link between the variables.

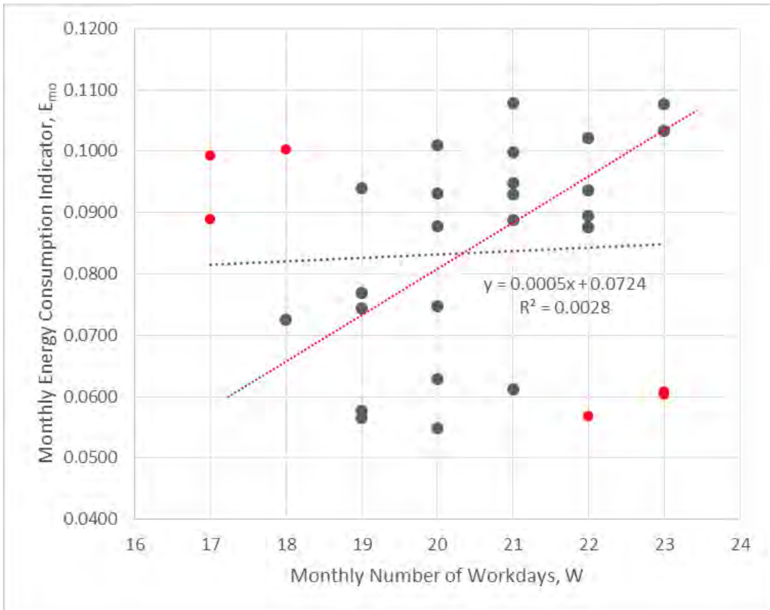

Figure 4.27: W plotted against E_{mo}: when the red data points are excluded from the dataset, the black regression line is replaced by the red one.

4.5 Summary

Field Investigation enabled the research process to understand the scope of solar energy harvesting within MCA's urban conditions and the impact of urban configurations on building solar potential in real life, while some observations helped generate input parameters for the simulation study. However, a comprehensive analysis of the collected numerical data resulted in some important findings regarding energy consumption in buildings:

1. Energy consumption is, individually, closely related to mean temperature, minimum temperature and maximum temperature squared – all showing positive relationships (positive slope of regression line).
2. Most, if not all, buildings in MCA are airconditioned. Cooling load dominates energy consumption in MCA buildings, and therefore a reduction in cooling load (e.g. by introducing natural ventilation) will significantly reduce energy demand.
3. Natural lighting is scarcely utilized in MCA buildings, hence the application of natural lighting could considerably reduce energy demand. However, the energy required for lighting in MCA buildings appears to be constant under different climatic conditions and is also insubstantial compared to airconditioning energy.
4. Monthly Mean Temperature, Monthly Maximum Temperature (extreme variable), Monthly Average Sunshine Hours, Monthly Number of Workdays and Eid-ul-fitr Month (categorical variable) are all statistically significant predictor variables for generating monthly energy consumption figures.

A reduction in the buildings' energy consumption increases the energy production to energy consumption ratio, which emphasizes the role of solar energy harvesting in buildings to meet energy demands. Adopting passive design strategies in MCA buildings is therefore highly recommended.

References

Kanters, J. & Wall, M., 2014. The impact of urban design decisions on net zero energy solar buildings in Sweden. *Urban, Planning and Transport Research: An Open Access Journal,* 2(1), pp. 312-332.

The Daily Star, 2019. *Trouble in Tongi, beyond,* Dhaka: The Daily Star.

WMO, 2017. *WMO Guidelines on the Calculation of Climate Normals,* Geneva: World Meteorological Organization.

CHAPTER 5: PARAMETRIC STUDY AND ANALYTICS

5.1 Introduction

In this chapter, all computational simulations that were performed for the parametric study and analyses concerning solar potential and its implications in the urban environment are delineated. This final phase of the research comprises experimentations in three categories: 1. Simulation study of existing buildings, 2. Simulation study of existing districts, and 3. Simulation study of projected districts. For each category, the criteria for simulation, input data, output data, simulation process, and the resulting dataset are outlined and documented in the following sections.

5.2 Simulation Study on Existing Buildings

This section deals with the thorough examination of the monthly solar potential of seven buildings listed in Table 4.2, namely Sonali Bank Bhaban (SBB), Janata Bank Bhaban (JBB), BCIC Building (BCIC), Senakallyan Bhaban (SKB), Krishi Bhaban (KRB), Agrani Bank Building (AGB), NCC Bank Building (NCC). These seven buildings were selected because their energy data for all months of the year from March 2019 to February 2020 were made available by DPDC, and their varying heights, orientations, profiles, and surrounding urban conditions make them particularly suitable for this study. The figures generated from simulation were utilized for a comparative study of the buildings' monthly energy consumption and possible amount of electricity generated from solar PV systems. However, the focus is on evaluating and analyzing the physical urban environment, along with urban climatic scenarios responsible for the monthly variation of solar potential across the studied buildings.

5.2.1 Criteria

Field Investigation provided the data for 3D modeling in Rhinoceros[9] by means of physical observations and reconnaissance surveys as described in Section 4.2.2. The 3D representation of the reference building was considered as the Test Geometry for solar radiation analysis using Grasshopper[10] and Ladybug[11],

---

[9] Rhinoceros is a CAD software for 3D modeling. See Section 3.4.1 for details.
[10] Grasshopper is a parametric modelling plugin for Rhinoceros. See Section 3.4.1 for details.
[11] Ladybug is an extension of Grasshopper for environmental analysis. See Section 3.4.2 for details.

while surrounding buildings, along with the ground plane, were taken as the Context Geometry. The Grasshopper script used for analysis is given in Figure D2 in Appendix D.

5.2.2 Input and Output

The input parameters for simulation are outlined in Section 3.4.2. In this experiment, the simulations were carried out on a monthly basis. The Grasshopper script generated the monthly PV potential for each month as separate numerical outputs for the simulation of each building.

5.2.3 Results and Observation

The results of the simulation are recorded in the E_{mpv} columns of Tables 5.1-4. Monthly energy consumption figures (E_m) and the corresponding monthly electricity generated from PV (E_{mpv}) are compared for each building.

Table 5.1: Monthly Energy Consumption (E_m) figures (field data) compared with Monthly Electricity Generated from PV (E_{mpv}) figures (obtained from simulation) for SBB and JBB.

		Sonali Bank Bhaban (SBB)			**Janata Bank Bhaban (JBB)**		
		E_m	**E_{mpv}**	**$S_m = E_{mpv} / E_m$**	**E_m**	**E_{mpv}**	**$S_m = E_{mpv} / E_m$**
Year	**Month**						
2019	**Mar**	448460	65503	14.61%	225858	58234	25.78%
	Apr	470288	65932	14.02%	312294	55385	17.73%
	May	476674	64714	13.58%	306716	52711	17.19%
	Jun	501782	55861	11.13%	317244	45172	14.24%
	Jul	458068	52582	11.48%	314089	43123	13.73%
	Aug	524072	55728	10.63%	355528	46813	13.17%
	Sep	458740	55120	12.02%	355520	47952	13.49%
	Oct	490886	57188	11.65%	318694	53111	16.67%
	Nov	373666	50985	13.64%	253369	49655	19.60%
	Dec	338082	50356	14.89%	200307	50002	24.96%
2020	**Jan**	302606	52762	17.44%	183232	51142	27.91%
	Feb	300352	54369	18.10%	183400	49965	27.24%
SUM		*5143676*	*681101*	*13.24%*	*3326251*	*603263*	*18.14%*

Table 5.2: Monthly Energy Consumption (E_m) figures (field data) compared with Monthly Electricity Generated from PV (E_{mpv}) figures (obtained from simulation) for BCIC and SKB.

		BCIC Building (BCIC)			Senakallyan Bhaban (SKB)		
		E_m	E_{mpv}	$S_m = E_{mpv} / E_m$	E_m	E_{mpv}	$S_m = E_{mpv} / E_m$
Year	**Month**						
2019	**Mar**	742670	62233	8.38%	655238	77915	11.89%
	Apr	897275	60996	6.80%	654860	78767	12.03%
	May	752743	59381	7.89%	689440	78762	11.42%
	Jun	740742	51373	6.94%	507458	69081	13.61%
	Jul	774928	48710	6.29%	763735	65255	8.54%
	Aug	837930	51807	6.18%	679548	68303	10.05%
	Sep	837155	51686	6.17%	772931	65893	8.53%
	Oct	751321	55441	7.38%	652006	68573	10.52%
	Nov	635200	51561	8.12%	522583	62874	12.03%
	Dec	470638	53359	11.34%	440410	64714	14.69%
2020	**Jan**	466952	54812	11.74%	397464	66371	16.70%
	Feb	434420	54134	12.46%	393749	65867	16.73%
SUM		*8341974*	*655494*	*7.86%*	*7129422*	*832375*	*11.68%*

Table 5.3: Monthly Energy Consumption (E_m) figures (field data) compared with Monthly Electricity Generated from PV (E_{mpv}) figures (obtained from simulation) for BCIC and SKB.

		Krishi Bhaban (KRB)			Agrani Bank Building (AGB)		
		E_m	E_{mpv}	$S_m = E_{mpv} / E_m$	E_m	E_{mpv}	$S_m = E_{mpv} / E_m$
Year	**Month**						
2019	**Mar**	655238	49906	7.62%	170560	18407	10.79%
	Apr	654860	46889	7.16%	255432	21655	8.48%
	May	689440	45069	6.54%	235916	23040	9.77%
	Jun	507458	39041	7.69%	166800	20813	12.48%
	Jul	763735	37063	4.85%	273000	19200	7.03%

		Krishi Bhaban (KRB)			Agrani Bank Building (AGB)		
		E_m	E_{mpv}	$S_m = E_{mpv} / E_m$	E_m	E_{mpv}	$S_m = E_{mpv} / E_m$
Year	**Month**						
	Aug	679548	39428	5.80%	270000	19213	7.12%
	Sep	772931	41042	5.31%	211200	16402	7.77%
2019	**Oct**	652006	45616	7.00%	217800	13886	6.38%
	Nov	522583	43894	8.40%	175800	10109	5.75%
	Dec	440410	45516	10.33%	144000	8965	6.23%
2020	**Jan**	397464	46433	11.68%	136800	10151	7.42%
	Feb	393749	44819	11.38%	116400	12671	10.89%
SUM		*7129422*	*524715*	*7.36%*	*2373708*	*194513*	*8.19%*

Table 5.4: Monthly Energy Consumption (E_m) figures (field data) compared with Monthly Electricity Generated from PV (E_{mpv}) figures (obtained from simulation) for NCC.

		NCC Bank Building (NCC)		
		E_m	E_{mpv}	$S_m = E_{mpv} / E_m$
Year	**Month**			
2019	**Mar**	190000	48964	25.77%
	Apr	228000	43877	19.24%
	May	222000	41999	18.92%
	Jun	242000	36744	15.18%
	Jul	270000	35230	13.05%
	Aug	230000	37431	16.27%
	Sep	248000	38956	15.71%
	Oct	244000	46482	19.05%
	Nov	206000	46880	22.76%
	Dec	168000	49892	29.70%
2020	**Jan**	178000	50187	28.19%
	Feb	180000	46275	25.71%
SUM		*2606000*	*522915*	*20.07%*

In Tables 5.1-4, the percentage of energy demand that can be met in each particular calendar month (S_m) is also included for each of the seven buildings. The primary observation is that the S_m values for some buildings (e.g. NCC and JBB) follow a higher trend than the other buildings, while some other buildings (e.g. KRB and BCIC) follow a lower trend. Moreover, some months, most notably December and January show greater percentage than the other months of the year. For monthly comparison, which should analyze the effect of climatic differences, Monthly Solar Fraction (S_{mo}) values for each building were listed in Table 5.5 and these figures were then analyzed in Section 5.2.4. For building-wise comparison, building features were identified (see Table 5.6-8) and compared on the basis of their solar performance in Section 5.2.5. An in-simulation image of each building is provided in Figures 5.1-7, in which the solar irradiation mapping of the facades of each building was also carefully observed. The simulation work was conducted using simplified models that are devoid of ignorable complexities, details, and insignificant building and street elements.

Table 5.5: Monthly Solar Fraction (S_{mo}) figures for seven buildings of MCA.

$$S_{mo} = S_m / \sum S_m$$

Month	SBB	JBB	BCIC	SKB	KRB	AGB	NCC
Jan	0.11	0.12	0.12	0.11	0.12	0.07	0.11
Feb	0.11	0.12	0.13	0.11	0.12	0.11	0.10
Mar	0.09	0.11	0.08	0.08	0.08	0.11	0.10
Apr	0.09	0.08	0.07	0.08	0.08	0.08	0.08
May	0.08	0.07	0.08	0.08	0.07	0.10	0.08
Jun	0.07	0.06	0.07	0.09	0.08	0.12	0.06
Jul	0.07	0.06	0.06	0.06	0.05	0.07	0.05
Aug	0.07	0.06	0.06	0.07	0.06	0.07	0.07
Sep	0.07	0.06	0.06	0.06	0.06	0.08	0.06
Oct	0.07	0.07	0.07	0.07	0.07	0.06	0.08
Nov	0.08	0.08	0.08	0.08	0.09	0.06	0.09
Dec	0.09	0.11	0.11	0.10	0.11	0.06	0.12

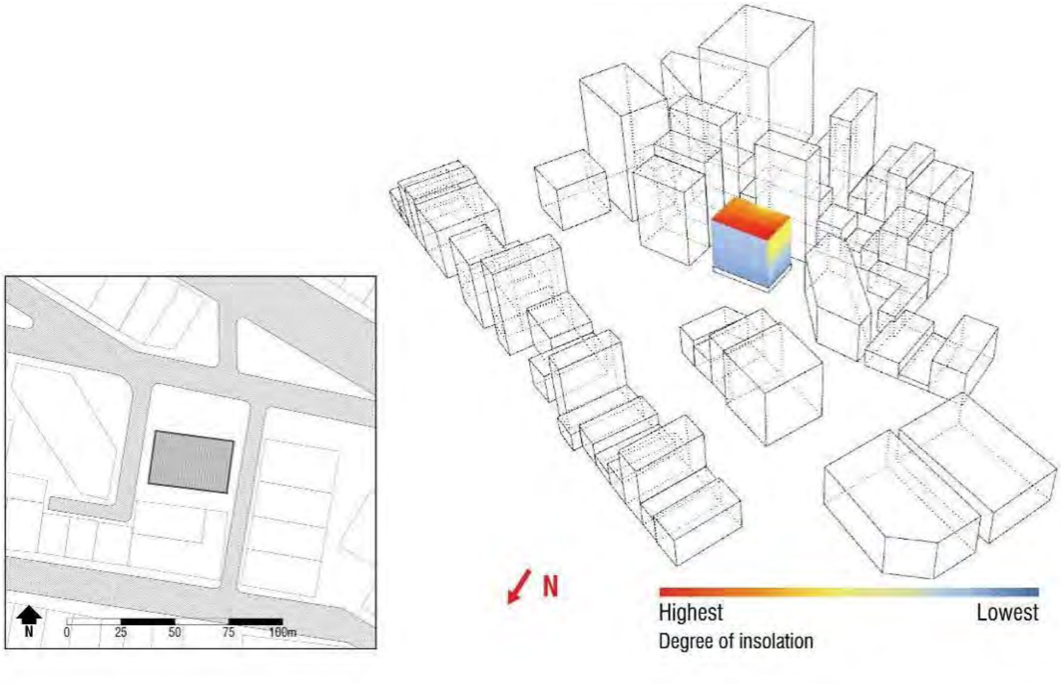

Figure 5.1: Aerial view showing surface insolation pattern for AGB above Ground Floor level. The streetside facade is the north facade, and a much higher building to its south causes overshadowing, affecting solar potential.

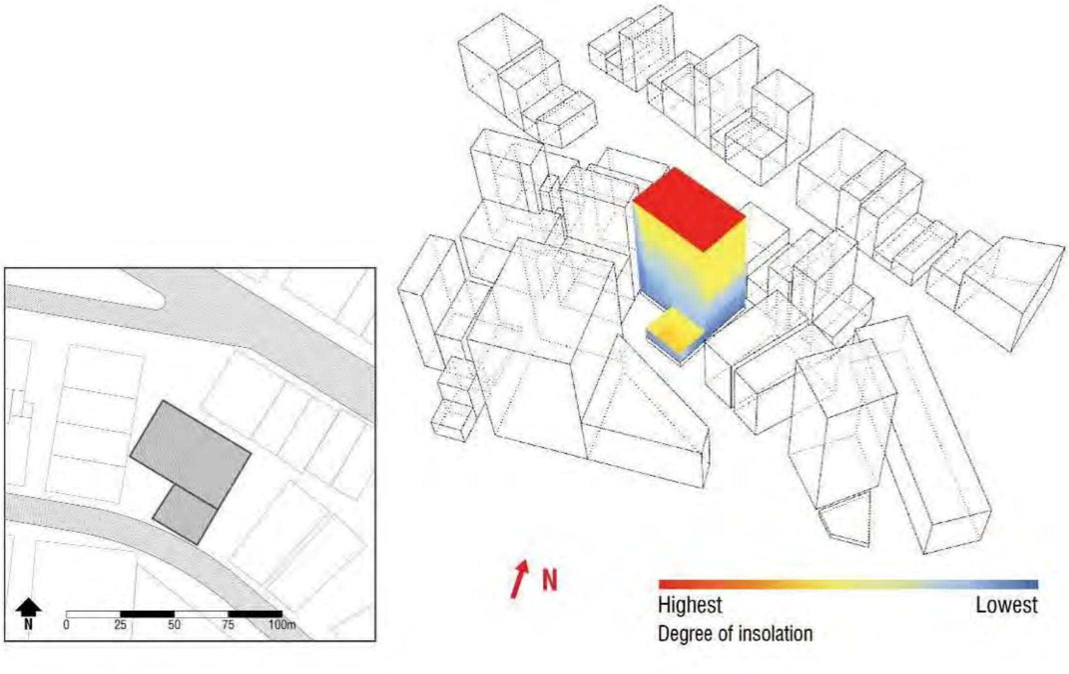

Figure 5.2: Aerial view showing surface insolation pattern for BCIC above Ground Floor level. The streetside facade faces south, but a higher building on the other side of the street causes overshadowing in the lower part.

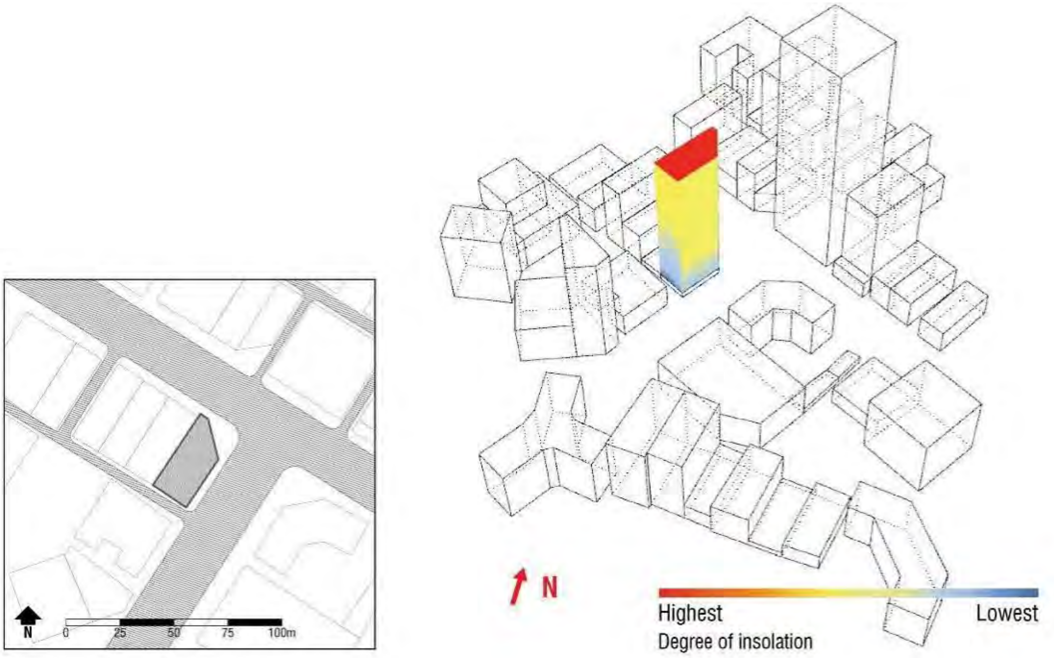

Figure 5.3: Aerial view showing surface insolation pattern for JBB above Ground Floor level. In terms of solar potential, JBB takes maximum advantage out of its openness to the south, and a non-shaded roof.

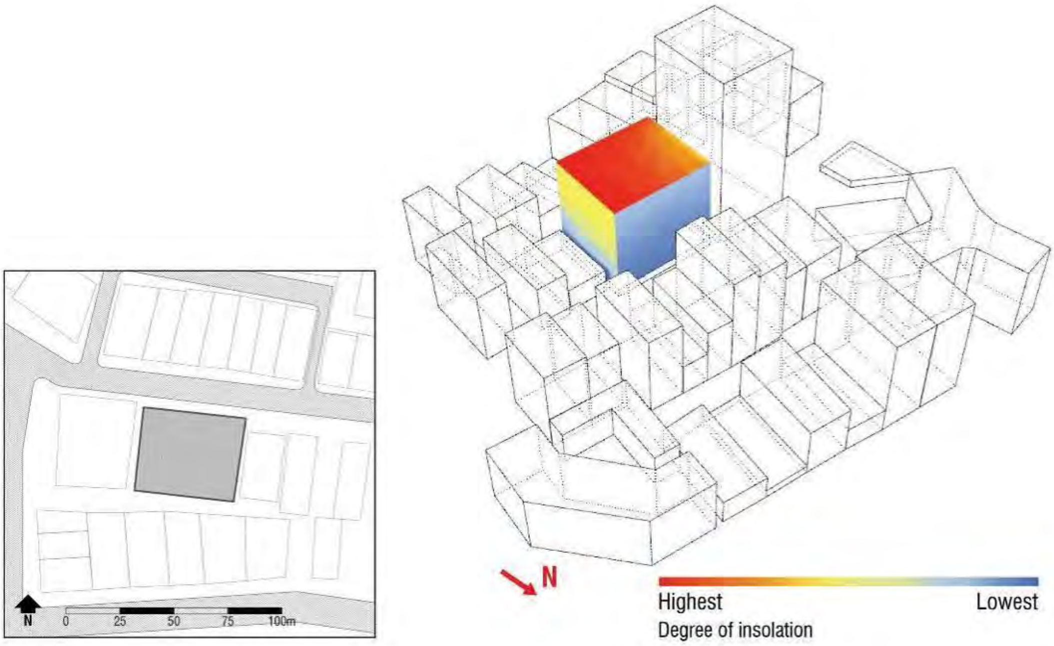

Figure 5.4: Surface insolation pattern for KRB above Ground Floor level. KRB's streetside facade is the north facade, and its west facade and roof is shaded by a much higher building to its west, undermining its solar potential.

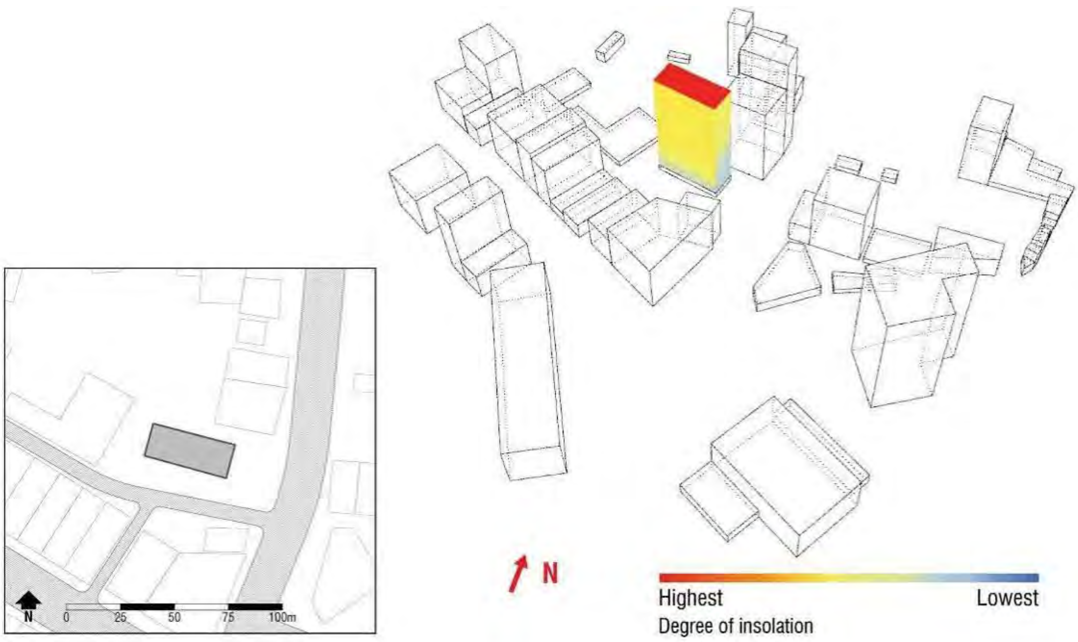

Figure 5.5: Surface insolation pattern for NCC. Solar energy production can be maximized because a wider facade of the building face minimally obstructed south, and its relative height ensures its roof is not shaded.

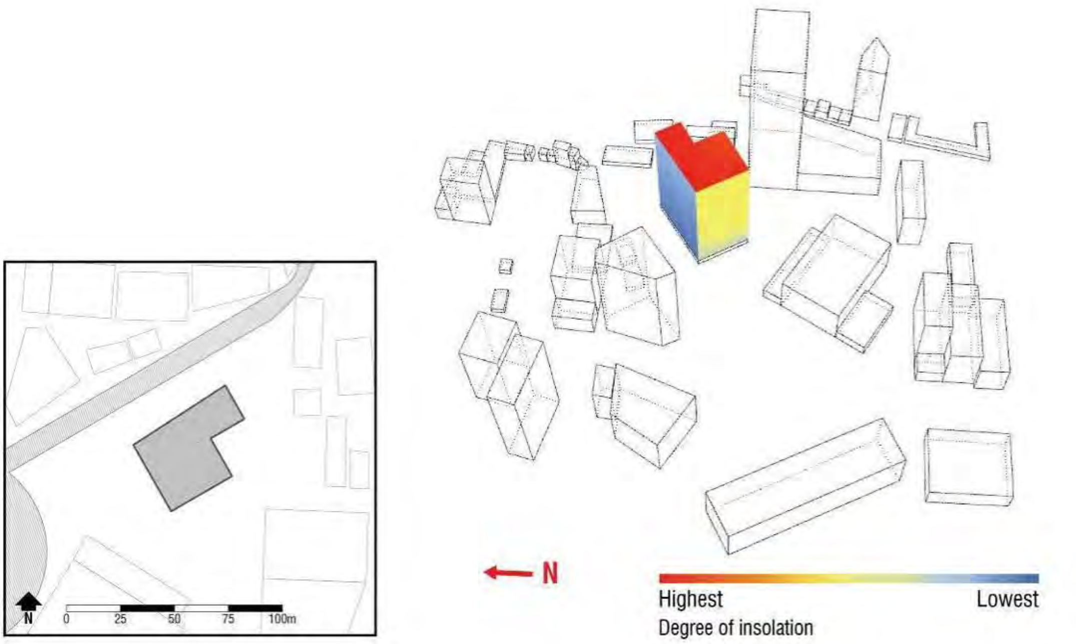

Figure 5.6: Aerial view showing surface insolation pattern for SKB. Although adjacent to the street, the building's largest facade faces the north and captures minimum insolation, which hurts its solar potential.

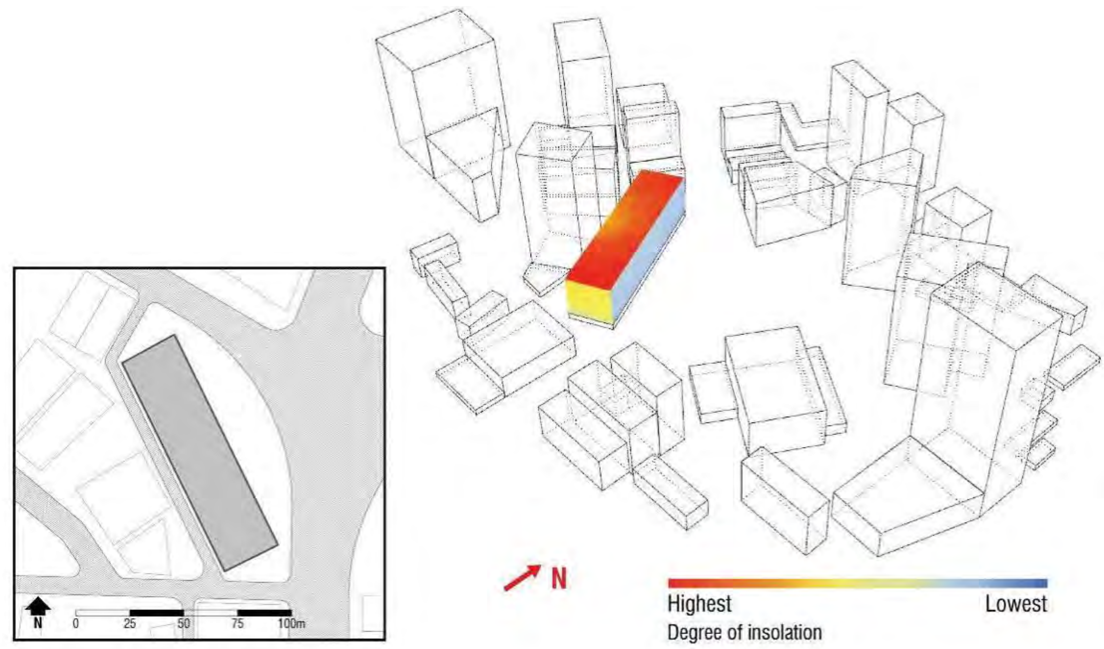

Figure 5.7: Surface insolation pattern for SBB. It is obvious that the roof is shaded partially by a building to its south-west, while insolation in its street facade, facing northeast, is poor.

Observations on building features that impact insolation on the buildings' surfaces are listed in Tables 5.6-8. Table 5.6 lists numerical data, whereas Tables 5.7 and 5.8 include qualitative information for each building. Figures 5.1-7 provide useful visuals that help the understanding of these data.

Table 5.6: Building feature study for seven buildings of MCA (1).

Building Name	Annual Energy Consumption Rate (E_r, kWh/m^2)	Annual Solar Performance Indicator (P.I. = E_{pv}/TFA kWh/m^2)	Possible Annual Energy Demand Met (%)	Ground Coverage (%)	Number of Stories	FAR = A_{bplot} / TFA	FSI = A_{plot} / TFA	Compactness Ratio (Comp = Env / TFA)
SBB	220	29	13.24%	65%	8	5.22	2.67	0.22
JBB	256	46	18.14%	48%	24	9.75	5.36	0.25
BCIC	284	22	7.86%	57%	20	9.07	7.00	0.17
SKB	233	27	11.68%	64%	21	13.45	5.55	0.17
KRB	328	24	7.36%	79%	12	9.51	8.12	0.18
AGB	248	20	8.19%	54%	10	5.89	3.32	0.23
NCC	213	43	20.07%	50%	20	10.00	5.09	0.23

Table 5.7: Building feature study for seven buildings of MCA (2).

Building Name	Orientation (Elongated along)[12]	Streetside Facade[13]	HVAC System	Overshadowing of South Facade[14]
SBB	NW - SE	EN	Split	Moderate
JBB	SW - NE	NE, ES	Split	Low
BCIC	WN - ES	SW	Split	High
SKB	WS - EN, L-shaped	NW, WS, SW	Central	Moderate
KRB	W - E, Square	N	Split	High
AGB	W - E	N	Split	High
NCC	W - E	E, S	Central	Low

Table 5.8: Building feature study for seven buildings of MCA (3).

Building Name	Relative Height of Roof[15]	Setback Conditions[16]	Major Blockade for Insolation	Facade Shading Conditions
SBB	Low	Wide	Higher buildings toward west	Shaded by Recess
JBB	Very High	Wide	Minor	Shaded by Recess
BCIC	Moderate	Narrow	Surrounded by highrise buildings of similar height	Shading Device Used
SKB	Moderate	Wide	31-story building toward south-east	Bare Glass
KRB	Low	Narrow	22-story building immediate west	Large Shading Device
AGB	Low	Wide	19 story building immediate south	Shading Device Used
NCC	High	Wide	Lower buildings toward south	Floor Slabs Extended

[12] This denotes the axis the building is elongated along, which is defined by a straight line from any point inside one discrete 15° azimuth angle category to another as given in Figure 3.5 in Section 3.5.2.

[13] This denotes the discrete 15° azimuth angle category outward facade normals direct to.

[14] 'High' refers that at least 75% of south-facing facades are shaded and unsuitable for PV deployment, while 'Moderate' and 'Low' accounts for 31-74% and <30% respectively.

[15] 'Very High' refers that the building is the tallest among the considered surrounding buildings; 'High' describes there are up to 2 surrounding buildings that are as tall or taller, 'Moderate' means that there are 3-6 surrounding buildings that are as tall or taller; 'Low' stands for buildings that are lower than most surrounding buildings.

[16] 'Wide' refers that all surrounding buildings maintain a minimum of 6m distance from the reference building, while 'Narrow' suggests that there is at least one that does not.

5.2.4 Analysis: Monthly Comparison

Figure 5.8 shows a graph with Monthly Solar Fraction (S_{mo}) plotted against each month as enumerated in Table 5.5. It is obvious from the concentration of data points that the S_{mo} values follow a general trend, which is depicted in Figure 5.9 with a polynomial regression line of order 3. This also helps to identify possible anomalies in the obtained data, for example, in June and in the particular case of AGB, which was previously observed in Figures 4.17 and 4.19.

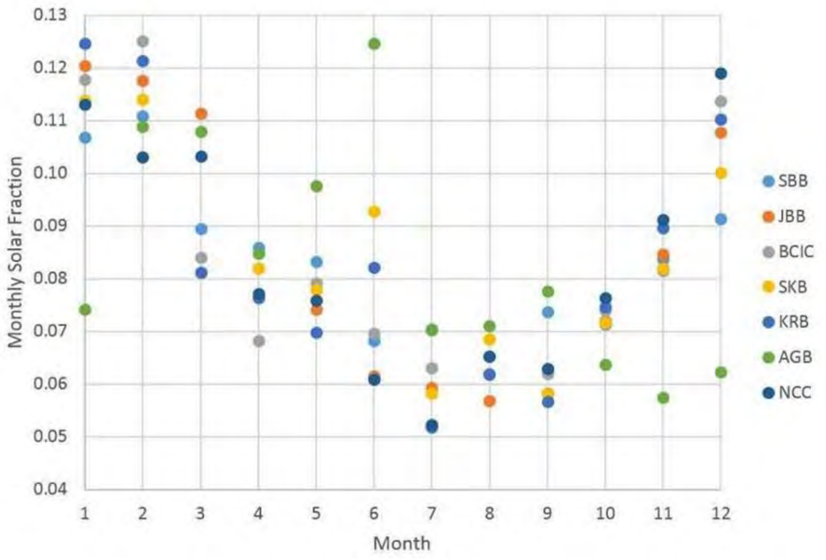

Figure 5.8: Fluctuations in the rate of solar contribution to meeting monthly energy demands depicted in a S_{mo} vs month-value graph.

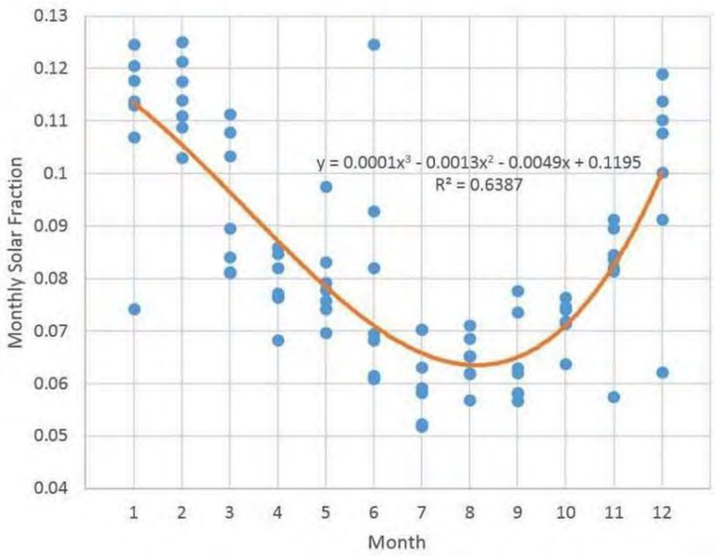

Figure 5.9: Trendline showing the pattern of fluctuation in monthly solar contribution over the year.

Key observations are:

1. Despite the sun's southward inclination, shortened days, and a reduction in solar intensity, PV solar systems can take advantage of clear skies and consistent sunshine in the months of December, January, and February to produce nearly as much electricity as in the months of June, July, and August (see Table 5.1-4).

2. Energy consumption heavily affects solar performance. Since energy consumption is low during December, January, and February, it results in a sharp increase in the possible energy demand met using PV systems. Figure 5.9 shows that S_{mo} values drop drastically in mid-year due to high levels of energy consumption and overcast skies impacting insolation.

3. A polynomial regression line of order 3 shows a good fit (R^2 = 0.6387) to the data points in the graph in Figure 5.9, which plots all S_{mo} values against month values. The curve is lopsided, implying that the lowest values of S_{mo} are found in late mid-year.

4. The highest proportion of energy demand met by solar energy is observed in January and the lowest in August. Moreover, the contribution of solar energy rises at a higher rate from August to December. In December, solar energy can make the third-highest contribution after January and February.

5. Weather variables impact both energy consumption and solar energy harvesting, and thus monthly solar contribution is also a combined effect of weather variables.

Monthly solar contribution to meeting energy demands can be predicted using a polynomial order 3 regression equation, provided the solar contribution of a particular month is known. This has been discussed in Section 6.3.2.

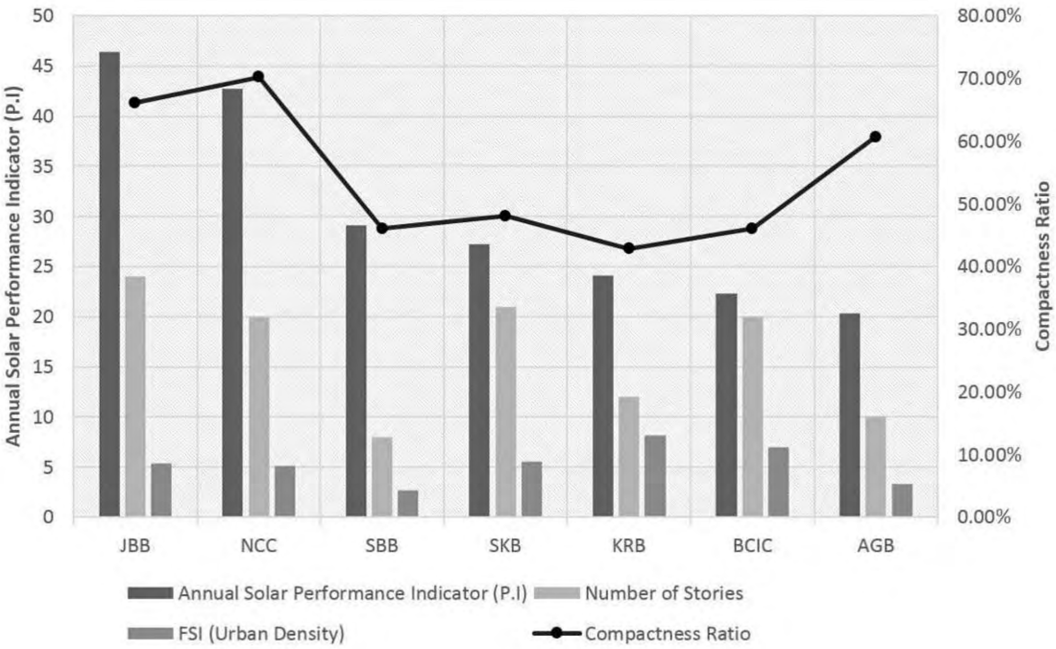

Figure 5.10: Multiple-axes graph visualizing numerical building data from Table 5.6 in descending order of the buildings' Annual Solar Performance Indicator (P.I.) from left to right.

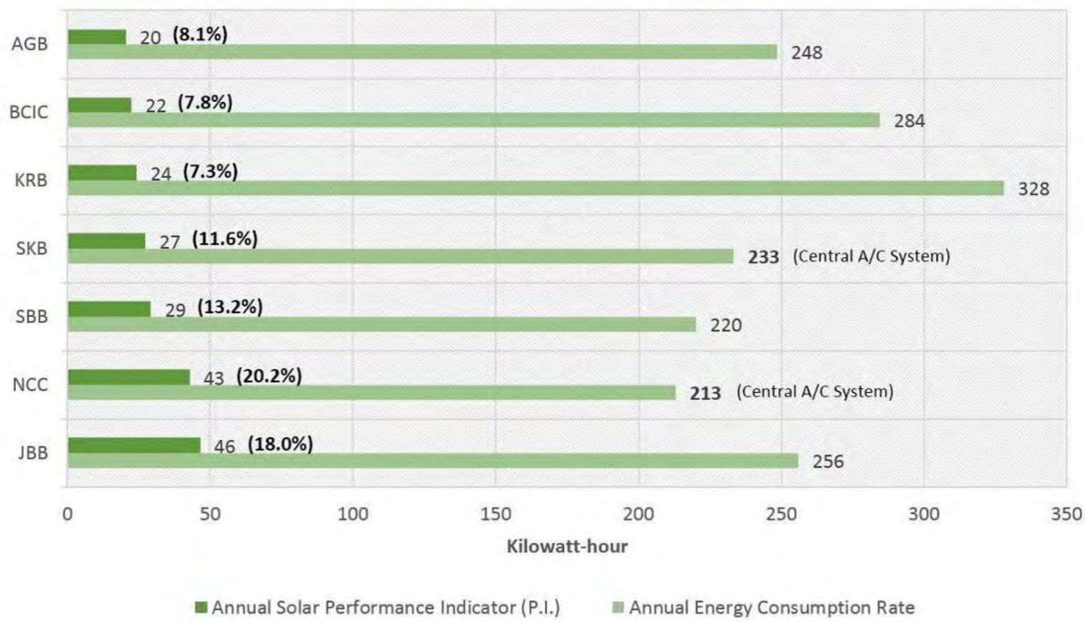

Figure 5.11: Graph showing the proportion of each building's possible yearly electricity generation using PV to the buildings' Annual Energy Consumption.

5.2.5 Analysis: Building-wise Comparison

Four building parameters, namely Annual Solar Performance Indicator (P.I.), Number of Stories, Urban Density (Floor Space Index - FSI), and Compactness Ratio from Table 5.6 are visualized in descending order of the buildings' Annual Solar Performance Indicator (P.I.) from left to right in Figure 5.10. The observations are given below:

1. Urban Density (FSI) shows an increasing trend, while Compactness Ratio shows a decreasing trend from left to right.

2. AGB has both a comparatively lower value of FSI and a comparatively higher value of Compactness Ratio, yet showing minimum solar potential per unit floor area. This can be explained from the observations given in Tables 5.5 and 5.6: AGB's only streetside facade is the North facade; the overshadowing of the south facade is maximum due to the impact of a much higher building to its south; the height of its roof with respect to its surrounding buildings is low – all affecting insolation.

3. In the cases of SKB and BCIC, the roof height is moderate compared to the surroundings, which affects facade insolation. Thus, despite being 20 or more stories in height, SKB and BCIC have lower solar potential (E_{pv}) per unit floor area compared to their tall counterparts such as JBB and NCC. This suggests that relative height is a key parameter.

4. Buildings to NCC's south impact its solar potential, resulting in lower P.I. than JBB, which enjoys unobstructed south. Therefore, the degree of shading received by the south-facing surfaces is an important factor.

5. Central A/C systems are more energy-efficient than split systems. Figure 5.11 shows that NCC takes the biggest advantage from PV systems to meet its energy demands – estimated to be 20.2%. This is because its energy consumption is relatively lower than other buildings. It takes significant advantage of its Central A/C system and its elongation along the East-to-West axis – significantly reducing solar heat gain.

6. Among other studied buildings, SKB also has a Central A/C system while having the third-lowest energy consumption figures; and SBB, having the second-lowest energy consumption figures, is not fully air-conditioned like the remaining studied buildings. It is evident from Field Investigation that A/C systems are responsible for the majority of energy consumed in commercial office buildings in MCA.

7. A low-rise building has a greater chance of having its surfaces overshadowed by other buildings. Nevertheless, SBB performs the third best in terms of solar potential despite being a low-rise building with a low compactness ratio – the reason can be attributed to its low FSI figures (see Figure 5.10).

5.2.6 Discussion on Key Findings

The principal observations from this study are listed below:

Building Height: Although tall buildings have relatively lower chances of being fully shaded by other buildings, higher buildings tend to show potentially lower solar performance (P.I.). Since taller buildings have a lower roof-to-facade area ratio, their solar performance is affected because roofs or horizontal surfaces dominate in terms of solar potential as opposed to facades or vertical surfaces.

Relative Height: Relative building height was found to be an important parameter, because the higher the building with respect to the surroundings, the lower is the chance for the roofs and facades to be shaded by surrounding buildings. This also implies that facades have a significant role in the solar potential of individual buildings.

Orientation: Although a building's orientation is not directly linked to solar irradiation in buildings, the key issues to consider are the degree of its openness to the south and the percentage of surface area facing open south. When the facade with the largest surface area faces the south without being obstructed by other buildings, the building's solar potential is maximized due to a higher degree of insolation.

Compactness Ratio: Compactness Ratio was found to have a positive effect on solar potential, subject to key issues of urban configurations such as urban density (FSI), relative building height, surrounding buildings shading the south-facing facades, and orientation of the streetside facade, etc.

Streetside Facade: The streetside facades of a building are of crucial importance. When these facades face the south, solar potential receives a boost. When they face the north, solar potential is affected.

To sum up, solar potential, when observed for the individual building in terms of its energy consumption, is not influenced strictly by any single factor but by the combined effect of several factors that regulate urban space.

5.3 Simulation Study of Existing Districts

This section deals with the solar potential study of existing business districts in Kawran Bazar and MCA. A 500m x 500m area was modeled for each district, and the possible amount of electricity that can be generated using PV systems was determined. 500m x 500m is the grid size for urban areas for carbon-emission studies (Dai, et al., 2020), and it complies with the Low-carbon Economy (LCE) concept. This area definition was also used in previous studies on the solar potential of urban areas (Brito, et al., 2017). Therefore, this area was deemed optimum for studying the district-level dynamics of solar potential and related factors such as surface orientation, street orientation, and density.

5.3.1 Criteria

Simulations were run only on an annual basis, taking all buildings within the area as the Test Geometry, with only the ground plane serving as the Context Geometry. The ground floor facade was omitted from calculations like all other experiments, but for single-story structures, the roof areas were considered separately for analysis. The Grasshopper script used for analysis is given in Figure D3 in Appendix D.

5.3.2 Input and Output

The input parameters for simulation are outlined in Section 3.4.2. In this experiment, separate simulations were carried out on a number of surface categories. Among horizontal surfaces, single-story buildings' roofs were categorized as Low Roofs (LR), and all higher roofs as Roofs (R). Vertical surfaces, i.e. facades were classified into 12 distinct categories: N, NE, EN, E, ES, SE, S, SW, WS, W, WN, and NW.[17] The integrated parametric interface generated the yearly PV potential for each model's constituent vertical and horizontal surface categories from the grasshopper script used.

5.3.3 Results and Observation

The amount of electricity that can be generated from PV deployment in each surface category is documented in tabular form in Tables 5.9 and 5.10. The overall PV potential of each district is compared on the basis of urban parameters such as Urban Density (FSI) in Table 5.11.

Table 5.9: Simulation output for various surface categories in KB district model and an estimation of their summation.

Surface Categories	Total Surface Area (m^2)	Qualified Surface Area (m^2) (>650 kWh/m^2)	Qualified Surface Percentage (%)	Electricity Generated from PV (GWh/year)
Roofs (R)	69580	69580	100	11.01
Low roofs (LR)	27481	27481	100	4.42
N	25485	0	0	0.00
NE	916	0	0	0.00
EN	33845	1281	3	0.08
E	25508	9707	38	0.68
ES	1640	571	34	0.05
SE	37695	17977	47	1.48
S	18728	8201	43	0.66
SW	357	229	64	0.02
WS	32396	17800	54	1.30
W	29063	11793	40	0.81
WN	297	0	0	0.00
NW	25485	0	0	0.00
TOTAL	*328477*	*175999*	*53*	*20.51*

[17] This categorization has been executed according to the direction of their outward surface normals falling within separate azimuth angle groups Figure 3.5 in Section 3.5.2

Table 5.10: Simulation output for various surface categories in MCA district model and an estimation of their summation.

Surface Categories	Total Surface Area (m²)	Qualified Surface Area (m²) (>650 kWh/m²)	Qualified Surface Percentage (%)	Electricity Generated from PV (GWh/year)
Roofs (R)	76999	76999	100	11.61
Low roofs (LR)	13304	13304	100	1.69
N	43786	0	0	0.00
NE	28532	0	0	0.00
EN	4846	62	1	0.00
E	55569	13934	25	0.97
ES	41223	16464	39	1.24
SE	4995	3888	77	0.30
S	44589	19796	44	1.62
SW	27786	16569	59	1.23
WS	3989	2504	62	0.20
W	54558	15994	29	1.08
WN	44936	868	1	0.05
NW	43786	0	0	0.00
TOTAL	*488898*	*170368*	*35*	*19.98*

Table 5.11: Comparison of data outcome of existing district simulation.

District Name	MCA	KB
Study Area	250000	250000
Total Floor Area (TFA)	654557	535990
Total Building Plot Area (m^2, approx.)	112878	121327
FAR	5.80	4.42
FSI	2.62	2.14
E_{pv} (GWh)	19.98	20.51
Facades' Contribution	33.46%	24.72%
E_{pv}/TFA (kWh/m^2)	30.52	38.26
(E_{pv}/TFA) x FAR	177.00	169.01
(E_{pv}/TFA) x FSI	79.92	82.02

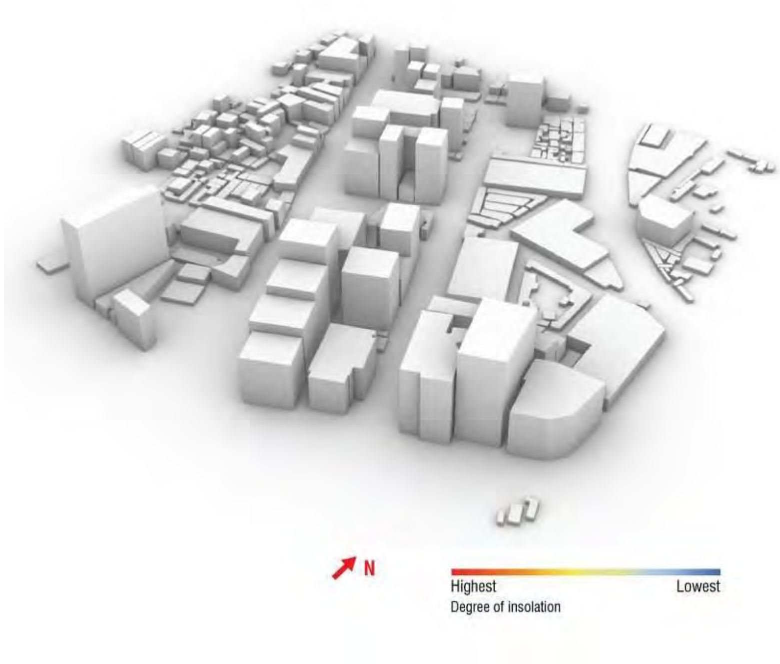

Figure 5.12: Rhinoceros model for a 500mx500m area in Kawran Bazar (KB).

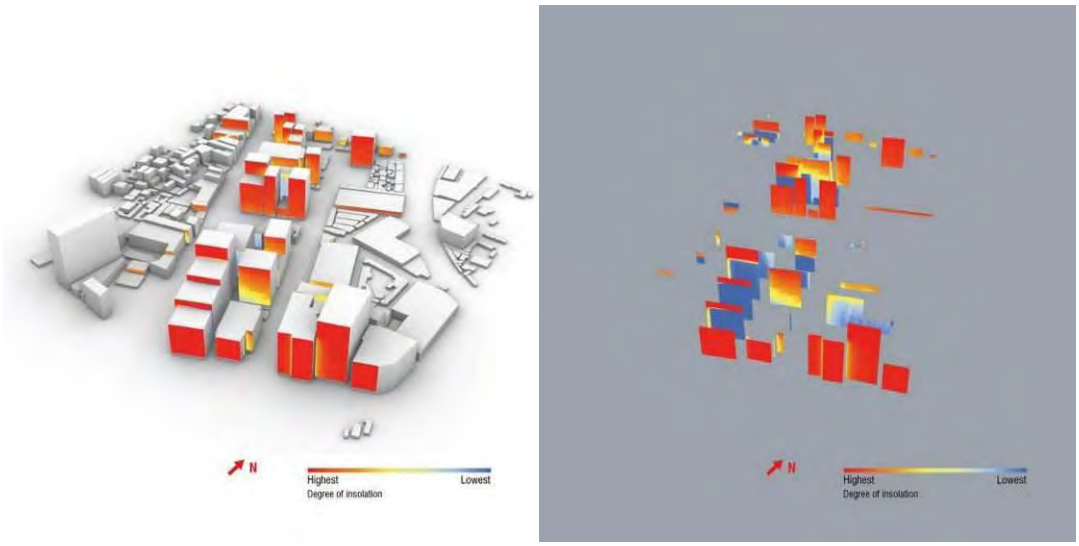

Figure 5.13: Insolation pattern for the "SE" surface category of KB district model (left image) and the SE surfaces separated from model to reveal overshadowing due to poor setback (right image).

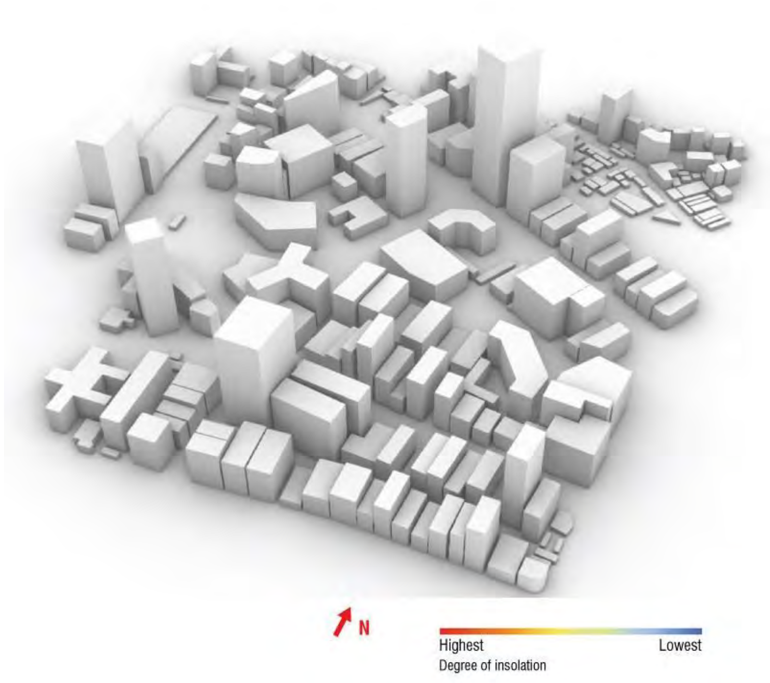

Figure 5.14: Rhinoceros model for a 500mx500m area in Motijheel Commercial Area (MCA).

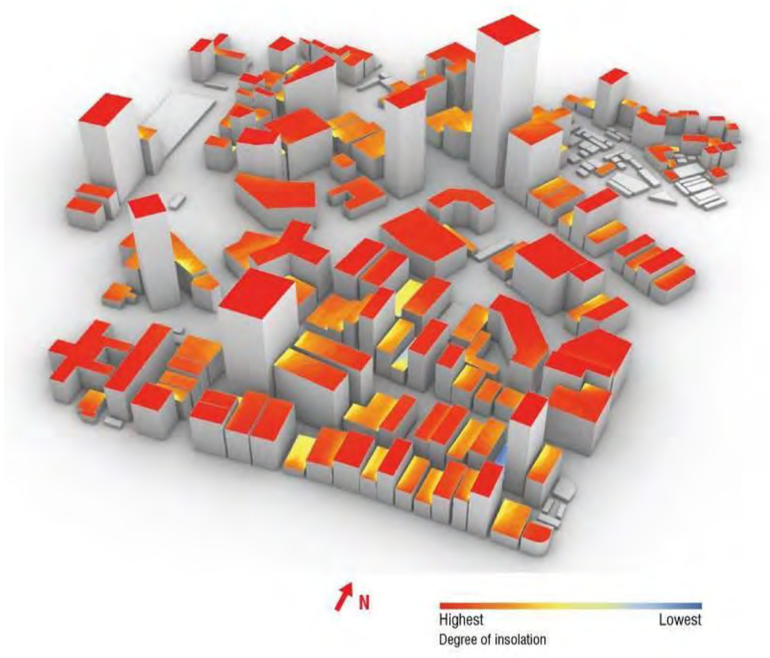

Figure 5.15: Insolation pattern for the "R" surface category of MCA district model, all of which are qualified for PV deployment.

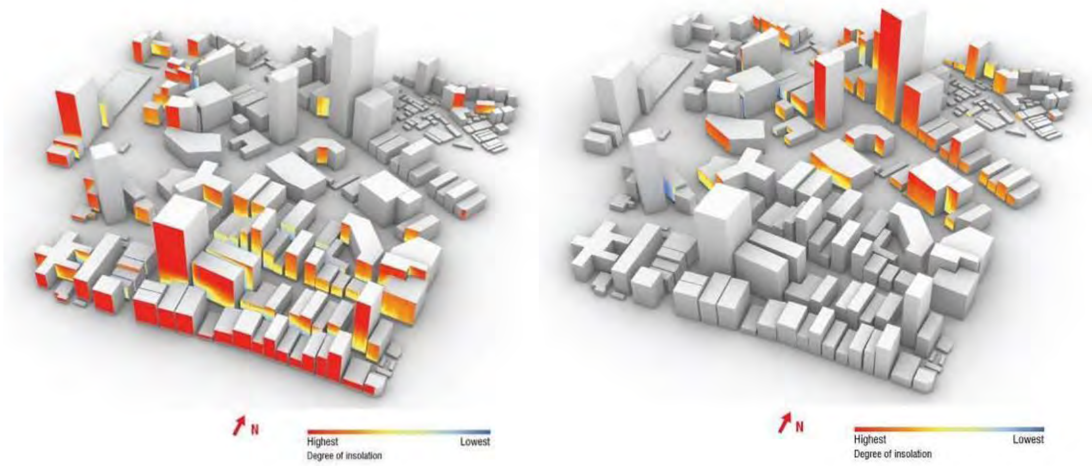

Figure 5.16: Insolation pattern for the "S" (left) and "SW" (right) surface category of the MCA district model. Surfaces of these categories are abundant due to the orientation of primary streets in the district.

5.3.4 Analysis

The contribution of each facade category to solar potential, as listed in Figures 5.9 and 5.10, can be better evaluated from the pie charts given in Figures 5.17 and 5.18. The major observations are:

- Almost all north-oriented surfaces (N, NE, EN, WN, NW) are unsuitable for PV deployment in the case of both districts (see Figures 5.17 and 5.18). All such surfaces have their outward surface normals within 37.5° CW/CCW rotation of absolute north azimuth.
- However, other facades contribute significantly (33.46% for MCA and 24.72% for KB; see Table 5.11) to the overall PV potential and are therefore very important to consider in district planning.
- Street orientation is a major factor in urban districts that regulates facade orientation and the overshadowing of facades. Streets running in the East-west direction resulted in a huge array of streetside facades facing south in MCA, while streets running along north-south resulted in the overshadowing of south facades (see Figure 5.13).
- FSI and FAR affect solar potential, which is why KB performs better (see Table 5.11). The (Epv/TFA) x FAR and (Epv/TFA) x FSI figures are

similar for both districts, implying that solar performance has a strong relationship with both FAR and FSI.

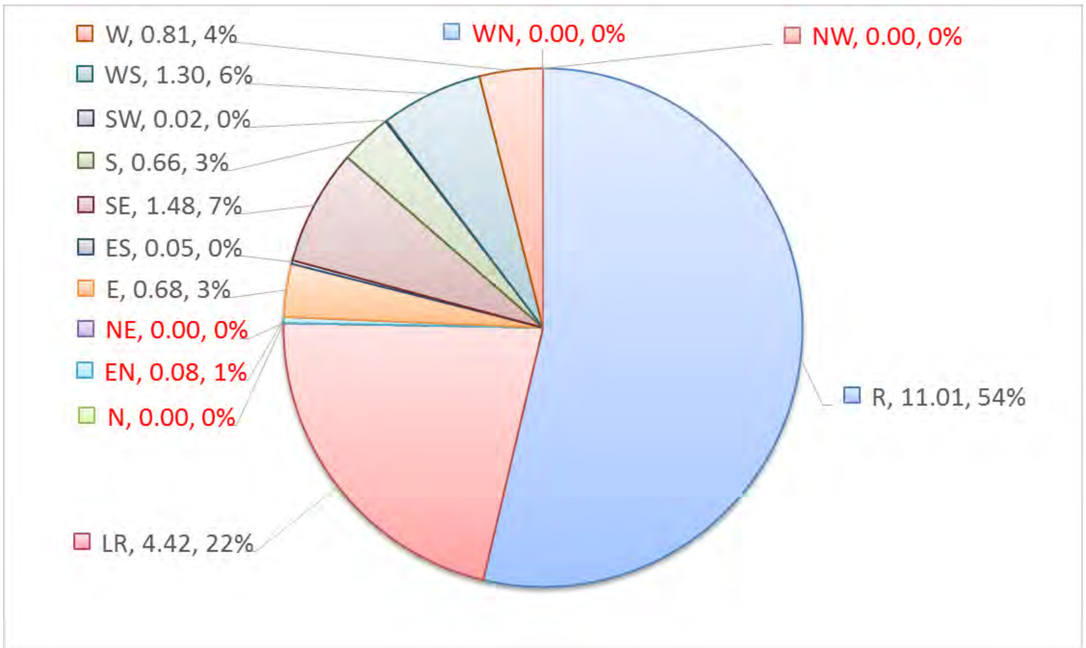

Figure 5.17: Pie chart illustrating the distribution of E_{pv} (GWh) across surface categories for KB highlighting dominant contribution of roofs (R and LR).

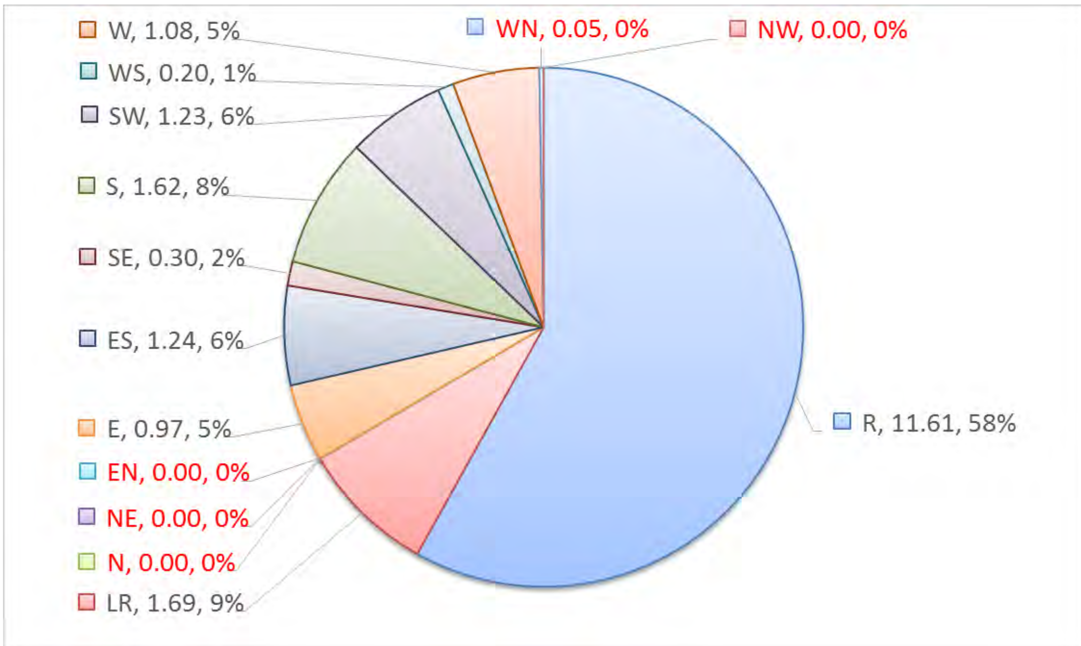

Figure 5.18: Pie chart illustrating the distribution of E_{pv} (GWh) across surface categories for MCA highlighting dominant contribution of roofs (R and LR).

5.3.5 Discussion on Key Findings

Below are the principal findings from the study:

Dominant Surface for PV Deployment: With facades accounting for 33.46% of the solar potential for MCA and 24.72% for KB, roofs or horizontal building surfaces dominate in terms of solar potential. However, in terms of total qualified areas (surfaces with irradiation of more than 650 kWh/m^2/year are deemed suitable for PV deployment), facades have 49.94% for MCA and 41.01% for KB (see Table 5.12). From the detailed figures given in Table 5.8, Table 5.12 summarises and compares overall numbers for Roofs and Facades. It is observed that roofs generate more electricity annually from comparatively less area and hence fewer PV panels, and are therefore more efficient and economic for solar harvesting. As described in Section 2.4.2, the use of optimum tilt angles for PV panels can further increase efficiency. Facades can also make use of tilt angles, for example, by using PV panels as shading devices or on top of shading devices, but in that case, the effect of mutual shading is likely to be more influential than when placed on the roofs due to the inclination of the sun.

Table 5.12: Contribution to overall solar potential and total PV deployment areas on roofs and facades for business districts MCA (Motijheel Commercial Area) and KB (Kawran Bazar).

District	MCA	KB
Total Qualified Surface Area (m^2)	180382	164621
Total Qualified Roof Area (m^2)	90303	97062
Total Qualified Facade Area (m^2)	90079	67559
Total Qualified Roof Area / Total Qualified Surface Area	50.06%	58.96%
Total Qualified Facade Area / Total Qualified Surface Area	49.94%	41.04%
Roofs' Contribution to Solar Potential	66.54%	75.28%
Facades' Contribution to Solar Potential	33.46%	24.72%

Omission of North Facade for PV Deployment: Little or no qualified surface areas for PV deployment could be identified among the facades with outward surface normals within a range of 75 degrees in the North, i.e. 37.5 degrees of both CW and CCW rotations from the absolute North azimuth. Therefore, these facades can be omitted for PV deployment.

Street Orientation: Street orientation is responsible for facades facing a particular direction. Since streetside facades are more suitable for solar harvesting than other facades, it is important to orient these facades to the south, which could be advantageous for solar harvesting. In the study of existing districts, streets running in the East-West direction were responsible for most of the qualified facade areas facing the south. This phenomenon was observed in the case of MCA, with the district having a superior solar potential. In the case of KB, however, a major street runs in the North-South direction, which causes overshadowing of south facades (see Figure 5.13).

Dominant Facades for PV Deployment: South facades were found to be performing better than other facades, especially the facades having surface normals within a range of 45° in the south i.e. 22.5 degrees CC and CCW rotation from the absolute south. Therefore, buildings, urban blocks, or districts having more unobstructed south facades should have an advantage over the ones that do not.

Urban Density: Urban Density (measured in FSI – Floor Space Index) is also found to have a negative effect on solar potential at the district level, after showing the same relationship at the building level.

Simulation study on existing districts showed that district solar potential is the complex effect of many factors combined, among which the effect of street orientation was prominent. Besides, the solar potential of various surface categories highlighted the efficiency of select surfaces such as roofs and south facades, which, if overshadowed, cause solar potential to drop drastically.

5.4 Simulation Study on Projected Districts

This section elaborates experimentation with a generic urban block commonly found in the newly planned commercial zones of Purbachal New Town proposed by RAJUK, Dhaka's Development Authority. This experimentation records, observes, and analyzes simulation responses in terms of solar potential to varying parameters of the urban block. Simulations were conducted using the same integrated parametric interface that was utilized in previous experimentations.

5.4.1 Criteria

The masterplan of Purbachal New Town utilized for finding a generic commercial urban block is given in Figure G1 in Appendix G. This masterplan offers the arrangement of plots of different sizes and combinations. A common arrangement of plots from the commercial zones was followed for modeling the urban block, an instance of which is given in Figure 5.19. The plot arrangement and street layout, which remain unchanged throughout the experiment, have been shown in Figure 5.20. Besides, Figure 5.20 also illustrates how some of the parameters used in the analysis were defined.

Figure 5.19: An instance of projected district model in Rhinoceros used for experimentation. The large open spaces are generated by streets around the reference urban block in the middle.

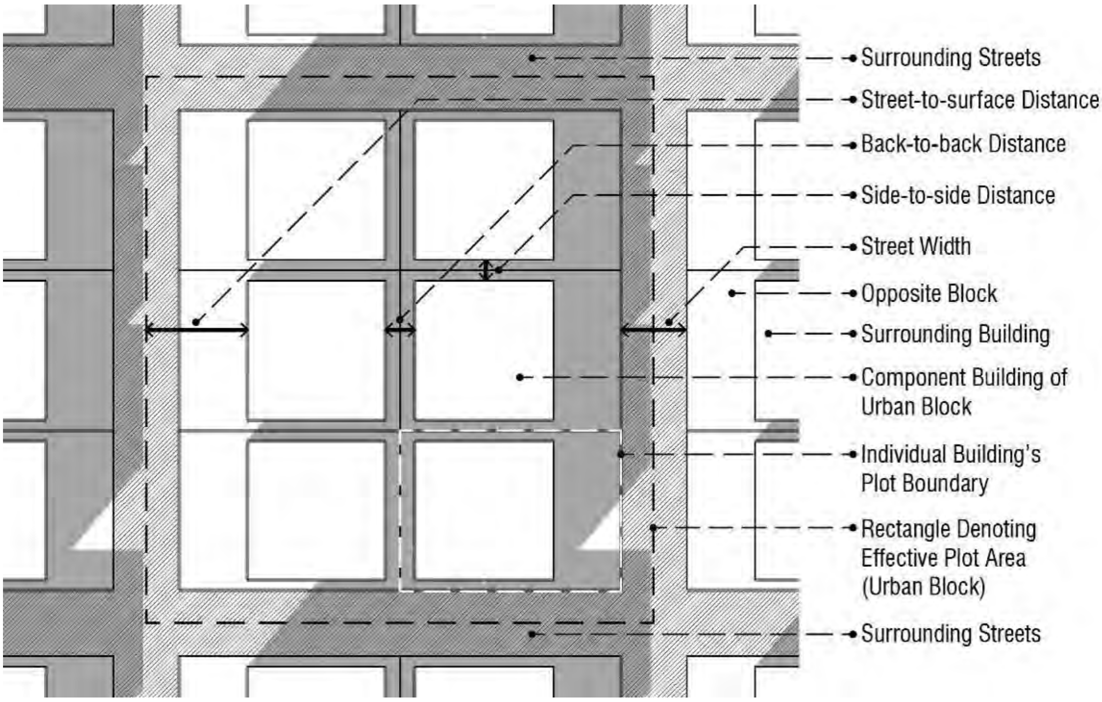

Figure 5.20: Site plan showing the plot boundaries for each building and the location of the street, and the demarcation of urban block parameters.

The generic urban block selected for the study consists of six buildings of the same height, each with a plot size of 21.95m x 30.48m, for every instance of simulation. The non-variation of height is justified because the FAR rule proposed by INB2008 restricts building height and a common tendency of the property owners is to take the maximum advantage out of the FAR rule. Throughout the experimentation, a minimum street width of 9.0m was kept fixed as per the recommendation of INB2008 for the particular plot size (GOB, 2008). Identical blocks were considered as surroundings, and therefore, identical buildings were set up on the other side of the street. The building layout was square. These features were maintained so that no particular orientation gets an undue bias in terms of solar potential. A 30° clockwise rotation was performed 5 times for obtaining 6 orientation instances of the projected district, all buildings' Ground Coverage (GC) was reduced 3 times for getting 4 instances of GC, all buildings were moved 2.62m closer to its access street 3 times so that there are 4 instances of the distance of the streetside surface from the street (see Street-to-surface Distance in Figure 5.20), and five instances of building height from 10 stories to 14 stories were included. Thus, there were in total 6 x 4 x 4 x 5 = 480 projected district models for which simulations were performed. Varying GC and Street-to-surface Distance (refer to Figure 5.20) results in changes in Side-to-side Distance and Back-to-back Distance (refer to Figure 5.20). The Grasshopper script used for each simulation is given in Figure D1 in Appendix D.

5.4.2 Input and Output

The input parameters for simulation are outlined in Section 3.4.2. For this experiment, all simulations were carried out on an annual basis to find out the yearly solar potentials of each instance of projected districts. All surfaces of the six buildings of the reference urban block were added as test geometry barring ground floor surfaces, while all other geometries in the projected district model including buildings on the opposite side of the street, ground floor facades, and the ground plane were considered as context geometry for simulation using Grasshopper and Ladybug. For each simulation, the Grasshopper script generated solar radiation mapping of the test geometry, along with an estimation of the amount of electricity that can be produced from PV systems. Figure 5.21-26 shows 2 separate cases of projected districts with varied numbers of GC and Street-to-surface Distance. 3 variations of building height are depicted for each case, and all 6 instances were rotated 90 degrees (clockwise/counterclockwise) from their default orientation (the longer block side facing absolute north and south azimuth directions was considered as the default orientation). GC, in this experiment, was considered as an urban block parameter and is different from GC when considered as a building parameter. This can be understood from Equations 2.4 and 2.5. The Effective Plot Area[18] ($\sum A_{plot}$) for calculating GC[19] for the urban block throughout the experiment is shown in Figure 5.20. The maximum allowable FAR in this case, according to INB2008, is 6.0 (GOB, 2008), which dictates building height as illustrated in

---

[18] Effective Plot Area is the summation of all plot areas (A_{plot}) of the urban block. Plot area refers to the building plot area (A_{bplot}) plus half the area of the adjacent street. See Section 2.6.1 for details.

[19] Ground Coverage of an urban block is the total footprint of all buildings of the block divided by Effective Plot Area. See Section 2.6.1 for details.

Table 5.12, where the corresponding Ground Coverage (GC) variations for this experiment are also included.

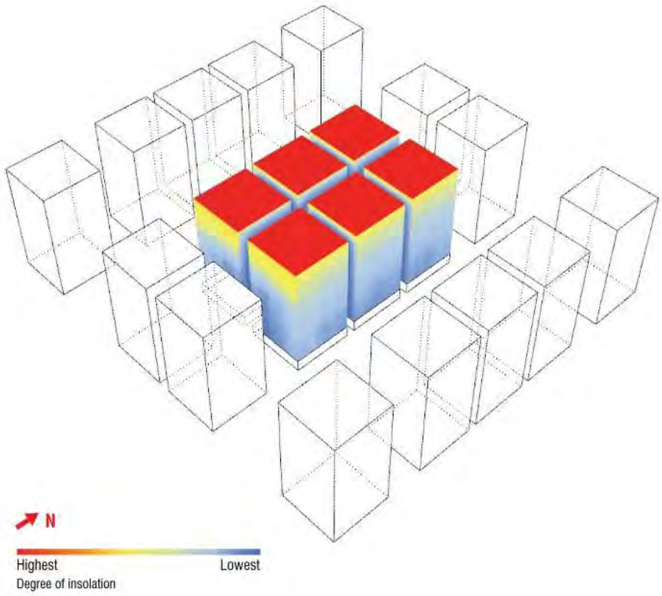

Figure 5.21: Insolation pattern for generic urban block with Ground Coverage = 41.81%, Street-to-surface Distance = 13.88, and Number of Stories = 10.

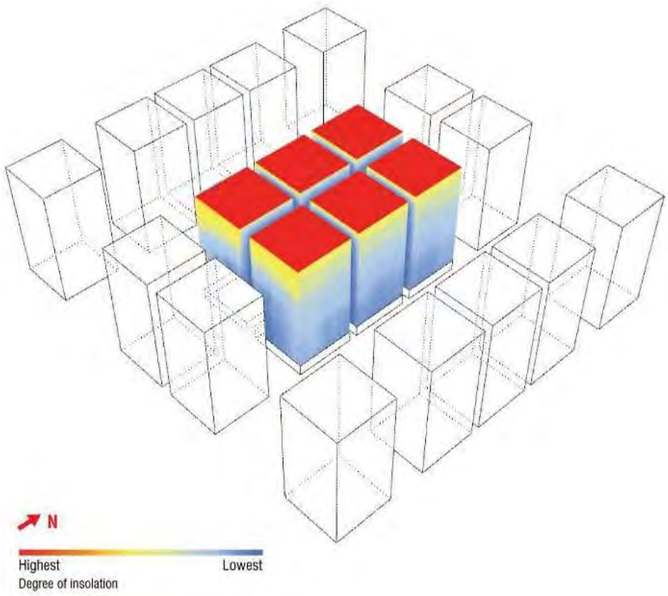

Figure 5.22: Insolation pattern for generic urban block with Ground Coverage = 41.81%, Street-to-surface Distance = 13.88m, and Number of Stories = 11.

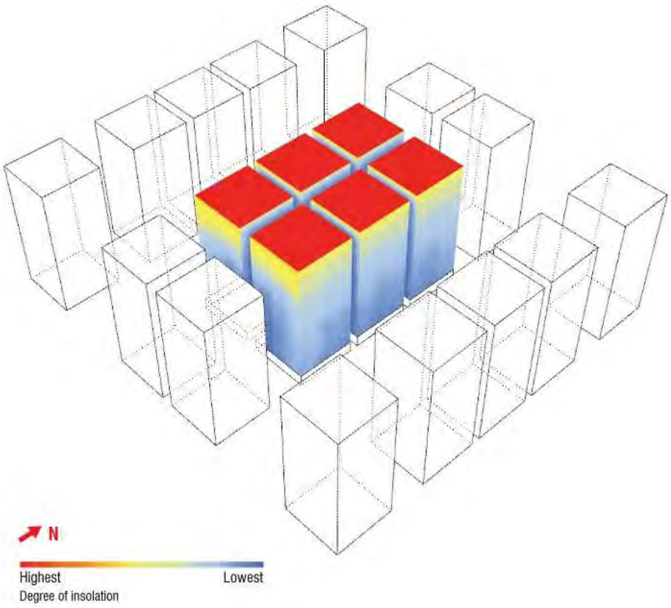

Figure 5.23: Insolation pattern for generic urban block with Ground Coverage = 41.81%, Street-to-surface Distance = 13.88m, and Number of Stories = 12.

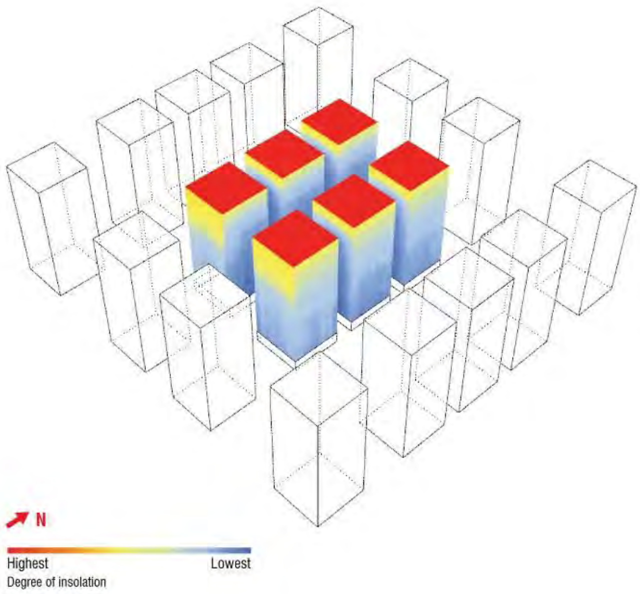

Figure 5.24: Insolation pattern for generic urban block with Ground Coverage = 35.38%, Street-to-surface Distance = 9.71m, and Number of Stories = 10.

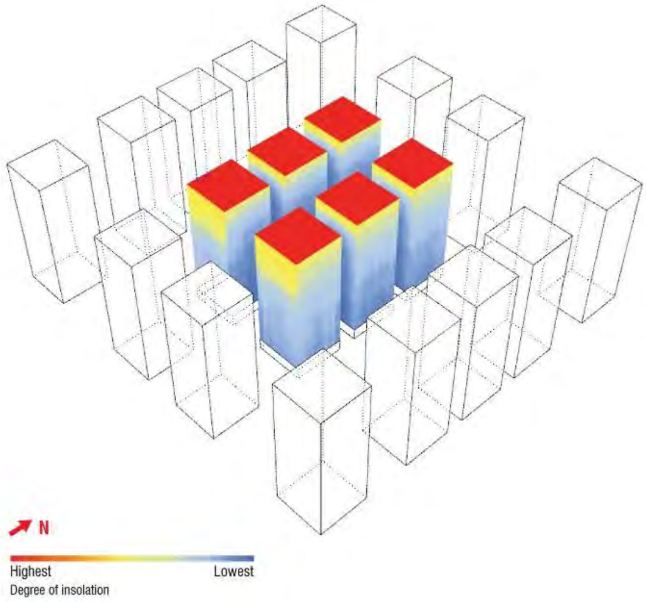

Figure 5.25: Insolation pattern for generic urban block with Ground Coverage = 35.38%, Street-to-surface Distance = 9.71m, and Number of Stories = 11.

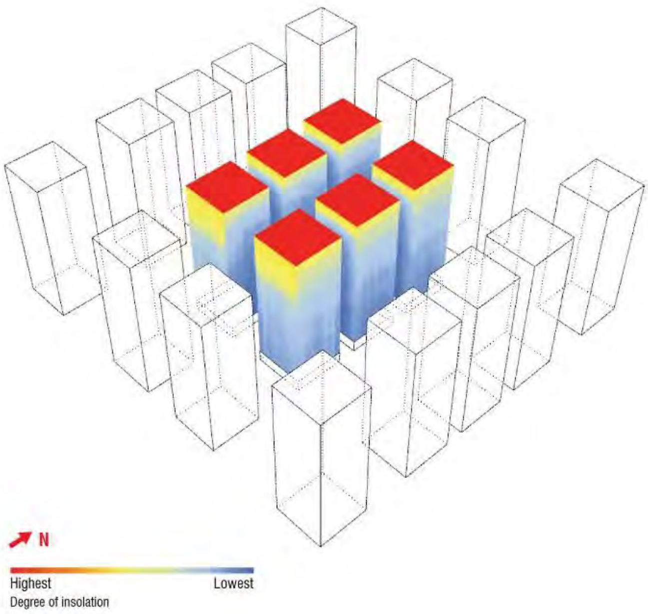

Figure 5.26: Insolation pattern for generic urban block with Ground Coverage = 35.38%, Street-to-surface Distance = 9.71m, and Number of Stories = 12.

Table 5.13: Ground Coverage (GC) values used in the experiment with projected districts and related parameters.

Ground Coverage (Building)	Ground Coverage (Urban Block)	Max. No. of Stories*	TFA (Building, m²)	TFA (Urban Block, m²)	Resulting Side-to-side Distance (m)**
54.55%	41.81%	11	4013	24080	2.84
50.00%	38.33%	12	4013	24080	3.66
46.15%	35.38%	13	4013	24080	4.38
42.86%	32.85%	14	4013	24080	5.01

* Maximum Number of Stories according to the Maximum Allowable FAR value of 6.0 recommended by INB2008.

** The minimum side-to-side distance according to INB2008 is 6m. Lower setback values were taken in favor of larger GC values for the square layout so that roof area is maximized.

It can also be observed from Table 5.13 that the Side-to-side Distance (see Figure 5.20) values change due to changes in GC values. Similarly, the Back-to-back Distance (see Figure 5.20) values change with changes in the GC and Street-to-surface Distance (see Figure 5.20) values due to the buildings' square layout. The minimum Back-to-back Distance used was 4.0m rising to a maximum of 12.9637m, whereas the minimum as recommended by INB2008 is 6m (GOB, 2008). On the other hand, the range of Street-to-surface Distance used was 6m – 14.9637m whilst the INB2008 minimum is 7.5m. However, the Back-to-back Distance parameter was not considered as an independent variable along with other parameters in data analysis. This is because when all three parameters including GC, Street-to-surface distance, and Back-to-back Distance are included as variables in a multiple linear regression analysis, the Back-to-back Distance variable's coefficient is returned zero.

5.4.3 Results and Observation

For each of the 480 instances, the Annual Solar Performance Indicator (P.I.) was calculated by dividing the Possible Annual Electricity Generation from PV (E_{pv}) figures (obtained from simulation) by Total Floor Area (TFA) of the urban block and was considered to be the dependent variable for data analysis. Seven variables, namely Number of Stories, Ground Coverage, Urban Density (FSI), Compactness Ratio, Street-to-Surface Distance, Side-to-side Distance, and CW/CCW Rotation of Azimuth Angle (°) were calculated for each instance of projected district models and were considered as independent variables. All these variables are listed in tabular form in Tables E13-17 in Appendix E, where each row represents the values of variables for a particular instance of a projected district model. It should be noted that the number of degrees was considered as the value for CW/CCW Rotation of Azimuth Angle (°) irrespective of whether it is a clockwise (CW) or a counterclockwise (CCW) rotation of the azimuth angle from the default orientation of the generic urban block. This is illustrated in Figure 5.27, which shows the default orientation at 0° rotation of the model with absolute north azimuth as the rotation axis.

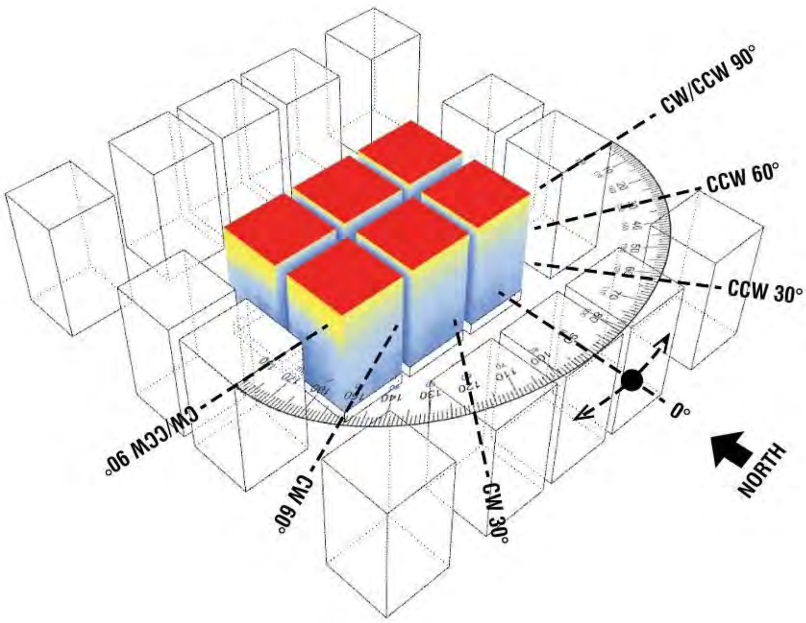

Figure 5.27: Orientation values for the rotation of azimuth angle. Both a CW and CCW rotation of 30 degrees were accounted for as a value of 30.

5.4.4 Analysis

Multiple linear regression was conducted with P.I. as the dependent variable and all other features (all variables listed in the first column of Table 5.14 except "Intercept") as independent variables. Table 5.14 shows the coefficients and P-values of all variables and the intercept.

Table 5.14: Coefficients and P-values of the Intercept and Independent Variables from Multiple Linear Regression.

Intercept / Variable	***Coefficients***	***P-value***
Intercept	-246.7873292	1.03769E-32
Number of Stories	-1.013491738	0.000198846
Ground Coverage	526.3799823	9.07891E-40
Urban Density (FSI)	-0.911393786	0.197635874
Compactness Ratio	0.529582151	0.324430057
Street-to-Surface Distance	0.016951516	0.01670597
Side-to-side Distance	21.17557653	9.46472E-41
CW/CCW Rotation of Azimuth Angle (°)	-0.013784235	1.08682E-60

The multiple linear regression model has an Adjusted R-square score of 0.9506. From the results of this analysis, it is observed that:

- The coefficients of two related variables, namely Number of Stories and Urban Density (FSI) are returned negative. This corresponds to the fact that density has a negative effect on solar potential.
- Moreover, Ground Coverage (GC)'s coefficient is returned to be 526.38, the highest positive value among the coefficients. This high value is returned because GC is a decimal fraction, and a positive value is the representation of a positive linear relationship, which signifies that the more the GC, the greater is the area of the roof – meaning a consequent increase in solar energy harvesting.
- Additionally, Compactness Ratio also shows a positive linear relationship with a coefficient of 0.53, because more surface area means a greater opportunity for solar harvesting with PV panels.
- The Street-to-surface Distance (coeff = 0.01695) has a relatively lower impact on solar performance (P.I.) for twofold reasons. Firstly, an increase in the Street-to-surface Distance with a resultant increase of insolation in streetside facades means a decrease in the Back-to-back distance between buildings and hence a reduction in the insolation of backward building surfaces. Secondly, this signifies that the solar

potential of vertical surfaces is significantly lower than the solar potential of horizontal surfaces in the context of Dhaka.

- However, the facades' importance in urban blocks' solar potential is still significant to be considered for PV deployment, which is verified by Side-to-side Setback's positive linear relationship (coeff = 21.18) with P.I.
- Another variable showing a negative relationship with P.I. is CW/CCW Rotation of Azimuth Angle (coeff = -0.01378), which is significant because the values used for this variable are large numbers, e.g. 0, 30, 60, and 90, compared to P.I. values. This can be interpreted easily. The more rotation from its default orientation of 0°, the less is the insolation in the surfaces of the urban block – because the longest side of the urban block faces the absolute south azimuth at the default orientation of experimentation. Therefore, the finding that south-facing facades get greater insolation is also established by the results of this experiment.
- Finally, all independent variables considered in the analysis provide useful information in the prediction of P.I., except for Urban Density and Compactness Ratio, which implies that these two variables are in fact functions of the other variables and can be omitted from the regression model. Each of Number of Stories, Ground Coverage, Street-to-Surface Distance, Side-to-side Distance, CW/CCW Rotation of Azimuth Angle (°) is assigned a P-value smaller than $\alpha = 0.05$ (see Table 5.14), which means that the null hypothesis can be rejected for each of them. On the contrary, Urban Density and Compactness Ratio are not statistically significant and should not be considered predictor variables.

The results were cross-validated by Scikit-learn's machine learning model using multiple linear regression and a train-test split of 80%-20% of the 480 samples of data, which can predict the dependent variable from each sample of independent variables from the test set with 94.49% accuracy (as opposed to the adjusted R-square score of 0.9506 for the aforementioned multiple regression model). The Pyhton code for this model is given in Appendix H.

Figure 5.28: Correlation matrix showing the extent to which the variables used in the experiment with projected district models are related to one another. The color scale at the right represents the relative degree of correlation.

The interrelationship among variables used in the multiple linear regression analysis can be better represented by the Scikit-learn heatmap shown in Figure 5.28. Key observations are:

1. The correlation matrix confirms the negative relationship of P.I. with each of Number of Stories, Urban Density (FSI) and CW/CCW Rotation of Azimuth Angle, and positive relationships with the remaining variables.

2. Additionally, it shows that Urban Density (FSI) is positively related to Ground Coverage and Number of Stories – while both positively impact FSI, each has an effect on P.I. which is opposite to the other.

3. Compactness Ratio’s negative relationship with Urban Density and Number of Stories is also justified – meaning that the higher the density, the less is the envelope area for solar harvesting per unit floor area, which usually results in decreased solar performance.

4. Thus, despite being insignificant predictor variables, Urban Density (FSI) and Compactness Ratio are interconnected variables and should individually have strong relationships with P.I., subject to the effect of other variables.

Final Regression Model:

The multiple linear regression model with Number of Stories, Ground Coverage, Street-to-Surface Distance, Side-to-side Distance, and CW/CCW Rotation of Azimuth Angle (°) as independent variables and P.I. as the dependent variable returns a slightly improved Adjusted R-square value of 0.9507, while the relationships with each variable are preserved (See Table 5.15). See Table E14-17 in Appendix E for detailed regression statistics.

Table 5.15: Coefficients and P-values of the Intercept and Independent Variables from the Final Regression Model.

Intercept / Variable	***Coefficients***	***P-value***
Intercept	-240.7346084	3.16082E-33
Number of Stories	-1.361321362	2.1695E-306
Ground Coverage	512.8515644	4.65332E-41
Street-to-Surface Distance	0.016951516	0.01666621
Side-to-side Distance	21.06220689	1.16256E-40
CW/CCW Rotation of Azimuth Angle (°)	-0.013784235	8.80854E-61

The exclusion of Urban Density (FSI) and Compactness Ratio from regression improve the model, which prompts us to individually scrutinize these variables.

Individual Relationship with Urban Density (FSI):

Despite not being a significant predictor variable of P.I. due to its P-value (which is greater than $\alpha = 0.05$, see Table 5.14), Urban Density or FSI, individually, has an obvious negative effect on solar performance (P.I.), and a polynomial regression line of order 2 shows a much better fit to the obtained data from the experiment with projected district models than a linear regression line (see Figure 5.29). An R-square value of 0.5406 suggests a moderately strong relationship, implying that it is possible to maximize solar performance for high-density urban settings by the manipulation of other factors (see the scattering of points in the middle).

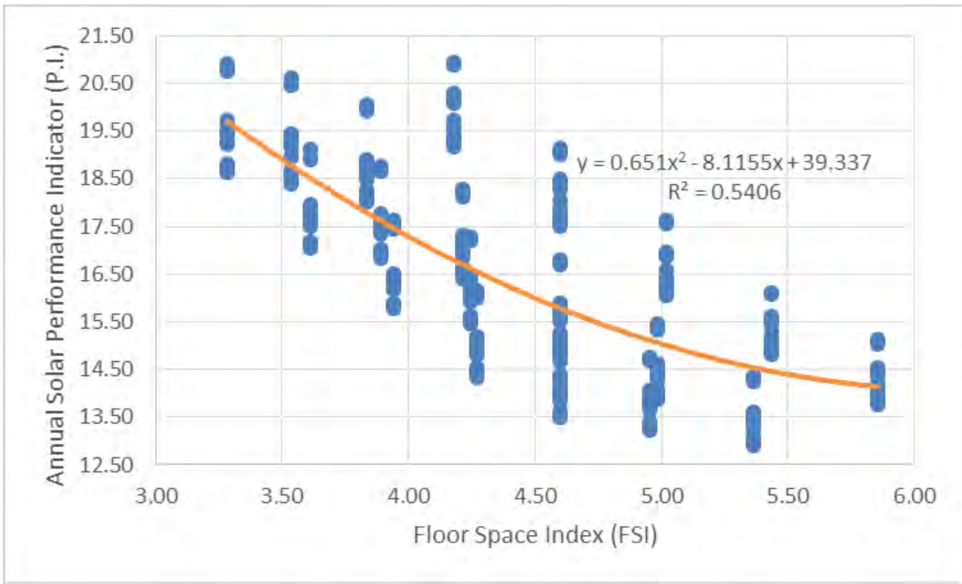

Figure 5.29: Effect of density (FSI) on solar potential per unit floor area (P.I.).

Upon further investigation with a separate experiment (see Figures 5.30-31) involving a modified urban block with much higher density values, it shows that the relationship of FSI to P.I. is similar. Higher density values were obtained by increasing the plot size to 30m x 30m because INB2008 recommends greater FAR values for larger plot sizes (GOB, 2008). FSI values also rise when there are more buildings per block. In this case, 8 buildings comprised the block as opposed to the previous 6. Keeping other variables unchanged, this experiments evaluates P.I. on the basis of increasing FSI values due to the increase of Number of Stories. While Figure 5.31 appears to verify the polynomial relationship illustrated in Figure 5.29, the spread of data points in both cases implies that even under high-density urban conditions (e.g. FSI > 5.0), it is possible to increase solar potential by working on predictor variables[20]. Figure 5.30 shows simulation images for 10, 13, and 17 stories for the separate

[20] In the experiment with projected districts, Number of Stories, Ground Coverage, Street-to-surface Distance, Side-to-side Distance, and CW/CCW Rotation of Azimuth Angle (°) were found to be the significant predictor variables for obtaining P.I.

experiment with an 8-building urban block utilizing MGC recommended by INB2008 for building plot size 30m x 30m. Figure 5.31 shows FSI vs P.I. plot for this higher-density urban block. 12 15° CW rotations of the azimuth angle were considered, while 8 FSI values correspond to the variation of Number of Stories from 10 to 17. FSI = 5.52 corresponds to the Maximum Allowable FAR for each building, 7.00, recommended by INB2008.

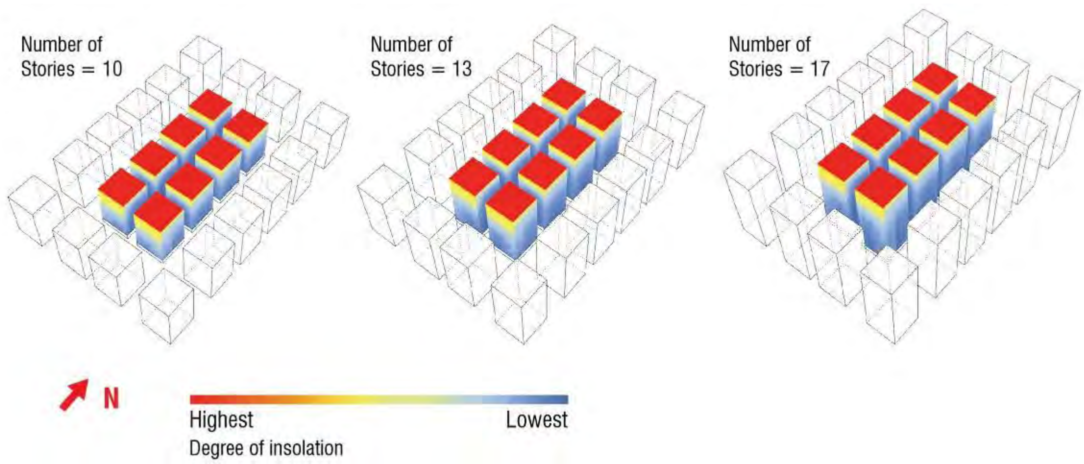

Figure 5.30: Insolation pattern for an 8-building block with 30mx30m plots.

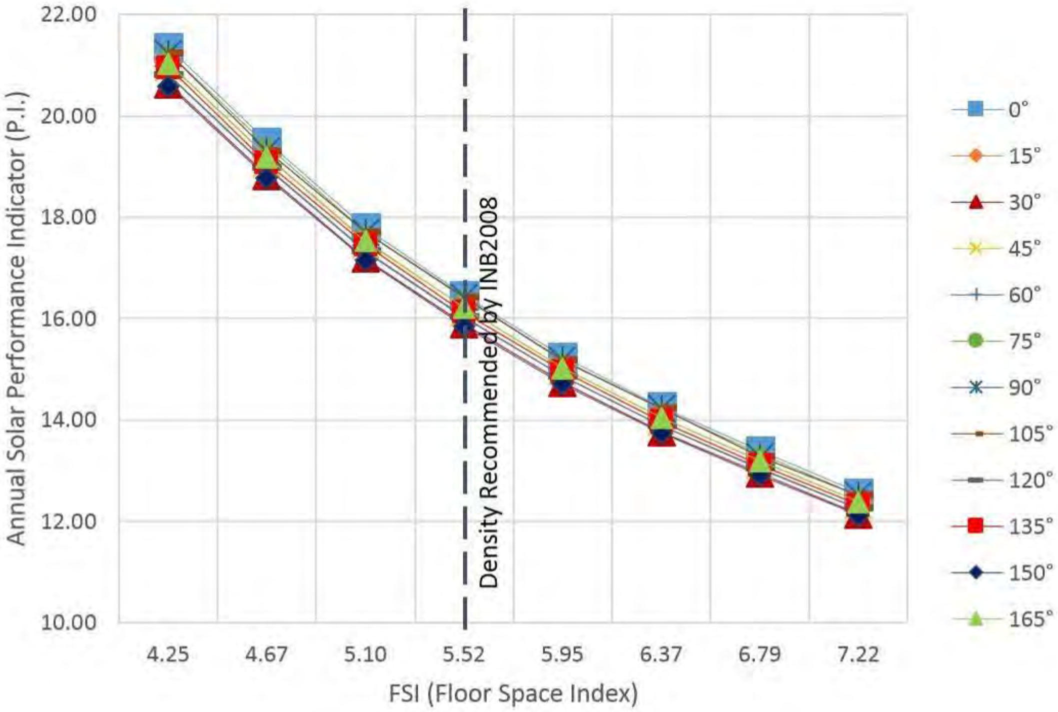

Figure 5.31: FSI vs P.I. plot for the 8-building block showing a similar relationship between density and solar potential per unit floor area.

Individual Relationship with Compactness Ratio:

Compactness Ratio (Comp) has a positive effect on the solar performance (P.I.) of the urban block, heavily subject to the effect of other factors such as Ground Coverage and CW/CCW Rotation of Azimuth Angle (°). Having said that, Compactness Ratio, in combination with other urban block parameters, has not turned out to be a significant predictor variable, which is evident from its P-value (it is greater than $\alpha = 0.05$, see Table 5.14). Besides, in combination with Urban Density (FSI), the other insignificant variable, it does not have a strong impact on P.I. A multiple linear regression analysis with Urban Density (FSI) and Compactness Ratio as independent variables and P.I. as the dependent variable returns a poor adjusted R-square value of 0.572624837. Figure 5.32 shows Comp vs P.I. plot with a linear regression line with a positive slope. An R-square value of 0.1296 indicates that the data points are loosely connected to the regression line, which suggests this relationship is heavily influenced by other factors. However, notice that the lowest compactness ratios have little option but to contribute poorly to solar performance, whereas its high values allow for both high and low solar performances.

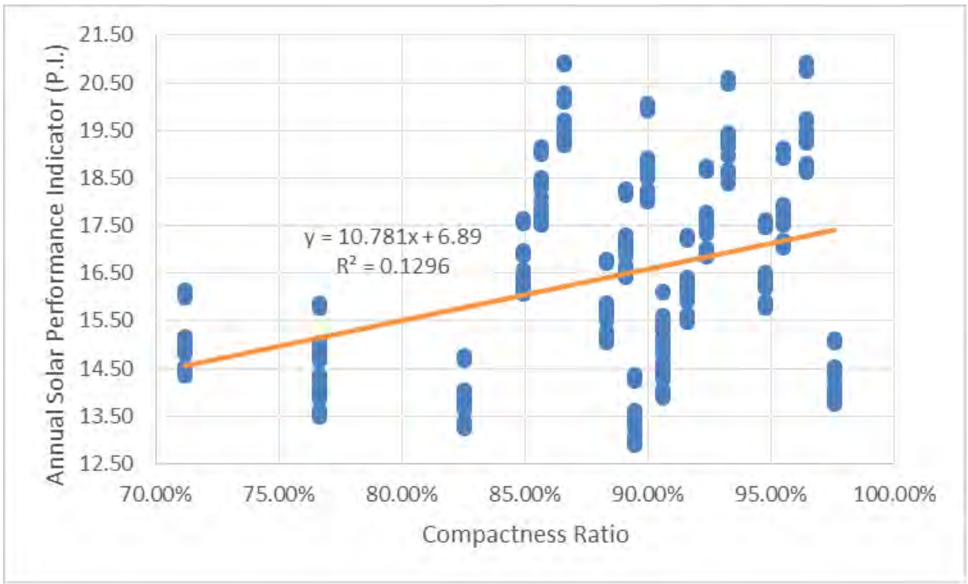

Figure 5.32: Effect of Compactness Ratio (Comp) vs on solar potential per unit floor area (P.I.).

Individual relationship with other variables:

Number of Stories: Number of Stories within the urban block was assumed identical for each building because if a building needs to maximize floor space, it must utilize the maximum advantage from FAR regulations. Since GC values were assumed identical for each building for any particular instance of projected districts, the Number of Stories corresponded. Number of Stories has a strong negative effect on solar potential: a polynomial regression of order 2 represents the relationship to P.I. better (see Figure 5.33) than the linear relationship assumed in multiple linear regression analysis. An R-square value of 0.8953 confirms a strong relationship. It can also be observed from Figure 6.1 that for higher buildings, it is more difficult to increase P.I. by the manipulation of other factors – evident from the decreasing extent of the scattering of data points as Number of Stories increase (for higher stories, e.g. 13 and 14, the jump in the value of P.I. for various instances of projected district models is relatively smaller in the graph). This is due to the diminishing roof-to-envelope area ratio and roof-to-floor area ratio, given that roofs are the most efficient collectors of solar energy.

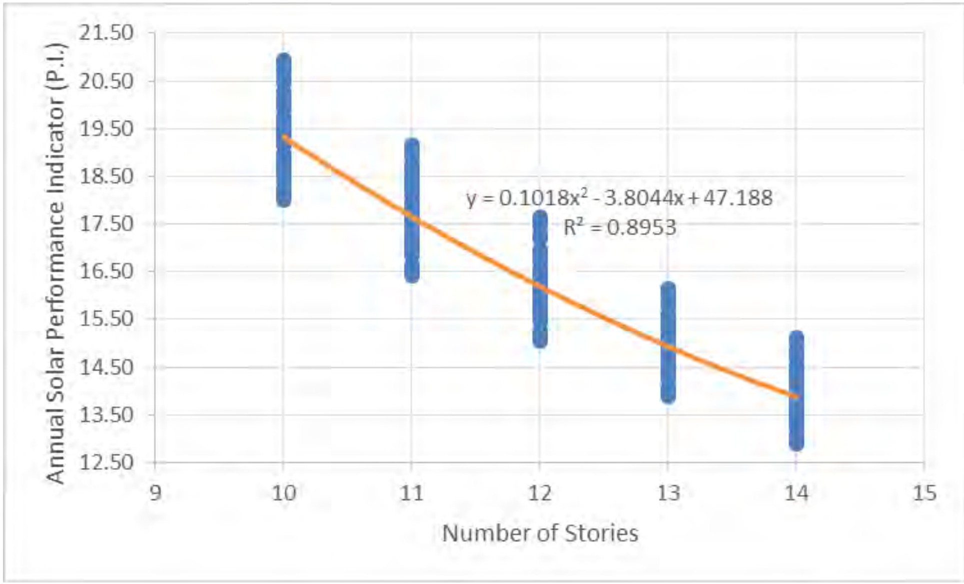

Figure 5.33: Effect of building height (Number of Stories) on solar potential per unit floor area (P.I.).

Ground Coverage: The four values of Ground Coverage (GC), an urban block parameter, do not show a clear individual relationship with P.I. However, at a lower GC, the spaces between buildings are wider and thus allow for more facade insolation. Moreover, lower GC values correspond to reduced floor areas, due to which P.I. (solar potential per unit floor area) increases. This phenomenon is clearly understood from Figure 5.34: the decrease of P.I. with increases in GC suggests that facades get lower insolation with increases in Street-to-surface Distance and Side-to-side Distance. However, a sudden increase of P.I. for the highest GC value implies that roof areas are significantly increased to have a telling impact on solar performance. An R-square value of 0.0253 for the poorly fit polynomial regression line of order 2 suggests that the effect of GC is heavily dependent on the effect of other factors.

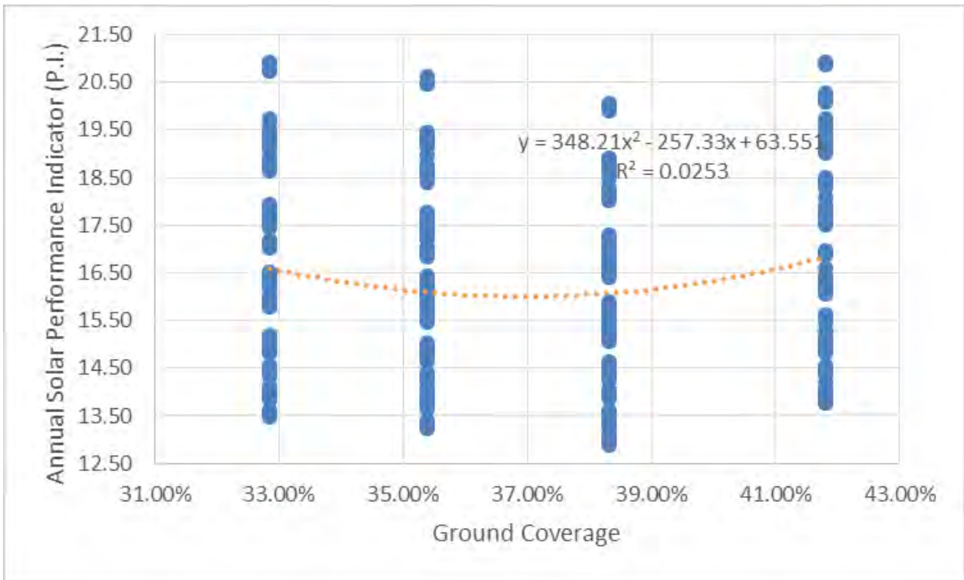

Figure 5.34: Effect of ground coverage (GC) on solar potential per unit floor area (P.I.).

Street-to-surface Distance: Street-to-surface Distance values do not show any clear relationship with P.I. Figure 5.35 shows that the data points, forming 4 vertical lines in each of the 4 clusters, can be easily separated in terms of GC values, which suggests that the effect of this parameter is subject to other dominant factors such as GC. Figure 5.35 also shows a poorly fit polynomial regression line of order 3 as further proof of the individual non-relationship. The effect of street-to-surface distance is almost nullified because of the reversing effect of Back-to-back distance.

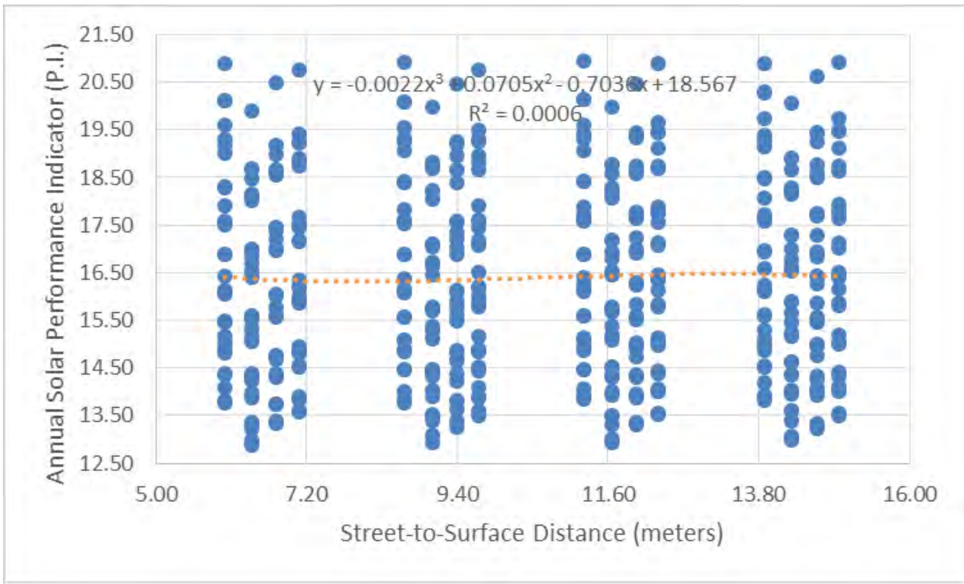

Figure 5.35: Effect of street-to-surface distance on solar potential per unit floor area (P.I.).

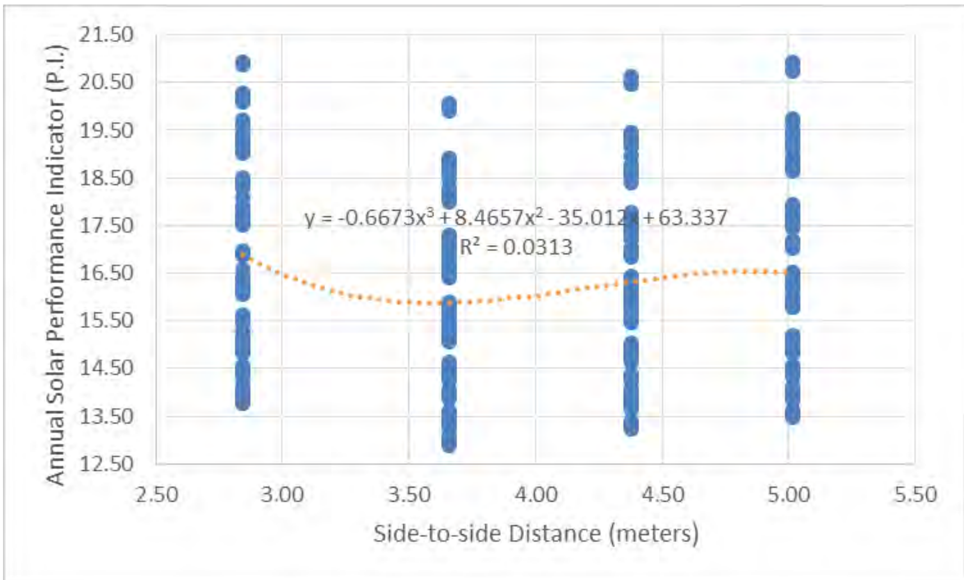

Figure 5.36: Effect of side-to-side distance on solar potential per unit floor area (P.I.).

Side-to-side Distance: In the experiment with projected districts, changes in the side-to-side distance values correspond to changes in GC values, and have the opposite effect on P.I. (see Figure 5.36). A poorly fit polynomial regression line of order 3 ($R^2 = 0.0313$) implies that there is no clear relationship, and its effect is heavily subject to the effect of other variables. Each vertical line of data points represents the effect of a separate Ground Coverage value in the graph shown in Figure 5.36.

CW/CCW Rotation of Azimuth Angle (°): Figure 5.37 shows a CW/CCW Rotation of Azimuth Angle (°) vs P.I. plot and a poorly fit polynomial regression line of order 3 ($R^2 = 0.0681$), meaning that the effect of rotation is heavily subject to the effect of other variables. Despite the loosely connected regression line, the relationship is much clearer because each vertical line of data points contains points of similar instances at a particular height of the vertical line. Although the relationship has a negative trend, notice that at 90° rotation, the block performs slightly better in terms of solar potential. This is because the shorter side of the urban block faces perfect north, and hence the area of non-qualified surfaces (<650 kWh/m^2) becomes minimum (largest sides of the urban block faces perfect east and perfect west).

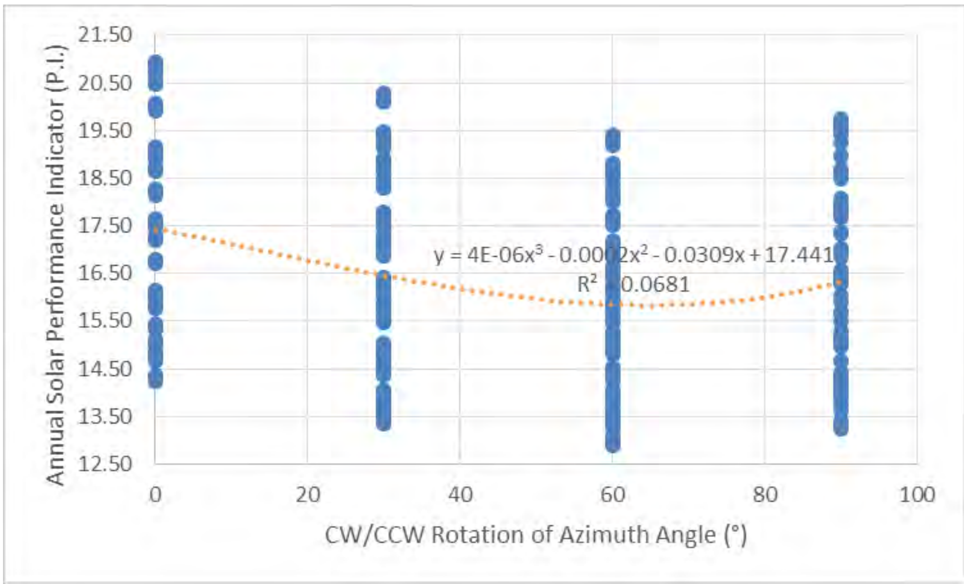

Figure 5.37: Effect of orientation (CW/CCW Rotation of Azimuth Angle, °) on solar potential per unit floor area (P.I.).

5.5 SUMMARY

Solar potential was investigated at the building level, the district level, and finally, the urban block level for the business districts of Dhaka, and its prospects were evaluated based on local urban conditions, significant urban parameters, building regulations, energy consumption, and weather variables. The key findings were:

1. For the individual building, relative height, surface orientation and level of obstructions are important parameters impacting solar potential.
2. Solar performance drops to the lowest during late mid-year (Jul-Aug).
3. Vertical surfaces that have outward surface normals within a rotation range of 37.5° (CW/CCW) of the north azimuth are unsuitable for PV deployment, whereas surfaces with exactly opposite outward surface normals contribute most efficiently to solar potential.
4. Roofs dominate in terms of contributing to solar potential, but the contribution of facades is too significant to be ignored.
5. Number of Stories, Ground Coverage, Street-to-surface Distance, Side-to-side Distance, and CW/CCW Rotation of Azimuth Angle (°) are all significant predictor variables for obtaining P.I. – a metric that measures the degree to which energy demand of the urban block can be met by harvesting solar energy. Although among these variables, only Number of Stories show a clear individual relationship, solar potential per unit floor area is dictated by the combined effect of these five variables.
6. The individual relationships of P.I. with Urban Density and Compactness Ratio imply that even within high-density urban areas with moderate envelope area per unit floor area, it is possible to increase solar potential per unit floor area by the manipulation of other factors such as by reducing Number of Stories, and by ensuring unobstructed, or minimally obstructed, roofs and south facades.

These findings will inform urban designers about monthly performance levels, the impact of the manner of arrangements of urban blocks within a business district, and the role of urban parameters that regulate the spaces between buildings in efficiently harnessing solar energy.

References

Brito, M. et al., 2017. The importance of facades for the solar PV potential of a Mediterranean city using LiDAR data. *Renewable Energy,* 111(2017), pp. 85-94.

Dai, S., Zuo, S. & Ren, Y., 2020. A spatial database of CO2 emissions, urban form fragmentation and city-scale effect related impact factors for the low carbon urban system in Jinjiang city, China. *Data in brief,* 29(2020), p. 105274.

GOB, 2008. *Bangladesh Gazette,* Dhaka: Government of Bangladesh.

CHAPTER 6: DISCUSSIONS AND CONCLUSION

6.1 Introduction

In previous chapters, investigations and analyses were conducted on findings from the literature, fieldwork, and simulation. The study culminated in the performative evaluation and analytics of buildings and urban settings. In this chapter, the findings from the overall research work were discussed and summarised so that urban design guidelines could be formulated based on the key research outcomes.

6.2 Findings

A summary of key findings from the overall research is presented in Table 6.1.

Table 6.1: Summary of key findings from research.

No.	Aspect	Key Finding
1	Weather variables vs energy consumption	Energy consumption shows positive individual relationships to each of mean temperature, minimum temperature, and maximum temperature squared (all with a positive slope of regression line).
2	Energy consumption pattern	Cooling load dominates energy consumption in the commercial buildings of MCA.
3	Energy consumption pattern	Natural lighting is scarcely utilized in the commercial buildings of MCA, while the energy required for lighting appears to be constant under different climatic conditions and is also insubstantial compared to airconditioning energy.
4	Predicting energy consumption	Monthly Mean Temperature, Monthly Maximum Temperature (extreme variable), Monthly Average Sunshine Hours, Monthly Number of Workdays, and Eid-ul-fitr Month (categorical variable) are all statistically significant predictor variables for predicting monthly energy consumption figures.
5	Solar contribution	Solar performance drops to the lowest during late mid-year (July-August) and rises to the highest during December, January, and February.

No.	Aspect	Key Finding
6	Surface orientation	Roofs contribute most significantly to solar potential, followed by south-facing facades. Therefore, keeping them unobstructed should be prioritized. North-facing facades should be excluded from PV deployment.
7	Street orientation	Streets running along the E-W direction could reduce overshadowing of south facades.
8	Urban block parameters regulating solar potential	Number of Stories, Ground Coverage, Street-to-surface Distance, Side-to-side Distance, and CW/CCW Rotation of Azimuth Angle (°) are all significant predictor variables for obtaining solar potential per unit floor area (P.I.). Although among these variables, only Number of Stories shows a clear individual relationship, P.I. is dictated by the combined effect of these five variables.
9	Density and envelope area	The individual relationships of P.I. with FSI and Comp imply that even within high-density urban areas with moderate envelope area per unit floor area, it is possible to increase P.I. by the manipulation of other factors such as by reducing stories, and by ensuring unobstructed, or minimally obstructed, roofs and south facades.

6.3 Urban Design Guidelines

6.3.1 Prediction of Solar Performance and Solar Potential

The important actors in urban development, for example, urban designers and policymakers are interested in the ratio of how much electricity can be contributed annually by solar energy systems in reference to the consumed electricity (Kanters & Wall, 2014). The Annual Solar Performance Indicator (P.I.) is a metric used in this research by which this ratio can be represented. If the P.I. of an urban block is greater than that of another, it can be said that a larger proportion of the annual energy demand of the first one can be met by electricity produced from solar energy systems, and vice versa. The P.I. (in kWh/m^2/year) of the generic urban block used in this research can be predicted using the following multiple linear regression equation (see Equation 6.1) if certain urban design parameters of that urban block are known.

$$P.I. = u_0 + u_1x_1 + u_2x_2 + u_3x_3 + u_4x_4 + u_5x_5 \quad (6.1)$$

In Equation 6.1, u_0 = -240.7346084; u_1 = -1.361321362; u_2 = 512.8515644; u_3 = 0.016951516; u_4 = 21.06220689; u_5 = -0.013784235; x_1 = Number of Stories; x_2 = Ground Coverage (decimal fraction); x_3 = Street-to-surface Distance (m); x_4 = Side-to-side Distance (m); x_5 = CW/CCW Rotation of Azimuth Angle (°).

From the predicted P.I., the solar potential or the electricity generated annually from PV (E_{pv}) can be calculated using the equation below:

$$E_{pv} = P.I. \times TFA \quad (6.2)$$

Here, TFA = Total Floor Area of the Urban Block.

6.3.2 Prediction of Monthly Solar Contribution

If the month value (January = 1, February = 2, and so on) and solar energy's percentage contribution to meeting energy demands (S_m) for a particular month are known, the percentage contribution can be predicted with 64% accuracy using the following equations.

$$S_{mo} = 0.0001x^3 - 0.0013x^2 - 0.0049x + 0.1195 \quad (6.3)$$

$$S_m(Month\ 2) = \frac{S_{mo}(Month\ 2)}{S_{mo}(Month\ 1)} \times S_m(Month\ 1) \quad (6.4)$$

To illustrate, assume that the contribution of solar energy to meeting energy demands of a particular building entity for March is 18%. We have to predict the contribution for July. Utilizing the month value of March and July, which respectively equal 3 and 7, we get S_{mo} (Month 1) and S_{mo} (Month 2) values to be 0.0997 and 0.0558 respectively. Given that S_m (Month 1) value is 18%, from equation 6.4, we get S_m (Month 2) value to be 10%, which is our desired value. However, this prediction cannot be used to predict annual solar contribution, in which case the sum of all monthly electricity generated from PV and the sum of all months' energy consumption need to be known.

6.3.3 Prediction of Monthly Energy Consumption

If the Monthly Mean Temperature (T_{avg}), Monthly Maximum Temperature (T_{max}), Monthly Average Sunshine Hours (S_{avg}), Monthly Number of Workdays (W) for a particular month, and whether or not it is an Eid-ul-fitr month are known, Equation 6.5, a multiple regression equation, can predict E_{mo} for a commercial building in MCA with 89% accuracy.

$$E_{mo} = w_0 + w_1 T_{avg} + w_2 {T_{max}}^2 - w_3 T_{max} - w_4 S_{avg} + w_5 W - w_6 R \quad (6.5)$$

Here, w_0 = 0.262453583; w_1 = 0.005041003; w_2 = 0.000275783; w_3 = 0.019421743; w_4 = 0.001189239; w_5 = 0.001793107 and w_6 = 0.016118018. R equals 1 if the given month is an Eid-ul-fitr month, and 0 otherwise.

Then, Equation 6.6 can help find the Monthly Energy Consumption (E_m) of a building if the building's Total Floor Area (TFA) and the building's Annual Energy Consumption Rate (E_r) are known.[21]

$$E_m = E_{mo} \times E_r \times TFA \quad (6.6)$$

6.3.4 Building Regulations in Reference to Urban Block Parameters

Ground Coverage (urban block parameter) was found to be an important parameter in terms of the solar potential of the urban block. This metric is dependent on the GC of each building of the block and street width. Local building regulations in Dhaka recommend MGC (Maximum Ground Coverage) and street width values for individual building plots. Urban areas should consider maximizing GC for the buildings to ensure large roof areas so that their solar potential is maximized.

Urban Density (Floor Space Index - FSI) affects solar potential and is dependent on FAR (individual building parameter) and street width values. However, urban areas must optimize density, which has a positive effect on the energy efficiency of urban districts. In order to optimize density, it is necessary

[21] This prediction assumes that energy consumption is strictly a function of Total Floor Area (TFA).

to optimize both FAR and street width, which are components of local building regulations. Wider streets are good for insolation and natural ventilation, but at the same time require more pavement areas. However, wider streets can be positive for urban areas if wide pedestrian pathways can be accommodated.

Compactness Ratio influences solar potential positively, and should therefore be considered as an important building parameter in the local building regulations. Currently, there is no recommendation in INB2008 regarding this parameter (GOB, 2008), but this study has shown that GC impacts compactness ratio positively. When an urban block is composed of identical buildings, the compactness ratio of a component building and that of the urban block are equal. A higher value of compactness ratio means a larger envelope area for solar harvesting. However, compactness ratio works efficiently only with considerations for some other important factors: the degree of building's openness to the south, the percentage of surface area facing open south, roof-to-envelope area ratio, and roof-to-floor area ratio.

Orientation is another parameter that could be addressed by local building regulations. However, unlike urban block orientation, the effect of building orientation on solar potential is not clear. In general, the more important issues to consider are surface orientation and street orientation. Building code should encourage larger facades facing open south, and major streets running in the east-west direction, which can make streetside facades face south. Additionally, it may encourage smaller building facades to face absolute north, which is often a conflicting requirement to larger facades facing south, but still the second-best option for orientation.

Besides, the urban block parameters Street-to-surface Distance and Side-to-side Distance can also be addressed by the components of local building regulations such as Front Setback, Back Setback, and Side Setback. **Setback** has turned out to be an influential factor in combination with other factors. Table 6.2 lists urban block parameters and the correspondings components of local building regulations in Dhaka.

Table 6.2: Urban Block Parameters and the local building regulations that control their values in Dhaka.

Ser.	Urban Block Parameter	Reference to Local Building Regulations
1	***Number of Stories***	FAR, MGC, Civil Aviation Rules
2	***Ground Coverage (GC)***	MGC, Street Width
3	***Urban Density (FSI)***	FAR, Street Width
4	***Compactness Ratio***	MGC, FAR (Not directly addressed in the regulations)
5	***Street-to-surface Distance***	Front Setback, Street Width
5	***Back-to-back Distance***	Back Setback
6	***Side-to-side Distance***	Side Setback
7	***CW/CCW Rotation of Azimuth Angle (°)***	Not addressed in the regulations

However, the incorporation of solar energy systems in building regulations needs to be supported by other issues such as fire safety, because fire hazards can result from PV systems due to overheating and system failures. Government incentives for solar energy harvesting in buildings, and the introduction of smart-grid systems can promote the usage of solar energy alongside building regulations and urban planning provisions.

6.4 Achievement of the Objectives

6.4.1 Objective one

To identify and study the components of the existing regulations responsible for the spatial arrangement of urban blocks in a business district in Dhaka in terms of insolation and overshadowing.

Theoretical Framework and Field Investigation enabled the understanding of the dynamics of insolation and overshadowing, and how the spaces between buildings impact them. Local building regulations shape the nature of spaces between buildings in Dhaka, and therefore, urban design parameters related to insolation and overshadowing were studied in reference to these regulations.

6.4.2 Objective two

To investigate the solar potential of urban surfaces of the said district at the urban block level.

Solar potential was investigated in three levels: the building level, the district level, and finally, the urban block level through Parametric Study and Analytics. A comprehensive understanding of energy consumption was developed through Theoretical Framework and Field Investigation, which was important for analyzing solar potential as a building dynamic.

6.4.3 Objective three

To explore possibilities for the development of urban design strategies that will potentially maximize solar energy harvesting in the business districts of Dhaka.

Parametric Study and Analytics also enabled the evaluation of urban design parameters, which helped to develop recommendations and design strategies for the business districts of Dhaka with a robust understanding of solar potential at the urban block level.

6.5 Recommendations

For the context of any tropical high-density city such as Dhaka, the results of this research highlight the necessity and importance of exploring innovative urban design strategies while the city aims to promote the efficient incorporation of solar energy. Alongside stakeholders and important players in the urban design process, the findings of this research will also provide insights for the general public and decision-makers in the city administration so that the city can build awareness toward clean energy and adopt policies well-suited for the implementation of renewable energy. Additionally, district planning strategies and building regulations could be modified in favor of solar harvesting by taking into account some key issues of spatial configurations of the urban block, the smallest unit of urban planning. Table 6.3 presents the findings of this study on how the solar potential of a commercial urban block within a business district in Dhaka could be maximized by addressing its spatial parameters.

Table 6.3: Recommendations for maximizing solar potential at urban block level for business districts in Dhaka.

No.	Urban Block Parameter	Recommendation for high solar potential per unit floor area
1	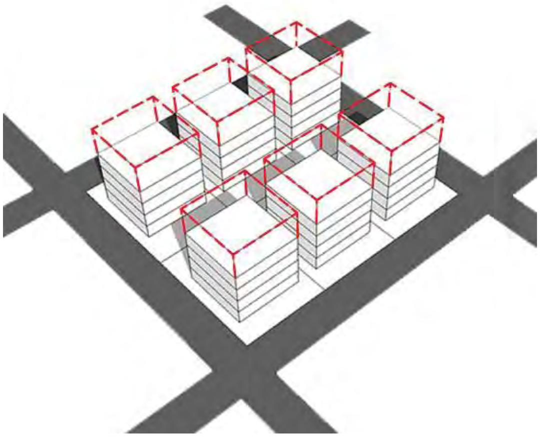 *Number of Stories*	▪ Reduce building height as much as possible by reducing the number of stories. ▪ FAR (Floor Area Ratio) rules for the individual building could be modified.
2	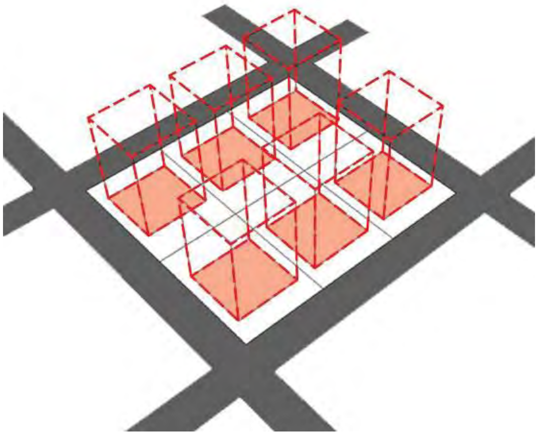 *Ground Coverage*	▪ Increase roof areas by utilizing the maximum allowable ground coverage. ▪ MGC (Maximum Ground Coverage) rules for the individual building could allow for more ground coverage.
3	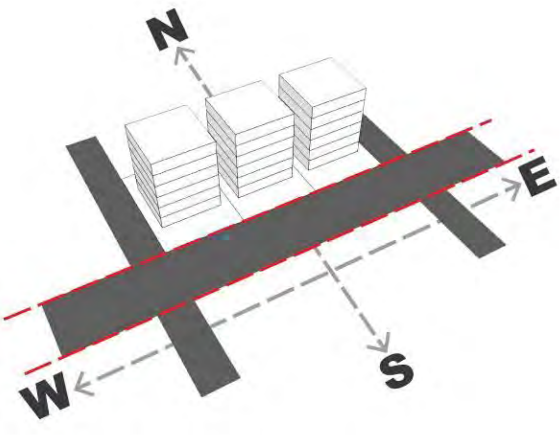 *Street Orientation*	▪ Orient major streets of the business district along the east-west direction to avoid the overshadowing of high-insolation facades. ▪ District planning and Detail Area Plan (DAP)[22] could allow for this strategy.

No.	Urban Block Parameter	Recommendation for high solar potential per unit floor area
4	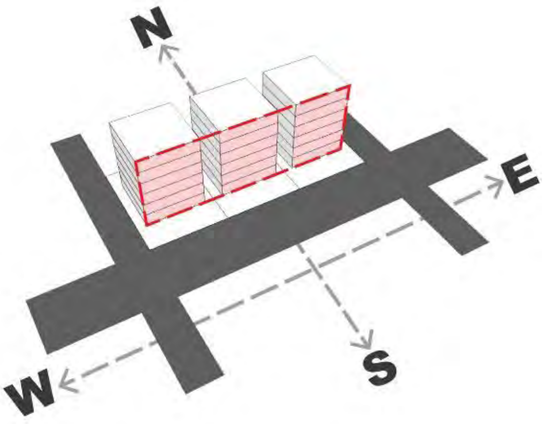 *Surface Orientation*	▪ Orient the largest facade areas to open south, or at least make south facades streetside facades. Also, avoid having taller buildings to the south. ▪ District planning and Detail Area Plan (DAP)[22] could allow for this provision.
5	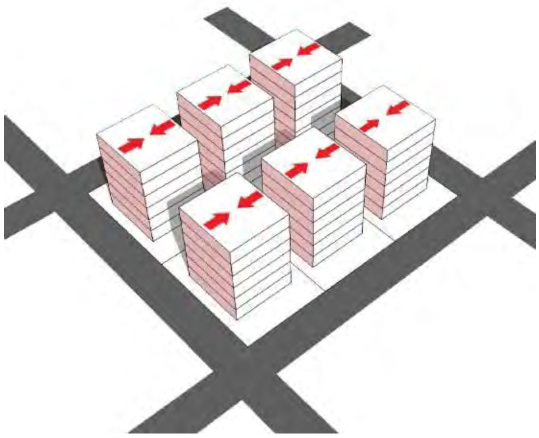 *Side-to-side Distance*	▪ After securing MGC, increase Side Setback as much as possible.
6	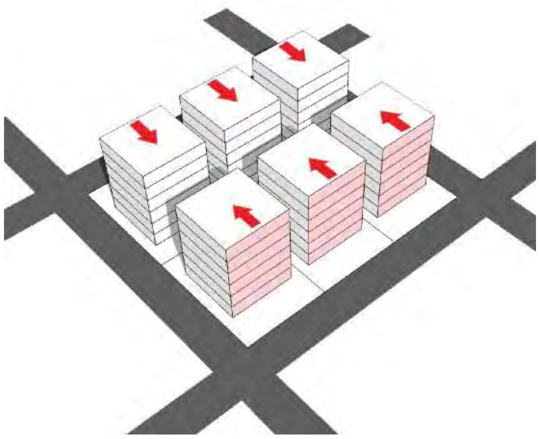 *Street-to-Surface Distance*	▪ After securing MGC, increase Front Setback as much as possible. ▪ Alternatively, increase Street Width. ▪ Street Width rules could be modified in the building regulations.

[22] See Section 2.5 for details about DAP (Detail Area Plan).

No.	Urban Block Parameter	Recommendation for high solar potential per unit floor area
7	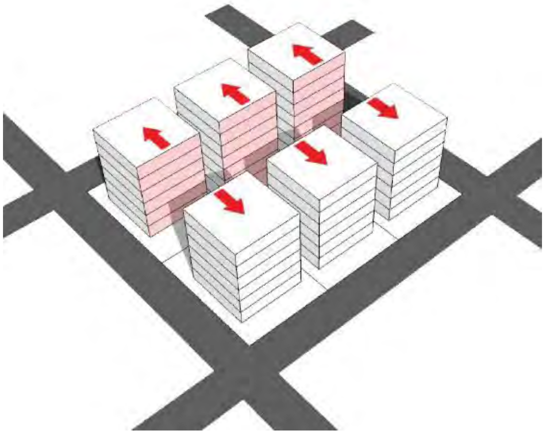 *Back-to-back Distance*	▪ After securing MGC, increase Back Setback as much as possible. ▪ Since increasing Ground Coverage is the priority, Setback rules could allow for smaller setbacks in favor of more ground coverage.
8	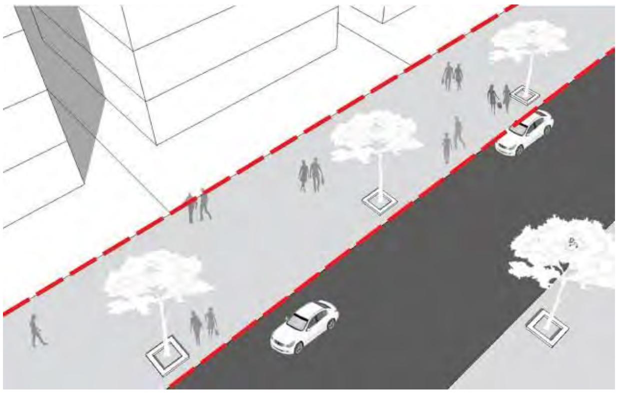 *Street Width*	▪ Compensate for larger street widths by accommodating wider pedestrian paths. ▪ District planning and Detail Area Plan (DAP) could acknowledge this issue.
9	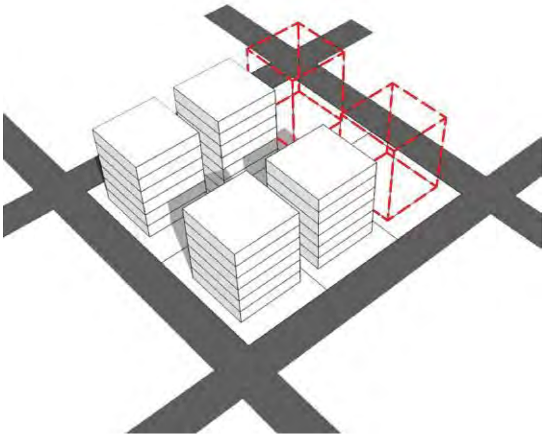 *Density*	▪ Maintain density by utilizing MGC rather than by increasing building height. ▪ Reduce density by reducing the number of buildings per block, thereby increasing streetside surface area per block. ▪ District planning and Detail Area Plan (DAP) could allow for this provision.

No.	Urban Block Parameter	Recommendation for high solar potential per unit floor area
10	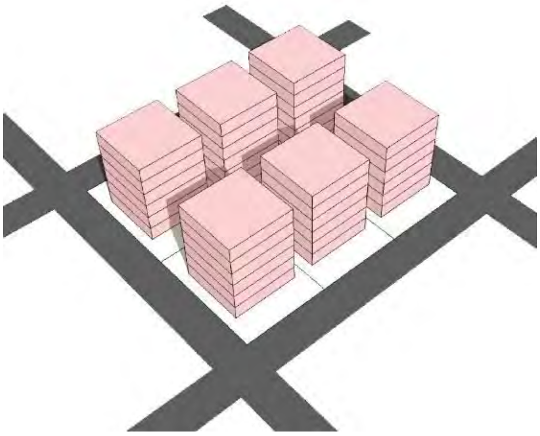 *Compactness Ratio*	▪ It is preferable to have more envelope area per unit floor area, but it is recommended to increase the proportion of roof area and facade area facing open south. ▪ Both district planning and building regulations could acknowledge this strategy.

6.6 Limitations and Areas for Further Research

This research focuses on commercial office buildings in the business districts in Dhaka and the urban settings that are comprised of these buildings. However, there are a few limitations of the study, and future research may consider working on a few aspects of this research as mentioned below:

1. The study on energy consumption considered three years' data from Field Investigation, whereas a larger dataset, which corresponds to a much longer period of time, could have generated more reliable results.
2. The estimation of energy consumption rate requires more rigorous study involving more building entities while identifying other factors such as energy consumption patterns in the interior, differences in interior activities, special circumstances, and detailed design issues which influence the consumption of energy. Future studies can address these issues, as well as the proportion of energy consumption that can be attributed to airconditioning, lighting, and other types of equipment.
3. The study on the solar potential of the projected district models assumes the same height and ground coverage for all component buildings, but

variations in these parameters can have an interesting effect on solar potential, as observed in the case of individual buildings. Future studies can study the effect of variations of building height within the urban block.

4. Tilt angles, which could increase the efficiency of solar systems, have been considered for neither facades nor roofs in this study. But the incorporation of tilt angles in future studies involving solar potential could generate interesting outcomes. While using tilt angles, the effect of mutual shading should also be considered.
5. This study considers orientation at 30° intervals for the study on projected districts. But reducing the interval and including more instances of orientation in the study could have generated more conclusive facts on orientation in urban settings.
6. Further studies should address how the significant urban parameters influencing solar potential, such as surface and street orientation, can be incorporated into the building code so that the solar potential of an urban area can be maximized. Other studies could address specific challenges such as maximizing solar potential for urban settings with high densities and low compactness ratios.

Overall, this study highlights the role of architecture, planning, and urban design in the design of modern cities so that they can explore the full potential of solar resources and meet local energy demands, while generating useful information for future research works on solar potential, energy, and environment.

References

GOB, 2008. *Bangladesh Gazette,* Dhaka: Government of Bangladesh.

Kanters, J. & Wall, M., 2014. The impact of urban design decisions on net zero energy solar buildings in Sweden. *Urban, Planning and Transport Research: An Open Access Journal,* 2(1), pp. 312-332.

BIBLIOGRAPHY

Agrawala, S. et al., 2003. *Development and Climate Change in Bangladesh: Focus on Coastal Flooding and the Sundarbans,* Dhaka: Organisation for Economic Co-operation and Development.

Ahmed, K. S., 1995. *Approaches to Bioclimatic Urban Design for the Tropics with Special Reference to Dhaka. (Doctor of Philosophy).* 1st ed. London: Architectural Association School of Architecture, London..

Ahmed, Z. N., 1994. *Assessment of residential sites in Dhaka with respect to solar radiation gains (Unpublished Ph. D. Thesis),* Leicester: De Montfort University, UK.

Amado, M. & Poggi, F., 2014. Solar urban planning: a parametric approach. *Energy Procedia,* 48(2014), pp. 1539-1548.

Arboit, M., Diblasi, A., Fernandez Llano, J. & de Rosa, C., 2008. Assessing the solar potential of low-density urban environments in Andean cities with desert climates: The case of the city of Mendoza, in Argentina. *Renewable Energy,* 33(2008), p. 1733–1748.

Banglapedia, 2015. *Dhaka, Geology.* [Online] Available at: http://en.banglapedia.org/index.php?title=Dhaka,_Geology [Accessed 24 April 2020].

Beckman, J. & Duffie, W., 1991. *Solar engineering of thermal processes.* 1st ed. New York: John Wiley & Sons, Inc.

Brito, M. et al., 2017. The importance of facades for the solar PV potential of a Mediterranean city using LiDAR data. *Renewable Energy,* 111(2017), pp. 85-94.

Chowdhury, S. A., 2018. *Indicative Tariff for Utility-Scale Solar IPP in Bangladesh,* Dhaka: Centre for Energy Research, United International University.

Compagnon, R., 2004. Solar and daylight availability in the urban fabric. *Energy and Buildings,* 36(2004), p. 321–328.

Dai, S., Zuo, S. & Ren, Y., 2020. A spatial database of CO2 emissions, urban form fragmentation and city-scale effect related impact factors for the low carbon urban system in Jinjiang city, China. *Data in brief,* 29(2020), p. 105274.

Deb, A., Bhuiyan, M. A. & Nasir, A., 2013. Prospects of Solar Energy in Bangladesh. *IOSR Journal of Electrical and Electronics Engineering (IOSR-JEEE),* 4(5), pp. 46-57.

Debnath, K. B., Hossain, M. T., Rezwan, S. M. & Iqbal, M. N., 2015. *Exploring the solar energy potential for multistoried commercial office buildings in a dense CBD area of a mega city.* Dhaka, ResearchGate.

Drone Media Imaging, 2021. *Solar Panels and Drone Thermal Imaging.* [Online] Available at: https://www.dronemediaimaging.co.uk/solar-panels-and-drone-thermal-imaging/
[Accessed 3 July 2021].

Farkas, K., et al., 2013. *IEA SHC Task 41: Solar Energy Systems in Architecture - Integration Criteria and Guidelines,* Paris, France: M. C. M. Probst, C. Roecker (editors).

GAISMA, 2020. *GAISMA.* [Online] Available at: https://www.gaisma.com/en/location/dhaka.html [Accessed 23 April 2020].

Ghosh, H. et al., 2002. *Measurement and Estimation of Sunshine Duration for Bangladesh,* Dhaka: Renewable Energy Research Center, University of Dhaka, Bangladesh.

Giani, M. et al., 2013. *A Design Approach for the Solar Optimization of Built Volumes.* Lausanne, s.n.

GOB, 2008. *Bangladesh Gazette,* Dhaka: Government of Bangladesh.

GOB, 2008. *Renewable Energy Policy of Bangladesh,* Dhaka: Power Division, Ministry of Power, Energy and Mineral Resources, Government of the People's Republic of Bangladesh.

Gomes, J., Diwan, L., Bernardo, R. & Karlsson, B., 2014. Minimizing the Impact of Shading at Oblique Solar Angles in a Fully Enclosed Asymmetric Concentrating PVT Collector. *Energy Procedia,* 57(2014), pp. 2176-2185.

Groat, L. & Wang, D., 2002. *Architectural Research Methods.* 1st ed. USA: John Wiley & Sons, Inc.

Haine, K. & Blumberga, D., 2016. Towards solar urban planning: a new step for better energy performance case of study Ibenbadis, Constantine (Algeria). *Energy Procedia,* 95(2016), pp. 145-152.

IEA, 2019. *World Energy Outlook 2019.* [Online] Available at: https://www.iea.org/reports/world-energy-outlook-2019 [Accessed 22 April 2020].

IEA, 2020. *IEA - International Energy Agency.* [Online] Available at: https://www.iea.org/data-and-statistics/charts/share-of-population-without-access-to-electricity-or-water-in-rural-areas-2017
[Accessed 27 April 2020].

IEA-PVPS, 2019. *Trends in Photovoltaic Applications 2019,* Stockholm, Sweden: IEA Photovoltaic Power Systems Programme.

Insectapedia, 2021. *Thermography 101: Thermal Imaging in Buildings.* [Online] Available at: https://inspectapedia.com/home_inspection/Thermography_Info.php [Accessed 3 July 2021].

Jelle, B. P. & Breivik, C., 2012. State-of-the-art building integrated photovoltaics. *Energy Procedia,* 20(2012), pp. 68-77.

Joarder, M. A. R., Ahmed, Z. N., Price, A. & Mourshed, M., 2009. *A simulation assessment of the height of light shelves to enhance daylighting quality in tropical office buildings under overcast sky conditions in Dhaka, Bangladesh.* Glasgow, Scotland, International Building Performance Simulation Association.

Kanters, J. & Horvat, M., 2012. Solar Energy as a Design Parameter in Urban Planning. *Energy Procedia,* pp. 1143-1152.

Kanters, J. & Wall, M., 2014. The impact of urban design decisions on net zero energy solar buildings in Sweden. *Urban, Planning and Transport Research: An Open Access Journal,* 2(1), pp. 312-332.

Kanters, J. & Wall, M., 2015. A planning process map for solar buildings in urban environments. *Renewable and Sustainable Energy Reviews,* p. 173–185.

Kanters, J., Wall, M. & Dubois, M.-C., 2014. Development of a Façade Assessment and Design Tool for Solar Energy (FASSADES). *Buildings,* 4(2014), pp. 43-59.

Kanters, J., Wall, M. & Dubois, M.-C., 2014. Typical values for active solar energy in urban planning. *Energy Procedia,* 48(2014), pp. 1607-1616.

Khan, A. H., Islam, A., Islam, M. & Rahman, M. S., 2015. *A systematic approach to find the optimum tilt angle for meeting the maximum energy demand of an isolated area.* Dhaka, Jahangirnagar University.

Košir, M., Capeluto, I. G., Krainer, A. & Kristl, Ž., 2014. Solar potential in existing urban layouts: Critical overview of the existing building stock in Slovenian context. *Energy Policy,* 69(2014), pp. 443-456.

Lam, J. C., Wan, K. K. & Yang, L., 2008. Sensitivity analysis and energy conservation measures implications. *Energy Conversion and Management,* 49(2008), pp. 3170-3177.

Lean, G., Hinrichsen, D. & Markham, A., 1990. *Atlas of the environment.* London: Arrow Books Ltd..

Lobaccaro, G., Fiorito, F., Masera, G. & Poli, T., 2012. District geometry simulation: a study for the optimization of solar façades in urban canopy layers. *Energy Procedia,* 30(2012), p. 1163 – 1172.

Lobaccaro, G. & Frontini, F., 2014. Solar energy in urban environment: how urban densification affects existing buildings. *Energy Procedia,* 48(2014), pp. 1559-1569.

Lobaccaro, G., Frontini, F., Masera, G. & Poli, T., 2012. SolarPW: A new solar design tool to exploit solar potential in existing urban areas. *Energy Procedia,* 30(2012), p. 1173 – 1183.

Nadim, M., Rashed, M. R. H., Muhury, A. & Mominuzzaman, S. M., 2016. *Estimation of Optimum Tilt Angle for PV Cell: a Study in Perspective of Bangladesh.* Dhaka, Institute of Electrical and Electronics Engineers (IEEE).

NOAA, 2020. *National Centers for Environmental Information.* [Online] Available at: https://www.ncdc.noaa.gov/ [Accessed 24 April 2020].

Obaidullah, M. & Sarkar, M., 2004. Performance and Life Cycle Cost Analysis of a Stand Alone PV Lighting System. *Journal of Energy & Environment,* 3(1), pp. 25-32.

O'Brien, W. T., Kennedy, C. A., Athienitis, A. K. & Kesik, T. J., 2010. The relationship between net energy use and the urban density of solar buildings. *Environment and Planning B Planning and Design,* 37(6), pp. 1002-1021.

Pedregosa, F. et al., 2011. Scikit-learn: Machine Learning in Python. *Journal of Machine Learning Research,* 12(2011), pp. 2825-2830.

Peng, C., Huang, Y. & Wu, Z., 2011. Building-integrated photovoltaics (BIPV) in architectural design in China. *Energy and Buildings,* pp. 3592-3598.

Roudsari, M. S., 2013. *Ladybug: A Parametric Environmental Plugin for Grasshopper to Help Designers Create an Environmentally Conscious Design.* Chambery, France, ResearchGate.

Sarralde, J. J., Quinn, D. J., Wiesmann, D. & Koen, S., 2015. Solar energy and urban morphology: Scenarios for increasing the renewable energy potential of neighbourhoods in London. *Renewable Energy,* 73(2015), pp. 10-17.

The Daily Star, 2019. *Trouble in Tongi, beyond,* Dhaka: The Daily Star.

Todorov, M., 2015. *Implementation of Solar Energy in Urban Planning,* Malmo: Lund University.

UN, 2018. *World Urbanization Prospects 2018.* [Online] Available at: https://population.un.org/wup/ [Accessed 22 April 2020].

VanderPlas, J., 2016. *Python Data Science Handbook.* 1st ed. Sebastopol(California): O'Reilly Media, Inc.

Verso, A., Martin, A., Amador, J. & Dominguez, J., 2015. GIS-based method to evaluate the photovoltaic potential in the urban environments: The particular case of Miraflores de la Sierra. *Solar Energy,* July, 117(2015), pp. 236-245.

Weatherbase, 2008. *Weatherbase: Historical Weather for Dhaka, Bangladesh.* [Online] Available at: http://www.weatherbase.com/weather/weather.php3?s=032914&refer=/ [Accessed 24 April 2020].

Wikipedia, 2020. *Geography of Bangladesh.* [Online] Available at: https://en.wikipedia.org/wiki/Geography_of_Bangladesh#Climate [Accessed 24 April 2020].

WMO, 2017. *WMO Guidelines on the Calculation of Climate Normals,* Geneva: World Meteorological Organization.

World Bank, 2008. *Policies for Mainstreaming Strategic Environmental Assessment in the Urban Development of Greater Dhaka,* Dhaka: World Bank.

Zhang, J. et al., 2019. Impact of urban block typology on building solar potential and energy use efficiency in tropical high-density city. *Applied Energy,* pp. 513-533.

APPENDICES

Appendix A:

Table A1: Summary of key findings of the research in relation to the objectives, methodologies, and concerned chapters.

Objective	Methods	Chapter	Key findings
Objective 1: To identify and study the components of the existing regulations responsible for the spatial arrangement of urban blocks in a business district in Dhaka in terms of insolation and overshadowing.	Theoretical Framework	Chapter 2	Theoretical Framework and Field Investigation enabled the understanding of the dynamics of insolation and overshadowing, and how the spaces between buildings impact them. Local building regulations shape the nature of spaces between buildings in Dhaka, and therefore, urban design parameters related to insolation and overshadowing were studied in reference to these regulations.
Objective 2: To investigate the solar potential of urban surfaces of the said district at the urban block level.	Theoretical Framework, Field Investigation, and Parametric Study and Analytics	Chapter 2, 4, and 5	Solar potential was investigated in three levels: the building level, the district level, and finally, the urban block level. A comprehensive understanding of energy consumption was developed, which was important for analyzing solar potential as a building dynamic.
Objective 3: To explore possibilities for the development of urban design strategies that will potentially maximize solar energy harvesting in the business districts of Dhaka.	Parametric Study and Analytics	Chapter 5	Parametric Study and Analytics also enabled the evaluation of urban design parameters, which helped to develop recommendations and design strategies for the business districts of Dhaka with a robust understanding of solar potential at the urban block level.

Appendix B: Key terms and concepts

Annual Solar Performance Indicator (P.I.): Electricity produced annually from PV per unit floor area, i.e. solar potential per unit floor area. See Section 3.5.2 for definition.

Compactness Ratio (Comp): Envelope area divided by total floor area. See Section 2.6.2 for definition.

Ground Coverage (GC): Building footprint divided by plot area. See Section 2.6.1 for definition.

Effective Plot Area (A_{plot} (building), or $\sum A_{plot}$ (urban block)): Effective Plot Area for a building (A_{plot}) is the building's designated plot area (A_{bplot}) plus half the area of the surrounding street. Effective Plot Area for an urban block ($\sum A_{plot}$) in the summation of all component buildings' Effective Plot Areas. See Section 2.6.1 for definition.

Energy Consumption Rate (E_r): Refers to Annual Energy Consumption Rate, which is defined by Annual Total Energy Consumption (E_y) divided by Total Floor Area (TFA). Monthly Energy Consumption Rate (E_{mr}) for a calendar month is that month's Energy Consumption (E_m) divided by TFA. See Section 3.5.2 for definition.

FAR: Total floor area (TFA) divided by building's designated plot area (A_{bplot}). See Section 2.6.1 for definition.

FSI (Urban Density): Floor Space Index. Calculated by dividing total floor area (TFA) by effective plot area ($\sum A_{plot}$). See Section 2.6.1 for definition.

Monthly Energy Consumption Indicator (E_{mo}): Monthly Energy Consumption (E_m) divided by Annual Energy Consumption (E_y), or Monthly Energy Consumption Rate (E_{mr}) divided by Annual Energy Consumption Rate (E_r). See Section 3.5.2 for definition.

Monthly Solar Fraction (S_{mo}): Percentage of energy demand met by solar energy in a month (S_m) divided by percentage met in a year (S_y). See Section 3.5.1 for definition.

Monthly Solar Performance Indicator (M.P.I.): Electricity produced monthly from PV (E_{mpv}) per unit floor area. See Section 3.5.2 for definition.

Solar Performance: Solar performance refers to P.I.

Solar Potential: Electricity produced annually from PV (E_{pv}). See Section 2.2 for definition.

Setback: Distance between plot boundary and the building surface closest to it. See Section 3.5.1 for definition.

TFA: Total Floor Area.

Urban Density (FSI): See FSI above.

Appendix C: Example Photogrammetry of Building Facades

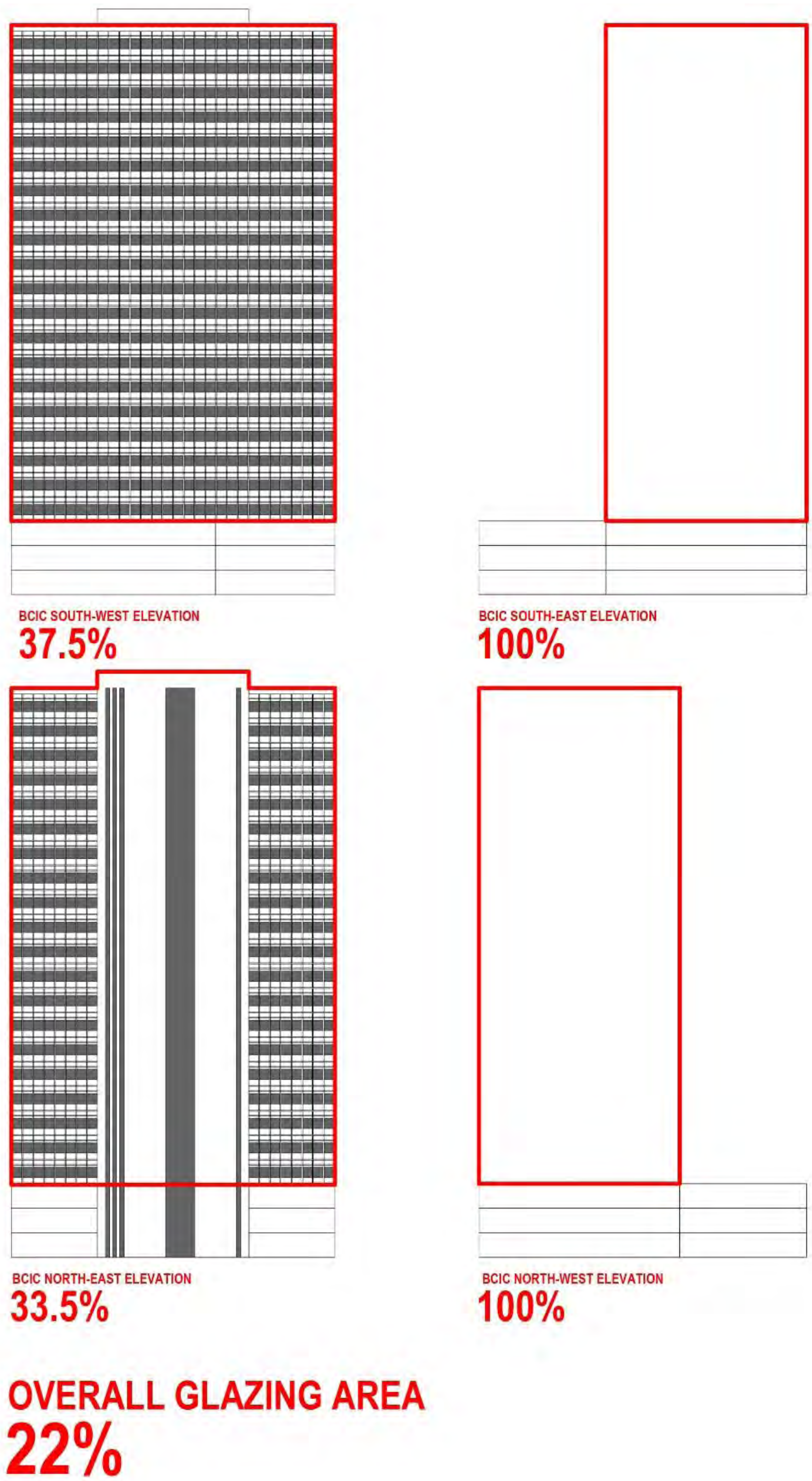

Figure I1: Photogrammetry of the facades of BCIC to calculate the percentage of glazing area. The bottom three floors were excluded from calculation because those areas do not qualify as suitable for PV deployment.

Appendix D: Grasshopper scripts

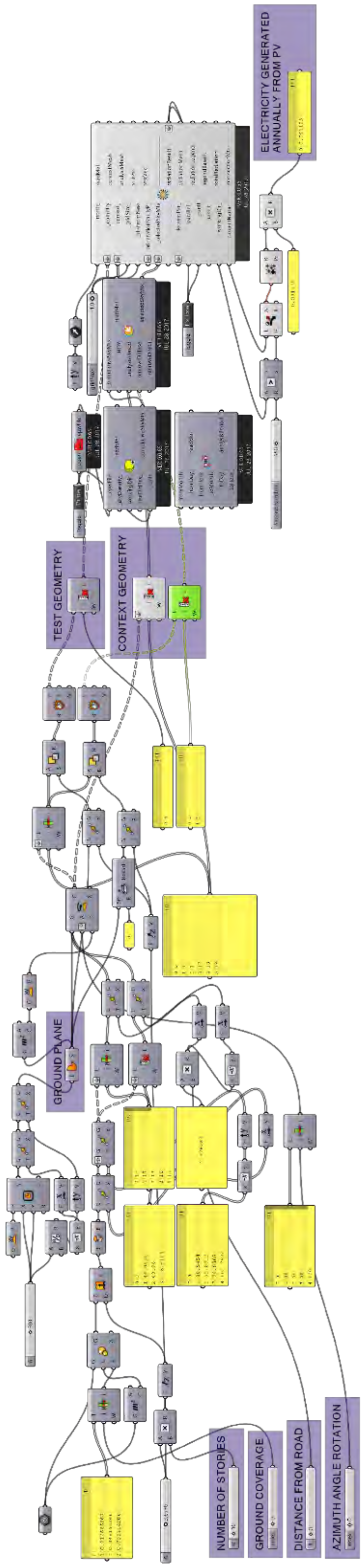

Figure D1: Grasshopper script used for simulation study of projected districts.

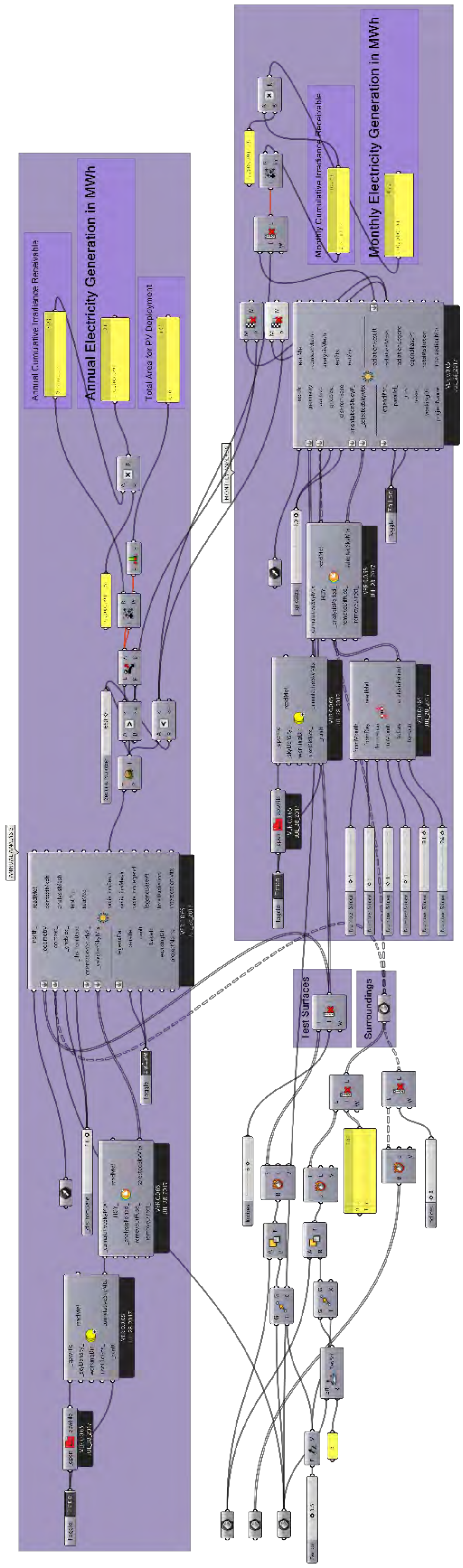

Figure D2: Grasshopper script used for simulation study of existing buildings.

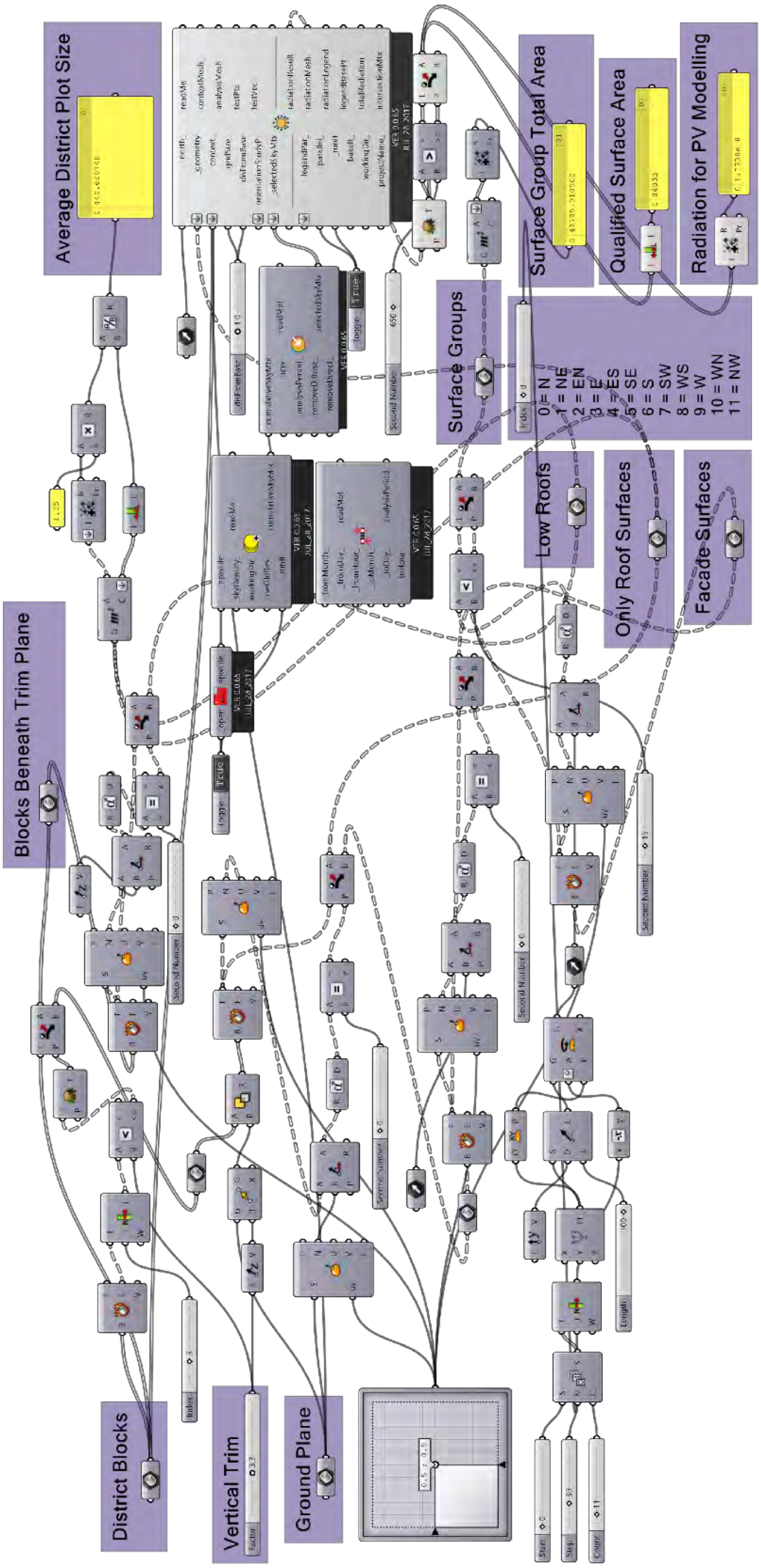

Figure D3: Grasshopper script used for simulation study of existing districts.

Appendix E: Detailed Data Tables

Table E1: List of Acronyms for Building Entities in MCA.

Acronym	Description
SBB	Sonali Bank Bhaban (Single Building)
JBB	Janata Bank Bhaban (Single Building)
BCIC	Bangladesh Chemical Industries Corporation Building (Single Building)
SKB	Senakallyan Bhaban (Single Building)
NAV	Navana (Multiple Buildings)
WAB	Wapda Building (Single Building)
KRB	Krishi Bhaban (Single Building)
AJC	Adamjee Court (Single Building)
AGB	Agrani Bank Building (Single Building)
NCC	NCC Bank Building (Single Building)
BDB	Bangladesh Bank Building (Single Building)
BBH	B.B. Hospital Zone (Single Building - features a single customer)
DIT	DIT Sub-station (Multiple Buildings)
PDB	PDB Design (Single Building)

Table E2: Monthly Energy Consumption in kWh and Corresponding Monthly Energy Consumption Indicator (E_{mo}) Figures for Building Entities in MCA (1).

Building Entities		**SBB**	**E_{mo}**	**JBB**	**E_{mo}**	**BCIC**	**E_{mo}**
Customer #		4		18		13	
YYYY	**MMM**						
2017	Jul	431766	0.0839	N/A	N/A	771112	0.0924
	Aug	575258	0.1118	N/A	N/A	879599	0.1054
	Sep	475958	0.0925	N/A	N/A	1136360	0.1362
	Oct	511536	0.0994	N/A	N/A	978574	0.1173
	Nov	450492	0.0876	N/A	N/A	752160	0.0902
	Dec	445338	0.0866	N/A	N/A	740016	0.0887
2018	Jan	312394	0.0607	N/A	N/A	502350	0.0602
	Feb	288094	0.0560	N/A	N/A	440934	0.0529
	Mar	512476	0.0996	N/A	N/A	731670	0.0877
	Apr	512084	0.0996	N/A	N/A	685662	0.0822
	May	374482	0.0728	N/A	N/A	904605	0.1084
	Jun	334662	0.0651	N/A	N/A	727827	0.0872
	Jul	528022	0.1027	N/A	N/A	909378	0.1090
	Aug	627646	0.1220	N/A	N/A	760027	0.0911
	Sep	463828	0.0902	N/A	N/A	823363	0.0987
	Dec	325496	0.0633	N/A	N/A	520997	0.0625
2019	Jan	379438	0.0738	N/A	N/A	534793	0.0641
	Feb	293152	0.0570	175867	0.0529	516685	0.0619
	Mar	448460	0.0872	225858	0.0679	742670	0.0890
	Apr	470288	0.0914	312294	0.0939	897275	0.1076
	May	476674	0.0927	306716	0.0922	752743	0.0902
	Jun	501782	0.0976	317244	0.0954	740742	0.0888
	Jul	458068	0.0891	314089	0.0944	774928	0.0929
	Aug	524072	0.1019	355528	0.1069	837930	0.1004
	Sep	458740	0.0892	355520	0.1069	837155	0.1004
	Oct	490886	0.0954	318694	0.0958	751321	0.0901
	Nov	373666	0.0726	253369	0.0762	635200	0.0761
	Dec	338082	0.0657	200307	0.0602	470638	0.0564
2020	Jan	302606	0.0588	183232	0.0551	466952	0.0560
	Feb	300352	0.0584	183400	0.0551	434420	0.0521

Table E3: Monthly Energy Consumption in kWh and Corresponding Monthly Energy Consumption Indicator (E_{mo}) Figures for Building Entities in MCA (2).

Buiding Entities		SKB	E_{mo}	NAV	E_{mo}	WAB	E_{mo}
Customer #		4		30		2	
YYYY	MMM						
2017	Jul	633548	0.0889	1568926	0.1201	84947	0.0759
	Aug	754085	0.1058	1468220	0.1124	116730	0.1043
	Sep	154200	0.0216	1295932	0.0992	109907	0.0982
	Oct	743556	0.1043	1372006	0.1050	100922	0.0902
	Nov	645354	0.0905	1308258	0.1001	80038	0.0715
	Dec	524703	0.0736	907072	0.0694	67724	0.0605
2018	Jan	389127	0.0546	737176	0.0564	61651	0.0551
	Feb	441346	0.0619	738344	0.0565	42100	0.0376
	Mar	590118	0.0828	1311628	0.1004	86361	0.0772
	Apr	708323	0.0994	1183399	0.0906	104082	0.0930
	May	650108	0.0912	1050339	0.0804	81203	0.0726
	Jun	409007	0.0574	1311375	0.1004	96595	0.0863
	Jul	744892	0.1045	1404306	0.1075	149094	0.1332
	Aug	706536	0.0991	1345944	0.1030	115482	0.1032
	Sep	804335	0.1128	1342181	0.1027	99591	0.0890
	Dec	454803	0.0638	779343	0.0597	67225	0.0601
2019	Jan	436404	0.0612	787595	0.0603	65728	0.0587
	Feb	384264	0.0539	794473	0.0608	66228	0.0592
	Mar	655238	0.0919	869869	0.0666	69139	0.0618
	Apr	654860	0.0919	1185028	0.0907	78124	0.0698
	May	689440	0.0967	1335385	0.1022	139443	0.1246
	Jun	507458	0.0712	1234515	0.0945	108743	0.0972
	Jul	763735	0.1071	1340197	0.1026	126464	0.1130
	Aug	679548	0.0953	1261334	0.0965	115066	0.1028
	Sep	772931	0.1084	1295886	0.0992	112986	0.1010
	Oct	652006	0.0915	1259538	0.0964	128961	0.1152
	Nov	522583	0.0733	1052843	0.0806	64336	0.0575
	Dec	440410	0.0618	810981	0.0621	85317	0.0762
2020	Jan	397464	0.0557	706175	0.0541	57120	0.0510
	Feb	393749	0.0552	712422	0.0545	33276	0.0297

Table E4: Monthly Energy Consumption in kWh and Corresponding Monthly Energy Consumption Indicator (E_{mo}) Figures for Building Entities in MCA (3).

Buiding Entities		**KRB**	**E_{mo}**	**AJC**	**E_{mo}**	**AGB**	**E_{mo}**
Customer #		10		6		2	
YYYY	**MMM**						
2017	Jul	N/A	N/A	721080	0.1130	147516	0.0621
	Aug	N/A	N/A	722690	0.1132	260912	0.1099
	Sep	N/A	N/A	600070	0.0940	183696	0.0774
	Oct	N/A	N/A	650480	0.1019	242416	0.1021
	Nov	N/A	N/A	601930	0.0943	154628	0.0651
	Dec	N/A	N/A	476900	0.0747	209308	0.0882
2018	Jan	N/A	N/A	458830	0.0719	261332	0.1101
	Feb	N/A	N/A	369030	0.0578	214280	0.0903
	Mar	N/A	N/A	687963	0.1078	276216	0.1164
	Apr	N/A	N/A	675760	0.1059	215908	0.0910
	May	N/A	N/A	572360	0.0897	209552	0.0883
	Jun	N/A	N/A	430700	0.0675	137144	0.0578
	Jul	N/A	N/A	730620	0.1145	255656	0.1077
	Aug	N/A	N/A	789860	0.1238	264636	0.1115
	Sep	N/A	N/A	786830	0.1233	215920	0.0910
	Dec	N/A	N/A	482670	0.0756	116548	0.0491
2019	Jan	N/A	N/A	406660	0.0637	134808	0.0568
	Feb	N/A	N/A	368170	0.0577	99400	0.0419
	Mar	337330	0.0801	411900	0.0645	170560	0.0719
	Apr	424084	0.1007	605940	0.0949	255432	0.1076
	May	265200	0.0630	596550	0.0935	235916	0.0994
	Jun	303315	0.0720	420910	0.0660	166800	0.0703
	Jul	432412	0.1027	707490	0.1109	273000	0.1150
	Aug	460141	0.1093	727740	0.1140	270000	0.1137
	Sep	480574	0.1141	710980	0.1114	211200	0.0890
	Oct	373441	0.0887	616170	0.0966	217800	0.0918
	Nov	317400	0.0754	491660	0.0770	175800	0.0741
	Dec	269123	0.0639	368330	0.0577	144000	0.0607
2020	Jan	327874	0.0779	378570	0.0593	136800	0.0576
	Feb	219943	0.0522	345590	0.0542	116400	0.0490

Table E5: Monthly Energy Consumption in kWh and Corresponding Monthly Energy Consumption Indicator (E_{mo}) Figures for Building Entities in MCA (4).

Buiding Entities		**NCC**	**E_{mo}**	**BDB**	**E_{mo}**	**BBH**	**E_{mo}**
Customer #		1		9		1	
YYYY	**MMM**						
2017	Jul	178000	0.0683	1498251	0.0901	N/A	N/A
	Aug	178000	0.0683	902439	0.0542	N/A	N/A
	Sep	184000	0.0706	N/A	N/A	N/A	N/A
	Oct	202000	0.0775	N/A	N/A	N/A	N/A
	Nov	192000	0.0737	N/A	N/A	N/A	N/A
	Dec	154000	0.0591	1388987	0.0835	47864	0.0615
2018	Jan	140000	0.0537	1107636	0.0666	44900	0.0577
	Feb	150000	0.0576	853642	0.0513	56936	0.0732
	Mar	194000	0.0744	1409309	0.0847	68080	0.0875
	Apr	210000	0.0806	1583055	0.0952	89484	0.1150
	May	214000	0.0821	1665907	0.1001	80696	0.1037
	Jun	202000	0.0775	N/A	N/A	78344	0.1007
	Jul	222000	0.0852	N/A	N/A	87620	0.1126
	Aug	226000	0.0867	1587424	0.0954	78032	0.1003
	Sep	222000	0.0852	1915089	0.1151	84412	0.1085
	Dec	168000	0.0645	1109200	0.0667	47952	0.0616
2019	Jan	186000	0.0714	833770	0.0501	47688	0.0613
	Feb	168000	0.0645	490113	0.0295	46484	0.0598
	Mar	190000	0.0729	1225455	0.0737	66284	0.0852
	Apr	228000	0.0875	2080654	0.1251	71788	0.0923
	May	222000	0.0852	1597024	0.0960	77264	0.0993
	Jun	242000	0.0929	1274358	0.0766	69276	0.0890
	Jul	270000	0.1036	1764597	0.1061	79812	0.1026
	Aug	230000	0.0883	1632051	0.0981	73060	0.0939
	Sep	248000	0.0952	1594127	0.0958	78228	0.1006
	Oct	244000	0.0936	1391999	0.0837	72948	0.0938
	Nov	206000	0.0790	1063141	0.0639	57148	0.0735
	Dec	168000	0.0645	896141	0.0539	44876	0.0577
2020	Jan	178000	0.0683	1021512	0.0614	43256	0.0556
	Feb	180000	0.0691	1093884	0.0658	44032	0.0566

Table E6: Monthly Energy Consumption in kWh and Corresponding Monthly Energy Consumption Indicator (E_{mo}) Figures for Building Entities in MCA (5).

Buiding Entities		**DIT**	**E_{mo}**	**PDB**	**E_{mo}**
Customer #		3		12	
YYYY	**MMM**				
2017	Jul	1023156	0.1050	N/A	N/A
	Aug	1554396	0.1596	N/A	N/A
	Sep	1077798	0.1106	N/A	N/A
	Oct	1144996	0.1175	N/A	N/A
	Nov	735470	0.0755	N/A	N/A
	Dec	910704	0.0935	N/A	N/A
2018	Jan	652784	0.0670	N/A	N/A
	Feb	432418	0.0444	N/A	N/A
	Mar	1028192	0.1055	N/A	N/A
	Apr	905492	0.0929	N/A	N/A
	May	865434	0.0888	N/A	N/A
	Jun	532946	0.0547	N/A	N/A
	Jul	1019190	0.1046	N/A	N/A
	Aug	960368	0.0986	N/A	N/A
	Sep	983220	0.1009	N/A	N/A
	Dec	676066	0.0694	204457	0.0536
2019	Jan	497954	0.0511	226926	0.0595
	Feb	768442	0.0789	206657	0.0542
	Mar	817998	0.0840	342965	0.0899
	Apr	1012442	0.1039	335748	0.0880
	May	871890	0.0895	400797	0.1050
	Jun	733564	0.0753	379694	0.0995
	Jul	1075932	0.1104	393239	0.1031
	Aug	896414	0.0920	373860	0.0980
	Sep	955060	0.0980	363731	0.0953
	Oct	853182	0.0876	387646	0.1016
	Nov	726946	0.0746	267442	0.0701
	Dec	623850	0.0640	203474	0.0533
2020	Jan	578588	0.0594	190093	0.0498
	Feb	596038	0.0612	176872	0.0464

Table E7: Median and Average Monthly Energy Consumption Indicator (E_{mo}) Figures and their differences for Building Entities in MCA.

Value Considering All Buiding Entities		MEDIAN E_{mo}	AVERAGE E_{mo}	(MEDIAN – AVERAGE)
YYYY	**MMM**			
2017	Jul	0.0895	0.0900	-0.0005
	Aug	0.1078	0.1045	0.0033
	Sep	0.0940	0.0889	0.0051
	Oct	0.1021	0.1017	0.0004
	Nov	0.0876	0.0832	0.0044
	Dec	0.0747	0.0763	-0.0016
2018	Jan	0.0602	0.0649	-0.0047
	Feb	0.0565	0.0581	-0.0016
	Mar	0.0877	0.0931	-0.0054
	Apr	0.0930	0.0950	-0.0020
	May	0.0888	0.0889	-0.0001
	Jun	0.0725	0.0755	-0.0030
	Jul	0.1076	0.1082	-0.0006
	Aug	0.1003	0.1032	-0.0029
	Sep	0.1009	0.1016	-0.0007
	Dec	0.0629	0.0625	0.0004
2019	Jan	0.0607	0.0610	-0.0003
	Feb	0.0577	0.0563	0.0014
	Mar	0.0769	0.0776	-0.0007
	Apr	0.0931	0.0961	-0.0030
	May	0.0947	0.0950	-0.0002
	Jun	0.0889	0.0847	0.0042
	Jul	0.1033	0.1038	-0.0005
	Aug	0.0993	0.1008	-0.0015
	Sep	0.0998	0.1003	-0.0005
	Oct	0.0937	0.0944	-0.0007
	Nov	0.0743	0.0731	0.0012
	Dec	0.0612	0.0613	-0.0001
2020	Jan	0.0568	0.0586	-0.0018
	Feb	0.0548	0.0542	0.0006

Table E8-E12: Detailed Results of Multiple Linear Regression Analysis with T_{max}^2, T_{max}, T_{avg}, S_{avg}, W, and R as independent variables and E_{mo} as the dependent variable.

Table E8: Summary output: Regression Statistics.

Regression Statistics	
Multiple R	0.954802848
R Square	0.911648479
Adjusted R Square	0.888600256
Standard Error	0.005847176
Observations	30

Table E9: Summary output: ANOVA (Analysis of Variance).

	df	*SS*	*MS*	*F*	*Significance F*
Regression	6	0.008113972	0.001352329	39.55395963	5.42076E-11
Residual	23	0.000786358	3.41895E-05		
Total	29	0.008900329			

Table E10: Summary output: Coefficients, Standard Error, t Stat and P-value.

	Coefficients	***Standard Error***	***t Stat***	***P-value***
Intercept	0.262453583	0.158060815	1.660459514	0.110395773
T_{max}^2	0.000275783	0.000144887	1.903429337	0.069572924
T_{max}	-0.019421743	0.009388332	-2.068710779	0.049994585
T_{avg}	0.005041003	0.000845443	5.962556958	4.43803E-06
S_{avg}	-0.001189239	0.000942592	-1.261668183	0.219714086
W	0.001793107	0.000779612	2.300000997	0.030859641
R	-0.016118018	0.005111649	-3.153193602	0.004448544

Table E11: (Continued) Lower 95%, Upper 95%, Lower 95.0%, Upper 95.0%.

	Lower 95%	***Upper 95%***	***Lower 95.0%***	***Upper 95.0%***
Intercept	-0.064520124	0.58942729	-0.064520124	0.58942729
T_{max}^2	-2.39395E-05	0.000575506	-2.39395E-05	0.000575506
T_{max}	-0.038842988	-4.9916E-07	-0.038842988	-4.9916E-07
T_{avg}	0.00329207	0.006789935	0.00329207	0.006789935

	Lower 95%	*Upper 95%*	*Lower 95.0%*	*Upper 95.0%*
S_{avg}	-0.003139139	0.000760662	-0.003139139	0.000760662
W	0.000180358	0.003405857	0.000180358	0.003405857
R	-0.026692269	-0.005543767	-0.026692269	-0.005543767

Table E12: Residual output: Predicted E_{mo} and Residuals.

Observation	*Predicted E_{mo}*	*Residuals*
1	0.101671234	-0.012206053
2	0.101101824	0.006742339
3	0.097936917	-0.003909029
4	0.094228735	0.007896716
5	0.078932163	0.008649559
6	0.067328887	0.007398895
7	0.063185304	-0.002965745
8	0.065710485	-0.009193781
9	0.085298808	0.002410647
10	0.088159673	0.00485581
11	0.092038323	-0.003202095
12	0.079924468	-0.007423514
13	0.106867536	0.000730531
14	0.09823703	0.00206478
15	0.100634007	0.000292876
16	0.064582706	-0.001714858
17	0.060669167	7.99966E-05
18	0.060719572	-0.003029223
19	0.076852563	3.61787E-05
20	0.092052024	0.001029725
21	0.10083598	-0.00609573
22	0.081498424	0.007423514
23	0.105598397	-0.002263912
24	0.096047272	0.003231354
25	0.10090799	-0.001133778
26	0.092791471	0.000907006
27	0.075541634	-0.0012007
28	0.054979708	0.006239378
29	0.057149981	-0.000346205
30	0.060139506	-0.005304682

Table E13: Values of variables for each instance of simulation with projected district models. Each row represents a separate instance. Values of dependent variable P.I. (E_{pv}/TFA, kWh/m^2) are given in bold.

Number of Stories	Ground Coverage	Urban Density (FSI)	Compactness Ratio	Street-to-surface Distance	Side-to-side Distance	CW/CCW Rotation of Azimuth Angle (°)	P.I.
10	41.81%	4.1813	86.59%	13.8788	2.8444	90	**19.7267**
10	41.81%	4.1813	86.59%	13.8788	2.8444	60	**19.3902**
10	41.81%	4.1813	86.59%	13.8788	2.8444	30	**20.2642**
10	41.81%	4.1813	86.59%	13.8788	2.8444	0	**20.9047**
10	41.81%	4.1813	86.59%	13.8788	2.8444	30	**20.2914**
10	41.81%	4.1813	86.59%	13.8788	2.8444	60	**19.2849**
10	41.81%	4.1813	86.59%	11.2525	2.8444	90	**19.6100**
10	41.81%	4.1813	86.59%	11.2525	2.8444	60	**19.4040**
10	41.81%	4.1813	86.59%	11.2525	2.8444	30	**20.1295**
10	41.81%	4.1813	86.59%	11.2525	2.8444	0	**20.9362**
10	41.81%	4.1813	86.59%	11.2525	2.8444	30	**20.1305**
10	41.81%	4.1813	86.59%	11.2525	2.8444	60	**19.3022**
10	41.81%	4.1813	86.59%	8.6263	2.8444	90	**19.5419**
10	41.81%	4.1813	86.59%	8.6263	2.8444	60	**19.3447**
10	41.81%	4.1813	86.59%	8.6263	2.8444	30	**20.0984**
10	41.81%	4.1813	86.59%	8.6263	2.8444	0	**20.9236**
10	41.81%	4.1813	86.59%	8.6263	2.8444	30	**20.0939**
10	41.81%	4.1813	86.59%	8.6263	2.8444	60	**19.2482**
10	41.81%	4.1813	86.59%	6.0000	2.8444	90	**19.5956**
10	41.81%	4.1813	86.59%	6.0000	2.8444	60	**19.3056**
10	41.81%	4.1813	86.59%	6.0000	2.8444	30	**20.1055**
10	41.81%	4.1813	86.59%	6.0000	2.8444	0	**20.8807**
10	41.81%	4.1813	86.59%	6.0000	2.8444	30	**20.1256**
10	41.81%	4.1813	86.59%	6.0000	2.8444	60	**19.1746**
10	38.33%	3.8328	90.00%	14.2854	3.6576	90	**18.6544**
10	38.33%	3.8328	90.00%	14.2854	3.6576	60	**18.2423**
10	38.33%	3.8328	90.00%	14.2854	3.6576	30	**18.9035**
10	38.33%	3.8328	90.00%	14.2854	3.6576	0	**20.0634**
10	38.33%	3.8328	90.00%	14.2854	3.6576	30	**18.9046**
10	38.33%	3.8328	90.00%	14.2854	3.6576	60	**18.1385**

Number of Stories	Ground Coverage	Urban Density (FSI)	Compactness Ratio	Street-to-surface Distance	Side-to-side Distance	CW/CCW Rotation of Azimuth Angle (°)	P.I.
10	38.33%	3.8328	90.00%	11.6591	3.6576	90	**18.5787**
10	38.33%	3.8328	90.00%	11.6591	3.6576	60	**18.1697**
10	38.33%	3.8328	90.00%	11.6591	3.6576	30	**18.7750**
10	38.33%	3.8328	90.00%	11.6591	3.6576	0	**19.9821**
10	38.33%	3.8328	90.00%	11.6591	3.6576	30	**18.7654**
10	38.33%	3.8328	90.00%	11.6591	3.6576	60	**18.0645**
10	38.33%	3.8328	90.00%	9.0329	3.6576	90	**18.6875**
10	38.33%	3.8328	90.00%	9.0329	3.6576	60	**18.2320**
10	38.33%	3.8328	90.00%	9.0329	3.6576	30	**18.7899**
10	38.33%	3.8328	90.00%	9.0329	3.6576	0	**19.9815**
10	38.33%	3.8328	90.00%	9.0329	3.6576	30	**18.8098**
10	38.33%	3.8328	90.00%	9.0329	3.6576	60	**18.0359**
10	38.33%	3.8328	90.00%	6.4066	3.6576	90	**18.4732**
10	38.33%	3.8328	90.00%	6.4066	3.6576	60	**18.1438**
10	38.33%	3.8328	90.00%	6.4066	3.6576	30	**18.6573**
10	38.33%	3.8328	90.00%	6.4066	3.6576	0	**19.9103**
10	38.33%	3.8328	90.00%	6.4066	3.6576	30	**18.6801**
10	38.33%	3.8328	90.00%	6.4066	3.6576	60	**18.0066**
10	35.38%	3.5380	93.27%	14.6441	4.3751	90	**19.2445**
10	35.38%	3.5380	93.27%	14.6441	4.3751	60	**18.6142**
10	35.38%	3.5380	93.27%	14.6441	4.3751	30	**19.4476**
10	35.38%	3.5380	93.27%	14.6441	4.3751	0	**20.6209**
10	35.38%	3.5380	93.27%	14.6441	4.3751	30	**19.4352**
10	35.38%	3.5380	93.27%	14.6441	4.3751	60	**18.5050**
10	35.38%	3.5380	93.27%	12.0179	4.3751	90	**19.4373**
10	35.38%	3.5380	93.27%	12.0179	4.3751	60	**18.6624**
10	35.38%	3.5380	93.27%	12.0179	4.3751	30	**19.3677**
10	35.38%	3.5380	93.27%	12.0179	4.3751	0	**20.4747**
10	35.38%	3.5380	93.27%	12.0179	4.3751	30	**19.3405**
10	35.38%	3.5380	93.27%	12.0179	4.3751	60	**18.5793**
10	35.38%	3.5380	93.27%	9.3916	4.3751	90	**18.9664**
10	35.38%	3.5380	93.27%	9.3916	4.3751	60	**18.6653**
10	35.38%	3.5380	93.27%	9.3916	4.3751	30	**19.2569**

Number of Stories	Ground Coverage	Urban Density (FSI)	Compactness Ratio	Street-to-surface Distance	Side-to-side Distance	CW/CCW Rotation of Azimuth Angle (°)	P.I.
10	35.38%	3.5380	93.27%	9.3916	4.3751	0	**20.4648**
10	35.38%	3.5380	93.27%	9.3916	4.3751	30	**19.2106**
10	35.38%	3.5380	93.27%	9.3916	4.3751	60	**18.3846**
10	35.38%	3.5380	93.27%	6.7653	4.3751	90	**18.9751**
10	35.38%	3.5380	93.27%	6.7653	4.3751	60	**18.6551**
10	35.38%	3.5380	93.27%	6.7653	4.3751	30	**19.1643**
10	35.38%	3.5380	93.27%	6.7653	4.3751	0	**20.4848**
10	35.38%	3.5380	93.27%	6.7653	4.3751	30	**19.1633**
10	35.38%	3.5380	93.27%	6.7653	4.3751	60	**18.5621**
10	32.85%	3.2853	96.41%	14.9637	5.0142	90	**19.7367**
10	32.85%	3.2853	96.41%	14.9637	5.0142	60	**18.7408**
10	32.85%	3.2853	96.41%	14.9637	5.0142	30	**19.4904**
10	32.85%	3.2853	96.41%	14.9637	5.0142	0	**20.9218**
10	32.85%	3.2853	96.41%	14.9637	5.0142	30	**19.4590**
10	32.85%	3.2853	96.41%	14.9637	5.0142	60	**18.6264**
10	32.85%	3.2853	96.41%	12.3374	5.0142	90	**19.6558**
10	32.85%	3.2853	96.41%	12.3374	5.0142	60	**18.7446**
10	32.85%	3.2853	96.41%	12.3374	5.0142	30	**19.4288**
10	32.85%	3.2853	96.41%	12.3374	5.0142	0	**20.8879**
10	32.85%	3.2853	96.41%	12.3374	5.0142	30	**19.4573**
10	32.85%	3.2853	96.41%	12.3374	5.0142	60	**18.6756**
10	32.85%	3.2853	96.41%	9.7112	5.0142	90	**19.4967**
10	32.85%	3.2853	96.41%	9.7112	5.0142	60	**18.8097**
10	32.85%	3.2853	96.41%	9.7112	5.0142	30	**19.2957**
10	32.85%	3.2853	96.41%	9.7112	5.0142	0	**20.7555**
10	32.85%	3.2853	96.41%	9.7112	5.0142	30	**19.2574**
10	32.85%	3.2853	96.41%	9.7112	5.0142	60	**18.6721**
10	32.85%	3.2853	96.41%	7.0849	5.0142	90	**19.4276**
10	32.85%	3.2853	96.41%	7.0849	5.0142	60	**18.7945**
10	32.85%	3.2853	96.41%	7.0849	5.0142	30	**19.2478**
10	32.85%	3.2853	96.41%	7.0849	5.0142	0	**20.7484**
10	32.85%	3.2853	96.41%	7.0849	5.0142	30	**19.2333**
10	32.85%	3.2853	96.41%	7.0849	5.0142	60	**18.7528**

Number of Stories	Ground Coverage	Urban Density (FSI)	Compactness Ratio	Street-to-surface Distance	Side-to-side Distance	CW/CCW Rotation of Azimuth Angle (°)	P.I.
11	41.81%	4.5994	85.69%	13.8788	2.8444	90	**18.0685**
11	41.81%	4.5994	85.69%	13.8788	2.8444	60	**17.7151**
11	41.81%	4.5994	85.69%	13.8788	2.8444	30	**18.4837**
11	41.81%	4.5994	85.69%	13.8788	2.8444	0	**19.1461**
11	41.81%	4.5994	85.69%	13.8788	2.8444	30	**18.5007**
11	41.81%	4.5994	85.69%	13.8788	2.8444	60	**17.5846**
11	41.81%	4.5994	85.69%	11.2525	2.8444	90	**17.8743**
11	41.81%	4.5994	85.69%	11.2525	2.8444	60	**17.7288**
11	41.81%	4.5994	85.69%	11.2525	2.8444	30	**18.4156**
11	41.81%	4.5994	85.69%	11.2525	2.8444	0	**19.0533**
11	41.81%	4.5994	85.69%	11.2525	2.8444	30	**18.4183**
11	41.81%	4.5994	85.69%	11.2525	2.8444	60	**17.6209**
11	41.81%	4.5994	85.69%	8.6263	2.8444	90	**17.8334**
11	41.81%	4.5994	85.69%	8.6263	2.8444	60	**17.6057**
11	41.81%	4.5994	85.69%	8.6263	2.8444	30	**18.3942**
11	41.81%	4.5994	85.69%	8.6263	2.8444	0	**19.0551**
11	41.81%	4.5994	85.69%	8.6263	2.8444	30	**18.4068**
11	41.81%	4.5994	85.69%	8.6263	2.8444	60	**17.5254**
11	41.81%	4.5994	85.69%	6.0000	2.8444	90	**17.9073**
11	41.81%	4.5994	85.69%	6.0000	2.8444	60	**17.5911**
11	41.81%	4.5994	85.69%	6.0000	2.8444	30	**18.2843**
11	41.81%	4.5994	85.69%	6.0000	2.8444	0	**19.0068**
11	41.81%	4.5994	85.69%	6.0000	2.8444	30	**18.3026**
11	41.81%	4.5994	85.69%	6.0000	2.8444	60	**17.5039**
11	38.33%	4.2161	89.09%	14.2854	3.6576	90	**17.0066**
11	38.33%	4.2161	89.09%	14.2854	3.6576	60	**16.6297**
11	38.33%	4.2161	89.09%	14.2854	3.6576	30	**17.3020**
11	38.33%	4.2161	89.09%	14.2854	3.6576	0	**18.2786**
11	38.33%	4.2161	89.09%	14.2854	3.6576	30	**17.3027**
11	38.33%	4.2161	89.09%	14.2854	3.6576	60	**16.5272**
11	38.33%	4.2161	89.09%	11.6591	3.6576	90	**16.9485**
11	38.33%	4.2161	89.09%	11.6591	3.6576	60	**16.5436**
11	38.33%	4.2161	89.09%	11.6591	3.6576	30	**17.1800**

Number of Stories	Ground Coverage	Urban Density (FSI)	Compactness Ratio	Street-to-surface Distance	Side-to-side Distance	CW/CCW Rotation of Azimuth Angle (°)	P.I.
11	38.33%	4.2161	89.09%	11.6591	3.6576	0	**18.2714**
11	38.33%	4.2161	89.09%	11.6591	3.6576	30	**17.1815**
11	38.33%	4.2161	89.09%	11.6591	3.6576	60	**16.4507**
11	38.33%	4.2161	89.09%	9.0329	3.6576	90	**17.0357**
11	38.33%	4.2161	89.09%	9.0329	3.6576	60	**16.6457**
11	38.33%	4.2161	89.09%	9.0329	3.6576	30	**17.0988**
11	38.33%	4.2161	89.09%	9.0329	3.6576	0	**18.2066**
11	38.33%	4.2161	89.09%	9.0329	3.6576	30	**17.1143**
11	38.33%	4.2161	89.09%	9.0329	3.6576	60	**16.4454**
11	38.33%	4.2161	89.09%	6.4066	3.6576	90	**16.8508**
11	38.33%	4.2161	89.09%	6.4066	3.6576	60	**16.5388**
11	38.33%	4.2161	89.09%	6.4066	3.6576	30	**16.9829**
11	38.33%	4.2161	89.09%	6.4066	3.6576	0	**18.1242**
11	38.33%	4.2161	89.09%	6.4066	3.6576	30	**17.0039**
11	38.33%	4.2161	89.09%	6.4066	3.6576	60	**16.4061**
11	35.38%	3.8918	92.36%	14.6441	4.3751	90	**17.7362**
11	35.38%	3.8918	92.36%	14.6441	4.3751	60	**16.9357**
11	35.38%	3.8918	92.36%	14.6441	4.3751	30	**17.7063**
11	35.38%	3.8918	92.36%	14.6441	4.3751	0	**18.7610**
11	35.38%	3.8918	92.36%	14.6441	4.3751	30	**17.6920**
11	35.38%	3.8918	92.36%	14.6441	4.3751	60	**16.8336**
11	35.38%	3.8918	92.36%	12.0179	4.3751	90	**17.7725**
11	35.38%	3.8918	92.36%	12.0179	4.3751	60	**16.9951**
11	35.38%	3.8918	92.36%	12.0179	4.3751	30	**17.6763**
11	35.38%	3.8918	92.36%	12.0179	4.3751	0	**18.7372**
11	35.38%	3.8918	92.36%	12.0179	4.3751	30	**17.6396**
11	35.38%	3.8918	92.36%	12.0179	4.3751	60	**16.9223**
11	35.38%	3.8918	92.36%	9.3916	4.3751	90	**17.3408**
11	35.38%	3.8918	92.36%	9.3916	4.3751	60	**17.0159**
11	35.38%	3.8918	92.36%	9.3916	4.3751	30	**17.5821**
11	35.38%	3.8918	92.36%	9.3916	4.3751	0	**18.6582**
11	35.38%	3.8918	92.36%	9.3916	4.3751	30	**17.5457**
11	35.38%	3.8918	92.36%	9.3916	4.3751	60	**16.8731**

Number of Stories	Ground Coverage	Urban Density (FSI)	Compactness Ratio	Street-to-surface Distance	Side-to-side Distance	CW/CCW Rotation of Azimuth Angle (°)	P.I.
11	35.38%	3.8918	92.36%	6.7653	4.3751	90	**17.3896**
11	35.38%	3.8918	92.36%	6.7653	4.3751	60	**17.0200**
11	35.38%	3.8918	92.36%	6.7653	4.3751	30	**17.4571**
11	35.38%	3.8918	92.36%	6.7653	4.3751	0	**18.6553**
11	35.38%	3.8918	92.36%	6.7653	4.3751	30	**17.4591**
11	35.38%	3.8918	92.36%	6.7653	4.3751	60	**16.9553**
11	32.85%	3.6138	95.50%	14.9637	5.0142	90	**17.9470**
11	32.85%	3.6138	95.50%	14.9637	5.0142	60	**17.1217**
11	32.85%	3.6138	95.50%	14.9637	5.0142	30	**17.7894**
11	32.85%	3.6138	95.50%	14.9637	5.0142	0	**19.1251**
11	32.85%	3.6138	95.50%	14.9637	5.0142	30	**17.7451**
11	32.85%	3.6138	95.50%	14.9637	5.0142	60	**17.0326**
11	32.85%	3.6138	95.50%	12.3374	5.0142	90	**17.8924**
11	32.85%	3.6138	95.50%	12.3374	5.0142	60	**17.1169**
11	32.85%	3.6138	95.50%	12.3374	5.0142	30	**17.7448**
11	32.85%	3.6138	95.50%	12.3374	5.0142	0	**19.1151**
11	32.85%	3.6138	95.50%	12.3374	5.0142	30	**17.7737**
11	32.85%	3.6138	95.50%	12.3374	5.0142	60	**17.0628**
11	32.85%	3.6138	95.50%	9.7112	5.0142	90	**17.9171**
11	32.85%	3.6138	95.50%	9.7112	5.0142	60	**17.1779**
11	32.85%	3.6138	95.50%	9.7112	5.0142	30	**17.6196**
11	32.85%	3.6138	95.50%	9.7112	5.0142	0	**18.9525**
11	32.85%	3.6138	95.50%	9.7112	5.0142	30	**17.5817**
11	32.85%	3.6138	95.50%	9.7112	5.0142	60	**17.0618**
11	32.85%	3.6138	95.50%	7.0849	5.0142	90	**17.6755**
11	32.85%	3.6138	95.50%	7.0849	5.0142	60	**17.1901**
11	32.85%	3.6138	95.50%	7.0849	5.0142	30	**17.5163**
11	32.85%	3.6138	95.50%	7.0849	5.0142	0	**18.9084**
11	32.85%	3.6138	95.50%	7.0849	5.0142	30	**17.5065**
11	32.85%	3.6138	95.50%	7.0849	5.0142	60	**17.1513**
12	41.81%	5.0175	84.93%	13.8788	2.8444	90	**16.5859**
12	41.81%	5.0175	84.93%	13.8788	2.8444	60	**16.2446**
12	41.81%	5.0175	84.93%	13.8788	2.8444	30	**16.9501**

Number of Stories	Ground Coverage	Urban Density (FSI)	Compactness Ratio	Street-to-surface Distance	Side-to-side Distance	CW/CCW Rotation of Azimuth Angle (°)	P.I.
12	41.81%	5.0175	84.93%	13.8788	2.8444	0	**17.6493**
12	41.81%	5.0175	84.93%	13.8788	2.8444	30	**16.9678**
12	41.81%	5.0175	84.93%	13.8788	2.8444	60	**16.1272**
12	41.81%	5.0175	84.93%	11.2525	2.8444	90	**16.4081**
12	41.81%	5.0175	84.93%	11.2525	2.8444	60	**16.2597**
12	41.81%	5.0175	84.93%	11.2525	2.8444	30	**16.8954**
12	41.81%	5.0175	84.93%	11.2525	2.8444	0	**17.5959**
12	41.81%	5.0175	84.93%	11.2525	2.8444	30	**16.8977**
12	41.81%	5.0175	84.93%	11.2525	2.8444	60	**16.1652**
12	41.81%	5.0175	84.93%	8.6263	2.8444	90	**16.3677**
12	41.81%	5.0175	84.93%	8.6263	2.8444	60	**16.1695**
12	41.81%	5.0175	84.93%	8.6263	2.8444	30	**16.8796**
12	41.81%	5.0175	84.93%	8.6263	2.8444	0	**17.5974**
12	41.81%	5.0175	84.93%	8.6263	2.8444	30	**16.8912**
12	41.81%	5.0175	84.93%	8.6263	2.8444	60	**16.0733**
12	41.81%	5.0175	84.93%	6.0000	2.8444	90	**16.4264**
12	41.81%	5.0175	84.93%	6.0000	2.8444	60	**16.1399**
12	41.81%	5.0175	84.93%	6.0000	2.8444	30	**16.8780**
12	41.81%	5.0175	84.93%	6.0000	2.8444	0	**17.5550**
12	41.81%	5.0175	84.93%	6.0000	2.8444	30	**16.8938**
12	41.81%	5.0175	84.93%	6.0000	2.8444	60	**16.0533**
12	38.33%	4.5994	88.33%	14.2854	3.6576	90	**15.6504**
12	38.33%	4.5994	88.33%	14.2854	3.6576	60	**15.2527**
12	38.33%	4.5994	88.33%	14.2854	3.6576	30	**15.8824**
12	38.33%	4.5994	88.33%	14.2854	3.6576	0	**16.7766**
12	38.33%	4.5994	88.33%	14.2854	3.6576	30	**15.8783**
12	38.33%	4.5994	88.33%	14.2854	3.6576	60	**15.1588**
12	38.33%	4.5994	88.33%	11.6591	3.6576	90	**15.6822**
12	38.33%	4.5994	88.33%	11.6591	3.6576	60	**15.1781**
12	38.33%	4.5994	88.33%	11.6591	3.6576	30	**15.7765**
12	38.33%	4.5994	88.33%	11.6591	3.6576	0	**16.7980**
12	38.33%	4.5994	88.33%	11.6591	3.6576	30	**15.7679**
12	38.33%	4.5994	88.33%	11.6591	3.6576	60	**15.0905**

Number of Stories	Ground Coverage	Urban Density (FSI)	Compactness Ratio	Street-to-surface Distance	Side-to-side Distance	CW/CCW Rotation of Azimuth Angle (°)	P.I.
12	38.33%	4.5994	88.33%	9.0329	3.6576	90	**15.6932**
12	38.33%	4.5994	88.33%	9.0329	3.6576	60	**15.2819**
12	38.33%	4.5994	88.33%	9.0329	3.6576	30	**15.7537**
12	38.33%	4.5994	88.33%	9.0329	3.6576	0	**16.7323**
12	38.33%	4.5994	88.33%	9.0329	3.6576	30	**15.7771**
12	38.33%	4.5994	88.33%	9.0329	3.6576	60	**15.1007**
12	38.33%	4.5994	88.33%	6.4066	3.6576	90	**15.5080**
12	38.33%	4.5994	88.33%	6.4066	3.6576	60	**15.1763**
12	38.33%	4.5994	88.33%	6.4066	3.6576	30	**15.5868**
12	38.33%	4.5994	88.33%	6.4066	3.6576	0	**16.6971**
12	38.33%	4.5994	88.33%	6.4066	3.6576	30	**15.5987**
12	38.33%	4.5994	88.33%	6.4066	3.6576	60	**15.0522**
12	35.38%	4.2456	91.60%	14.6441	4.3751	90	**16.2725**
12	35.38%	4.2456	91.60%	14.6441	4.3751	60	**15.5587**
12	35.38%	4.2456	91.60%	14.6441	4.3751	30	**16.4205**
12	35.38%	4.2456	91.60%	14.6441	4.3751	0	**17.2962**
12	35.38%	4.2456	91.60%	14.6441	4.3751	30	**16.4222**
12	35.38%	4.2456	91.60%	14.6441	4.3751	60	**15.4598**
12	35.38%	4.2456	91.60%	12.0179	4.3751	90	**16.2937**
12	35.38%	4.2456	91.60%	12.0179	4.3751	60	**15.5972**
12	35.38%	4.2456	91.60%	12.0179	4.3751	30	**16.2642**
12	35.38%	4.2456	91.60%	12.0179	4.3751	0	**17.2270**
12	35.38%	4.2456	91.60%	12.0179	4.3751	30	**16.2303**
12	35.38%	4.2456	91.60%	12.0179	4.3751	60	**15.5223**
12	35.38%	4.2456	91.60%	9.3916	4.3751	90	**15.9145**
12	35.38%	4.2456	91.60%	9.3916	4.3751	60	**15.6157**
12	35.38%	4.2456	91.60%	9.3916	4.3751	30	**16.1353**
12	35.38%	4.2456	91.60%	9.3916	4.3751	0	**17.2001**
12	35.38%	4.2456	91.60%	9.3916	4.3751	30	**16.1022**
12	35.38%	4.2456	91.60%	9.3916	4.3751	60	**15.4793**
12	35.38%	4.2456	91.60%	6.7653	4.3751	90	**16.0429**
12	35.38%	4.2456	91.60%	6.7653	4.3751	60	**15.6254**
12	35.38%	4.2456	91.60%	6.7653	4.3751	30	**16.0260**

Number of Stories	Ground Coverage	Urban Density (FSI)	Compactness Ratio	Street-to-surface Distance	Side-to-side Distance	CW/CCW Rotation of Azimuth Angle (°)	P.I.
12	35.38%	4.2456	91.60%	6.7653	4.3751	0	**17.2151**
12	35.38%	4.2456	91.60%	6.7653	4.3751	30	**16.0251**
12	35.38%	4.2456	91.60%	6.7653	4.3751	60	**15.5662**
12	32.85%	3.9423	94.74%	14.9637	5.0142	90	**16.5041**
12	32.85%	3.9423	94.74%	14.9637	5.0142	60	**15.8532**
12	32.85%	3.9423	94.74%	14.9637	5.0142	30	**16.4157**
12	32.85%	3.9423	94.74%	14.9637	5.0142	0	**17.6263**
12	32.85%	3.9423	94.74%	14.9637	5.0142	30	**16.3959**
12	32.85%	3.9423	94.74%	14.9637	5.0142	60	**15.7977**
12	32.85%	3.9423	94.74%	12.3374	5.0142	90	**16.4667**
12	32.85%	3.9423	94.74%	12.3374	5.0142	60	**15.8363**
12	32.85%	3.9423	94.74%	12.3374	5.0142	30	**16.3518**
12	32.85%	3.9423	94.74%	12.3374	5.0142	0	**17.5514**
12	32.85%	3.9423	94.74%	12.3374	5.0142	30	**16.3703**
12	32.85%	3.9423	94.74%	12.3374	5.0142	60	**15.7902**
12	32.85%	3.9423	94.74%	9.7112	5.0142	90	**16.5113**
12	32.85%	3.9423	94.74%	9.7112	5.0142	60	**15.8999**
12	32.85%	3.9423	94.74%	9.7112	5.0142	30	**16.2195**
12	32.85%	3.9423	94.74%	9.7112	5.0142	0	**17.4545**
12	32.85%	3.9423	94.74%	9.7112	5.0142	30	**16.1937**
12	32.85%	3.9423	94.74%	9.7112	5.0142	60	**15.7741**
12	32.85%	3.9423	94.74%	7.0849	5.0142	90	**16.3455**
12	32.85%	3.9423	94.74%	7.0849	5.0142	60	**15.9015**
12	32.85%	3.9423	94.74%	7.0849	5.0142	30	**16.1864**
12	32.85%	3.9423	94.74%	7.0849	5.0142	0	**17.4546**
12	32.85%	3.9423	94.74%	7.0849	5.0142	30	**16.1861**
12	32.85%	3.9423	94.74%	7.0849	5.0142	60	**15.8724**
13	41.81%	5.4356	90.59%	13.8788	2.8444	90	**15.2865**
13	41.81%	5.4356	90.59%	13.8788	2.8444	60	**14.9892**
13	41.81%	5.4356	90.59%	13.8788	2.8444	30	**15.5966**
13	41.81%	5.4356	90.59%	13.8788	2.8444	0	**16.1085**
13	41.81%	5.4356	90.59%	13.8788	2.8444	30	**15.6175**
13	41.81%	5.4356	90.59%	13.8788	2.8444	60	**14.8746**

Number of Stories	Ground Coverage	Urban Density (FSI)	Compactness Ratio	Street-to-surface Distance	Side-to-side Distance	CW/CCW Rotation of Azimuth Angle (°)	P.I.
13	41.81%	5.4356	90.59%	11.2525	2.8444	90	**15.1241**
13	41.81%	5.4356	90.59%	11.2525	2.8444	60	**14.9391**
13	41.81%	5.4356	90.59%	11.2525	2.8444	30	**15.5820**
13	41.81%	5.4356	90.59%	11.2525	2.8444	0	**16.1162**
13	41.81%	5.4356	90.59%	11.2525	2.8444	30	**15.5843**
13	41.81%	5.4356	90.59%	11.2525	2.8444	60	**14.8608**
13	41.81%	5.4356	90.59%	8.6263	2.8444	90	**15.0852**
13	41.81%	5.4356	90.59%	8.6263	2.8444	60	**14.8968**
13	41.81%	5.4356	90.59%	8.6263	2.8444	30	**15.5642**
13	41.81%	5.4356	90.59%	8.6263	2.8444	0	**16.1146**
13	41.81%	5.4356	90.59%	8.6263	2.8444	30	**15.5748**
13	41.81%	5.4356	90.59%	8.6263	2.8444	60	**14.8288**
13	41.81%	5.4356	90.59%	6.0000	2.8444	90	**15.1521**
13	41.81%	5.4356	90.59%	6.0000	2.8444	60	**14.8824**
13	41.81%	5.4356	90.59%	6.0000	2.8444	30	**15.4710**
13	41.81%	5.4356	90.59%	6.0000	2.8444	0	**16.0782**
13	41.81%	5.4356	90.59%	6.0000	2.8444	30	**15.4864**
13	41.81%	5.4356	90.59%	6.0000	2.8444	60	**14.8108**
13	38.33%	4.9827	90.59%	14.2854	3.6576	90	**14.3601**
13	38.33%	4.9827	90.59%	14.2854	3.6576	60	**14.0400**
13	38.33%	4.9827	90.59%	14.2854	3.6576	30	**14.6348**
13	38.33%	4.9827	90.59%	14.2854	3.6576	0	**15.4570**
13	38.33%	4.9827	90.59%	14.2854	3.6576	30	**14.6352**
13	38.33%	4.9827	90.59%	14.2854	3.6576	60	**13.9556**
13	38.33%	4.9827	90.59%	11.6591	3.6576	90	**14.3145**
13	38.33%	4.9827	90.59%	11.6591	3.6576	60	**13.9958**
13	38.33%	4.9827	90.59%	11.6591	3.6576	30	**14.5229**
13	38.33%	4.9827	90.59%	11.6591	3.6576	0	**15.3905**
13	38.33%	4.9827	90.59%	11.6591	3.6576	30	**14.5241**
13	38.33%	4.9827	90.59%	11.6591	3.6576	60	**13.9149**
13	38.33%	4.9827	90.59%	9.0329	3.6576	90	**14.4146**
13	38.33%	4.9827	90.59%	9.0329	3.6576	60	**14.0467**
13	38.33%	4.9827	90.59%	9.0329	3.6576	30	**14.4633**

Number of Stories	Ground Coverage	Urban Density (FSI)	Compactness Ratio	Street-to-surface Distance	Side-to-side Distance	CW/CCW Rotation of Azimuth Angle (°)	P.I.
13	38.33%	4.9827	90.59%	9.0329	3.6576	0	**15.3906**
13	38.33%	4.9827	90.59%	9.0329	3.6576	30	**14.4764**
13	38.33%	4.9827	90.59%	9.0329	3.6576	60	**13.9002**
13	38.33%	4.9827	90.59%	6.4066	3.6576	90	**14.2505**
13	38.33%	4.9827	90.59%	6.4066	3.6576	60	**13.9875**
13	38.33%	4.9827	90.59%	6.4066	3.6576	30	**14.3616**
13	38.33%	4.9827	90.59%	6.4066	3.6576	0	**15.3332**
13	38.33%	4.9827	90.59%	6.4066	3.6576	30	**14.3793**
13	38.33%	4.9827	90.59%	6.4066	3.6576	60	**13.8750**
13	35.38%	4.5994	76.66%	14.6441	4.3751	90	**15.0052**
13	35.38%	4.5994	76.66%	14.6441	4.3751	60	**14.3293**
13	35.38%	4.5994	76.66%	14.6441	4.3751	30	**14.9766**
13	35.38%	4.5994	76.66%	14.6441	4.3751	0	**15.8683**
13	35.38%	4.5994	76.66%	14.6441	4.3751	30	**14.9646**
13	35.38%	4.5994	76.66%	14.6441	4.3751	60	**14.2430**
13	35.38%	4.5994	76.66%	12.0179	4.3751	90	**15.0305**
13	35.38%	4.5994	76.66%	12.0179	4.3751	60	**14.3693**
13	35.38%	4.5994	76.66%	12.0179	4.3751	30	**14.9390**
13	35.38%	4.5994	76.66%	12.0179	4.3751	0	**15.8500**
13	35.38%	4.5994	76.66%	12.0179	4.3751	30	**14.9131**
13	35.38%	4.5994	76.66%	12.0179	4.3751	60	**14.3127**
13	35.38%	4.5994	76.66%	9.3916	4.3751	90	**14.6673**
13	35.38%	4.5994	76.66%	9.3916	4.3751	60	**14.3792**
13	35.38%	4.5994	76.66%	9.3916	4.3751	30	**14.8709**
13	35.38%	4.5994	76.66%	9.3916	4.3751	0	**15.7726**
13	35.38%	4.5994	76.66%	9.3916	4.3751	30	**14.8377**
13	35.38%	4.5994	76.66%	9.3916	4.3751	60	**14.2317**
13	35.38%	4.5994	76.66%	6.7653	4.3751	90	**14.6712**
13	35.38%	4.5994	76.66%	6.7653	4.3751	60	**14.3757**
13	35.38%	4.5994	76.66%	6.7653	4.3751	30	**14.7619**
13	35.38%	4.5994	76.66%	6.7653	4.3751	0	**15.7709**
13	35.38%	4.5994	76.66%	6.7653	4.3751	30	**14.7613**
13	35.38%	4.5994	76.66%	6.7653	4.3751	60	**14.3090**

Number of Stories	Ground Coverage	Urban Density (FSI)	Compactness Ratio	Street-to-surface Distance	Side-to-side Distance	CW/CCW Rotation of Azimuth Angle (°)	P.I.
13	32.85%	4.2709	71.18%	14.9637	5.0142	90	**15.1853**
13	32.85%	4.2709	71.18%	14.9637	5.0142	60	**14.4224**
13	32.85%	4.2709	71.18%	14.9637	5.0142	30	**15.0333**
13	32.85%	4.2709	71.18%	14.9637	5.0142	0	**16.1571**
13	32.85%	4.2709	71.18%	14.9637	5.0142	30	**15.0010**
13	32.85%	4.2709	71.18%	14.9637	5.0142	60	**14.3344**
13	32.85%	4.2709	71.18%	12.3374	5.0142	90	**15.1284**
13	32.85%	4.2709	71.18%	12.3374	5.0142	60	**14.4287**
13	32.85%	4.2709	71.18%	12.3374	5.0142	30	**14.9814**
13	32.85%	4.2709	71.18%	12.3374	5.0142	0	**16.1315**
13	32.85%	4.2709	71.18%	12.3374	5.0142	30	**15.0033**
13	32.85%	4.2709	71.18%	12.3374	5.0142	60	**14.3729**
13	32.85%	4.2709	71.18%	9.7112	5.0142	90	**15.1574**
13	32.85%	4.2709	71.18%	9.7112	5.0142	60	**14.5178**
13	32.85%	4.2709	71.18%	9.7112	5.0142	30	**14.8768**
13	32.85%	4.2709	71.18%	9.7112	5.0142	0	**16.0140**
13	32.85%	4.2709	71.18%	9.7112	5.0142	30	**14.8474**
13	32.85%	4.2709	71.18%	9.7112	5.0142	60	**14.4247**
13	32.85%	4.2709	71.18%	7.0849	5.0142	90	**14.9477**
13	32.85%	4.2709	71.18%	7.0849	5.0142	60	**14.5403**
13	32.85%	4.2709	71.18%	7.0849	5.0142	30	**14.8174**
13	32.85%	4.2709	71.18%	7.0849	5.0142	0	**15.9872**
13	32.85%	4.2709	71.18%	7.0849	5.0142	30	**14.8092**
13	32.85%	4.2709	71.18%	7.0849	5.0142	60	**14.5101**
14	41.81%	5.8538	97.56%	13.8788	2.8444	90	**14.1969**
14	41.81%	5.8538	97.56%	13.8788	2.8444	60	**13.9237**
14	41.81%	5.8538	97.56%	13.8788	2.8444	30	**14.5232**
14	41.81%	5.8538	97.56%	13.8788	2.8444	0	**15.1236**
14	41.81%	5.8538	97.56%	13.8788	2.8444	30	**14.5385**
14	41.81%	5.8538	97.56%	13.8788	2.8444	60	**13.8231**
14	41.81%	5.8538	97.56%	11.2525	2.8444	90	**14.0483**
14	41.81%	5.8538	97.56%	11.2525	2.8444	60	**13.9328**
14	41.81%	5.8538	97.56%	11.2525	2.8444	30	**14.4740**

Number of Stories	Ground Coverage	Urban Density (FSI)	Compactness Ratio	Street-to-surface Distance	Side-to-side Distance	CW/CCW Rotation of Azimuth Angle (°)	P.I.
14	41.81%	5.8538	97.56%	11.2525	2.8444	0	**15.0754**
14	41.81%	5.8538	97.56%	11.2525	2.8444	30	**14.4761**
14	41.81%	5.8538	97.56%	11.2525	2.8444	60	**13.8518**
14	41.81%	5.8538	97.56%	8.6263	2.8444	90	**14.0121**
14	41.81%	5.8538	97.56%	8.6263	2.8444	60	**13.8397**
14	41.81%	5.8538	97.56%	8.6263	2.8444	30	**14.4547**
14	41.81%	5.8538	97.56%	8.6263	2.8444	0	**15.0737**
14	41.81%	5.8538	97.56%	8.6263	2.8444	30	**14.4645**
14	41.81%	5.8538	97.56%	8.6263	2.8444	60	**13.7747**
14	41.81%	5.8538	97.56%	6.0000	2.8444	90	**14.0761**
14	41.81%	5.8538	97.56%	6.0000	2.8444	60	**13.8282**
14	41.81%	5.8538	97.56%	6.0000	2.8444	30	**14.3665**
14	41.81%	5.8538	97.56%	6.0000	2.8444	0	**15.0348**
14	41.81%	5.8538	97.56%	6.0000	2.8444	30	**14.3809**
14	41.81%	5.8538	97.56%	6.0000	2.8444	60	**13.7578**
14	38.33%	5.3660	89.43%	14.2854	3.6576	90	**13.3790**
14	38.33%	5.3660	89.43%	14.2854	3.6576	60	**13.0666**
14	38.33%	5.3660	89.43%	14.2854	3.6576	30	**13.6046**
14	38.33%	5.3660	89.43%	14.2854	3.6576	0	**14.3667**
14	38.33%	5.3660	89.43%	14.2854	3.6576	30	**13.6053**
14	38.33%	5.3660	89.43%	14.2854	3.6576	60	**12.9861**
14	38.33%	5.3660	89.43%	11.6591	3.6576	90	**13.3169**
14	38.33%	5.3660	89.43%	11.6591	3.6576	60	**13.0031**
14	38.33%	5.3660	89.43%	11.6591	3.6576	30	**13.5053**
14	38.33%	5.3660	89.43%	11.6591	3.6576	0	**14.3654**
14	38.33%	5.3660	89.43%	11.6591	3.6576	30	**13.5023**
14	38.33%	5.3660	89.43%	11.6591	3.6576	60	**12.9258**
14	38.33%	5.3660	89.43%	9.0329	3.6576	90	**13.3918**
14	38.33%	5.3660	89.43%	9.0329	3.6576	60	**13.0833**
14	38.33%	5.3660	89.43%	9.0329	3.6576	30	**13.4935**
14	38.33%	5.3660	89.43%	9.0329	3.6576	0	**14.3175**
14	38.33%	5.3660	89.43%	9.0329	3.6576	30	**13.5157**
14	38.33%	5.3660	89.43%	9.0329	3.6576	60	**12.9238**

Number of Stories	Ground Coverage	Urban Density (FSI)	Compactness Ratio	Street-to-surface Distance	Side-to-side Distance	CW/CCW Rotation of Azimuth Angle (°)	P.I.
14	38.33%	5.3660	89.43%	6.4066	3.6576	90	**13.2401**
14	38.33%	5.3660	89.43%	6.4066	3.6576	60	**12.9952**
14	38.33%	5.3660	89.43%	6.4066	3.6576	30	**13.3459**
14	38.33%	5.3660	89.43%	6.4066	3.6576	0	**14.2452**
14	38.33%	5.3660	89.43%	6.4066	3.6576	30	**13.3603**
14	38.33%	5.3660	89.43%	6.4066	3.6576	60	**12.8909**
14	35.38%	4.9532	82.55%	14.6441	4.3751	90	**13.9362**
14	35.38%	4.9532	82.55%	14.6441	4.3751	60	**13.3275**
14	35.38%	4.9532	82.55%	14.6441	4.3751	30	**14.0509**
14	35.38%	4.9532	82.55%	14.6441	4.3751	0	**14.7696**
14	35.38%	4.9532	82.55%	14.6441	4.3751	30	**14.0547**
14	35.38%	4.9532	82.55%	14.6441	4.3751	60	**13.2382**
14	35.38%	4.9532	82.55%	12.0179	4.3751	90	**13.9643**
14	35.38%	4.9532	82.55%	12.0179	4.3751	60	**13.3584**
14	35.38%	4.9532	82.55%	12.0179	4.3751	30	**13.8936**
14	35.38%	4.9532	82.55%	12.0179	4.3751	0	**14.7380**
14	35.38%	4.9532	82.55%	12.0179	4.3751	30	**13.8625**
14	35.38%	4.9532	82.55%	12.0179	4.3751	60	**13.2989**
14	35.38%	4.9532	82.55%	9.3916	4.3751	90	**13.6256**
14	35.38%	4.9532	82.55%	9.3916	4.3751	60	**13.3768**
14	35.38%	4.9532	82.55%	9.3916	4.3751	30	**13.8173**
14	35.38%	4.9532	82.55%	9.3916	4.3751	0	**14.6664**
14	35.38%	4.9532	82.55%	9.3916	4.3751	30	**13.7864**
14	35.38%	4.9532	82.55%	9.3916	4.3751	60	**13.2622**
14	35.38%	4.9532	82.55%	6.7653	4.3751	90	**13.7375**
14	35.38%	4.9532	82.55%	6.7653	4.3751	60	**13.3812**
14	35.38%	4.9532	82.55%	6.7653	4.3751	30	**13.7349**
14	35.38%	4.9532	82.55%	6.7653	4.3751	0	**14.7381**
14	35.38%	4.9532	82.55%	6.7653	4.3751	30	**13.7341**
14	35.38%	4.9532	82.55%	6.7653	4.3751	60	**13.3302**
14	32.85%	4.5994	76.66%	14.9637	5.0142	90	**14.1196**
14	32.85%	4.5994	76.66%	14.9637	5.0142	60	**13.5502**
14	32.85%	4.5994	76.66%	14.9637	5.0142	30	**14.0350**

Number of Stories	Ground Coverage	Urban Density (FSI)	Compactness Ratio	Street-to-surface Distance	Side-to-side Distance	CW/CCW Rotation of Azimuth Angle (°)	P.I.
14	32.85%	4.5994	76.66%	14.9637	5.0142	0	**15.0340**
14	32.85%	4.5994	76.66%	14.9637	5.0142	30	**14.0108**
14	32.85%	4.5994	76.66%	14.9637	5.0142	60	**13.4832**
14	32.85%	4.5994	76.66%	12.3374	5.0142	90	**14.0720**
14	32.85%	4.5994	76.66%	12.3374	5.0142	60	**13.5545**
14	32.85%	4.5994	76.66%	12.3374	5.0142	30	**14.0035**
14	32.85%	4.5994	76.66%	12.3374	5.0142	0	**15.0345**
14	32.85%	4.5994	76.66%	12.3374	5.0142	30	**14.0144**
14	32.85%	4.5994	76.66%	12.3374	5.0142	60	**13.5101**
14	32.85%	4.5994	76.66%	9.7112	5.0142	90	**14.0997**
14	32.85%	4.5994	76.66%	9.7112	5.0142	60	**13.6090**
14	32.85%	4.5994	76.66%	9.7112	5.0142	30	**13.8895**
14	32.85%	4.5994	76.66%	9.7112	5.0142	0	**14.8920**
14	32.85%	4.5994	76.66%	9.7112	5.0142	30	**13.8601**
14	32.85%	4.5994	76.66%	9.7112	5.0142	60	**13.5012**
14	32.85%	4.5994	76.66%	7.0849	5.0142	90	**13.8971**
14	32.85%	4.5994	76.66%	7.0849	5.0142	60	**13.6083**
14	32.85%	4.5994	76.66%	7.0849	5.0142	30	**13.8444**
14	32.85%	4.5994	76.66%	7.0849	5.0142	0	**14.8631**
14	32.85%	4.5994	76.66%	7.0849	5.0142	30	**13.8441**
14	32.85%	4.5994	76.66%	7.0849	5.0142	60	**13.5809**

Table E14-17: Multiple linear regression model specifications with Number of Stories, Ground Coverage, Street-to-surface Distance, Side-to-side Distance and CW/CCW Rotation of Azimuth Angle (°) as independent variables and Annual Solar Performance Indicator (P.I.) as the dependent variable.

Table E14: Regression Statistics.

Regression Statistics	
Multiple R	0.97531399
R Square	0.951237379
Adjusted R Square	0.950723006
Standard Error	0.453896015
Observations	480

Table E15: ANOVA (Analysis of Variance).

	df	*SS*	*MS*	*F*	*Significance F*
Regression	5	1904.991097	380.9982194	1849.312077	3.0628E-308
Residual	474	97.65423492	0.206021593		
Total	479	2002.645332			

Table E16: Coefficients, Standard Error, t Stat and P-value.

	Coefficients	*Standard Error*	*t Stat*	*P-value*
Intercept	-240.7346084	18.52992218	-12.99166862	3.16082E-33
Number of Stories	-1.361321362	0.014649431	-92.92656974	2.1695E-306
Ground Coverage	512.8515644	34.62883588	14.80995683	4.65332E-41
Street-to-surface Distance	0.016951516	0.00705573	2.402517818	0.01666621
Side-to-side Distance	21.06220689	1.43087304	14.71982929	1.16256E-40
CW/CCW Rotation of Azimuth Angle (°)	-0.013784235	0.000721288	-19.11058081	8.80854E-61

Table E17: Lower 95%, Upper 95%, Lower 95.0%, Upper 95.0%.

	Lower 95%	*Upper 95%*	*Lower 95.0%*	*Upper 95.0%*
Intercept	-277.1455601	-204.3236567	-277.1455601	-204.3236567
Number of Stories	-1.390107221	-1.332535503	-1.390107221	-1.332535503
Ground Coverage	444.8065473	580.8965815	444.8065473	580.8965815
Street-to-surface Distance	0.003087139	0.030815893	0.003087139	0.030815893
Side-to-side Distance	18.25056803	23.87384574	18.25056803	23.87384574
CW/CCW Rotation of Azimuth Angle (°)	-0.015201553	-0.012366917	-0.015201553	-0.012366917

Appendix F: Field Data Samples

Monthly Operation Data (MOD)
(Feeder & Tariff wise Import & Sold Unit)
Table-2

Name of the Circle : Motijheel

Month : Feb'2020

Name of the Division : Network Operation & Customer Service Motijheel

Sl No.	Name of Feeder	Consumer & Unit Sold (KWH)	Tariff Category LT-A	LT-C1	LT-C2	LT-D1	LT-D2	LT-E	MT-1	MT-2	MT-3	MT-4	MT-5	Total	Import Unit	System Loss
01	Sugar Bhaban U/G	Number of Customer	0	0	0	0	0	0	0	2	0	0	0	2	71129	6.52
		Sold Unit	0	0	0	0	0	0	0	66492	0	0	0	66492		
02	Sonali Bank RMU	Number of Customer	0	0	0	0	0	0	0	4	0	0	0	4	321300	6.52
		Sold Unit	0	0	0	0	0	0	0	300352	0	0	0	300352		
03	Janata Bank 11KV O/H	Number of Customer	0	1	4	0	0	50	0	18	1	0	0	74	296616	6.55
		Sold Unit	0	1495	1568	0	0	49853	0	183400	40872	0	0	277188		
04	BCIC 11KV O/H	Number of Customer	0	0	0	0	0	0	0	13	0	0	0	13	464819	6.54
		Sold Unit	0	0	0	0	0	0	0	434420	0	0	0	434420		
05	B.B. DIT Gate RMU	Number of Customer	0	0	0	0	0	0	5	0	0	0	0	5	123587	6.51
		Sold Unit	0	0	0	0	0	0	115542	0	0	0	0	115542		
06	B.B. Hospital Zone RMU	Number of Customer	0	0	0	0	0	0	0	1	0	0	1	2	110268	6.51
		Sold Unit	0	0	0	0	0	0	0	44032	0	0	59058	103090		
07	PDB Design 11KV O/H	Number of Customer	363	1	4	0	0	43	1	12	0	0	1	425	317669	6.56
		Sold Unit	49978	655	261	0	0	26437	1027	176872	0	0	41600	296830		
08	Senakallyan U/G	Number of Customer	0	0	0	0	0	0	0	4	0	0	0	4	421212	6.52
		Sold Unit	0	0	0	0	0	0	0	393749	0	0	0	393749		
09	Navana 11KV O/H	Number of Customer	0	0	1	0	1	33	0	30	0	0	0	65	838178	6.56
		Sold Unit	0	0	801	0	5995	63976	0	712422	0	0	0	783194		
10	Inner Circular Road 11KV O/H	Number of Customer	4497	604	16	18	17	341	13	8	0	0	2	5516	1455827	6.57
		Sold Unit	641081	428933	34433	15597	23397	97862	72139	19764	0	0	26932	1360138		
11	DIT Sub-station RMU	Number of Customer	0	0	0	0	0	0	0	3	0	0	0	3	637610	6.52
		Sold Unit	0	0	0	0	0	0	0	596038	0	0	0	596038		
12	Modhumita via Ovisar 11KV O/H	Number of Customer	5522	26	40	21	1	377	53	14	0	0	1	6055	1292055	6.57
		Sold Unit	801416	16063	11300	12838	120	140838	89661	127495	0	0	7472	1207203		
13	Wapda Building RMU	Number of Customer	0	0	0	0	0	4	0	2	0	0	0	6	36961	6.52
		Sold Unit	0	0	0	0	0	1276	0	33276	0	0	0	34552		
14	Dilkusha 11KV O/H	Number of Customer	1	0	0	2	2	22	0	20	0	0	0	47	412997	6.55
		Sold Unit	334	0	0	696	840	29888	0	354188	0	0	0	385946		
15	Krishi Bhaban 11KV O/H	Number of Customer	0	0	0	0	0	0	0	10	0	0	0	10	235308	6.53
		Sold Unit	0	0	0	0	0	0	0	219943	0	0	0	219943		
16	B.B. Staff Quarter RMU	Number of Customer	0	0	0	0	0	0	0	0	0	0	0	0	0	0.00
		Sold Unit	0	0	0	0	0	0	0	0	0	0	0	0		
17	DIT 11KV O/H	Number of Customer	0	0	4	0	1	14	0	17	0	0	0	36	240508	6.55
		Sold Unit	0	0	1021	0	0	12703	0	211031	0	0	0	224755		
18	Adamjee Court U/G	Number of Customer	0	0	0	0	0	0	0	6	0	0	0	6	369694	6.52
		Sold Unit	0	0	0	0	0	0	0	345590	0	0	0	345590		
19	Motijheel Nearest	Number of Customer	14	0	0	0	0	23	0	17	0	1	0	55	379695	6.55
		Sold Unit	1598	0	0	0	0	25506	0	327437	0	284	0	354825		
20	Arambag 11KV O/H	Number of Customer	3157	194	8	8	27	358	9	12	3	0	5	3781	1280276	6.56
		Sold Unit	447851	183433	6467	7123	47845	198675	19438	85356	72312	0	127790	1196290		
21	Box culvert 11KV O/H	Number of Customer	1744	554	23	4	2	281	4	17	0	0	1	2630	1212544	6.59
		Sold Unit	313662	476559	18887	6153	540	148295	12105	148594	0	0	7800	1132595		
22	Agrani Bank U/G	Number of Customer	0	0	0	0	0	0	0	2	0	0	0	2	124505	6.51
		Sold Unit	0	0	0	0	0	0	0	116400	0	0	0	116400		
23	Fakirapool Water Tank 11KV O/H	Number of Customer	421	143	4	1	5	210	2	16	0	0	1	803	556674	6.57
		Sold Unit	70752	153646	9649	1155	2760	100673	526	150727	0	0	30213	520101		
24	Mohamadan Club 11KV O/H	Number of Customer	0	0	0	0	0	5	0	14	0	0	1	20	328253	6.56
		Sold Unit	0	0	0	0	0	6146	0	300421	0	0	153	306720		
25	NCC Bank U/G	Number of Customer	0	0	0	0	0	0	0	1	0	0	0	1	192533	6.51
		Sold Unit	0	0	0	0	0	0	0	180000	0	0	0	180000		
26	Station Road 11KV O/H	Number of Customer	3672	26	16	14	1	401	20	17	2	0	3	4172	1117562	6.57
		Sold Unit	504121	32745	4819	10854	1877	167194	36429	149278	33904	0	102936	1044157		
27	Bangladesh Bank	Number of Customer	90	2	0	4	0	37	2	9	0	0	4	148	1266253	6.56
		Sold Unit	21255	177	0	2307	0	6058	3794	1093884	0	0	55652	1183127		
	Total	Number of Customer	**19481**	**1551**	**120**	**72**	**57**	**2199**	**109**	**269**	**6**	**1**	**20**	**23885**	**14104033**	**6.56**
		Sold Unit	**2852048**	**1293706**	**89206**	**56723**	**83374**	**1075380**	**350661**	**6771161**	**147088**	**284**	**459606**	**13179237**		

Figure F1: A Sample Monthly Report from DPDC.

Appendix G: Documents

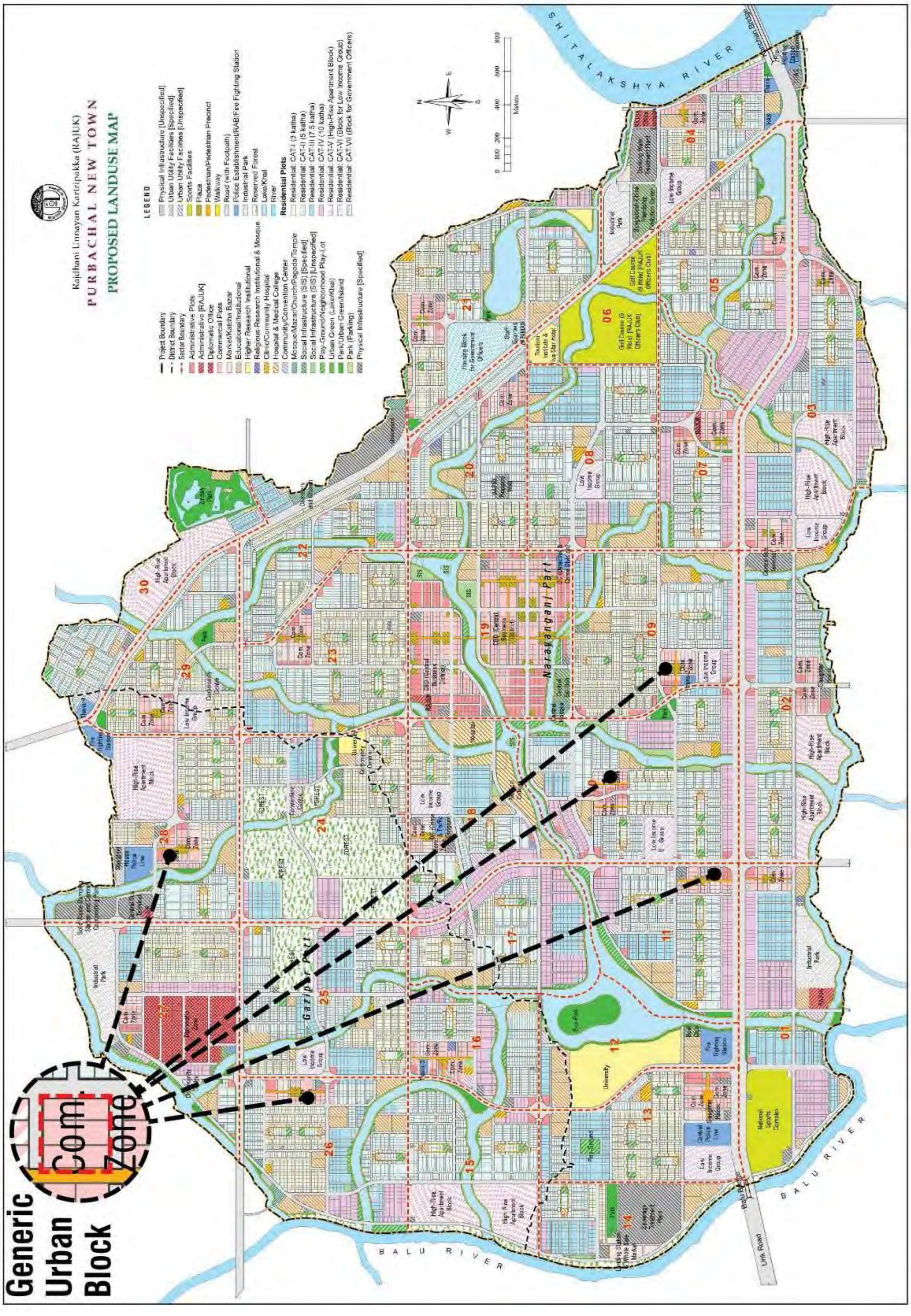

Figure G1: Proposed Landuse Map of Purbachal New Town by Rajuk – Dhaka's Development Authority, showing the generic commercial block.

Appendix H: Python Code for Machine Learning Model

In [1]:

```
import pandas as pd
from datetime import datetime
import numpy as np
from sklearn.linear_model import LinearRegression
import matplotlib.pyplot as plt
```

In [2]:

```
col_list = ["Number of Stories", "Ground Coverage", "Urban Density (FSI)", "Compactness Ratio", "Street-to-Surface Distance", "Side-to-side Distance", "CW/CCW Rotation of Azimuth Angle (°)", "P.I."]
block_data = pd.read_csv("data_simulation.csv", engine='python', usecols=col_list)
block_data = block_data.loc[:480]
# data preview
block_data.head()
```

In [3]:

```
# extraction of independent and dependent variables
X = block_data.iloc[:, 0:-1].values
y = block_data.iloc[:, -1].values
```

In [4]:

```
# visualizing data
# creation of correlation matrix
import seaborn as sns
sns.heatmap(block_data.corr())
```

In [5]:

```
# splitting into train set and test set
from sklearn.model_selection import train_test_split
X_train, X_test, y_train, y_test = train_test_split(X, y, test_size = 0.2, random_state = 0)
```

In [6]:

```
# fitting multiple linear regression to train set
from sklearn.linear_model import LinearRegression
regressor =  LinearRegression()
regressor.fit(X_train, y_train)
```

In [7]:

```
y_pred = regressor.predict(X_test)
```

In [8]:

```
print(regressor.coef_)
print(regressor.intercept_)
```

In [9]:

```
from sklearn.metrics import r2_score
r2Score = r2_score(y_test, y_pred)

print(r2Score)
```

Sources of this code:
1. Python Data Science Handbook by Jake VanderPlas
2. www.stackoverflow.com
3. Applied Machine Learning in Python: an online non-credit course authorized by University of Michigan and offered through Coursera